DISSERTATION

INTERACTIONS BETWEEN FLOW HYDRAULICS AND CHANNEL MORPHOLOGY IN STEP-POOL STREAMS

Submitted by

Andrew C. Wilcox

Department of Geosciences

In partial fulfillment of the requirements

for the Degree of Doctor of Philosophy

Colorado State University

Fort Collins, Colorado

Summer 2005

COLORADO STATE UNIVERSITY

May 10, 2005

WE HEREBY RECOMMEND THAT THE DISSERTATION PREPARED UNDER OUR SUPERVISION BY ANDREW C. WILCOX ENTITLED INTERACTIONS BETWEEN FLOW HYDRAULICS AND CHANNEL MORPHOLOGY IN STEP-POOL STREAMS BE ACCEPTED AS FULFILLING IN PART REQUIREMENTS FOR THE DEGREE OF DOCTOR OF PHILOSOPHY

Committee on Graduate Work

_____

_____

_____

_____
Advisor

_____
Department Head

ABSTRACT OF DISSERTATION

INTERACTIONS BETWEEN FLOW HYDRAULICS AND MORPHOLOGY IN STEP-POOL STREAM CHANNELS

This research investigated interactions between hydraulics and morphology in step-pool channels, an important class of steep mountain stream channels, using physical modeling and field studies. Flow resistance dynamics in step-pool channels were examined through physical modeling in a laboratory flume configured to resemble a step-pool channel. Over 400 flume runs were completed using a factorial design in which variables contributing to flow resistance in step-pool channels were manipulated in order to both measure resistance partitioning between grains, steps, and large woody debris (LWD) and to quantify the effects of changes in LWD configurations, step geometry, discharge, and slope on total flow resistance. Analysis of partitioning between LWD, spill, and grain roughness showed that LWD and spill over steps were responsible for the largest components of total resistance and that grain roughness was a small component of total resistance. Flume experiments documented significant interaction effects between steps, grains, and LWD, illustrating the synergistic effect of roughness features on hydraulics in these channels and providing insight into the errors in simple additive approaches to resistance partitioning. Approaches to resistance partitioning that assume that sources of resistance are isolated and additive were found to inflate the values of components that are quantified by subtraction from measurable components, likely as a result of interactions between roughness features.

Discharge strongly influenced resistance dynamics: it had the largest effect on total resistance of all variables tested; altered resistance partitioning between spill, LWD, and grains; and had highly significant interactions with all other variables, thereby mediating the effect of LWD configuration and other factors on resistance. LWD position, density, orientation, and step geometry also had highly significant effects on flow resistance.

Spatial and temporal patterns of hydraulics and energy dissipation in step-pool channels were also examined in a field setting using measurements of three-dimensional velocity and turbulence structure. Contributions to overall velocity vector magnitudes and especially to turbulence intensities from vertical and cross-stream flow components were substantial, creating three-dimensionality in overall flow characteristics compared to lower-gradient systems. Variation in hydraulics both spatially, between positions upstream and downstream from steps, and temporally, with changing discharge, resulted largely from changes in the streamwise velocity component. Spatial variations in hydraulic characteristics in the study reach reflected the form drag and spill resistance generated by step-pool sequences consisting of LWD and/or large clasts.

The combined results of the flume and field investigations illustrate several aspects of the interactions between hydraulics and channel morphology in step-pool channels. Whereas bed roughness features in these channels create very large flow resistance values at lower discharges, the drag created by LWD and step-pool sequences is diminished substantially with increasing discharge, suggesting a greater sensitivity of hydraulics to discharge variations in step-pool channels than in low-gradient channels. Further, the hydraulic effect of LWD is substantial in these systems and results from both

form drag from LWD pieces and spill resistance contributions from step-forming LWD, suggesting that forced step-pool systems containing LWD have higher flow resistance and morphologic and hydraulic complexity compared to steep channels lacking LWD. Reductions in LWD abundance as a result of land-use activities may have significantly altered flow resistance dynamics and associated morphologic characteristics in these channels.

Andrew C. Wilcox

Department of Geosciences

Colorado State University

Fort Collins, CO 80523

Summer 2005

ACKNOWLEDGMENTS

First and foremost, I would like to thank my advisor, Dr. Ellen Wohl, for her mentorship, support, and friendship during my doctoral studies. I have learned a great deal from Ellen about being a scientist and geomorphologist, and I have gained great respect for her ability to achieve both prodigious academic productivity and balance between work and play. Ellen also provided financial support, including obtaining the main NSF grant that funded the first part of my doctoral studies, arranging teaching assistant positions and research fellowships, and conference funding. I was also fortunate that Ellen allowed me to ride her globe-trotting coattails to field work in New Zealand and Italy.

I am also grateful to my committee members, Drs. Deborah Anthony, Brian Bledsoe, and Jonathan M. Nelson for their guidance, advice, and critical reviews, all of which have improved my work. In particular, Jon has challenged me to dig deeper into the theoretical and quantitative aspects of my research, has shared some of his deep understanding of river mechanics with me, and has spent long hours with me looking at my data and pondering its implications.

My doctoral research has been funded in part by National Science Foundation grant EAR-9902440. Field work was also supported by a Geological Society of America Research Grant and a Warner-Chevron grant. I am also grateful for an Edward M. Warner Research Fellowship and for fellowships from Colorado State University's College of Natural Resources and the American Water Resources Association.

I would like to thank several undergraduate research assistants, Julie Kray, Glen Vallance, Robert Turner, Joe Dartt, and Karla Schmidt, for their yeoman work in

collecting and processing the mountains of data generated during my research. They provided invaluable assistance running the flume at the Engineering Research Center and processing data. Julie Kray and Glen Vallance also spent long days standing in very cold water, occasionally supplemented by snow or thunderstorms, helping collect field data. I also thank Francesco Comiti for assistance with data collection and collaborations on studies of mountain rivers.

Thanks also to Chad Lipscomb, Michael Robeson, Christopher Thornton, and Junior Garza at Colorado State University's Engineering Research Center for assistance with flume setup and operation. Others that have assisted my work include Dr. Philip Chapman for advice on statistical analyses, Tracy Phelps for assistance with data processing, Laurie Porth and Manuel Martinez (U.S. Forest Service) for East St. Louis Creek discharge data and logistical support, and Craig Huhta (SonTek) for providing insights on the FlowTracker ADV.

I would also like to thanks the friends that helped nourish my soul by climbing, skiing, biking, and playing music with me during my Ph.D.

My parents, Cynda and Philip Wilcox, have been a source of constant support and love throughout my academic career and life. They instilled in me the value of education, hard work, integrity, and public service.

Finally, I would like to deeply thank my wife, Alisa Wade. I am grateful not only for her help with flume and field work and artistic and editorial assistance, but more importantly for the love, companionship, patience, laughter, listening, and willingness to put up with my work habits that have sustained and supported me through my Ph.D.

TABLE OF CONTENTS

CHAPTER 1. INTRODUCTION

Step-pool channels are an important class of mountain channels that are characterized by repeating sequences of boulder, log, or bedrock steps over which flow plunges into pools. Sequences of step-pool features occur in channels with gradients of 0.02 to 0.2 m/m (Wohl and Grodek, 1994; Montgomery and Buffington, 1997; Chartrand and Whiting, 2000), resulting in stepped profiles in which elevation loss is concentrated in large steps separated by low-gradient pools (Keller and Swanson, 1979).

Despite a growing body of recent research describing the morphologic characteristics of step-pool channels, significant gaps in knowledge of the processes operating in these channels remain, particularly in relation to hydraulics, sediment transport, and the role of large woody debris (LWD). Because early research in fluvial geomorphology tended to focus on low-gradient alluvial channels, research on physical processes in steep stream channels has lagged behind related work on lower-gradient channels. Understanding of physical processes in step-pool channels is important, because these channels constitute a large proportion of channel length in mountain stream networks and provide habitat for a variety of aquatic species (Wohl, 2000a). Furthermore, because of the position of step-pool channels in the headwaters of many drainage networks, processes in these channels strongly influence water and sediment discharge to downstream areas, thereby affecting flooding, water supply, reservoir sedimentation, and downstream aquatic and riparian habitat. In Colorado, controls on the morphology of mountain stream channels have been debated in the context of controversies over instream flows for channel maintenance purposes (Gordon, 1995).

The interactions between hydraulic driving forces and the resisting forces created by roughness elements such as step-pool sequences and LWD in steep channels are poorly understood, hindering advances in analyses of flow, channel form, and sediment transport processes in step-pool channels and limiting understanding of how steep channels are different from the low-gradient channels on which much fluvial geomorphic knowledge is based. Understanding the hydraulics of step-pool channels, including velocity structure, turbulence characteristics, controls on hydraulic resistance, and the role of large woody debris (LWD), is critical to developing insight into the mechanics and morphology of these channels. Improved understanding of flow resistance in mountain stream channels is needed because of the implications of flow resistance dynamics for channel form and stability, sediment transport, and aquatic habitat. Further, because stage-discharge relationships are governed by flow resistance, increased understanding of the controls on flow resistance is needed to improve estimates of velocity and discharge in step-pool channels. Existing equations for estimating flow resistance or sediment transport in lower-gradient channels have substantial error when applied to step-pool and other high-gradient systems (Mussetter, 1989; Jarrett, 1992; Marcus et al., 1992; Yager et al., 2002; Curran and Wohl, 2003). Management concerns in headwater streams, including the impacts of land-use on woody debris loading and the potential for associated stream restoration efforts, also highlight the need for improved understanding of the role of LWD in step-pool channels. Although the morphologic role of LWD has been well documented in low-gradient systems, existing studies in step-pool channels have largely neglected LWD.

1.1 Study objectives

The research presented here investigates the interactions between flow hydraulics and channel morphology in step-pool stream channels. Three related aspects of hydraulics and morphology in step-pool channels are explored: (1) large woody debris and controls on total flow resistance; (2) flow resistance partitioning between steps, grains, and LWD; and (3) spatial and temporal variations in three-dimensional hydraulics.

The objectives of the first component of this research are to (1) determine the relative effect of step-pool structures, LWD, grain roughness from non-step-forming clasts, discharge, and slope on flow resistance; (2) assess the role of interactions between these resistance components in altering flow resistance dynamics; and (3) evaluate how variations in LWD configurations affect hydraulic resistance in step-pool channels. The second aspect of my research, which explores the partitioning of flow resistance in step-pool channels, (1) measures the fractional contributions of grain, spill, and debris resistance to total resistance; (2) tests the effect of discharge, slope, and LWD density on partitioning; and (3) evaluates a range of methods for quantifying resistance partitioning. The third avenue of research treated here investigates (1) the three-dimensional character of velocity and turbulence in step-pool channels; (2) how velocity and turbulence vary with discharge; and (3) the effect of step-pool bed morphology on spatial variations in hydraulics.

The broad goals of this work are to increase understanding of basic physical processes in this important class of mountain rivers, in an effort to address some of the gaps in our knowledge of step-pool channels discussed above and to develop insight into

the mechanics and morphology of these channels. This work also seeks to elucidate how step-pool channels differ from low-gradient stream channels in terms of hydraulics and their interactions with bed morphology. Another unifying theme of this work is the objective of increasing understanding of the effect of LWD on hydraulics and flow resistance in step-pool channels. Resulting insights may in turn shed light on management and restoration of woody debris in headwater streams and into how widespread reductions in LWD abundance in headwater streams have altered the hydraulics and morphology of these channels. In addition, all of these investigations are intended to contribute to analyses of sediment transport dynamics, discharge estimation, and assessment of aquatic habitat characteristics in steep stream channels.

1.2 Research overview

My investigation of hydraulics and morphology in step-pool channels comprised flume and field components. Flow resistance dynamics in step-pool channels, including controls on total resistance and the partitioning of resistance between steps, grains, and LWD, were investigated through physical modeling using a laboratory flume configured to resemble a step-pool channel. Over 400 flume runs were completed using a factorial design in which variables contributing to flow resistance in step-pool channels were manipulated in order to both measure resistance partitioning between grains, steps, and large woody debris (LWD) and to quantify the effects of changes in LWD configurations, step geometry, discharge, and slope on total flow resistance. This approach allowed testing of the effect of numerous LWD configurations on flow resistance, including LWD density, orientation, piece length, arrangement, and position; measurement of both the

main effects of different variables on flow resistance and of interactions among resistance features; and testing of multiple methods of flow resistance partitioning.

My research also examined spatial and temporal patterns of hydraulics and energy dissipation in step-pool channels using field measurements of three-dimensional velocity and turbulence structure. Repeat measurements of hydraulic characteristics were performed using a FlowTracker acoustic Doppler velocimeter in a step-pool channel in the Colorado Rockies. To examine the effects of spatial variations in the channel on flow hydraulics, thalweg velocity profiles were measured at positions associated with different bed morphologies, and to examine the effects of temporal variations, these measurements were repeated at five different discharges.

This dissertation is organized around the three lines of inquiry described above: (1) large woody debris and controls on total flow resistance; (2) flow resistance partitioning between steps, grains, and LWD; and (3) spatial and temporal variations in three-dimensional hydraulics in step-pool channels. One chapter is devoted to each of these investigations; these chapters are organized in the form of journal papers, with separate sections describing background and relevant literature, methods, results, and discussion. Preceding these chapters a more extensive review of existing knowledge regarding step-pool channels and flow resistance partitioning is presented. Data collected in the course of this research are presented in a series of appendices.

CHAPTER 2. BACKGROUND

This dissertation, in examining the interactions between hydraulics and morphology in step-pool channels, builds on a wide range of research areas in geomorphology and hydraulic engineering. These include previous studies of morphology and hydraulics in step-pool channels, investigations of the physical role of large woody debris in stream channels, analyses of flow resistance dynamics and resistance partitioning, and studies of turbulence and three-dimensional hydraulics in lower-gradient systems. This chapter provides background information and reviews selected literature related to these topics.

2.1 Step-pool channels

Descriptions of the morphology of step-pool streams in terms of relationships between step length, step height, grain size, stream gradient, and channel width (e.g., Grant et al., 1990; Wohl and Grodek, 1994; Chin, 1999a; Chartrand and Whiting, 2000) and of the variance in these relationships (Zimmermann and Church, 2001) have been emphasized in previous step-pool research. For example, Chin (1999a), based on field surveys in step-pool channels in the Santa Monica Mountains, California, found strong correlations between step length and slope (inverse relationship) and between step height and slope (positive relationship). Chin (1999a) concludes that step-pool morphology is controlled by both particle size, which exerts causality over step height, and discharge, which controls step wavelength. Wohl and Grodek (1994) found that boulder and bedrock steps in ephemeral channels exhibited strong correlations between the height and

spacing of steps and channel slope. In these channels, ephemeral flows are not large enough to submerge step-forming clasts, suggesting different formative processes than in perennial channels where high flows that submerge clasts are presumed to be responsible for step formation. Wohl and Grodek (1994) conclude that slope is the dominant control on flow structure and scales of turbulence, which are reflected by step characteristics.

Many of the previous studies of step-pool channels have focused on channels in which steps are clast-formed and LWD is absent (Hayward, 1980; Wohl and Grodek, 1994; Chin, 1999a; Lenzi, 2001; Lee and Ferguson, 2002). Woody debris is prevalent in many step-pool channels, however, and steps formed entirely or partially by LWD are sometimes referred to as forced steps (Montgomery and Buffington, 1997). Several studies have described the effects of LWD on channel morphology and flow hydraulics in steep headwater streams (Keller and Swanson, 1979; Bisson et al., 1987; Lisle, 1995; Curran and Wohl, 2003; Faustini and Jones, 2003), as discussed further in Chapter 3.

Several hypotheses have been advanced to explain the formation of step-pool features. Based on flume studies, Whittaker and Jaeggi (1982) theorized that particle sorting, armoring of the bed surface, and formation of antidunes at high (near-critical) flows and under conditions of low sediment supply may give rise to step-pool structures. Grant and Mizuyama (1992) also produced flume results that supported the antidune hypothesis. Chin (1999b) tested the antidune theory of step-pool formation in a field setting, comparing data on step wavelength for streams in the Santa Monica Mountains to predicted antidune wavelengths based on laboratory results. Chin (1999b) also used hydraulic calculations to estimate the depth and velocity of flows capable of mobilizing step-pool features and to define the domain of step formation (as characterized by Froude

number and critical shear stress), comparing these reconstructed flow conditions to the theoretical domain for antidune formation indicated by experimental data (Kennedy, 1963; Whittaker and Jaeggi, 1982). This analysis indicated general agreement between step-pool wavelengths and reconstructed hydraulic conditions for step formation from field studies and those predicted by the laboratory-based antidune model. Observations at the lower range of step-pool gradients (0.02–0.04 m/m) showed the best agreement with antidune theory, and reaches at the higher range of step-pool slopes (0.06–0.12 m/m) showed poor agreement with antidune theory, likely as a result of the presence of larger, less mobile roughness elements in these steeper channels (Chin, 1999b).

Mechanisms other than antidunes have also been invoked in explaining step-pool formation. Based on flume and field results, Abrahams et al. (1995) proposed that step-pool features are a channel adjustment to maximize flow resistance, whereby step spacing and geometry evolve to conditions of maximum flow resistance. Many measurements of step-pool geometry, however, do not conform to the conditions suggested by either the antidune or maximum flow resistance hypotheses (Curran and Wilcock, 2005).

Zimmerman and Church (2001) estimated bed shear stresses in a step-pool channel during a high flow (median annual flood) to investigate why channels remain stable during such flows, contrary to predictions based on Shields or similar criteria that high flows should be able to transport large clasts that form the channel boundary. They found that, for estimating bed stresses in step-pool units, pool gradient is more relevant than overall channel gradient, which, when used in the Shields equation, overestimates size of boulders that can be moved by a given flow. They also examined step-pool geometric relations and variations with gradient, concluding that the high variation of

step-pool wavelength, step height, residual pool depth, and pool length that they observed is indicative of the randomness of step location and structure. Zimmerman and Church (2001) found no convincing evidence that special conditions govern the formation of step-pool features or that the spacing of such features is regular. Rather, they suggest that subject to energy constraints that are stricter at higher gradients, step location is determined by the random occurrence of large clasts that behave as keystones for step formation, form hydraulic jumps downstream, and cause scour of downstream pools and expenditure of a large proportion of the stream's energy.

The effects of step-pool morphology on hydraulics were characterized in a field setting by Wohl and Thompson (2000). They indicate that, based on measurement of velocity profiles in East St. Louis Creek, CO, sites downstream from bed steps (where flow over steps plunges into downstream pools) appear to be dominated by wake turbulence from mid-profile shear layers associated with roller eddies. In contrast, sites upstream from steps, at steps, and in runs appear to be dominated by bed-generated turbulence. They suggest that wake-generated turbulence leads to higher energy dissipation in step-pool reaches relative to more uniform-gradient reaches such as runs. Wohl (2000b) further suggests that energy dissipation in steep reaches occurs as a result of flow separation and turbulence generated by bed and wall undulations. Comparison of bedrock and alluvial reaches indicates that as the bed becomes more undulating, proportionally more energy is dissipated within the flow as turbulence and shearing (as in alluvial reaches) rather than being applied to erosion of channel boundaries (as in bedrock reaches) (Wohl, 2000b). Additional studies related to the effects of step-pool sequences on flow resistance partitioning are described below.

2.2 Flow resistance partitioning

Total flow resistance in stream channels can be partitioned into components that are related to specific channel features, and such partitioning has implications for hydraulics, sediment transport, and channel morphology. Resistance partitioning has typically been expressed in terms of bed shear stress, friction slope, or Darcy-Weisbach friction factor. Other variables that are related to flow resistance, including shear velocity, flow depth, or Shields parameter, can be also partitioned into distinct components (Einstein and Barbarossa, 1952; Julien, 1998).

Flow resistance is typically discussed in terms of the resisting force exerted by the boundary on the flow, but it can be equally viewed in terms of drag on the boundary, because these forces must be equal and opposite (Middleton and Southard, 1984). Two kinds of fluid forces act at all points on the boundary: pressure forces, which act normal to the boundary, and viscous shear stress, which acts tangential to the solid surface. The sum of viscous and pressure forces acting on individual roughness elements on the boundary comprises the overall drag on the boundary, or conversely the overall resistance to fluid flow; this boundary resistance equates to boundary shear stress when expressed as average force per unit area (Middleton and Southard, 1984).

Various divisions have been proposed for characterizing flow resistance components in self-formed, alluvial rivers. Many authors suggest a basic separation of total resistance into grain and form resistance components. For example, bed shear stress (τ_b) can be expressed as the sum of grain shear stress (τ_b'), which describes the shear stress acting on particles in the bed, and form shear stress (τ_b''): $\tau_b=\tau_b'+\tau_b''$ (Julien, 1998). Einstein and Barbarossa (1952) were among the first to partition bed resistance,

by dividing hydraulic radius (R) into R that would result in the absence of bed irregularities, where only skin friction was present (R'), and the extra hydraulic radius, compared to the case of skin friction alone, resulting from bed irregularities (R'').

Numerous other types of resistance can be identified, many of which are subsets of the form resistance category. These include internal distortion resistance caused by boundary features that create eddies and secondary circulations, such as bars, bends, individual boulders, bed undulations, and bank outcrops (Leopold et al., 1964); free surface or spill resistance from waves and hydraulic jumps (Leopold et al., 1964; Bathurst, 1993); resistance from woody debris (e.g., Gippel, 1995) and aquatic vegetation (Petryk and Bosmajian, 1975; Nepf, 1999); and drag on sediment particles in transport (Whiting and Dietrich, 1990; Carbonneau and Bergeron, 2000).

The dominant types of flow resistance typically vary depending on channel type and position in the channel network. Prestegaard (1983a) suggested that individual grains create the most resistance in headwater streams, bedforms dominate resistance in mid-reaches of stream networks, and resistance from channel bends increases in importance at lower gradients. Bathurst (1993) noted that resistance is dominated by ponding in step-pool channels, form drag on boulders in boulder-bed channels, bed material and pool-riffle sequences in gravel-bed channels, and transient bedforms in sand-bed channels.

Various components of flow resistance are discussed in more detail below, and methods that have been proposed for measuring or calculating these components are described.

2.2.1 Grain resistance

Grain resistance represents the channel bed roughness that causes energy losses as a result of skin friction and form drag on individual grains in the bed (Einstein and Barbarossa, 1952; Parker and Peterson, 1980). In plane-bed channels, which lack bedforms, total resistance is typically assumed to equal grain resistance, and values for total bed shear stress, shear velocity, Chezy coefficient, Darcy-Weisbach friction factor, and Manning coefficient are equivalent to their grain components (Julien, 1998). Some authors have suggested that grain roughness can be dominant in gravel- and cobble-bed streams (Bray, 1982; Knighton, 1998). Identification of grain resistance contributions can be complicated in coarse-bedded channels where individual particles create substantial form drag (Bathurst, 1993).

Grain resistance is largely a function of relative submergence (d/D_x, where d is flow depth and D_x is a characteristic grain-size scale). The effect of grain resistance is therefore diminished with increasing depth or discharge (Knighton, 1998; Wohl, 2000a), although the proportion of total resistance attributable to grain resistance may increase with increasing stage as other resistance components are drowned out (Parker and Peterson, 1980), as explored further in Chapter 4. Knighton (1998) notes that the rate at which flow resistance decreases (because of a decreasing effect of grain roughness) decreases at higher discharge, and that the rate of change of velocities may also therefore be slower at higher discharges.

Grain resistance is usually approximated by some version of the relation originally proposed by Keulegan (1938) based on the logarithmic law of the wall:

$$\frac{u}{u_*} = \frac{1}{\kappa}\ln\left(\frac{d}{k_s}\right) + 6 = \frac{1}{\kappa}\ln\left(11\frac{d}{k_s}\right) \qquad \text{(Eq. 2.1)}$$

where u is mean velocity, u_* is shear velocity, k_s is roughness height, d is flow depth (used here instead of hydraulic radius), and κ is von Karman's constant and is usually set equal to 0.4.

Many authors have used the Keulegan relation to estimate grain roughness, although little consensus exists on selection of a characteristic scale to represent k_s. Various values have been developed based on flume and field data, including, for gravel-bed rivers, $k_s=1.25D_{35}$ to $k_s=3.5D_{90}$ (Millar and Quick, 1994), $k_s=3.5D_{84}$ and $k_s=6.8D_{50}$ (these values include form roughness, but the author suggests that grain roughness is predominant) (Bray, 1982); and for sand-bed rivers, $k_s=2D_{90}$ (Kamphuis, 1974), a value that was adopted by Parker and Peterson (1980) for use in gravel-bed rivers. Julien (1998) suggests that $k_s=3D_{90}$ is usually a good approximation over a range of stream types.

Estimates of grain resistance using Keulegan-type equations are convenient and widely used because once an appropriate scale for roughness height (k_s) is selected, this method requires only measurements of flow depth (or hydraulic radius in channels with small width-to-depth ratios) and grain size. Characterizing k_s is not straightforward, however, because roughness height may be a function of characteristic scales other than a single representative grain size (e.g., D_{84}, D_{90}) and is influenced by the concentration and sorting of bed roughness elements (Prestegaard, 1983a; Wiberg and Smith, 1991; Gomez, 1993). In addition, because the Keulegan relation (Equation 2.1) is based on the logarithmic law of the wall, using Keulegan-type relations to calculate grain roughness assumes that velocity profiles are logarithmic. Wiberg and Smith (1991) showed theoretically, however, that the logarithmic formula for resistance, with velocity

depending primarily on flow depth and the D_{84} of the vertically oriented axis of clasts, adequately represents mean velocity even in flows with non-logarithmic near-bed velocity profiles and large values of relative roughness. In steep channels, deviations from logarithmic profiles are significant, as discussed further below.

2.2.2 Form resistance

Form resistance arises from drag created by features developed in the bed material (Leopold et al., 1964; Griffiths, 1989; Parker, 2004). This form drag occurs because localized flow separation can create pressure differentials upstream and downstream from objects in the bed, creating a pressure-gradient force that resists flow and causes viscous energy losses downstream from these objects (Tritton, 1988; Roberson and Crowe, 1993). Parker and Peterson (1980) suggest that resistance characteristics of sand and gravel-bed streams are distinguished by bed mobility and bedform type, with dunes dominating form resistance in sand-bed streams (Kennedy, 1975) and pool-riffle structure and its associated bars creating form resistance in gravel-bed streams. In steep mountain channels, form resistance is created by large individual clasts and step-pool sequences. In addition, large woody debris can be an important source of form resistance in all channel types where it is present (Shields and Gippel, 1995; Manga and Kirchner, 2000; Curran and Wohl, 2003). Until relatively recently, most studies of form resistance focused on sand-bed streams, where form resistance is often the dominant component of flow resistance.

Form resistance in sand-bed streams

In sand-bed streams, where the shape of the bed is easily modified, the types and relative importance of form roughness can vary substantially depending on flow conditions (Knighton, 1998). Sand-bed channels are characterized by a progression of bedforms that develop with increasing flow intensity and that produce different levels of flow resistance, including ripples, dunes, washed-out dunes, plane bed, antidunes with standing waves, antidunes with breaking waves, and chutes and pools (Simons and Richardson, 1966). Friction factor values increase as ripples transition to dunes, decrease as dunes are washed out, and remain relatively low until breaking waves develop and cause energy losses (Simons and Richardson, 1966). Form resistance associated with dunes can be particularly large and arises due to expansion losses in the separation zone downstream from dune crests (Engelund, 1966; Julien, 1998), varying as a function of dune steepness, relative dune height, and the Froude number (Julien, 1998). A variety of methods have been developed for estimating resistance due to bedforms in sand-bedded rivers (e.g., Engelund, 1966; Brownlie, 1982; van Rijn, 1984; Wright and Parker, 2004).

Form resistance in gravel-bed streams

The contribution of bar resistance to total resistance in gravel-bed, pool-riffle channels has been evaluated in several studies (Parker and Peterson, 1980; Prestegaard, 1983b; Hey, 1988). Mechanisms that create resistance from bars include expansion losses in the lee of the fronts of bars, formation of antidunes and standing waves on portions of the bars that are near or exceeding critical flow, losses in riffles when the flow is sufficiently shallow that the riffles act as hydraulic controls, and alignment losses at

low flow when flow threads its way through exposed portions of the bars (Parker and Peterson, 1980).

Studies of resistance partitioning in gravel-bed rivers have reached differing conclusions regarding the contribution of bar resistance at high flows. Hey (1988), in a study of 62 sites in the United Kingdom with gradients of 0.0012–0.0215 m/m, found that bar resistance caused 7–86% of total resistance during high flows. Parker and Peterson (1980) concluded, based on analysis of flume data and field data from gravel-bed rivers in Alberta, that bedforms in gravel-bed streams appear to have a minimal effect on total resistance at flow levels associated with dominant discharges, because bar patterns are drowned out, but that bedform (bar) contributions may be substantial at lower stages. Their study adopted a slope-based division for estimating bar resistance, whereby total energy slope consists of energy slope resulting from grain resistance (S_g, calculated using equation 2.1) and energy slope resulting from bar resistance (S_b) (i.e., $S=S_g+S_b$).

Prestegaard (1983b) found that at bankfull discharges, bar resistance accounted for 50–75% of total resistance in 12 gravel-bed reaches with gradients of 0.0012–0.036 m/m, pool-riffle sequences, high width-to-depth ratios, and low sinuosities. In this analysis, grain roughness was estimated using the Parker and Peterson (1980) method, and the remainder of total resistance was assigned to bar roughness. Prestegaard (1983b) suggests that these data support the hypothesis that the stability of channel morphologies at bankfull stage may result in part from an equal partitioning of resistance among the main resistance components. In steeper study reaches where resistance stemmed from turbulence around individual boulders but was assigned to bar resistance, the importance of bar resistance may have been overestimated (Prestegaard, 1983b).

Bedforms other than bars associated with pool-riffle sequences can also create form roughness in gravel-bed streams. Cluster bedforms, consisting of a single obstacle protruding above neighboring clasts, in combination with accumulations upstream and downstream from the larger particle, have been described as the dominant microtopographic feature in gravel-bed rivers (Brayshaw, 1985). Robert et al. (1992; 1996) examined the effects of local transitions in bed roughness from smoother to rougher zones, as occur in the presence of protuberances (analogous to Brayshaw's cluster bedforms). These studies found that at roughness transitions associated with protruding clasts, local boundary shear stress and roughness length substantially increase, and downstream from the transition, near-bed flow velocity decreased (Robert et al., 1992). Roughness transitions were found to dominate the structure of turbulent boundary layers by affecting dominant coherent structures, with sweep motions becoming dominant in near-bed regions over rough surfaces (Robert et al., 1996). These findings support the notion that the dominant mechanism of flow resistance or energy dissipation in gravel-bed rivers may be associated with vortex shedding around large clasts (Robert et al., 1996).

Form resistance in mountain rivers

For evaluating flow resistance in mountain rivers, Bathurst (1985) suggests three scales of roughness: large-scale ($d/D_{84}<1$), intermediate-scale ($1<d/D_{84}<4$), and small-scale ($d/D_{84}>4$) roughness. In cases of large-scale roughness, individual large particles effectively create form resistance, blurring the distinction between grain resistance and form resistance.

Bathurst (1985) examines variations in resistance among mountain rivers and methods of evaluating resistance coefficients in these rivers, including Hey's (1979) semi-log resistance equation. Research by Jarrett (1984) implies that steep channels would have higher velocities and lower flow resistance than would be predicted by semi-log equations, especially in areas of intermediate-scale roughness where non-log velocities would be most pronounced (Bathurst 1985). Bathurst (1985) showed that flow resistance in streams with large-scale roughness, slopes greater than 0.005 m/m, and high Froude numbers was substantially overestimated by the Hey (1979) equation and varied considerably according to the roughness scale and the interaction between resistance components. Bathurst (1985) proposed a modified version of Hey's equation to more closely approximate intermediate and large-scale roughness conditions:

$$\left(\frac{8}{f}\right)^{1/2} = 5.62\log\left(\frac{d}{D_{84}}\right) + 4 \qquad \text{(Eq. 2.2)}$$

although he notes that this equation also contains considerable error.

Jarrett (1984) observed two-part, S-shaped velocity profiles in high-gradient streams. These S-shaped profiles arise where low-velocity flow occurs near the bed, between large boulders, changing fairly abruptly to high-velocity flow above the boulders. Knighton (1998) notes that for a given depth, larger roughness elements (i.e., reduced relative submergence) result in a steeper velocity gradient towards the bed. Byrd et al. (2000) examined velocity profiles measured in a steep (0.034 m/m), cobble-boulder stream (South Boulder Creek, CO), finding that 40% of the profiles were quasi-linear in form, 10% were nearly logarithmic, and the remaining 50% had various forms. Bathurst (1978) notes that in the case of large-scale roughness, the logarithmic velocity profile is disrupted and roughness elements act individually, producing resistance based on the sum

of drag forces around individual objects. Overall resistance in cases of large-scale roughness depends mainly on roughness geometry, which includes the size, shape, spacing and size distribution of large roughness elements, and to a lesser extent on channel geometry (Bathurst, 1978). These results indicate that in the case where large clasts create intermediate-scale and large-scale roughness (Bathurst 1985), velocity profiles are commonly non-logarithmic.

In addition to the effect of individual boulders creating large-scale roughness, form resistance in high-gradient streams can also be generated by step-pool bedforms. Step-pool sequences can create considerable roughness by causing ponding upstream from steps and spill resistance below steps, where plunging flow results in abrupt changes in velocity and dissipation of flow energy. Curran (1999) and MacFarlane (2001) estimated resistance partitioning estimates in step-pool channels in the Washington Cascades. Both authors found that spill resistance created by step-pool bedforms accounted for the largest component of total resistance. Spill resistance is generated by waves and turbulence at locations of sharp velocity reductions (Leopold et al., 1964). Curran's (1999) results are discussed further below in the context of debris resistance. Lee and Ferguson (2002) also examined flow resistance in step-pool streams using flume and field studies, finding that resistance varied strongly with discharge and that equations based on the log law, where k_s was scaled to step D_{84}, performed unexpectedly well in predicting resistance.

2.2.3 Debris resistance

Form resistance created by woody debris can be significant where LWD is present (Gippel, 1995; Shields and Gippel, 1995; Buffington and Montgomery, 1999; Manga and Kirchner, 2000). Young (1991) completed a flume study designed to quantify the hydraulic effects of LWD in lowland rivers, including the assumed flood-control benefits that have been used to justify LWD removal from rivers. Young measured the hydraulic effect in terms of the observed rise in stage upstream from LWD pieces mounted on frames in a flume with a slope of 0.025 m/m. Young examined the relationship between Relative Frontal Area (RFA) of LWD (a measure of obstruction caused by LWD) vs. % Stage Rise (%SR), and he also tested the effects of LWD angle, spacing, diameter, and height above bed on stage. Young observed a large reduction in %SR with streamwise angle (i.e., angled pieces caused a lower %SR than perpendicular LWD), and testing of LWD spacing indicated that %SR increased up to a certain spacing; above which LWD groups acted independently and effects on %SR declined. Young also found that the stage height rise caused by LWD increased with increasing proximity of LWD to the bed. Young concludes that increases in stage height associated with values of RFA that would be typical in lowland rivers are small, but where RFA is unusually high (e.g., large jams or in constricted reaches), increases in stage height are substantial, and LWD removal in these circumstances would improve flood conveyance in lowland rivers.

Woody debris can greatly influence energy dissipation in small to mid-sized high-gradient mountain channels by creating stepped profiles where large amounts of stream energy are dissipated in falls, cascades, hydraulic jumps, and concentrated turbulence sites associated with debris (Keller and Swanson, 1979). Keller and Swanson (1979)

note that in small western Oregon streams, debris influences 30–80% of a stream's elevation loss, and that the relative effect of large woody debris on energy dissipation decreases with channel slope.

Methods have also been developed for calculating form resistance caused by LWD based on the assumption that drag created by woody debris is governed by the same factors as drag on a cylinder, as described further in Chapter 4. One study using this approach, by Shields and Gippel (1995), calculated that in two low-gradient, sand-bed reaches, LWD had accounted for 15–40% and 1–10% of total resistance prior to its removal, with the lower contribution in the latter reach resulting from the greater amount of resistance attributed to bends in that reach.

Manga and Kirchner (2000) examined how LWD affects partitioning of flow resistance using field measurements from a spring-dominated stream, where discharge is nearly constant, combined with simple theoretical models, to quantify effects of LWD on hydraulic resistance at both local and reach-averaged scales. Manga and Kirchner determined the drag force on LWD by attaching springs to the end of a log in the field, observations of the orientation of the stretched springs and the magnitude of spring stretching, and calculations using Hooke's law. They show that the drag force on an individual floating log is the same as the theoretical drag value calculated for widely spaced cylinders at similar Reynolds numbers. They then estimate the partitioning of shear stress between LWD and streambeds, using both simple theoretical models and field measurements of water surface slope. Manga and Kirchner's results indicate that although LWD occupies less than 2% of streambed area, LWD contributes approximately half of total flow resistance. Increasing volumes of LWD result in increases in total shear

stress (via increases in stage) and increases in the contribution of LWD to total stress (Manga and Kirchner 2000).

Curran (1999) conducted field surveys along step-pool channels containing LWD in the Washington Cascades in order to estimate flow resistance contributions from grain, form, and spill components, with LWD contributing to both form and spill resistance. She used the Shields and Gippel (1995) method for calculating form resistance created by LWD pieces and the Millar and Quick (1994) form of the Keulegan equation for calculating grain resistance. Spill resistance was then derived by subtracting grain and form (debris) components from total resistance. This analysis indicated that, on average, grain resistance and form resistance from LWD accounted for less than 10% of total resistance, with the remaining 90% or more being assigned to spill resistance. Curran also indicated that total flow resistance was not correlated with LWD loading or other LWD characteristics. MacFarlane (2001), in a companion study examining resistance in streams without LWD, found lower flow resistances than recorded by Curran, indirectly providing evidence that LWD can substantially increase total flow resistance.

2.2.4 Other sources of flow resistance

Other types of flow resistance include resistance from channel bends, which appears to increase in importance at lower gradients where channels are more sinuous (Leopold et al., 1960), resistance from bank irregularities (Chow, 1959; Knighton, 1998), resistance from aquatic vegetation, modeling of which has employed some of the same methods as are used to evaluate LWD resistance (Nepf, 1999), and flow resistance from sediment in transport, either as suspended load or bedload. Knighton (1998) suggests

that suspended sediment, by increasing viscosity, dampens turbulence and thereby reduces resistance. For example, experiments by Vanoni and Nomicos (1960) found that suspended sediment load could reduce resistance by 5–28%, although the effect of suspended load on flow resistance is likely small in natural streams except at very high concentrations (Knighton 1998). Recent studies, however, have indicated that the effects of suspended sediment on flow resistance are ambiguous; these studies have found that suspended sediment may either amplify or damp turbulence, depending on values of flow variables (e.g., velocity, turbulent-length scale) and sediment transport variables (e.g., particle size, concentration) (Carbonneau and Bergeron, 2000).

Bedload in transport was traditionally believed to increase flow resistance by extracting momentum from the flow and thereby reducing near-bed velocities, with the effect depending on the thickness of the moving bedload layer (Whiting and Dietrich, 1990; Carbonneau and Bergeron, 2000). For example, Wiberg and Rubin (1989) found that momentum extraction by saltating grains was significant, although other data indicate that momentum extraction by saltating grains is minor (Whiting and Dietrich, 1990). Whiting and Dietrich (1990) detected no difference in roughness with transport stage, suggesting that momentum is dissipated by the drag of the bed in a similar fashion whether grains are saltating or the bed is immobile. This occurs because as velocity increases, momentum extraction by the bed increases as a result of increased drag on mobile and immobile grains, with fine sediment moving below the tops of large grains and coarse grains moving slowly enough relative to the fluid that flow resistance is indistinguishable from the immobile-bed case. Carbonneau and Bergeron (2000) found that the effect of adding bedload on turbulence and mean velocity varied between flume

runs with smooth versus rough beds; in two of three flume runs with rough beds, adding bedload resulted in reduced turbulence and increased mean velocity.

Research into the relative contributions of various components of flow resistance to total resistance, and into methods for measuring these components, remains an open and important area of inquiry with implications for discharge estimation and for understanding morphologic and sediment transport dynamics. These topics are explored further in the context of step-pool channels in subsequent chapters.

CHAPTER 3. CONTROLS ON FLOW RESISTANCE IN STEP-POOL STREAM CHANNELS

Abstract

Flow resistance dynamics in step-pool channels were examined through physical modeling using a laboratory flume configured to resemble a step-pool channel. Over 400 flume runs were completed using a factorial design in which variables contributing to flow resistance in step-pool channels were manipulated in order to measure the effects of changes in large woody debris (LWD) configurations, step geometry, discharge, and slope on total flow resistance. Flume experiments documented significant two-way and three-way interaction effects between steps, grains, and LWD, illustrating the complexity of flow resistance in these channels and highlighting difficulties in roughness prediction. In particular, steps and LWD showed a synergistic effect on hydraulics, creating substantially greater resistance in combination than the sum of their contributions individually. Discharge strongly influenced resistance dynamics: it had the largest effect on total resistance of all variables tested and had highly significant interactions with all other variables, thereby mediating the effect of LWD configuration and other factors on resistance. These results suggest that the discharge-dependence of flow resistance conditions is greater in step-pool channels than in lower-gradient systems. Step geometry and LWD density, position on steps, and orientation also had highly significant effects on flow resistance. LWD pieces located near the lip of steps, analogous to step-forming debris in step-pool channels, created substantially higher flow resistance than pieces

located further upstream on step treads, suggesting that LWD position on steps may be more important than overall LWD density in affecting flow resistance.

3.1 Introduction

Step-pool bedforms are ubiquitous in steep, headwater stream channels and provide an important means of energy dissipation in these high-energy systems. Flow resistance is generated in step-pool channels by the form drag of step-forming roughness features, including large clasts and/or logs, and by a tumbling flow regime in which critical or supercritical flow over step crests plunges into downstream pools, where velocity abruptly decreases and hydraulic jumps and roller eddies generate substantial turbulence (Peterson and Mohanty, 1960; Wohl and Thompson, 2000). Sequences of step-pool features occur in channels with gradients of 0.02 to 0.2 m/m (Wohl and Grodek, 1994; Montgomery and Buffington, 1997; Chartrand and Whiting, 2000), resulting in stepped profiles in which elevation loss is concentrated in large steps separated by low-gradient pools (Keller and Swanson, 1979). In confined, steep-gradient streams, where lateral adjustments are not available for dissipating energy (Chin, 1989), step-pool bedforms and the hydraulic resistance they create limit the stream energy available for sediment transport (Heede, 1981) and have been hypothesized to represent a channel adjustment to maximize flow resistance (Abrahams et al., 1995).

Recent research on step-pool channels has had two primary areas of emphasis: (1) descriptions of the morphology of step-pool streams in terms of relationships between step length, step height, grain size, stream gradient, and channel width (e.g., Grant et al., 1990; Wohl and Grodek, 1994; Chin, 1999a; Chartrand and Whiting, 2000), as well as

the variance in these relationships (Zimmermann and Church, 2001); and (2) investigations of processes responsible for the formation of step-pool features, as discussed further below. Many of the previous studies of step-pool channels have focused on channels in which steps are clast-formed and large woody debris (LWD) is absent (e.g., Hayward, 1980; Wohl and Grodek, 1994; Chin, 1999a; Lenzi, 2001; Lee and Ferguson, 2002). Woody debris is prevalent in many step-pool channels, however, and historically may have been much more so prior to widespread LWD removal from stream channels and reduced recruitment of LWD due to timber harvest practices (Bisson et al., 1987; Montgomery et al., 2003). The effects of LWD on hydraulics, sediment transport and storage, channel morphology, and habitat and substrate diversity have been well documented across a range of channel types, but especially in gravel-bed pool-riffle channels (Bilby and Likens, 1980; Lisle, 1986; Robison and Beschta, 1990; Shields and Smith, 1992; Nakamura and Swanson, 1993; Smith et al., 1993; Gippel, 1995; Richmond and Fausch, 1995; Abbe and Montgomery, 1996; Buffington and Montgomery, 1999; Gurnell et al., 2002; Faustini and Jones, 2003).

A subset of these studies has described the effects of LWD on channel morphology and flow hydraulics in steep headwater streams (Keller and Swanson, 1979; Bisson et al., 1987; Lisle, 1995; Curran and Wohl, 2003; Faustini and Jones, 2003). Woody debris, by creating channel obstructions either alone or in conjunction with large clasts, causes formation of step-pool features, sometimes referred to as forced steps (Montgomery and Buffington, 1997), which in turn are responsible for substantial portions of the energy dissipation and elevation loss in steep channels (Keller and Swanson, 1979; Heede, 1981; Curran and Wohl, 2003; Faustini and Jones, 2003).

Studies in the Pacific Northwest indicate that LWD steps are higher, create larger pools and longer low-gradient reaches upstream, and store finer sediment than steps formed only by boulders, resulting in greater variability in channel gradients and bed particle size, greater flow depths, and more widely spaced steps (Faustini and Jones, 2003; MacFarlane and Wohl, 2003). Jackson and Sturm (2002), working in Washington's coast ranges, found that small wood (diameters 10–40 cm) can also be an important step-forming agent in first- and second-order streams with widths <4 m, although pools were often poorly developed below such steps. Comparison of step-pool streams with and without LWD in the Washington Cascades found lower flow resistances in streams without LWD than recorded in LWD streams, providing evidence that LWD can substantially increase total flow resistance (Curran and Wohl, 2003; MacFarlane and Wohl, 2003). In particular, step-forming wood has a much greater influence on flow resistance than wood not incorporated in steps (Curran and Wohl, 2003).

Because manipulation of roughness variables and direct measurement of hydraulic parameters in steep, turbulent streams is extremely difficult, physical modeling using laboratory flume experiments provides an opportunity to isolate and investigate basic processes in these channels. Previous flume studies have examined step-forming mechanisms (Whittaker and Jaeggi, 1982; Grant and Mizuyama, 1992), step spacing (Maxwell and Papanicolaou, 2001; Curran and Wilcock, 2005), pool scour below steps (Comiti, 2003), and flow resistance for step-pool systems without woody debris roughness (Ashida et al., 1986; Abrahams et al., 1995; Maxwell and Papanicolaou, 2001; Lee and Ferguson, 2002). Flume studies have been used to document large variations in resistance with discharge, and observations that velocity consistently increases more

rapidly than flow depth with discharge suggest that driving forces increase more rapidly than form drag in step-pool channels (Lee and Ferguson, 2002). Flume studies have also produced a number of hypotheses about step-forming mechanisms. For example, Whittaker and Jaeggi (1982) used flume studies to theorize that particle sorting, armoring of the bed surface, and formation of antidunes at high (near-critical) flows and under conditions of low sediment supply may give rise to step-pool structures, and Grant and Mizuyama (1992) produced flume results that supported the antidune hypothesis. Based on flume and field results, Abrahams et al. (1995) proposed that step spacing and geometry evolve to conditions of maximum flow resistance. Many measurements of step-pool geometry, however, do not conform to the conditions suggested by either the antidune or maximum flow resistance hypotheses (Curran and Wilcock, 2005).

Previous flume experiments have also investigated LWD dynamics, including debris entrainment and transport (Braudrick et al., 1997; Braudrick and Grant, 2000), the effect of LWD on channel bed scour (Beschta, 1983; Cherry and Beschta, 1989; Beebe, 2000; Wallerstein et al., 2001), the effect of woody debris on stage in lowland rivers (Young, 1991), and drag coefficients associated with various debris configurations, sizes and submergences (Gippel et al., 1992; Wallerstein et al., 2002). Gippel et al. (1992) used force measurements on model LWD to determine how various LWD configuration factors affect drag coefficient (C_D). They found that LWD orientation, blockage effect (the proportion of the flow's cross-section areaal occupied by LWD), and shielding effect (LWD spacing, or density) had the greatest effects on drag, whereas length-to-diameter ratio and LWD depth from the bed had much smaller effects. Young (1991) recorded similar results as Gippel et al. (1992), illustrating the effects of LWD piece orientation

and spacing on percent stage rise upstream from LWD pieces. Wallerstein *et al.* (2002) found that logs positioned near the free surface (i.e., with low submergence values) have drag coefficients that are consistently higher than published values for cylinders because of their contribution to surface wave formation.

These works have collectively provided insights into the hydraulics and morphology of step-pool channels and into the role of LWD in creating flow resistance in lower-gradient channels. Controls on hydraulic resistance in step-pool channels and the hydraulic effects of LWD in these channels are poorly understood, however, reflecting a general lag in research on physical processes in steep stream channels behind related work on lower-gradient channels. Improved understanding of these topics is needed because of the implications of flow resistance dynamics for channel form and stability, sediment transport, and aquatic habitat. Because of the position of step-pool channels in the headwaters of many drainage networks, processes in these channels strongly influence water and sediment discharge to downstream areas, thereby affecting flooding, water supply, reservoir sedimentation, and aquatic and riparian habitat. Further, because stage-discharge relationships are governed by flow resistance, increased understanding of the controls on flow resistance is needed to improve estimates of velocity and discharge in step-pool channels. Existing equations for estimating flow resistance or sediment transport in lower-gradient channels have substantial error when applied to step-pool and other high-gradient systems (Bathurst, 1985; Mussetter, 1989; Jarrett, 1992; Marcus et al., 1992; Yager et al., 2002; Curran and Wohl, 2003). Management concerns in headwater streams, including the impacts of land-use on woody debris loading and the

potential for associated stream restoration efforts, also highlight the need for improved understanding of the role of LWD in step-pool channels.

The study described here used flume modeling to investigate flow resistance dynamics in step-pool channels. By manipulating variables contributing to flow resistance via a series of flume runs, I sought to (1) measure the relative effect of step-pool structures, large woody debris (LWD), non-step-forming grains, discharge, and slope on flow resistance; (2) assess the role of interactions between these resistance components in altering flow resistance dynamics; and (3) measure how variations in LWD configurations affect hydraulic resistance in step-pool channels. This flume experiment was also used to explore the partitioning of resistance in step-pool channels between grains, spill over step-pool bedforms, and debris resistance, as reported in Chapter 4. The results of this work are intended to increase understanding of the role of large woody debris (LWD) and other controls on flow resistance in step-pool channels in order to develop insight into the mechanics and morphology of these channels, to provide guidance for stream restoration and other management concerns in steep channels, and to elucidate how flow resistance dynamics in step-pool channels compare to lower-gradient systems.

3.2 Methods

Darcy-Weisbach friction factor was measured for over 400 flume runs in order to test the effect of numerous variables contributing to flow resistance in step-pool channels, including discharge, grains, steps, slope, and LWD density, orientation, piece length, arrangement, and position. Roughness configurations were manipulated using a series of

factorial experiments in which multiple combinations of variables contributing to resistance were tested, allowing estimates of both the main effects of different variables on flow resistance and of interactions among resistance features.

3.2.1 Flume configuration

The flume study was performed at Colorado State University's Engineering Research Center using a recirculating flume (Figure 3.1) that is 10-m long and 0.6-m wide, with a rectangular cross-section and smooth sidewalls. Flow was delivered to the flume via pipes and pumps from a reservoir of water shared by several flumes, and a cobble-filled baffle was used to dissipate flow energy at the upstream end of the flume. For each flume run, the discharge was set by manually adjusting valves on the pipes delivering water to the flume until the target discharge was attained, as indicated by pressure transducer readings and rating curves to convert pressure to discharge. Five discharges were tested: 4, 8, 16, 32, and 64 L/s. These discharges were selected to represent a range of low-flow to high-flow conditions, resulting in varying relative submergence of roughness features and Froude numbers. Because I sought to examine

Figure 3.1. Side-view photograph of flume, at slope of 0.14 m/m. Flume length is 10 m and width is 0.6 m. Flume is straight; distortion in photograph results from photographic methods.

the effect of a range of flow conditions on flow resistance, exact scaling of Froude number between the flume model and prototype step-pool streams was not applied. Flow for all flume runs was fully turbulent, allowing relaxation of Reynolds number scaling (Peakall et al., 1996). Flume runs were completed at three bed slopes intended to represent the range of slopes found in step-pool channels: 0.05, 0.10, and 0.14 m/m.

In order to simulate step-pool bedforms and to create spill resistance, step-pool sequences were constructed using plywood for the step treads and wood blocks (two-by-fours) for the step risers. Step geometry was scaled to mimic the following geometric tendencies of step-pool sequences observed in nature: (1) many step-pool channels are characterized by step height (H)-step length (L)-bed slope (S) ratios ($H/L/S$) between 1 and 2 (Abrahams et al., 1995; Curran and Wohl, 2003; MacFarlane and Wohl, 2003), a range that has been hypothesized to maximize flow resistance in step-pool channels (Abrahams et al., 1995); (2) H variations with S are limited (Grant et al., 1990; Curran and Wohl, 2003); and (3) L varies inversely with S (Chin, 1989; Grant et al., 1990; Wohl and Grodek, 1994; Wooldridge and Hickin, 2002). By adopting a fixed step height of 0.1 m and decreasing step length from 1.4 m at S=0.05 m/m to 0.5 m at S=0.14 m/m, a consistent $H/L/S$ ratio of 1.4 was achieved for flume runs in which steps were present (Figure 3.2). The $H/L/S$ ratio of 1.4 created a reverse gradient on step treads, whereby flow depths were greatest at the upstream end of each step tread, simulating a pool, and lowest at the downstream end of the step tread, simulating a step lip. In order to isolate the effect of steps on flow resistance, flume runs were also completed with a plane-bed configuration.

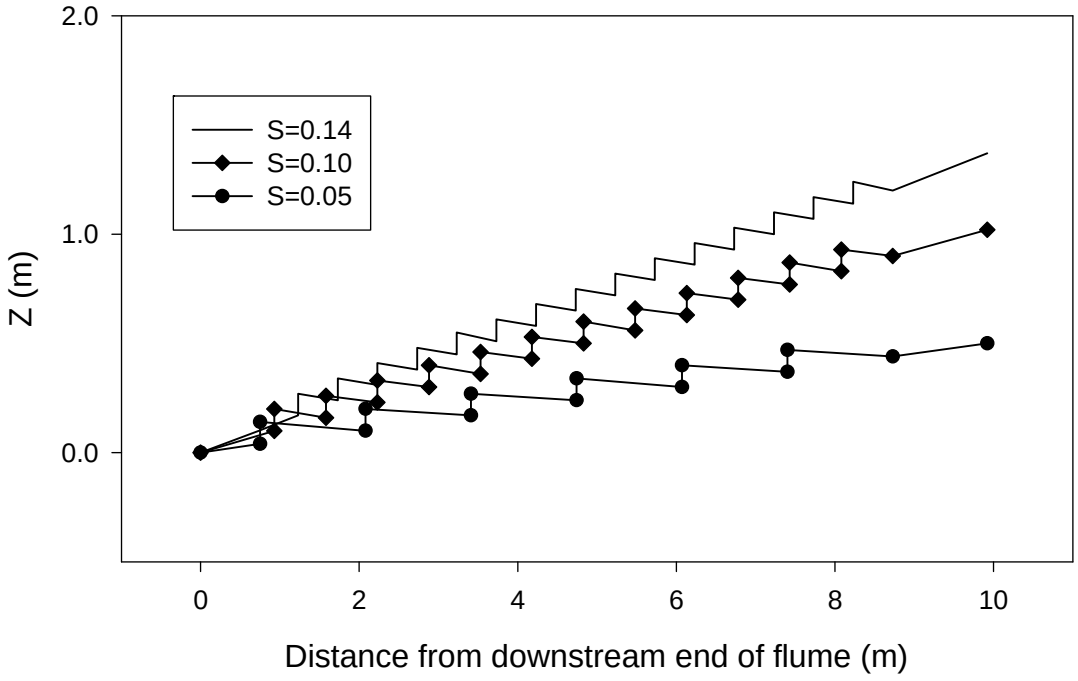

Figure 3.2. Longitudinal bed profiles illustrating step geometry at the three flume slopes tested here. A step height-step length-bed slope (*H*/*L*/*S*) ratio of 1.4 was maintained across the three slopes, with step length increasing as slope decreased and step height held constant.

All flume runs were completed with a non-erodible boundary and no sediment transport. The flume substrate consisted of either smooth plywood or fine gravel glued to the bed of the flume, depending on the roughness configuration being tested. For flume runs incorporating grain resistance, fine gravel with a median size (D_{50}) of 15 mm (D_{84}=22 mm) was glued to the bed of the flume (for plane-bed runs) or the step treads (for step-pool runs). This grain size mixture generally produced relative roughness ratios (D_{84}/d_{bf}, where d_{bf} is bankfull flow depth) within the range of 0.3–0.8 suggested by Montgomery and Buffington (1997) for step-pool channels, although grain size heterogeneity was lower here than in natural step-pool channels because construction materials, rather than large clasts, were used to create steps.

Because investigating the effects of various LWD configurations on flow resistance in step-pool channels was a central objective of this study, numerous woody debris configurations were established by varying LWD density, length, orientation, and arrangement. PVC cylinders (2.5-cm diameter) were fixed to the bed (with steps and grains present) and/or flume walls to represent LWD and debris resistance. LWD densities were set at four levels: high, medium, low, and none. High, medium, and low density LWD configurations corresponded to 10%, 5%, and 2.5% bed coverage by LWD (LWD area/bed area), or 2.3, 1.2, and 0.6 pieces/channel width, respectively. The high-density configuration scales with field results from small streams (<10 m width) within old-growth forests in western Washington indicating average LWD densities of 2.2–2.4 pieces/channel width (Bilby and Ward, 1989).

Three LWD orientations were tested: all pieces perpendicular to flow (Figure 3.3a), all pieces ramped at a 30–45 degree angle from the flume wall (Figure 3.3b), and a combination of perpendicular and ramped pieces (Figure 3.3c). I also tested the effect of three different LWD piece lengths/shapes: long cylinders (0.6 m, equal to flume width) (Figure 3.3a–c), short cylinders (0.3 m, or half the flume width) (Figure 3.4a), and rootwad pieces (short cylinders with 3-way branched PVC junctions attached to the ends to simulate rootwads; Figure 3.4b). Flume tests of three LWD arrangements were also completed: single pieces resting on the bed (Figures 3.3, 3.4), pieces vertically stacked in pairs (Figure 3.5a), and pieces arranged into LWD jams (Figure 3.5b). To create "jams", long and short pieces were interlocked with both perpendicular and ramped orientations. Flume runs for each LWD configuration were repeated at three densities, three slopes,

3.3a

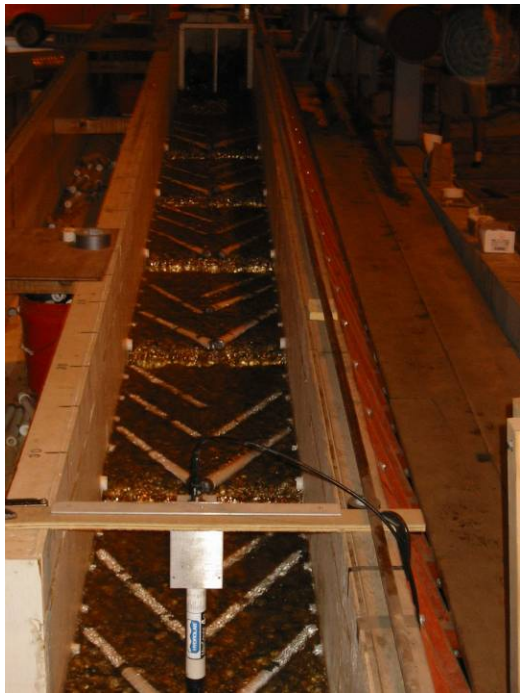

3.3b

3.3c

Figure 3.3. Orientations tested as part of factorial test of the effect of LWD configuration on friction factor; piece length=long: (a) perpendicular (high density, *S*=0.14 m/m), (b) ramped (high density, *S*=0.05 m/m), (c) combination (medium density, *S*=0.14 m/m). Conductivity probe used for salt dilution measurements of velocity is shown in foreground of (b).

3.4a **3.4b**

Figure 3.4. Piece lengths tested as part of factorial test of the effect of LWD configuration on friction factor: (a) short (high density, combination orientation), (b) rootwad (high density, perpendicular orientation). Long pieces were also tested, as shown in Figure 3.3.

3.5a **3.5b**

Figure 3.5. Arrangements tested as part of factorial test of the effect of LWD configuration on friction factor: (a) stacked (high density, perpendicular), (b) jams. Single pieces were also tested (Figures 3.3, 3.4).

and two discharges (8 and 32 L/s; a subset of these runs were completed at all five discharges). The variables tested in the flume are summarized in Table 3.1.

Table 3.1. Variables tested for their effect on flow resistance

Variables (Factors)	**Levels**				
Discharge (L/s)	4	8	16	32	64
Bed slope (m/m)	0.05	0.1	0.14		
LWD density	None	Low	Medium	High	
LWD orientation	Perpendicular	Ramped	Combination		
LWD length	Long	Short	Rootwad		
LWD arrangement	Single	Stacked	Jam		
LWD position	Near-lip	Away from lip			
Steps	Yes	No			
Grains	Yes	No			

LWD pieces were spaced evenly on each step tread, with the number of pieces on each step tread depending on the density, piece length, and step length. Because each short piece covered half as much of the bed as a long piece, twice as many short pieces as long pieces were used to maintain a given LWD density. For example, the high density LWD configuration comprised either 30 long pieces or 60 short pieces distributed over the length of the flume (Figures 3.3a, 3.4a). Because step length varied with slope based on the *H*/*L*/*S* criterion discussed above, with shorter step treads at steeper slopes, the number of pieces per step was proportional to step length, in order to keep densities consistent at different slopes. For example, at the steepest slope (0.14 m/m), two long pieces were placed on each of 15 steps to create the high-density configuration (Figure 3.3a), whereas at the lowest slope (0.05 m/m), five long pieces were placed on each of six steps to create an equivalent high-density configuration (Figure 3.3b). Medium and low

density LWD configurations were achieved by progressively removing the upstream-most pieces on each step tread. LWD pieces were therefore more likely to be located near the step lip at lower-density configurations. Alternate configurations, in which LWD pieces were preferentially positioned further upstream on the step tread rather than at the step lip, were also tested for a small number of runs, as described further below.

3.2.2 Calculation of total flow resistance

Once the particular bed configuration, slope, and discharge of interest were established, total hydraulic resistance for each flume run was measured in terms of Darcy-Weisbach friction factor (*f*):

$$f = \frac{8gRS_f}{V^2} \qquad \text{(Eq. 3.1)}$$

where g=gravitational acceleration (m/s^2), R=hydraulic radius (m), S_f=friction slope, and V=flow velocity (m/s). Reach-averaged velocity (V) was measured using a salt tracer and a Hydrolab Minisonde 4.0 conductivity probe, with salt added to a fixed point at the upstream end of the flume and the passage of the salt pulse over a fixed distance recorded by the conductivity probe at the downstream end. Travel time was determined based on the time difference between salt addition at the upstream end and the conductivity peak at the downstream end, as measured by a synchronized watch and data logger. Five to six repetitions of velocity measurements were carried out for each flume configuration and discharge, and the average of these was used to calculate f_{total} for each run. Flow depth (d) was used in place of hydraulic radius (R) in Equation 3.1, as is appropriate for flume simulations such as this one where the bed is rough but the walls are smooth (Williams, 1970). Average flow depth was back-calculated based on measured discharge and

velocity and the fixed flume width (w) using the continuity equation for discharge ($Q=wdv$). Each subrun lasted as long as necessary for salt concentrations to return to background levels; typically 1–10 minutes depending on discharge. Flow resistance results are expressed here in terms of Darcy-Weisbach friction factor because it is dimensionless, can be partitioned into distinct, additive components (Julien, 1998), and has been recommended for use in open channels (ASCE, 1963). Friction factor can be easily converted to other terms that are also commonly used in analyses of flow resistance, such as Manning's n, boundary shear stress (τ), or $(1/f)^{0.5}$.

The slope term in Equation 3.1 properly refers to friction slope (S_f), which is only equivalent to bed slope (S_o) under conditions of steady uniform flow. Although the flow deviated from steady uniform conditions in the flume on a local basis, I assumed that on a reach-averaged basis, $S_f=S_o$, justifying the use of bed slope (S_o) in calculations of friction factor. To estimate the error introduced by the use of S_o rather than S_f in Equation 3.1, S_f was measured and calculated for a subset of flume runs. Friction slope can be calculated as the change in total head over the length of the flume ($S_f = dH/dx$); total head (H) is:

$$H = z + d + \frac{v^2}{2g} \qquad \text{(Eq. 3.2)}$$

where z is bed elevation, d is local flow depth, and v is local velocity. For calculating H at various positions along the flume's longitudinal profile, flow depths were measured at the center-line of the flume along a longitudinal profile, using a point gage. Turbulence and unsteadiness in the flow caused rapid fluctuations in the water surface elevation in some locations, especially at the base of steps, reducing the accuracy of depth measurements. Local velocity at each position was back-calculated from the measured depth at that position and discharge. Friction slope was then determined based on the

change in H over the length of the flume. This differed from the method used to calculate friction factor (Equation 3.1), where reach-averaged velocity was measured with a salt tracer and flow depths were back-calculated by continuity. Measured S_f values differed from S_o values by less than 5%. The reasonable agreement between S_f and S_o suggests that over the length of the flume, steady uniform flow conditions are approximated and the use of S_o in Equation 3.1 is justified.

Reach-averaged depths based on point-gage measurements were also used, in combination with salt-tracer velocities and the continuity equation for discharge, to develop independent estimates of Q for selected runs. This provided a means of testing the accuracy of the pressure transducer-based discharge measurements. These tests revealed problems with flow calibration at one of the target discharges during one phase of the study. Although the problem was corrected, I was only able to repeat a subset of the compromised flume runs; a small number of other runs were eliminated from future analysis.

Based on the guidelines of Julien (1998) and Williams (1970), no sidewall correction factor was applied to measured friction factor values. Julien (1998) suggests that such a correction is only needed for smooth-walled flumes when the flume width is less than five times the average flow depth, in which case the sidewall resistance is different than bed resistance. For nearly all the flume runs completed here, the width-to-depth ratio was greater than five; the median w:d for all runs was approximately nine. Application of an empirical sidewall-correction equation proposed by Williams (1970) to my flume data suggested that sidewall resistance had small effects on measured friction factors, increasing f from <1–7% (average 3%) compared to the friction factor associated

with bed roughness only. This error was considered small enough that uncorrected *f* values were used in subsequent analysis. These results agreed with Williams' (1970) finding that, in experiments of varying flow depths in a 0.6-m width flume (equal to the width of the flume used here), sidewall effects were nearly or completely absent.

3.2.3 Analytical methods

In order to evaluate the effect of the variables in Table 3.1 on flow resistance, Darcy-Weisbach friction factor was measured for flume runs in a factorial experimental design, in which multiple factor-level combinations of the independent variables were tested. The advantage of a factorial design is that it allows analysis of interaction effects between the variables of interest, in addition to the effects of the variables acting individually (i.e., main effects). Two-way, three-way, and higher-order interaction effects may be present, depending on the number of factors tested. For example, a two-way interaction is present between two variables, or factors, if the difference in mean responses for two levels of a factor varies across levels of the second factor (Ott and Longnecker, 2001). Three-way interactions can indicate that the difference in mean responses for levels of one factor change across combinations of levels of two other factors, or that the pattern of two-way interactions between the first two factors varies across the levels of the third factor (Ott and Longnecker, 2001). Presence of a significant higher-order (e.g., 3-way) interaction indicates that analysis of lower-order (e.g., 2-way) interactions and main effects of factors included in the high-order interaction should account for the potential effect of the high-order interaction.

A series of factorial experiments were completed on subsets of the variables in Table 3.1, allowing investigation of the controls on total resistance and interactions between sources of resistance using the factor-level combinations of greatest relevance to step-pool channels. This approach resulted in a total of 404 flume runs, organized into the following factorial experiments: (1) LWD configuration, in which multiple combinations of LWD density, orientation, piece length, and arrangement were measured at three slopes and two discharges (n=210); (2) LWD position, in which the effect of placing LWD pieces preferentially near step lips or away from step lips was tested for three position configurations at two discharges (n=12); (3) Step-grain-LWD, in which flume runs were completed with and without steps and grains at four LWD configurations, three slopes, and five discharges (n=180); and (4) Step geometry, in which three $H/L/S$ geometries were repeated at four discharges (n=12) (Table 3.2). Certain flume runs were

Table 3.2. Factorial experiments performed to investigate controls on total resistance. In the factor-level combinations column, the number of levels for each factor is shown in parentheses.

Factorial experiment name	Factor-level combinations tested	Number of flume runs	Comments
LWD configuration	Density (3) Orientation (3) Length (3) Arrangement (2) Q (2) S (3)	210	Length and arrangement combined for statistical analyses; steps and grains present
LWD position	LWD position (3) Density (2) Q (2)	10	Tests of effect of proximity of LWD pieces to step lips; steps and grains present
Step-Grain-LWD	Grains (2) Steps (2) S (3) Q (5) LWD density (4)	168	All LWD pieces long-single-perpendicular
Step geometry	Step geometry (3) Q (4)	12	Tests of effect of step height:step length

used in more than one factorial test, causing the sum of the number of runs in these tests to add up to more than 404. Additional detail on each of these factorial experiments is provided in the Analysis section below.

Analyses of variance (ANOVAs) were performed on each factorial experiment in order to examine main effects and interactions between variables, with friction factor as the dependent variable. Log transformations were applied to friction factor values for statistical analyses in order to stabilize variances, although friction factor results are presented below in terms of untransformed values for ease of interpretation. Although analysis of higher-order interactions (4-way and 5-way) was possible for some of the factorial experiments conducted here, the ANOVA models only included main effects, two-way interactions, and, for the LWD configuration test, three-way interaction terms. Higher-order interactions were treated as error because of the difficulty of interpreting the meaning of such high-order interactions, creating a conservative test of variability and significance levels. The relative importance of the flow-resistance variables tested here and of their interactions was evaluated based on the *p*-values and sums-of-squares produced by ANOVAs for each modeled main effect and interaction term. Least-squares means (LS-means) and *p*-values of differences were also calculated for significant terms to elucidate differences between the roughness effects of various factor-level combinations.

3.3 Analysis

In order to facilitate and clarify reporting of the various factorial experiments and statistical tests performed here, the methods, results, and discussion of each grouping of flume runs are combined in the following section.

3.3.1 Overview of combined results

The broad effects of the variations in discharge (Q), slope (S), and bed roughness tested here are illustrated by the wide range in measured friction factors. For runs with steps and grains, f varied by two orders of magnitude, from 0.2 (no LWD, Q = 64 L/s, S=0.05 m/m) to 30 (high density, stacked, perpendicular LWD, Q = 8 L/s, S=0.14 m/m). Friction factors for runs without steps, grains, or LWD (i.e., smooth plane-bed configuration) were substantially lower and less variable; all were between 0.04 and 0.11 over five different discharges and three slopes.

In addition to the factorial experiments listed in Table 3.2, an unbalanced ANOVA combining all flume runs was performed to assess broad patterns of flow resistance. Main effects and two-way interactions among the following factors were tested: Q, S, steps (presence/absence), grains (presence/absence), and LWD (all LWD variables were combined into a LWD presence/absence factor). Several runs were excluded from statistical analysis because of flow calibration problems, resulting in an ANOVA on 388 runs. Although steps, grains, and LWD are included in this model, the effects of these factors under varying discharge and slope conditions, including interaction effects between these factors, were further explored using the more detailed factorial experiments described below and are discussed within the context of those

experiments. Here I focus on the overall effects of discharge and slope on flow resistance.

Discharge had the strongest influence on resistance of all factors tested and was inversely correlated with friction factor (Figure 3.6). Discharge mediated the effects of all other variables by determining the relative submergence of roughness objects on the bed. High discharges tended to drown out differences in f_{total} caused by varying roughness configurations (steps, grains, LWD), resulting in less variance in measured friction factors as Q increased (Figure 3.6; note log scale on y-axis).

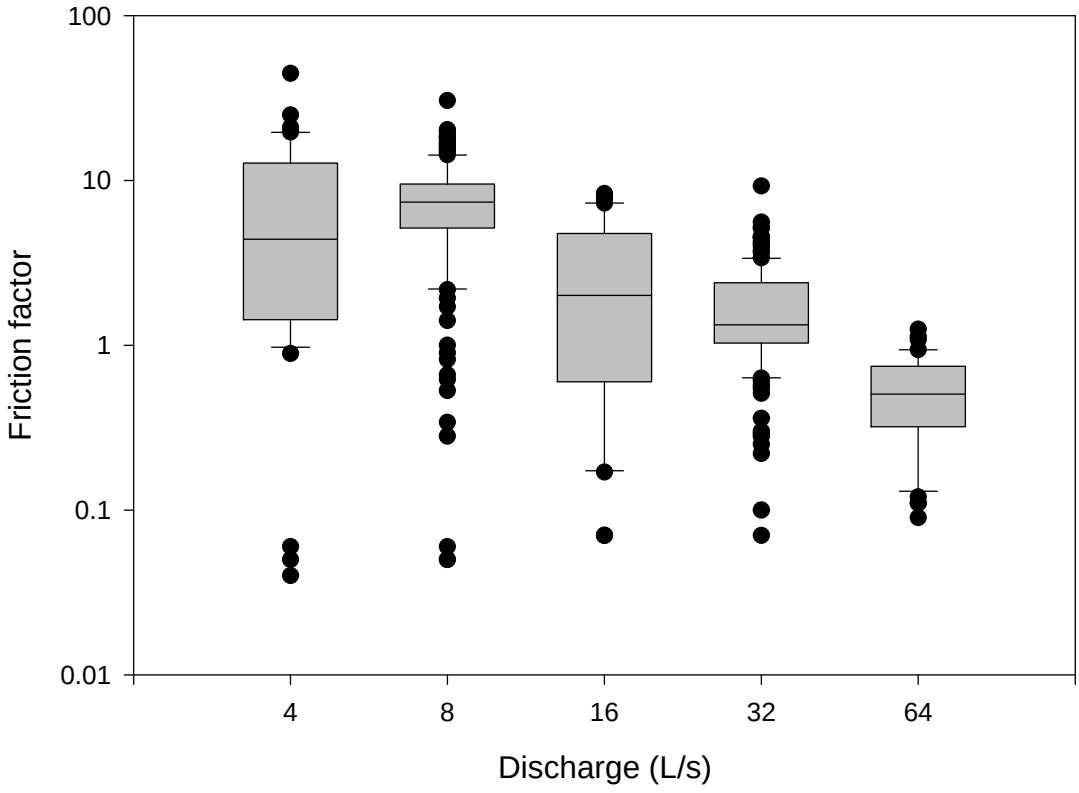

Figure 3.6. Distribution of friction factors (*f*) at different discharge (*Q*) levels for all flume runs, illustrating inverse relationship between *Q* and *f*. The spread in the data (boxes represent 25th–75th percentiles, error bars above and below boxes show 10th and 90th percentiles) reflects the influence of varying bed roughness configurations (LWD, steps, grains) and slopes. For example, all values below *f*=0.1 represent smooth plane-bed runs. Note that the median for 8 L/s is higher than for 4 L/s because the 8 L/s results include many more runs with LWD. The number of runs represented here is as follows: 4 L/s (n=38), 8 L/s (n=146), 16 L/s (n=38), 32 L/s (n=130), and 64 L/s (n=36).

Discharge effects are illustrated by analysis of LS-means, which indicate that the lowest four discharge levels (4, 8, 16, and 32 L/s) produced significantly different friction factors ($p<0.01$), but that the highest two discharge levels (32 and 64 L/s) were not significantly different from each other ($p=0.07$), averaging over all other variables. The mediating effect of Q was measured in terms of interaction effects between discharge and other variables in the factorial experiments discussed below. The effect of slope on friction factor was also significant, although much less so than for other factors. Averaging over other variables, friction factor increased approximately linearly with slope, reflecting the collinearity between slope and friction factor expressed in Equation 3.1.

The sharp decrease in friction factor as discharge increased occurred because velocity increased more rapidly with discharge, on average, than depth (width remained constant). This is illustrated by the at-a-station hydraulic geometry relations (Leopold and Maddock, 1953) for velocity and discharge, which were as follows for all flume runs combined:

$$v=0.073Q^{0.64} \qquad \text{(Eq. 3.3)}$$

$$d=0.022Q^{0.36} \qquad \text{(Eq. 3.4).}$$

The influence of changes in velocity on flow resistance is magnified in terms of friction factor because the velocity term is squared in the Darcy-Weisbach equation, whereas depth varies linearly with friction factor (Equation 3.1).

3.3.2 Effect of LWD configuration on flow resistance

Effect of LWD density, orientation, length, arrangement

The largest factorial experiment performed here was designed to test the effect of LWD configuration, including LWD density, orientation, piece length, and arrangement, on flow resistance with steps and grains present. This factorial experiment comprised 210 flume runs in which friction factor was measured for 36 different LWD configurations, with steps and grains present, at two discharges (8 and 32 L/s) and three bed slopes (0.05, 0.10, 0.14 m/m). The 36 different LWD configurations resulted from combinations of three LWD densities (low, medium, high), three orientations (perpendicular, ramped, combination), and four combinations of length and arrangement variables (long single, short single, long stacked, rootwad single) ("LWD test" in Table 3.2). This analysis is six runs short of a full factorial (36 LWD configurations * 3 slopes * 2 discharges = 216) because one of the LWD configurations (orientation=combination, length-arrangement=rootwad single) was not tested at S=0.14 m/m. Nevertheless, the 210 flume runs described here allowed analysis of both the main effects of LWD variables (density, orientation, length-arrangement) on flow resistance and of how these LWD variables interacted with each other and with discharge and slope.

An initial analysis of subsets of these runs, with the piece length and arrangement variables separated (length = short, long, rootwad; arrangement = single, stacked), suggested that both of these had small effects on friction factor compared to the other variables (Q, S, density, and orientation) and did not show an interaction effect with each other. Length and arrangement were therefore combined into one factor with four levels

to facilitate statistical analysis. Some length-arrangement combinations (e.g., short stacked, rootwad stacked) were not tested.

Statistical analyses of the "LWD configuration" runs were based on a factorial ANOVA model that included main effects and two-way and three-way interactions. This factorial documented numerous two-way and three-way interactions that were significant at α=0.05, particularly between *Q* and other variables (Table 3.3). Significant three-way

Table 3.3. ANOVA results for "LWD configuration" factorial analysis of 210 flume runs, showing main effects, 2-way interactions, and 3-way interactions. Results that are significant at α=0.01 are shown in bold; those that are significant at α=0.05 are shown in italics.

Source	DF	Type III SS	Mean Square	F Value	Pr > F
Main effects					
Q	1	128.05	128.05	3955.9	**<.0001**
Density	2	13.00	6.50	200.7	**<.0001**
Orientation	2	10.59	5.29	163.6	**<.0001**
Slope	2	7.25	3.62	112.0	**<.0001**
Length	3	2.67	0.89	27.5	**<.0001**
2-way interactions					
Q*slope	2	0.91	0.46	14.1	**<.0001**
Q*length	3	1.80	0.60	18.5	**<.0001**
Q*density	2	1.06	0.53	16.4	**<.0001**
Q*orientation	2	0.27	0.14	4.2	*0.0186*
Density*slope	4	1.66	0.41	12.8	**<.0001**
Density*length	6	1.19	0.20	6.1	**<.0001**
Density*orientation	4	0.15	0.04	1.2	0.3408
Length*slope	6	1.79	0.30	9.2	**<.0001**
Orientation*length	6	0.80	0.13	4.1	**0.0011**
Orientation*slope	4	0.06	0.01	0.5	0.7628
3-way interactions					
Q*density*slope	4	0.83	0.21	6.4	**0.0001**
Q*density*orientation	4	0.18	0.05	1.4	0.2318
Q*density*length	6	0.07	0.01	0.4	0.9063
Q*length*slope	6	0.66	0.11	3.4	**0.0047**
Q*orientation*length	6	0.47	0.08	2.4	*0.0317*
Q*orientation*slope	4	0.17	0.04	1.3	0.262
Density*orientation*slope	8	0.68	0.09	2.6	*0.0124*
Density*orientation*length	12	0.93	0.08	2.4	**0.01**
Density*length*slope	12	0.43	0.04	1.1	0.3635
Orientation*length*slope	11	1.04	0.09	2.9	**0.0025**

interactions were observed between the three LWD factors (density*orientation*length-arrangement) and between discharge, slope and LWD factors (Q*density*S, Q*length-arrangement*S, Q*orientation*S, density*orientation*S, orientation*length*S). Many combinations of these variables also produced significant two-way interactions. The presence of significant two-way interactions between Q and all of the LWD factors, as described further below, highlights the extent to which discharge mediated the effects of LWD on flow resistance.

All three LWD variables included in the factorial ANOVA (density, orientation, and the combined length-arrangement variable) had highly significant main effects on f (p<0.0001). Among these variables, LWD density had the highest F value and sum of squares, suggesting that varying the density of LWD affected flow resistance to a greater extent than did varying piece orientation, length, or arrangement. Medium and low densities of LWD resulted in f values 71% and 56% as large as high-density configurations, averaged over all discharges and other variables. Density effects were mediated by discharge, illustrating the highly significant two-way Q*density interaction effect. At high discharges, the relative difference between densities was slightly greater (medium and low densities produced f values 68% and 42% as large as high-density configurations), although the absolute difference was smaller because of the overall damping effect of increasing discharge on flow resistance (Figure 3.7). Slope also mediated the effect of debris density, resulting in a significant S*density effect. The effect of LWD density decreased with decreasing slope, such that at the lowest slope (S=0.05 m/m), no significant difference was observed between medium and high LWD densities. This response likely reflects variation in the number of pieces per step as step

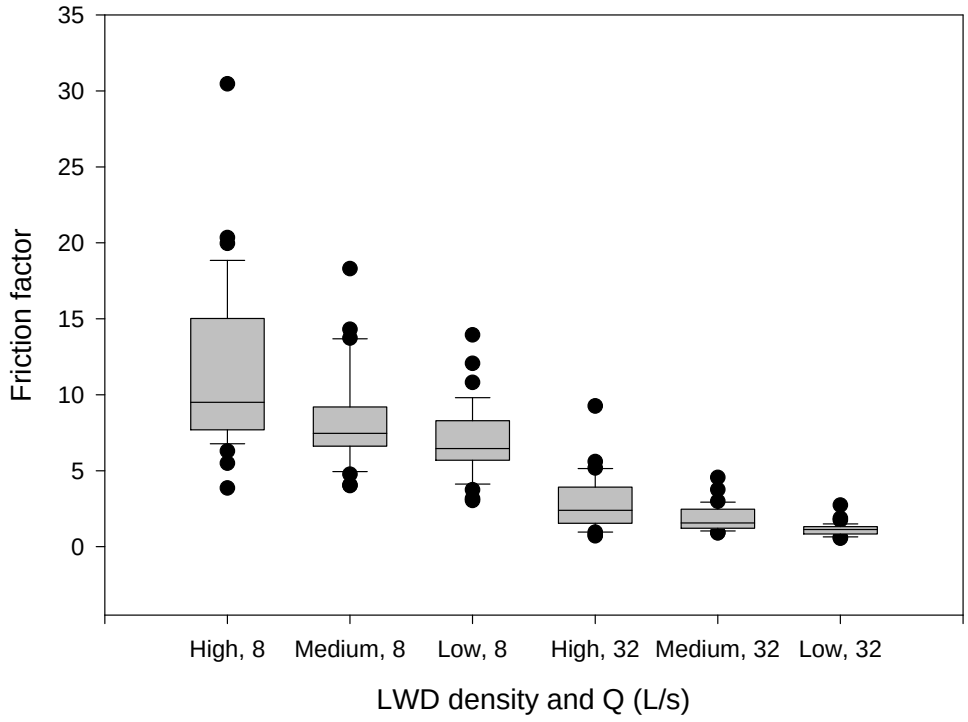

Figure 3.7. LWD density versus friction factor, by *Q*, for 210 flume runs that tested the effect of different LWD configurations on flow resistance.

length varied: at lower slopes, higher densities of LWD result in more pieces being placed on the step tread, where they are less effective, but no change in the number of "step-forming", at-lip pieces.

Debris orientation effects on flow resistance were nearly as large as density effects in the factorial ANOVA. Rotation of pieces 30–40 degrees from the flume wall produced flow resistances that were, on average, slightly more than half of those recorded for perpendicular pieces for all discharges combined. Flume runs with combinations of perpendicular and ramped pieces resulted in friction factors that were intermediate, on average, between perpendicular-only and ramped-only configurations, suggesting a roughly linear relationship between orientation and flow resistance within the range of

30–90 degrees. The slope of this relationship differs with discharge, however; a smaller but still significant orientation effect was observed at higher discharges than at lower discharges, illustrating the *Q**orientation interaction effect (Figure 3.8).

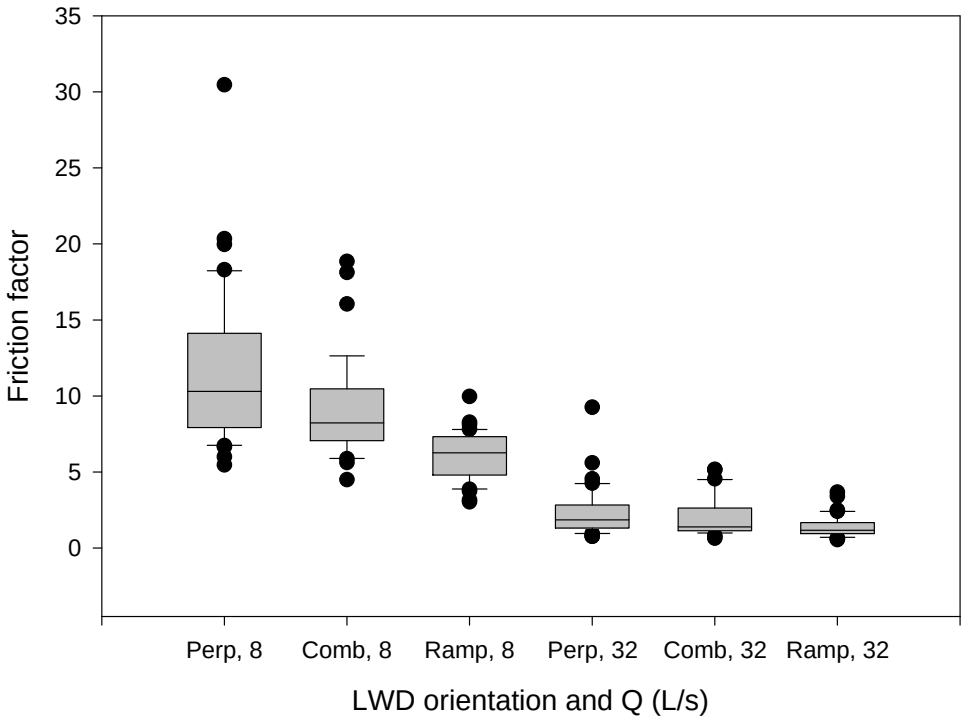

Figure 3.8. LWD orientation versus friction factor, by *Q*, for 210 flume runs that tested the effect of different LWD configurations on flow resistance. LWD orientations include perpendicular ("Perp"), combination of perpendicular and ramped ("Comb") and ramped at 30–45˚ ("Ramp").

The main effect of the combined piece length-arrangement variable was small compared to effects of other factors in this factorial ANOVA, although it was still highly significant (Table 3.3). The piece length-arrangement variable interacted strongly with other variables, however. For example, both discharge and slope strongly mediated the effect of piece length and arrangement on flow resistance, resulting in highly significant *Q**length and *S**length interaction effects and a three-way *Q***S**length effect. The

*Q**length interaction is illustrated by the varying effects of length at high (32 L/s) versus low (8 L/s) *Q*. Although long-single pieces created significantly higher resistance than short-single and rootwad pieces at low *Q* (α=0.05), these configurations had statistically indistinguishable effects on friction factor at high *Q*. Overall, pieces with rootwads affixed produced similar friction factor values as short single pieces. Friction factors associated with rootwad pieces were significantly lower than for long single and long stacked pieces but were not significantly different than those for short single pieces.

Averaging over other variables, vertically stacked pieces created significantly higher resistance than single pieces, although this effect also varied with discharge. Flow resistances created by stacked pieces were not significantly different than those for single (long and short) pieces at low *Q*, but differences between these arrangements were highly significant at high *Q*. This response reflects the ability of stacked pieces to continue to exert considerable drag on the flow at high discharges, because of their greater relative submergence than single pieces, which are drowned out at high flows. Flume runs with stacked arrangements produced the highest friction factors recorded in this experiment at both 8 and 32 L/s (stacked arrangements were not tested at other discharges): *f*=30 for *Q*=8 L/s and *f*=9.3 for *Q*=32 L/s (density=high, length= long, orientation=perpendicular, *S*=0.14 m/m). This configuration, which included stacked pieces at the lip of each step (Figure 3.5a), produced high flow resistances by damming and ponding the flow, thereby reducing velocities and increasing flow depths.

These results build on previous flume and field work in lower-gradient channels regarding the effect of LWD configuration on flow resistance. In terms of the effect of LWD density on hydraulics, somewhat different dynamics were observed here than in

previous studies. Although flow resistance increased with LWD density, under certain conditions changing from medium to high densities of model LWD had no effect on friction factor, suggesting a diminishing density effect. Previous work has also illustrated that once cylinder diameter is sufficiently close (i.e., once density is high enough), wake interference reduces the average drag compared to isolated cylinders. For example, Gippel et al. (1992) found that wake interference took effect at a spacing of less than four cylinder diameters. Diminishing density effects were observed here at much greater spacings, however; my medium and high density configurations corresponded to spacings of approximately 20 and 10 cylinder diameters, respectively. This is likely because in this study, spacing and density effects of LWD were conflated with "position" effects. That is, at higher densities, a greater number of LWD pieces were located further upstream on step treads, where flow depths and relative submergence of LWD pieces were greater because of the reverse gradient of steps in my flume, compared to lower density configurations. Position effects are explored further below, but the key point here is that the diminishing effect of LWD pieces on hydraulics as LWD density increases may take effect earlier (i.e., at wider spacings) in step-pool channels than in low-gradient channels because not all potential LWD positionings along a given step-pool sequence will result in similar flow resistance.

The effects of piece orientation on flow resistance documented here agree with results from lower-gradient flume tests. Earlier flume studies (Young, 1991; Gippel et al., 1992) have expressed the hydraulic effect of LWD in terms of afflux or percent stage rise. These studies found that debris angled 20–40˚ to the flow produced one-third to one-half the afflux produced by perpendicular LWD (Young, 1991; Gippel et al., 1992).

Orientation effects were dampened for more complex shapes designed to more closely approximate real debris (Gippel et al. 1992), however, and field measurements of the drag on model woody debris found that orientation had no significant effect on apparent drag coefficient (Hygelund and Manga, 2003).

Although my flume results suggested that piece length was less important than other variables in affecting friction factor, in natural channels length likely has an important indirect effect on flow resistance via its influence on piece stability. Woody debris pieces that are longer than bankfull width have been found to be more stable than shorter pieces extending only partway into the channel (Lienkaemper and Swanson, 1987; Hilderbrand et al., 1998). This may be even more important in steep, high-energy channels, where channel-spanning pieces may be more likely to contribute to step-pool formation than shorter pieces, although this effect was not modeled here because fixed LWD pieces were employed.

The rootwad configuration, which was also modeled as a component of piece length, was also found not to have a significantly different effect on flow resistance than other configurations. Rootwads were modeled here because of field evidence of the important physical role of rootwads compared to woody debris lacking rootwads (Lienkaemper and Swanson, 1987). Greater rootwad effects may have been observed if rootwads were placed so as to protrude into the center of the flume, rather than flush with the flume walls (Figure 3.4b); the latter configuration was chosen to approximate rootwad arrangements that would be most likely to be stable in steep channels.

Additional LWD configurations

The hydraulic effects of additional LWD configurations that were not part of the factorial experiment described above were also investigated. In tests of the effect of organizing LWD pieces into jams, in which long and short pieces were interlocked with varying orientations (Figure 3.5b), jams did not produce significantly different friction factors than evenly spaced single pieces (including long single, short single, and rootwad configurations), averaging over density, slope, and discharge. For certain discharges, slopes or densities, the flow resistance created by jams was significantly different than one or more of the other length-arrangement configurations. For example, jams resulted in significantly different (lower) friction factors than long stacked pieces at 32 L/s and at high densities, but were not significantly different from stacked or any other configurations at 8 L/s or at medium or low densities. Overall, however, the effect of organizing pieces into jams instead of other length-arrangement combinations was small.

I also completed a series of flume runs to test the effect of LWD position by varying whether pieces were placed near the step lip or further upstream on the step tread, comparing three configurations in terms of proximity of pieces to step lips. These "position" configurations, which employed long single perpendicular pieces at a bed slope of 0.05 m/m, were repeated at two discharges and two densities, creating a factorial test on 10 flume runs (Table 3.2). These tests documented a strong effect ($p<0.0001$) of LWD position on friction factor. Clustering of pieces near step lips produced friction factors that were more than double those observed when logs were clustered further upstream on the step tread, averaging over two discharges and densities (mean f=6.0 for "near-lip" configurations versus mean f=2.5 for "upstream on step tread" configurations).

No significant difference was observed between two different clustering configurations in which no pieces were at the step lip, but the distance from the lip was varied.

These results, in conjunction with the field observations of Curran and Wohl (2003), illustrate the importance of LWD position on flow resistance in step-pool channels. LWD pieces placed near the lip of steps, rather than further upstream along step treads, maximize flow resistance. "Near-lip" pieces create a damming effect, increasing ponding upstream, and interact with step-forming clasts to increase the effective height of steps, thereby increasing the vertical fall over steps and the associated spill resistance as flow plunges into downstream pools. LWD pieces placed further upstream along steps have less interaction with steps and, although they do create some flow resistance on their own, the overall effect is less than the resistance effect introduced by the step-debris interaction.

In natural step-pool channels, near-lip, step-forming LWD pieces are likely to trap other woody debris and to form debris jams, potentially resulting in greater overall stability for the debris formation and having a substantial influence on channel morphology (Keller and Swanson, 1979). Debris jams also have a large effect on physical processes in lower-gradient channels (e.g., O'Connor and Ziemer, 1989; Montgomery et al., 2003). In this context, my finding that organization of LWD pieces into jams did not create significantly different flow resistances than other configurations was unexpected. Although the implication may be that jams do not have a notably different effect on hydraulics and channel morphology than individual step-forming pieces in step-pool channels, it is also likely that failure to adequately capture the complexity of natural debris jams influenced my results.

3.3.3 Effect of steps and grains on flow resistance

Factorial experiments were also completed to evaluate the effect of steps and grains on flow resistance, as well as interaction effects between steps, grains, LWD, discharge, and slope. These experiments entailed completion of flume runs both with and without steps, with and without grains, at four LWD densities (none, low, medium, high), five discharges and three slopes. As discussed above, these tests treated steps as a distinct roughness entity from grains and LWD in order to isolate the resistance effect of steps, even though non-bedrock steps are indeed composed of these elements. Because these tests were intended to test interactions between LWD, steps, and grains, rather than the effect of varying LWD configurations, all LWD pieces in this analysis were long, single, and perpendicular; i.e, LWD length, orientation, and arrangement were kept constant. This resulted in a factorial analysis of 180 flume runs that tested several interactions of interest, including grain*debris, step*grain, and step*debris, as well as expanding the range of discharges evaluated compared to the LWD tests described above. Certain combinations of variables were not tested, resulting in an unbalanced factorial. For example, the configuration with no steps or grains (smooth plane bed) was not tested in combination with LWD, and the plane-bed with grains and LWD configuration was only tested at two of the three slopes. In addition, 12 runs were excluded from the statistical analysis because of flow calibration problems incurred during these runs, resulting in an ANOVA on 168 runs (Table 3.2). The results presented here are based on an ANOVA model containing only main effects and two-way interaction terms. A preliminary analysis including three-way interactions indicated that, although some three-

way interactions between Q and other variables were significant at $\alpha = 0.05$, these terms could be omitted at minimal predictive cost to the model.

These experiments illustrated both the highly significant main effects ($p<0.0001$) of steps and grains on flow resistance and the importance of interactions between steps, grains, and LWD in creating flow resistance. Adding steps substantially increased flow resistance compared to plane-bed configurations; friction factors for plane-bed runs were, on average, approximately 15% as large as step runs for smooth substrates (no grains) and 25% as large as step runs when grains were present. The effect of adding grains was smaller than the step effect; flume runs with no grain roughness (i.e., with smooth plywood substrate) produced friction factors approximately one-third as large as runs with grains for plane-bed configurations and half as large for runs with steps, averaging over other variables. In addition to the step*grain interaction effect ($p=0.0056$) illustrated here, two-way interactions between steps and debris and grains and debris were also significant at $\alpha=0.01$. Analysis of LS-means for the grain*debris interaction, which had the highest significance level of the various interactions between grains, steps, and debris ($p<0.0001$), shows that the effect of grains on flow resistance decreases as LWD density increases. Visual observation of flume runs suggest that this is because at low debris densities, flow depths were insufficient to fully submerge debris pieces at low flow if grains were absent, reducing debris drag, whereas the presence of grains resulted in full submergence of debris pieces at low debris densities. At high debris densities, in contrast, debris drag alone created sufficient flow depths to submerge debris pieces whether grains were present or not. The linkage of the grain*debris interaction to stage also reflects the

presence of a three-way *Q**grain*debris interaction, as was indicated by preliminary statistical tests that included three-way interactions.

The two-way step*debris interaction (p=0.0013) illustrates how the presence of LWD density can increase the flow resistance effect of steps. LS-means (and interaction plots) show that the difference in flow resistance between plane-bed and step configurations is substantially greater for runs with LWD than when LWD is absent (Figure 3.9). This effect is analogous to the "LWD position" effect discussed above, whereby presence of LWD pieces near the lip of steps increases the effective step height and the resulting spill resistance as flow plunges over the steps. The implications of such interactions for roughness partitioning are explored further in Chapter 4.

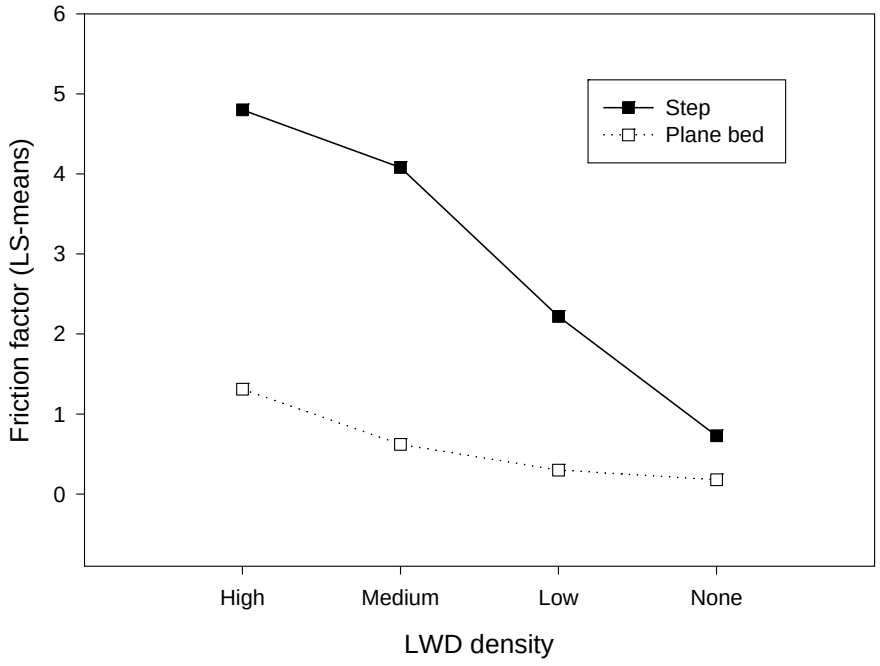

Figure 3.9. Interaction plot of Step*LWD interaction, based on "step-grain-LWD" factorial ANOVA, showing how presence or absence of steps affects momentum extraction by LWD.

A significant two-way interaction between slope and steps was also observed. As slope increased, a greater number of steps were present over the length of the flume, resulting in greater energy dissipation and flow resistance associated with flow overfalls over steps. At lower slopes, step-generated flow resistance (i.e., spill resistance) was reduced. Steps also interacted significantly with discharge. The LS-means for the Q*step and Q*grain interactions, both of which were highly significant (p<0.0001), show that presence of steps or grains had a much greater effect on resistance at low flows than at high flows, further illustrating the effectiveness of high discharge in drowning out bed roughness.

A final set of flume runs tested the effect of step geometry on flow resistance. Whereas the flume runs in the factorial experiments described above maintained a consistent step geometry (H/L/S), based on the scaling criteria described above, in this set of runs step geometry was varied by holding both step height and slope constant and varying step length. Three steps lengths were tested at H=0.1 m and S=0.10 m/m: L=0.5 m, 1.0 m, 1.4 m. The resulting step geometries produced H/L/S values of 2, 1.4 (the standard used in most flume runs here), and 0.7 and H/L values of 0.2, 0.1, and 0.07, respectively. Flume runs comparing these three geometries were completed for four discharges; no LWD was used in these runs. These tests indicated that step geometry highly affects flow resistance (p<0.0001), with more closely spaced steps increasing flow resistance compared to more widely spaced steps, over the range of geometries tested here. The widest step spacing (H/L/S = 0.7) produced only approximately 30% as much flow resistance as the closest step spacing (H/L/S = 2), averaging over discharges (Figure 3.10). More closely spaced steps with shorter step treads result in more frequent overfalls

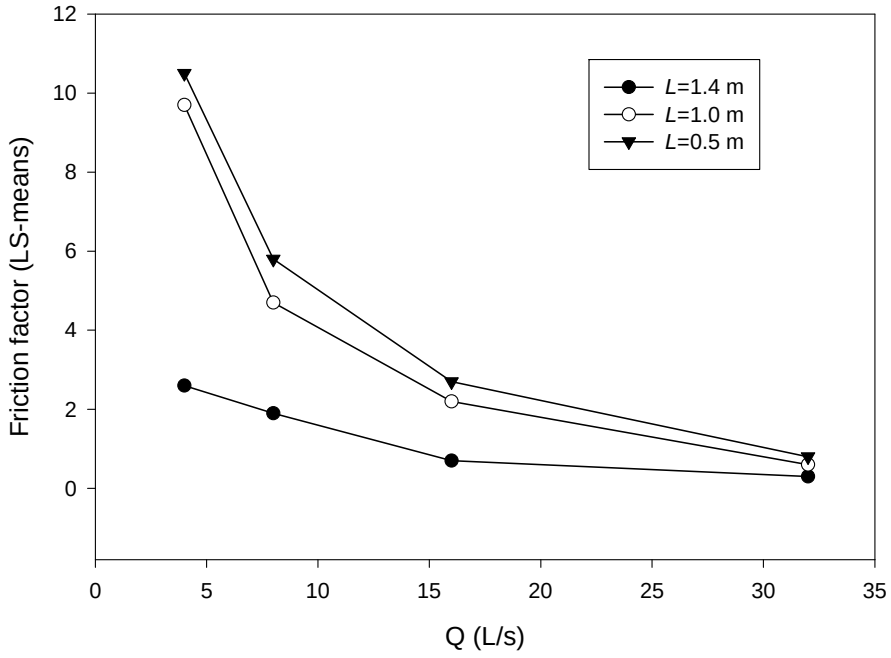

Figure 3.10. Effect of step geometry, illustrating increase in flow resistance resulting from closer step spacing, especially at lower *Q*. Tests were conducted at *S*=0.10 m/m, with *H*=0.1 m.

of flow, increasing flow resistance by creating more spill resistance. The effect observed in the step geometry tests was therefore analogous to the *S**step interaction described above.

These results build on previous flume and field investigations of the effects of step geometry on flow resistance. As noted above, Abrahams et al. (1995) suggested that step-pool channels are adjusted such that step spacing and geometry correspond to conditions of maximum flow resistance, whereby *H*/*L*/*S* values are typically between one and two. I did not measure a large enough range of *H*/*L*/*S* values at multiple slopes to test the maximum flow resistance hypothesis, but my results did show that substantially higher friction factors occurred for *H*/*L*/*S* values in the 1–2 range than for values below this range. These results also agree with MacFarlane and Wohl's (2003) observation of a

significant positive correlation between H/L and flow resistance in step-pool streams lacking LWD. Such a relationship was not observed in LWD-loaded reaches studied by Curran and Wohl (2003). Both of these studies found that $H/L/S$ values were typically between one and two; the mean for non-LWD reaches ($H/L/S$=1.82) was higher than for LWD-loaded reaches ($H/L/S$=1.36) (MacFarlane and Wohl, 2003). Field studies have found that many lower-gradients step-pool channels (S<0.075 m/m) fall outside of the $H/L/S$ = 1–2 range, however, suggesting that as gradient increases, the degree to which steps control energy dissipation increases.

3.4 Discussion

Flume experiments such as this one provide a quantitative basis for analysis of the effects of numerous roughness variables and of their interactions in creating total resistance. Manipulation of roughness variables to the extent that was performed here is infeasible in natural channels, and measurement of hydraulic parameters in steep, turbulent streams is challenging. A novel aspect of this work was the use of a factorial design for documenting interaction effects between roughness variables, which frequently turned out to be important. Although the idea that interaction effects between roughness features are important is intuitive, predictive efforts have typically neglected such interaction effects, and I know of no previous efforts that have measured the importance of interactions between resistance elements.

Interaction effects among roughness features, although not necessarily identified as such, have been observed in step-pool channels in field settings. For example, Keller and Swanson (1979) observed that the relative effect of large woody debris on energy

dissipation decreases with channel slope, in agreement with the two-way LWD density*slope interaction recorded in this flume study (Table 3.3). Step*debris interactions have been observed where large, step-forming boulders create accumulation loci for LWD, thereby creating larger steps that in turn trap finer sediment upstream and alter associated grain roughness (Faustini and Jones, 2003). In wood-rich pool-riffle channels, hydraulic roughness created by LWD and other sources of form drag have been found to cause textural fining, likely by reducing the shear stresses applied to the bed and available for sediment transport (Buffington and Montgomery, 1999).

3.4.1 Discharge effects on flow resistance

The discharge-dependence of roughness conditions, which was illustrated here in terms of highly significant two-way interactions between discharge and bed roughness variables, has also been well documented in field conditions across a range of channel types (Beven et al., 1979; Hayward, 1980; Jarrett, 1992; Bathurst, 2002; Lee and Ferguson, 2002; Heritage et al., 2004) and with respect to resistance associated with LWD (Lisle, 1986; Shields and Smith, 1992; Gippel, 1995). My flume data support Chin's (2003) conceptual model describing the effect of discharge variations in step-pool channels. This model suggests that the role of step-pool sequences varies temporally such that at low flows, when the vertical fall of flow over steps is most pronounced, the effectiveness of steps in reducing stream energy is maximized, whereas flow resistance and energy dissipation decrease as flow increases and the water surface profile flattens (Chin, 2003). The effect of changing discharge on relative submergence and flow resistance patterns in step-pool channels can also be conceptualized in terms of the

difference between nappe flow and skimming flow, which are engineering terms used to describe flow over stepped structures such as spillways (Chanson, 1994). At lower flows, steps produce nappe flow, in which the flow bounces over each step as a series of free-fall jets. Under these conditions, which are most analogous to high-gradient step-pool sequences in which steps are closely spaced, relative submergence of steps is low, allowing the steps and any roughness objects on the step treads to exert considerable drag on the flow and to create high flow resistances. At higher flows, a transition to skimming flow, where water flows become more parallel to a plane between successive step lips (Chanson, 1994), drowns out steps and dramatically decreases flow resistance.

The hydraulic geometry results presented here (Equations 3.3, 3.4) and the similar results of Lee and Ferguson (2002) show that the strong discharge-dependence of flow resistance in step-pool channels is driven by more rapid increases in velocity than in depth with discharge. This effect was exaggerated in the flume results presented here and those of Lee and Ferguson (2002) because a rectangular cross-section channel was employed, forcing changes in discharge to be entirely accommodated by changes in velocity and depth, but not in width. This geometry is a reasonable approximation of natural step-pool channels up to their bankfull level, however, because steeper channels tend to have low width-to-depth ratios and quasi-rectangular cross-sections compared to low-gradient channels. Comparison of my hydraulic geometry results to those reported for lower-gradient systems suggest substantially larger increases in velocity with discharge than in lower-gradient rivers. For example, average exponents reported for rivers in the Great Plains and Southwest for increases in velocity and depth with discharge were 0.34 and 0.40, respectively (Leopold and Maddock, 1953), compared to

0.64 and 0.36 here (Equations 3.3, 3.4). Other studies have confirmed the general pattern of depth increasing somewhat more rapidly than velocity with discharge in lower-gradient systems (Ferguson, 1986).

These results also indicate that the effect of discharge on flow resistance is substantially greater in step-pool channels than in lower-gradient streams. In lower-gradient streams, bed roughness materials are typically entirely submerged even at low flows, and discharge increases produce more subtle increases in relative submergence. Relative submergence of bed roughness features such as LWD and large clasts changes rapidly with discharge in step-pool channels, however, resulting in a strong stage- and discharge-dependence of flow resistance in such channels (Bathurst, 1985; Bathurst, 2002). The transition from a flow regime resembling nappe flow, in which wake-interference flow and turbulence generation at the base of steps produce flow resistance (Wohl and Thompson, 2000), to skimming flow, resulting in marked decreases in flow resistance, as described here and in Lee and Ferguson (2002), is also absent from lower-gradient systems.

3.4.2 Implications for flow resistance prediction in steep channels

The range of friction factors measured here (0.04–44) is at the low end of the range reported for step-pool channels in field studies (0.1–9000) (Beven et al., 1979; Mussetter, 1989; Lee, 1998; Curran and Wohl, 2003; MacFarlane and Wohl, 2003). These field data for the most part represent low-flow conditions; my flume results suggest that analogous friction factor values for high-flow conditions would be substantially lower.

Flume values of friction factor may also be low compared to field values because the complexity of roughness features in step-pool channels was by necessity simplified in my flume model. The treatment of steps as a distinct roughness feature, separate from grains and woody debris and constructed using two by fours, was one key simplification. Although steps in natural channels are composed of large clasts and/or woody debris (with the exception of bedrock steps), steps were treated as distinct features here to facilitate identification of distinct contributions of steps (spill resistance), grains on step treads, and form resistance from woody debris to flow resistance, as well as their interactions. Because this experiment did not treat grains as step-forming agents and sources of form resistance, as discussed in Chapter 4, grain roughness was also oversimplified. Whereas step-pool channels typically exhibit a strongly bimodal grain size distribution, with boulder-sized step-forming clasts and smaller (gravel/cobble) sediments in pools, a relatively narrow range of grain sizes was employed here.

Debris roughness was also oversimplified, given the use of smooth, evenly spaced PVC cylinders of a fixed diameter to represent LWD, three-way PVC junction attachments to represent rootwads (Figure 3.4b), and arrangements of short and long pieces to represent debris jams (Figure 3.5b). Previous flume studies modeling the effects of LWD have also employed smooth cylinders (Young, 1991; Gippel et al., 1992; Braudrick et al., 1997; Wallerstein et al., 2001). In addition, the use of immobile grains, LWD and steps prevented analysis of how feedbacks between increasing discharge and transport of sediment and LWD, including destruction of step-pool sequences and/or pool scour at high flow, would affect flow resistance dynamics. Moreover, because the flume

walls were smooth and straight, bank roughness and channel curvature effects were not modeled here.

Although predictive equations for dependent variables of interest are a common product of flume studies, no such model for flow resistance in step-pool channels is developed here. Condensing the results of my flume runs into a predictive equation for flow resistance, although possible, was not a goal of this study and would have limited applicability to natural channels in light of the design simplifications discussed above and the absence of variables such as step-forming grain size from my flume model.

3.4.3 Implications for stream restoration

Stream restoration efforts have typically focused on pool-riffle channels and have commonly employed LWD placement as a means of promoting pool scour and other habitat objectives (Bisson et al., 1987; Hilderbrand et al., 1997; Larson et al., 2001; Roni and Quinn, 2001). The evidence of the important hydraulic role of LWD in step-pool channels presented here and in field studies suggests that stream restoration efforts incorporating LWD placement may also be merited in steep streams where LWD abundances have been reduced by land-use practices. Restoring LWD in mountain stream channels could, by increasing flow depths and reducing flow velocities, create more complex aquatic habitats, promote sediment storage, promote step formation, and contribute to scour of deeper plunge pools.

Although stream restoration efforts are not typically framed in the context of maximizing flow resistance, many stream restoration objectives, such as creating low-velocity refugia or habitat complexity (Bisson et al., 1987; Brookes and Shields, 1996), are fundamentally related to flow resistance. Attempting to maximize flow resistance in

high-energy steep channels (e.g., through LWD placement) may therefore promote achievement of habitat objectives. Such an approach would be a departure from typical river management practices in low-gradient rivers, which have often sought to minimize flow resistance in order to minimize flood risk and to maximize channel conveyance (Gippel et al., 1992; Gippel et al., 1996). Maximizing resistance in headwater areas, in addition to advancing habitat objectives, could also reduce downstream flood risks by slowing the delivery of high flows to higher-order channels.

The flume results presented here, in conjunction with related field observations cited above, provide guidance for how LWD placement can be employed to maximize flow resistance in step-pool channels. LWD pieces placed near the lip of steps, rather than further upstream along step treads, are especially likely to maximize flow resistance. In "near-lip" positions, LWD pieces interact with step-forming clasts to increase the effective height of steps, creating a damming effect upstream and increasing the vertical overfall into downstream pools and associated pool scour. LWD pieces placed further upstream along steps have less interaction with steps and, although they do create some flow resistance on their own, the overall effect is less than the resistance effect introduced by the step*debris interaction. Increases in LWD density beyond a certain amount are therefore likely to have diminishing effects in terms of flow resistance, although LWD pieces located along step treads likely provide important microhabitats and habitat complexity for aquatic organisms. My results also suggest that vertical stacking of LWD pieces increases flow resistance compared to equivalent distributions of single pieces resting on the bed, although such configurations are unlikely to be stable unless they consist of channel-spanning pieces. Further, the LWD orientation effects documented

here suggest that restoration efforts using pieces oriented perpendicular to flow will maximize flow resistance compared to other piece orientations, although, as with non step-forming pieces, non-perpendicular orientations may be important for habitat diversity. Perpendicular pieces may also trap both coarse and fine sediment, promoting formation of new steps.

Woody debris restoration efforts in step-pool channels may only be effective within a relatively narrow range of channel sizes. Field observations in the Oregon Coast Range suggest that log steps are most common in third-order streams, because lower-order streams are typically highly confined and large fallen trees may remain perched above the channel, whereas higher-order streams have stream power sufficient to remove instream LWD before log steps can fully develop (Marston, 1982). In small headwater channels, relatively small wood (10–40 cm diameter) may be more important in step formation than larger wood (Jackson and Sturm, 2002).

3.5 Conclusions

The flume results reported here provide new insights into controls on hydraulic resistance in step-pool channels. The factorial experimental design employed here allowed measurement of interactions between LWD configurations, steps, grains, discharge, and slope and of the relative importance of roughness variables. Interactions between roughness variables, including significant two-way and three-way interaction effects between steps, grains, and LWD, strongly influenced flow resistance dynamics, highlighting the difficulties of flow resistance prediction in step-pool channels. For example, steps and woody debris combine to create substantially greater flow resistance

than the drag created by these features individually. Flow resistance dynamics and the effect of bed roughness configurations were also mediated by discharge, which had the largest effect on total resistance of all variables tested and had highly significant interactions with all other variables. A discharge-dependence of roughness conditions occurs in many channel types, but the effect appears to be more marked in step-pool channels because velocity increases more rapidly than depth as discharge increases. Step geometry and LWD density, position on steps, and orientation also had highly significant effects on flow resistance. LWD position appears to have a particularly important effect on flow resistance and, in some cases, mediates LWD density effects, where additional pieces located along step treads rather than near step lips have only small incremental effects on flow resistance.

These results suggest that reductions in LWD abundance in mountain channels caused by management activities have likely substantially decreased overall flow resistance in step-pool channels and may have greatly increased the shear stress applied to the bed and available for sediment transport, potentially altering sediment-transport dynamics and aquatic habitat suitability. These changes may have also caused transitions from forced step-pool morphologies to step-pool, step-riffle, cascade, or bedrock morphologies (Montgomery and Buffington, 1997). Management or restoration approaches in headwater stream channels that seek to maximize flow resistance through LWD placement or retention may achieve benefits in terms of sediment storage and aquatic habitat diversity.

CHAPTER 4: FLOW RESISTANCE PARTITIONING IN STEP-POOL CHANNELS

Abstract

In step-pool stream channels, flow resistance is created primarily by bed sediments, spill over step-pool bedforms, large woody debris (LWD), but partitioning between these roughness sources is poorly understood. In order to measure resistance partitioning between grains, steps, and LWD, variables contributing to flow resistance in step-pool channels were manipulated via a series of laboratory flume runs. A factorial design was employed, whereby total resistance was measured for flume runs with and without grains, steps, and LWD, and at multiple slopes, discharges, and LWD configurations. Independent estimates of resistance partitioning were developed using published formulas for grain resistance and a cylinder drag-based approach for calculating debris resistance. In addition, I employed a variety of methods of isolating and measuring resistance components and found that additive partitioning approaches inflate the values of "unmeasurable" components, an effect that is likely especially significant where interactions between roughness features are important, as they are in step-pool channels. Flume measurements indicated that the combined form-resistance effect of LWD and spill over steps dominated total resistance, regardless of the partitioning approach employed, and that grain roughness was a small component of total resistance. The relative contributions of grain, spill, and debris resistance depended on discharge, with debris resistance dominating at higher discharges, and to a lesser extent on debris density, with greater debris roughness at higher debris densities. Cylinder-drag

approaches substantially underestimate debris resistance in step-pool channels because such methods are unable to account for interaction effects between steps and debris, by which woody debris contributes to flow resistance both by increasing the spill effect of steps and by generating form drag.

4.1 Introduction

Total flow resistance in stream channels can be partitioned into components that are related to specific channel features, and such partitioning has implications for hydraulics, sediment transport, and channel morphology. A number of variables that are related to flow resistance, including bed shear stress, friction slope, Darcy-Weisbach friction factor, shear velocity, and flow depth, can be partitioned into distinct components (Einstein and Barbarossa, 1952; Julien, 1998). For example, Darcy-Weisbach friction factor can be partitioned as follows:

$$f_{total} = f_{grain} + f_{form} \quad \text{(Eq. 4.1)}$$

where f_{grain} is friction factor caused by grains in the absence of bedforms, f_{form} is the additional flow resistance created by bedforms or other sources of form drag, and f_{total} is total flow resistance:

$$f_{total} = \frac{8gRS_f}{V^2} \quad \text{(Eq. 4.2)}$$

where g is gravitational acceleration (m/s^2), R=hydraulic radius (m), S_f=friction slope, and V=flow velocity (m/s).

Grain resistance represents the channel bed roughness that causes energy losses as a result of skin friction and form drag on individual grains in the bed (Einstein and Barbarossa, 1952; Parker and Peterson, 1980). In plane-bed channels, which lack

bedforms, total resistance is typically assumed to equal grain resistance (i.e., $f_{total}=f_{grain}$) (Julien, 1998). Where bedforms or other sources of resistance may be present, grain resistance is usually approximated by some version of the relation originally proposed by Keulegan (1938) for calculating the resistance created by a rough bed alone and based on the logarithmic law of the wall. The Keulegan relation can be expressed in terms of friction factor as follows:

$$f_{grain} = \left[2.03 \log\left(\frac{12.2d}{k_s} \right) \right]^{-2} \qquad \text{(Eq. 4.3)}$$

where f_{grain} is the grain resistance component of Darcy-Weisbach friction factor, d is flow depth, and k_s is roughness height (modified from Einstein and Barbarossa, 1952). Roughness height is often expressed as mD_x, where m is a coefficient that typically ranges from 1 to 7 and D_x is some characteristic grain size (usually D_{50}, D_{84}, or D_{90}) (Kamphuis, 1974; Bray, 1982; Millar and Quick, 1994; Julien, 1998). Grain resistance in the Keulegan relation is therefore a function of relative submergence of bed particles (d/D_x).

Form resistance arises from pressure drag on irregularities of the bed surface that create flow separation (Leopold et al., 1964; Griffiths, 1989; Parker, 2004). The relative importance of grain versus form resistance and the dominant sources of form resistance typically vary depending on channel type and position in the channel network. Bedforms, including dunes and other transient bedforms in sand-bed channels and bars and pool-riffle sequences in gravel-bed streams, can dominate resistance in mid-reaches of stream networks, and resistance from channel bends increases in importance at lower gradients (Leopold et al., 1960; Leopold et al., 1964; Parker and Peterson, 1980;

Bathurst, 1993). In addition, large woody debris can be an important source of form resistance in all channel types where it is present (Shields and Gippel, 1995; Manga and Kirchner, 2000; Curran and Wohl, 2003).

In this paper I investigate the partitioning of flow resistance in step-pool channels. For the purposes of this study, three main types of flow resistance in step-pool channels were identified: spill resistance, debris resistance where large woody debris (LWD) is present, and grain resistance, where:

$$f_{total} = f_{grain} + f_{spill} + f_{debris}. \qquad \text{(Eq. 4.4)}$$

Spill resistance is generated by waves and turbulence at locations of sharp velocity reductions (Leopold et al., 1964) and may be particularly important in step-pool channels as a result of the tumbling flow over steps that characterizes these channels. Field studies of resistance partitioning in step-pool channels in the Washington Cascades suggested that spill resistance accounts for 90% or more of total resistance in step-pool channels containing LWD (Curran and Wohl, 2003).

Studies of lower-gradient systems have found that flow resistance created by woody debris can be significant (Gippel, 1995; Shields and Gippel, 1995; Buffington and Montgomery, 1999; Manga and Kirchner, 2000). For example, Manga and Kirchner (2000) used field measurements and simple theoretical models to show that in a spring-dominated stream in which LWD occupies less than 2% of streambed area, LWD contributes approximately half of total flow resistance. Shields and Gippel (1995) calculated that in two low-gradient reaches, LWD had accounted for 15–40% and 1–10% of total resistance prior to its removal, with the lower contribution in the latter reach resulting from the greater amount of resistance attributed to bends in that reach. Woody

debris has also been found to have a significant effect on physical processes in step-pool streams where it is present (Keller and Swanson, 1979; Lisle, 1995; Curran and Wohl, 2003; Faustini and Jones, 2003). The role of LWD has been largely neglected in the literature on step-pool channels, however; most previous studies of step-pool channels have focused on systems where LWD is absent (Hayward, 1980; Wohl and Grodek, 1994; Chin, 1999a; Lenzi, 2001; Lee and Ferguson, 2002).

This work seeks to increase understanding of interactions between hydraulic driving forces and the resisting forces created by roughness elements such as step-pool sequences and LWD in steep channels. These topics are poorly understood, hindering advances in analyses of flow, channel form, and sediment transport processes in step-pool channels and of how steep channels are different from the low-gradient channels upon which much fluvial geomorphic knowledge is based. In particular, this study investigates the contribution of LWD to hydraulics and flow resistance in these channels, which may in turn shed light on forestry management issues and on how widespread reductions in LWD abundance in headwater streams have altered the hydraulics of these channels.

In this paper the partitioning of flow resistance in step-pool channels is investigated using flume modeling in which flow resistance is measured both for isolated components of flow resistance and for multiple bed roughness combinations. Estimates of the fractional contributions of grain, spill, and debris resistance to total resistance are developed, and the effects of discharge, slope, and LWD density on partitioning are tested. The flume modeling is also employed to test errors associated with standard methods for quantifying resistance partitioning, whereby resistance is assumed to be additive and resistance components that are difficult to measure are indirectly estimated

by subtraction from measurable terms. Finally, independent estimates of resistance partitioning are developed, using published equations for grain resistance and cylinder drag-based estimates of debris resistance, for comparison to flume results.

4.2 Methods

4.2.1 Flume configuration

I investigated the partitioning of flow resistance in step-pool channels using flume measurements of Darcy-Weisbach friction factor (f_{total}) and a factorial design that allowed isolation and measurement of the relative contributions of flow resistance from grains (f_{grain}), spill over steps (f_{spill}), and woody debris (f_{debris}). This was achieved by completing a series of flume runs in which f_{total} was measured for bed configurations with and without grains, steps, and debris at various slopes and discharges, altering one of the independent variables contributing to flow resistance at a time and holding others constant. Total flow resistance (f_{total}) was calculated using Equation 4.2 and flume measurements of reach-averaged velocity (based on salt dilution), flow depth, and bed slope (see Chapter 3 for further details).

The flume study was performed at Colorado State University's Engineering Research Center using a flume that is 10-m long and 0.6-m wide, with a rectangular cross-section and smooth sidewalls. Flume runs were completed at three slopes intended to represent the range of slopes found in step-pool channels: 0.05, 0.10, and 0.14 m/m, and at five discharges selected to produce varying relative submergence of roughness features and Froude numbers: 4, 8, 16, 32, and 64 L/s. A relatively uniform mixture of grain sizes (D_{50}=15 mm, D_{84}=22 mm) was glued to the bed in order to create grain

roughness without any sediment transport. In order to simulate step-pool sequences and to create spill resistance, step risers and treads were constructed using wood blocks (two-by-fours) and plywood. Step-pool sequences were constructed with a step height (H)-step length (L)-bed slope (S) ratio ($H/L/S$) of 1.4 (Abrahams et al., 1995), creating a reverse gradient on each step tread. PVC cylinders (2.5-cm diameter) were fixed to the bed and/or flume walls to represent LWD and debris resistance. A total of 220 flume runs, reflecting combinations of resistance from grains, steps, and debris at multiple slopes and discharges, were performed for the partitioning analysis presented in this paper. Additional flume runs were also performed for a companion component of this flume study that examined controls on total flow resistance and the effect of a range of different LWD configurations, which were established by varying LWD density, length, orientation, and arrangement, on flow resistance (Chapter 3). The paper describing that study provides additional details on the flume configuration used here (Chapter 3).

4.2.2 Test of additive partitioning approach

Many studies of resistance partitioning employ the same basic method, whereby total resistance is divided into 1) one or more components that can be measured or calculated, and 2) a component that is difficult to measure directly using existing methods. The difficult-to-measure component, which is often the focus of the particular study, is estimated by measuring total resistance (using Equation 4.2 or an analogous resistance equation) and subtracting the measurable components. This approach is based on the premise that flow resistance is additive (Einstein and Barbarossa, 1952), such that:

$$f_{total} = f_{measurable} + f_{unmeasurable} \quad \text{(Eq. 4.5a)}$$

$$f_{unmeasurable} = f_{total} - f_{measurable}. \quad \text{(Eq. 4.5b)}$$

Because direct measurement of form resistance is difficult, previous analyses of resistance partitioning have often employed this additive approach to quantify the relative contributions of form resistance and grain resistance (Einstein and Barbarossa, 1952; Parker and Peterson, 1980; Prestegaard, 1983b; Curran and Wohl, 2003; MacFarlane and Wohl, 2003). Grain resistance is treated as the measurable component, calculated using Equation 4.3 or an analogous expression based on relative roughness, and form resistance is the unmeasurable component, calculated as the leftover value in Equation 4.5b (*Form resistance = Total resistance – Grain resistance)*. This additive approach has been used to quantify bar resistance in gravel-bed rivers (Parker and Peterson, 1980; Prestegaard, 1983b), spill and debris resistance in step-pool channels (Curran and Wohl, 2003; MacFarlane and Wohl, 2003), resistance to overland flow (Hu and Abrahams, 2004) and resistance associated with bedload transport (Gao and Abrahams, 2004).

For example, estimates of resistance partitioning between grains, spill, and form drag from LWD in step-pool channels were developed by Curran and Wohl (2003) using this additive approach. A form of the Keulegan equation was used to calculate grain resistance, a method developed by Shields and Gippel (1995) for calculating form resistance created by LWD pieces was used to calculate debris resistance, and f_{total} was measured for a series of stream reaches using surveys of reach-average slope, hydraulic radius or depth, and velocity. Spill resistance, which was treated as the "unmeasurable" component, was then derived by subtracting grain and form (debris) components from total resistance:

$$f_{spill} = f_{total} - f_{grain} - f_{debris}. \qquad \text{(Eq. 4.6)}$$

Many of the studies employing this approach have achieved a similar result: the unmeasurable, or "leftover" component is estimated to be the largest contributor to total flow resistance (Einstein and Barbarossa, 1952; Prestegaard, 1983b; Curran and Wohl, 2003; MacFarlane and Wohl, 2003). The consistency of these findings, regardless of whether the leftover value represents bar resistance, spill resistance, or some other component of flow resistance that is difficult to measure, suggests that the additive method may at least partly predetermine the outcome and inflate the values of any leftover term(s). Whereas the additive approach assumes that resistance components are isolated, combinations of resistance components often produce interaction effects that can substantially increase total resistance, as discussed in Chapter 3. Any additional flow resistance resulting from such interaction effects is assigned to the unmeasurable components, potentially inflating their value. Further, the leftover or unmeasurable terms are sensitive to any error in calculations of the terms on the right side of (5b).

I tested the sensitivity of partitioning estimates to the additive method by calculating grain, spill, and debris resistance using various "orderings". I took advantage of the factorial design employed here, in which friction factor was measured for numerous combinations of grains (presence/absence), steps (presence/absence), and model LWD (multiple configurations), to calculate resistance components using four separate "orderings," as follows:

1) grains, then steps, then debris ($f_{grain} + f_{spill} + f_{debris}$)
2) grains, then debris, then steps ($f_{grain} + f_{debris} + f_{spill}$)
3) steps, then grains, then debris ($f_{spill} + f_{grain} + f_{debris}$)

4) steps, then debris, then grains ($f_{spill} + f_{debris} + f_{grain}$)

Values of f_{grain}, f_{spill} and f_{debris} calculated by these four methods and values of their fractional contribution to f_{total} could then be compared. Additional potential ordering combinations, in which debris was measured first in the absence of steps or grains, followed by addition of steps and grains, were not tested.

For Method 1, in order to measure grain resistance, Darcy-Weisbach friction factor (f_{total}) was measured for flume runs with a plane-bed configuration (only grains on the bed and no steps or debris) at three slopes and five discharges (Figure 4.1a). Adopting the assumption that

$$f_{total} = f_{grain} \qquad \text{(Eq. 4.7)}$$

for these run produced 15 different f_{grain} values, although one slope-discharge combination (S=0.05 m/m, Q=32 L/s) was eliminated from subsequent analysis because of flow calibration problems. A simple optimization procedure was then applied to determine values of roughness height (k_s) in Equation 4.3, for various slopes and discharges, such that Equation 4.3 would calculate the friction factor values measured in the flume for these 14 plane-bed runs. The resulting values of k_s ranged from 0.06 to 0.12 m, or 2.6-5.4*D_{84}. These values were used in Equation 4.3 to calculate f_g for subsequent flume runs with steps and debris present, producing values of f_g that vary with the ratio of flow depth to characteristic grain size, according to Equation 4.3. This approach was designed to measure the grain resistance contribution from grains on step treads, rather than the form resistance created by large, step-forming clasts in step-pool channels.

Next, spill resistance values were calculated by measuring f_{total} for runs with steps and grains (but no debris) at three slopes and five discharges (Figure 4.1b) and then subtracting out the grain resistance values derived using (3) for each of those runs:

$$f_{spill} = f_{total} - f_{grain}. \qquad \text{(Eq. 4.8)}$$

This method produced f_{spill} values for each of 14 slope-discharge combinations. These f_{spill} values were then carried over and applied to subsequent runs in which model LWD was added.

Third, debris resistance was calculated by measuring total resistance for 102 runs with steps, grains, and debris. These runs comprised various combinations of different woody debris configurations, including three densities (low, medium, high), two lengths (long and short), two orientations (perpendicular and ramped at a 30–45 degree angle from the flume wall), and two arrangements (single and stacked). Configurations with long, single, perpendicular pieces (Figure 4.1c) were tested at five discharges, and other configurations were tested at two discharges (8 and 32 L/s). All configurations were repeated at three slopes. To derive values for f_{debris}, for each of these runs, Equation 4.4 was rearranged as follows:

$$f_{debris} = f_{total} - f_{grain} - f_{spill}. \qquad \text{(Eq. 4.9)}$$

Values for f_{grain} were calculated using Equation 4.3 and the k_s values I determined based on plane-bed runs, and values for f_{spill} from Equation 4.8 were carried over for specific slope-discharge combinations. Using this additive approach, I determined the fractional contribution of f_{grain}, f_{spill}, and f_{debris} to f_{total} for 99 runs (3 of the 102 runs were eliminated because of flow calibration errors), representing an array of discharges, slopes, and LWD densities, orientations, lengths, and arrangements.

4.1a **4.1b** **4.1c**

Figure 4.1. Flume configurations used in partitioning analysis: (a) plane-bed configuration, where $f_{total} = f_{grain}$; (b) steps with grains configuration, shown with Q=8 L/s at S=0.14 m/m, where $f_{spill} = f_{total} - f_{grain}$ (Method 1); (c) steps with grains and LWD (density=high, orientation=perpendicular, length=long) configuration.

Whereas in Method 1, total resistance was partitioned by calculating f_{grain}, then f_{spill}, then f_{debris}, for Method 2, I calculated f_{grain}, then f_{debris}, then f_{spill}. For Method 2, grain resistance was determined as in Method 1, based on plane-bed with grain runs and Equation 4.3. Next, f_{total} was measured for plane-bed with LWD runs, in which long-single-perpendicular pieces were added at different densities (Figure 4.2a). These tests were completed at four discharges and two slopes. Based on these runs, f_{debris} was calculated for multiple slope-discharge combinations as:

$$f_{debris} = f_{total} - f_{grain}. \qquad \text{(Eq. 4.10)}$$

Finally, for runs with steps, grains, and LWD (Figure 4.1c), spill resistance was calculated as the leftover value using Equation 4.6. Because f_{debris} values from plane-bed runs could only be carried over to subsequent step runs with the same LWD configurations (long-single-perpendicular, at two slopes), Method 2 comprised a total of only 24 runs.

For Method 3, I calculated f_{spill}, then f_{grain}, then f_{debris}. Flume runs with smooth plywood steps (no grains, no debris) (Figure 4.2b) were completed at three slopes and five discharges, where:

$$f_{total} = f_{spill}. \qquad \text{(Eq. 4.11)}$$

These "step without grain" runs, which can be viewed as analogous in some respects to bedrock step-pool sequences, were used to determine baseline values of spill resistance at each slope and discharge. Grain resistance was then calculated by measuring total resistance for "step with grain" runs, in which grains were glued to the step treads, and

4.2a **4.2b** **4.2c**

Figure 4.2. Flume configurations used in partitioning analysis: (a) plane-bed with LWD (density=high, orientation=perpendicular, length=long) configuration, where $f_{debris} = f_{total} - f_{grain}$ (Method 2); (b) steps without grains configuration (S=0.14 m/m), where $f_{total} = f_{spill}$ (Methods 3 and 4); (c) steps without grains, with LWD configuration, where $f_{debris} = f_{total} - f_{spill}$ (Method 4).

then subtracting out the baseline spill resistance value determined using Equation 4.11 for a given slope and discharge:

$$f_{grain} = f_{total} - f_{spill}. \qquad \text{(Eq. 4.12)}$$

Finally, friction factor was measured for runs with steps, grains, and model LWD, and f_{debris} was calculated as in Method 1 (Equation 4.9), for the same 99 runs. Methods 1 and 2 result in different estimates of f_{grain} and f_{spill}, but produce the same estimates of f_{debris}, because f_{debris} is in both cases calculated as the remainder or leftover value.

Method 4 employed a similar procedure, starting with smooth steps and calculating f_{spill} as in Method 3; then adding long, single, perpendicular debris to smooth steps (Figure 4.2c), at three densities, four discharges, and three slopes; and finally calculating f_{grain} as the leftover value in runs with steps, grains, and LWD. Method 4 comprised 36 runs.

Among the four ordering methods described above, I further explored the results of Method 1 in terms of how the observed partitioning dynamics (i.e., fractional contributions of f_{grain}, f_{spill}, and f_{debris}) varied with discharge, slope, and LWD density. Analyses of variance were performed to assess the main effects and two-way interactions between the independent variables (Q, S, and LWD density) on % f_{grain}, % f_{spill}, and % f_{debris}. A more detailed analysis of the controls on total resistance is presented in Chapter 3.

4.2.3 Grain resistance calculations

As discussed above, studies of flow resistance partitioning have typically calculated grain resistance using empirical and/or theoretically based equations. For

comparison with my flume-derived f_{grain} values, I also calculated f_{grain} using two published equations for grain resistance, both of which are based on some measure of relative submergence (d/D_x) (Parker and Peterson, 1980; Bathurst, 2002). The equation of *Parker and Peterson* (1980), which employs a variation on Equation 4.3, was developed for gravel-bed rivers and can be expressed as:

$$f_{grain} = 8 * \left[2.5 \ln\left(\frac{11d}{2D_{90}} \right) \right]^{-2} \qquad \text{(Eq. 4.13)}$$

where k_s=2D$_{90}$ (after Kamphuis, 1974) and represents grain resistance only.

I also tested a power-law relationship developed for calculating bed grain roughness, including form roughness created by large clasts and skin friction, in steep (S<0.008 m/m) channels (Bathurst, 2002). The Bathurst (2002) equation does not assume a logarithmic velocity profile and can be expressed as follows:

$$f_{grain} = 8 * \left[3.1 \left(\frac{d}{D_{84}} \right)^{0.93} \right]^{-2} . \qquad \text{(Eq. 4.14)}$$

These equations were applied to 154 flume runs with grains glued to the bed, including both plane-bed and step runs and representing a range of Q, S, and LWD configurations. To solve Equations 4.13 and 4.14, I used flow depths for each flume run and D_x values determined from sieving of the sediments used in the bed of the flume to represent grain roughness, where D_{84}=22 mm and D_{90}=23 mm.

4.2.4 Cylinder drag calculations of debris resistance

In addition to the flume-measured values of debris resistance developed using the additive approaches described above, f_{debris} was calculated based on calculations of form

drag associated with woody debris. This approach is referred to here as the "cylinder drag" method because it assumed that drag created by woody debris is governed by the same factors as drag on a cylinder. The procedure draws on methods developed in several previous studies (Ranga Raju et al., 1983; Gippel et al., 1992; Shields and Gippel, 1995; Manga and Kirchner, 2000; Hygelund and Manga, 2003). The downstream force on a submerged log can be calculated as follows:

$$F_d = \frac{\rho C_D^{app} \bar{u}^2 A \sin\theta}{2} \qquad \text{(Eq. 4.15)}$$

where F_d is drag force acting on a piece of LWD, ρ is density of water, C_d^{app} is apparent drag coefficient, u is depth-averaged approach velocity, A is submerged cross-sectional area of the LWD piece, and θ is the angle of the LWD piece relative to downstream. Whereas C_d is the drag coefficient in flow without boundary effects (i.e., in an infinitely large volume of fluid under steady conditions), C_d^{app} is the drag coefficient measured for a specific set of geometric and hydraulic conditions and corrected for the blockage effect of LWD (Ranga Raju et al., 1983; Shields and Gippel, 1995; Manga and Kirchner, 2000).

Data on C_d values for various model LWD configurations analogous to those employed in my study have been developed from measurements with a dynamometer in a towing carriage and a flume (Gippel et al., 1992). The following relationship for translating C_d values into values of C_d^{app} appropriate for use in cylinder-drag calculations has been proposed:

$$C_d^{app} = \frac{C_d}{a\left[1 - B\right]^b} \qquad \text{(Eq. 4.16)}$$

where a and b are experimentally determined coefficients and B is blockage ratio (Ranga Raju et al., 1983; Shields and Gippel, 1995). The blockage ratio is the ratio of the frontal

area of an object to the cross-sectional flow area and, for a cylindrical-shaped LWD piece, is defined as:

$$B = \frac{L' d_{LWD} \sin\theta + \pi\left(\frac{d_{LWD}}{2}\right)^2 \cos\theta}{A_{flow}} \qquad \text{(Eq. 4.17)}$$

where L' is piece length, d_{LWD} is submerged cylinder diameter, and A_{flow} is cross-sectional area of the flow (Gippel et al., 1992). For pieces oriented perpendicular to the flow (θ=90°), (17) reduces to $B = \left(L' d_{LWD}\right) / A$, and, where piece length is the same as flow width, $B = d_{LWD} / d$.

Data from flume studies suggest that, for blockage ratios between 0.03 and 0.4, a and b in Equation 4.16 are approximately one and two, respectively (Gippel et al., 1992; Shields and Gippel, 1995). Field measurements of drag coefficients for model LWD, however, found no relationship between B and C_d^{app} and that at larger B values, C_d^{app} was approximately 2.1 (Hygelund and Manga, 2003).

Once the drag force associated with debris has been determined, τ_{debris} can be calculated by dividing drag force acting on the LWD (Equation 4.15), by the area of the bed covered by debris, producing:

$$\tau_{debris} = \frac{\rho C_D^{app} \overline{u}^2 d_{LWD}}{2X} \qquad \text{(Eq. 4.18)}$$

where X is distance between logs (Nelson et al., 1993; Hygelund and Manga, 2003). For evenly spaced perpendicular pieces, X is equal to reach length divided by the number of pieces. τ_{debris} can then be converted into the debris component of Darcy-Weisbach friction factor:

$$f_{debris} = \frac{8\tau_{debris}}{\rho \overline{u}^2} = \frac{4C_D^{app} d_{lwd}}{X}. \qquad \text{(Eq. 4.19)}$$

Equation 4.19, which is similar to the equation proposed by Shields and Gippel (1995) for calculating form resistance resulting from LWD formations, assumes that wake interference effects between LWD pieces are minimal. Because approach velocity (u) cancels out, calculation of f_{debris} by this method does not require data on approach velocities, and Equation 4.18 can be omitted.

I used Equation 4.19 to calculate f_{debris} for 135 flume runs containing model LWD, including plane-bed and step runs. To determine values of C_d^{app}, I used Equation 4.16 with a=1 and b=2 and Equation 4.17, flume-measured blockage ratios based on LWD dimensions and orientation with respect to cross-sectional area of flow for each flume run, and C_d values derived by Gippel et al. (1992). The 135 runs tested here are a subset of the total number of LWD runs completed (Chapter 3) and represent those configurations for which C_d values were available in Gippel et al. (1992), as explained below (Table 4.1). This analysis only included runs with B >0.5, because at higher values Equation 4.16 is invalid. High blockage ratios (B>0.5) occurred at low discharges where model LWD pieces were either barely submerged or not fully submerged.

Gippel et al. (1992) measured drag force for a number of model LWD configurations, and many of their measurements employed model debris with similar dimensions and orientations as were used in my study, in a flume with the same width as my flume (0.6 m). For flume tests employing single and stacked pieces oriented perpendicular to flow, C_d values appropriate for the cylinder dimensions used here were derived based on the following empirical relationships developed by Gippel et al. (1992):

Single perpendicular pieces (L'/d_{lwd}<21): $C_d = 0.81\left(\frac{L'}{d_{lwd}}\right)^{0.062}$ (Eq. 4.20)

Stacked perpendicular pieces (L'/d_{lwd}<5.2): $C_d = 0.89\left(\frac{L'}{d_{lwd}}\right)^{0.174}$. (Eq. 4.21)

These equations produced C_d values ranging from 0.94 to 1.37 for perpendicular pieces (Table 4.1). For perpendicular stacked configurations, my L'/d_{lwd} =12, beyond the range of the data used to develop Equation 4.21.

Gippel et al. (1992) also reported C_d values for cylinders oriented at various angles to the flow, including values of approximately C_d =0.6 and C_d =0.75 for cylinders oriented 30 and 45 degrees to the flow direction, respectively. Based on these values, a C_d value of 0.7 was adopted here for ramped pieces, which were oriented between 30 and 45 degrees to the flow (Table 4.1).

Table 4.1. Drag coefficient (C_d) values employed in calculations of debris resistance for various model LWD configurations, based on data from Gippel et al. (1992).

LWD configuration	LWD length (L') (m)	LWD diameter (d_{lwd}) (m)	LWD orientation (^{o} to flow)	C_d
Long single	0.6	.0254	90	0.99
Long single	0.6	.0254	30–45	0.7
Short single	0.3	.0254	90	0.94
Long stacked	0.6	.051	90	1.37

4.3 Results

4.3.1 Test of additive partitioning approach

The comparison of different ordering methods for partitioning estimates shows that the order in which resistance components were added to the flume substantially influenced partitioning results (Table 4.2). This analysis illustrates that, using the additive approach, whichever resistance component is added last and is calculated as the

leftover value is inflated compared to the other methods of estimating the same component's contribution. The average of the fractional contributions of grain, spill, and debris resistance to total resistance for the runs tested using these four methods is shown in Table 4.2 and Figure 4.3; results for Method 1 are also shown in Figure 4.4. These are averages across varying debris densities, discharges, and slopes; the large standard deviations around the means are attributable to these variations.

Table 4.2. Results of test of additive approach to resistance partitioning, showing average contributions to f_{total} for runs with steps, grains, and LWD, for four methods in which ordering of calculation of resistance components was varied. These data represent varying debris densities, discharges, and slopes, all of which combine with measurement errors to produce the large standard deviations around mean values.

Method	Ordering	$\%f_{grain}$	$\%f_{spill}$	$\%f_{debris}$	Number of flume runs
1	1) grain, 2) step, 3) LWD	8±8	33±20	59±20	99
2	1) grain, 2) LWD, 3) step	9±11	74±25	17±17	24
3	1) step, 2) grain, 3) LWD	32±19	10±10	59±20	99
4	1) step, 2) LWD, 3) grain	28±24	12±10	59±26	36

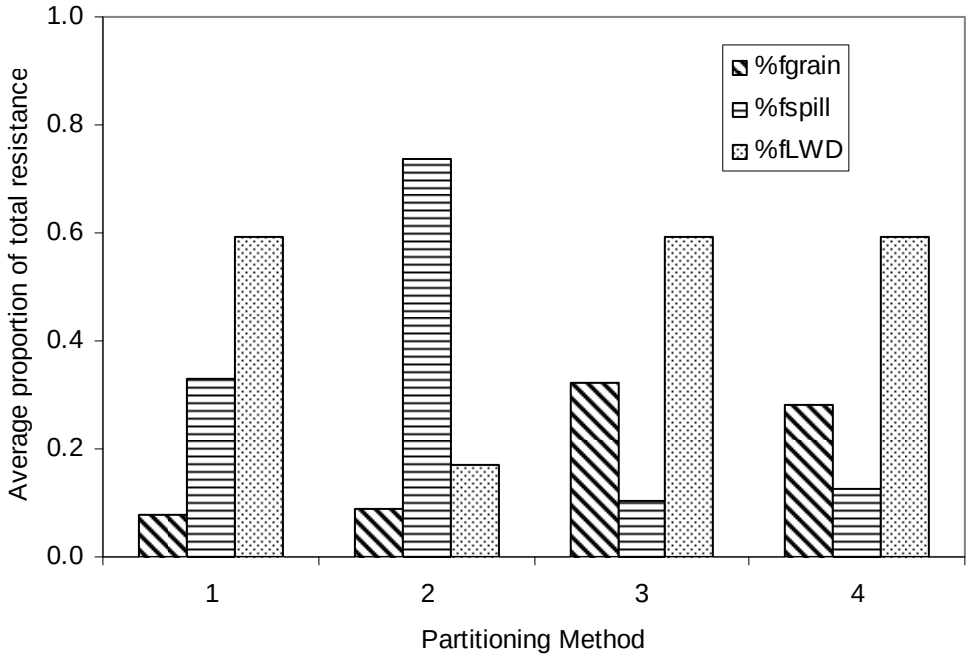

Figure 4.3. Results of test of additive approach to measuring partitioning between grain, spill, and debris resistance, based on four methods of measuring resistance components in flume.

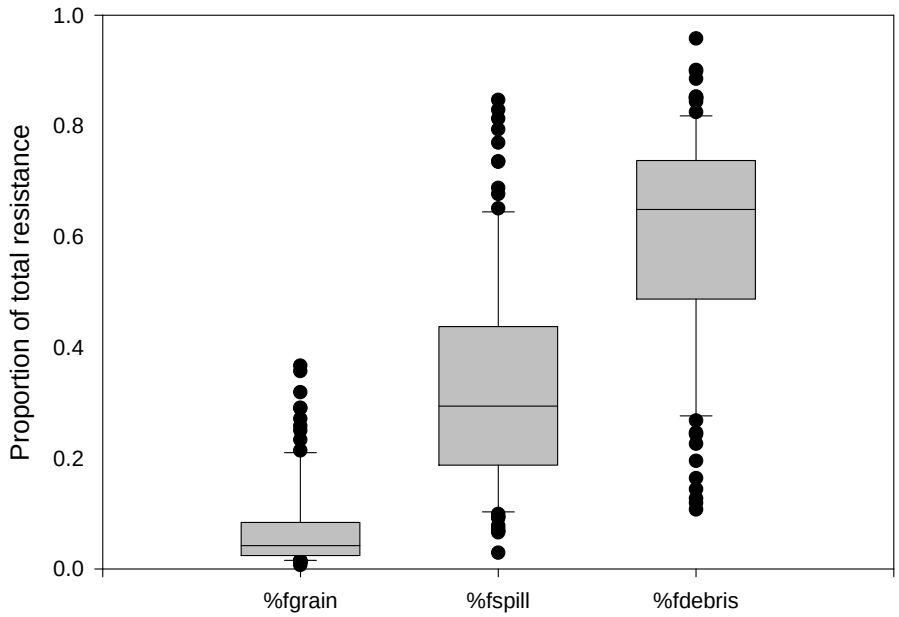

Figure 4.4. Fractional contributions of grain, spill and debris resistance to total flow resistance for 99 runs with grains, steps, and LWD, where $f_{grain} + f_{spill} + f_{debris} = 1$ for each run. These results are based on Method 1, in which f_{grain} is calculated using a Keulegan relation, f_{spill} is calculated from runs with steps and grains ($f_{spill} = f_{total} - f_{grain}$), and f_{debris} is calculated as $f_{debris} = f_{total} - f_{spill} - f_{grain}$. These data represent varying debris densities, discharges, and slopes, producing the observed spread around mean values (boxes represent 25th–75th percentiles, error bars above and below boxes show 10th and 90th percentiles).

All methods in which woody debris contributions are calculated with steps present (Methods 1, 3, 4) indicate that debris resistance is responsible for slightly less than 60% of total flow resistance, whereas the method in which debris was added to plane-bed configurations (Method 2) resulted in a much smaller f_{debris} contribution. Calculations of the spill resistance contribution were especially sensitive to ordering, ranging from 10% when smooth steps were added first and $f_{total} = f_{spill}$ (Methods 3 and 4) to 74% for Method 2, where spill resistance is the leftover value for runs with steps, grains, and debris (Equation 4.6). Grain resistance contributions were also sensitive to ordering but were never more than approximately one-third of the total. For methods in which f_{grain} was calculated using Equations 4.3 and 4.7, grain resistance was on the order

of 10% of the total, whereas higher f_{grain} contributions (~1/3) were estimated for methods in which f_{grain} was calculated as a leftover value (Method 4 and Equation 4.12).

Several conclusions can be drawn that are insensitive to ordering (i.e., that apply to all four methods). First, form resistance consisting of spill resistance (from steps) and debris resistance combined is responsible for the largest proportion of total flow resistance (68–92%). Second, grain resistance is a relatively small component of total resistance (8–32%) when steps and/or debris were present. Third, the conclusion of Curran Wohl (2003) that spill resistance is dominant in step-pool channels is supported only if one considers f_{debris} for runs with steps to be part of the f_{spill} term. This analysis also suggested that whichever resistance component was added first and measured in isolation (either steps or grains) accounted for only 10% of the resistance that would occur if steps, grains, and LWD were all present (Table 4.2).

4.3.2 Controls on resistance partitioning

The values reported in Table 4.2 represent averages for flume runs representing a range of discharges, slopes, and LWD configurations. Statistical analyses of the results of Method 1 show that the relative contributions of grain, spill, and debris resistance in these runs were strongly mediated by discharge, which had highly significant effects (p<0.0001) on $\%f_{grain}$, $\%f_{spill}$, and $\%f_{debris}$ in analyses of variance. Based on the magnitude of the sums-of-squares and p values, discharge effects on partitioning were substantially larger than those of slope or LWD density. The contribution of f_{spill} to total resistance was inversely proportional to discharge, suggesting that at higher discharges, steps were drowned out and had a smaller effect on the water surface profile, resulting in

a lower spill resistance contribution (Figure 4.5). From low to moderate discharges (4–16 L/s), % f_{debris} increased as debris pieces became fully submerged, beyond which % f_{debris} leveled off. At low discharges (4 and 8 L/s), % f_{spill} and % f_{debris} were typically similar in magnitude, whereas % f_{debris} dominated at higher discharges when steps were drowned out (Figure 4.5). Percent grain resistance increased with increasing discharge, reflecting the greater sensitivity of f_{total} to changes in Q than of f_{grain} (Figure 4.5).

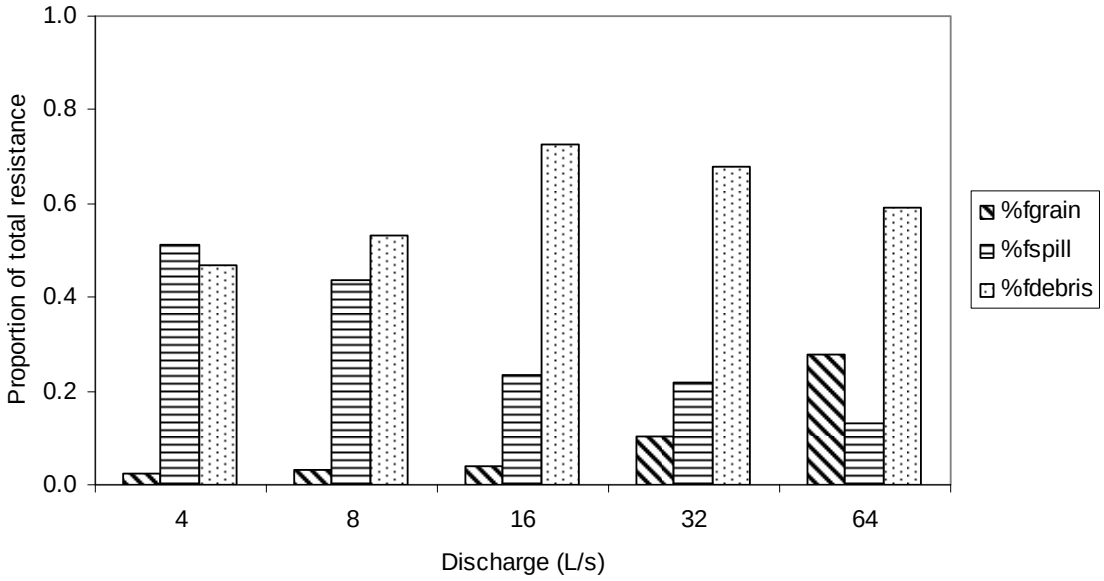

Figure 4.5. Effect of discharge on partitioning between grains, spill, and LWD, based on Method 1 results for 99 flume runs.

Debris density also significantly influenced resistance partitioning, with higher f_{debris} contributions at higher model LWD densities (Figure 4.6). At high debris densities, an average of 68% of total resistance was attributable to debris when grains, steps, and debris were present, whereas %f_{debris} averaged 49% at low debris densities. Conversely,

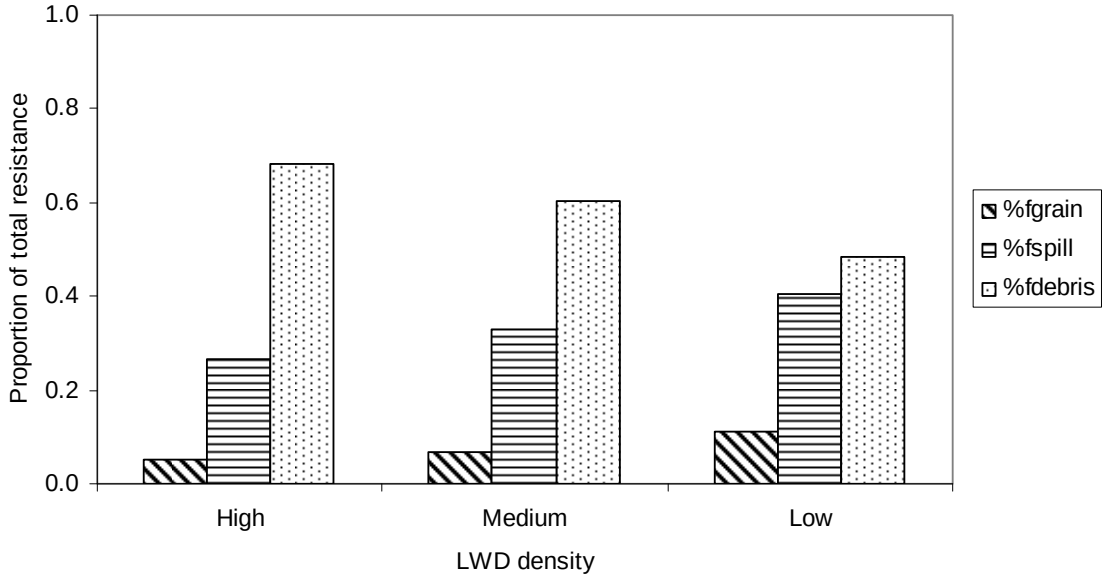

Figure 4.6. Effect of LWD density on partitioning between grains, spill, and LWD, based on Method 1 results for 99 runs.

the contributions of spill and grain resistance to f_{total} both decreased with increasing debris density (Figure 4.6).

Slope significantly affected $\%f_{spill}$ (p=0.0025). This is likely attributable to the step geometry employed here, whereby a greater number of steps were present over the length of the flume at higher slopes (see Chapter 3 for details), creating more opportunity for spill resistance generation as flow plunges over steps. Examination of the least-squares means for the Q^*S interaction shows that this slope effect was only present at low discharges; high discharges drowned out any slope effect on $\%f_{spill}$. The effect of slope on $\%f_{debris}$ was marginally significant and was not significant for $\%f_{grain}$.

4.3.3 Independent calculations of resistance partitioning

Grain resistance

Comparisons of grain resistance values generated by Equations 4.13 and 4.14 with measured f_{grain} showed that for nearly all runs, these equations produced lower estimates of f_{grain} than my "fitted Keulegan" method (Figure 4.7). For flume runs with steps (f_{grain}<0.5, Figure 4.7), Equation 4.13 (Parker and Peterson, 1980) produced the closest results to my fitted Keulegan values, underestimating f_{grain} by an average of 29%, compared to an average underestimate of 41% by Equation 4.14. For plane-bed runs (f_{grain}=0.2–1.2, Figure 4.7), the Bathurst (2002) equation performed slightly better than that of Parker and Peterson (1980). Employing Equations 4.13 and 4.14 to estimate the contribution of grain resistance to f_{total} indicates even smaller grain resistance contributions (3–6% of f_{total}, on average) than estimated in Method 1 above.

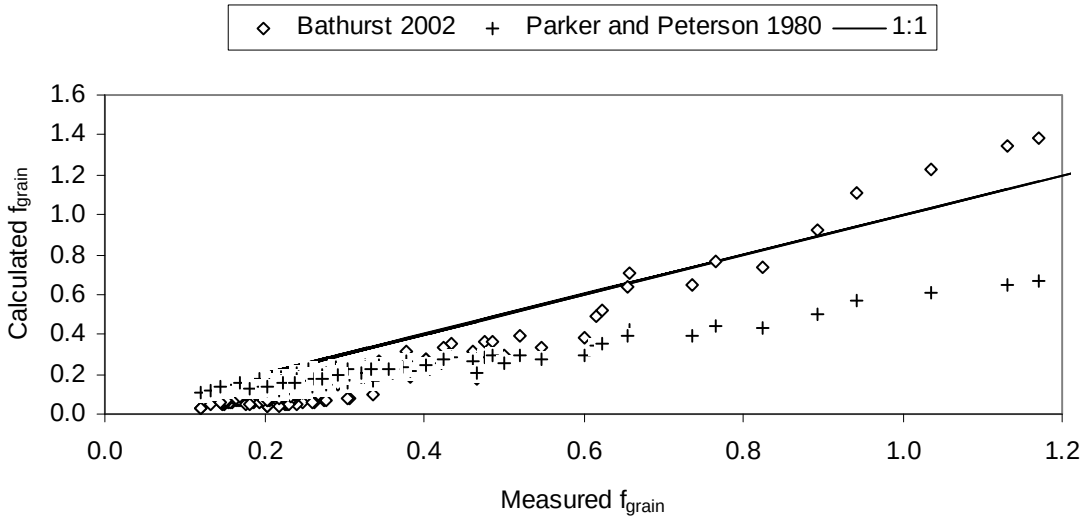

Figure 4.7. Comparison of grain resistance calculated for 154 flume runs. Values on x-axis are from flume measurements, using a Keulegan relation with k_s values developed from plane-bed runs. Values on y-axis are from the Bathurst (2002) and Parker and Peterson (1980) equations for grain resistance. Solid line shows 1:1 agreement with measured f_{grain} results.

The deviations between these equations and flume-based estimates of f_{grain} illustrate the influence of the roughness height parameter (k_s) employed to calculate f_{grain}. These results suggest that partitioning approaches that rely on empirical equations to calculate grain resistance and then apply methods such as Equations 4.8–4.10 are susceptible to errors in the calculation of f_{grain}.

Field surveys of step-pool channels containing LWD have also found that Keulegan-type equations produce resistance estimates that are a small fraction of f_{total} (Curran and Wohl, 2003). In contrast, flume and field studies by Lee and Ferguson (2002) indicated that Keulegan-type equations in which roughness height (k_s) was scaled to step D_{84} performed unexpectedly well in predicting total resistance in step-pool channels without woody debris, despite the importance of resistance sources other than skin friction in these streams.

Debris resistance

Estimates of debris resistance using the cylinder drag-based approach consistently underestimated f_{debris} for runs with steps, grains, and debris, compared to the f_{debris} estimates generated by additive Method 1 (Figure 4.8). Differences in f_{debris} values between these methods may be caused by several factors. As discussed above, the additive approach inflates f_{debris} values (for Method 1) by incorporating step-debris interaction effects into f_{debris}, whereas the drag approach does not account for such effects. The drag-based method may introduce error in a number of steps, especially in the conversion of C_d to C_d^{app}. Further, the drag-based method does not account for

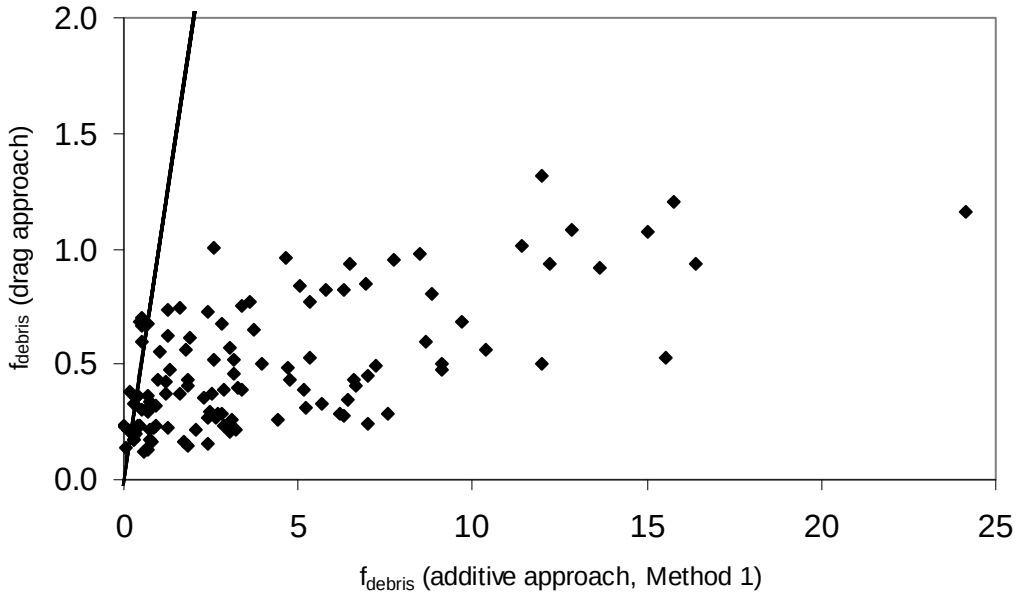

Figure 4.8. Comparison of f_{debris} calculated by additive partitioning approach (Method 1), where $f_{debris} = f_{total} - f_{spill} - f_{grain}$, versus cylinder drag approach, where f_{debris} is calculated based on cylinder drag coefficients, approach velocities, and LWD spacing, for runs with steps. Solid line illustrates 1:1 relationship between these methods.

interaction effects between LWD and other roughness elements. For plane-bed runs only, the agreement between the cylinder drag and additive Method 2 results for f_{debris}, was good, however (r^2=0.94 for a logarithmic trendline) (Figure 4.9). This suggests that the cylinder-drag approach is more appropriate for calculating the resistance created by debris pieces resting on a plane bed than for LWD on steps because of the additional resistance produced by LWD-step interactions.

4.4 Discussion

My tests of the additive approach to resistance partitioning, whereby a component of flow resistance that is difficult to directly measure is quantified by subtracting values calculated for some measurable components of resistance from total resistance, showed

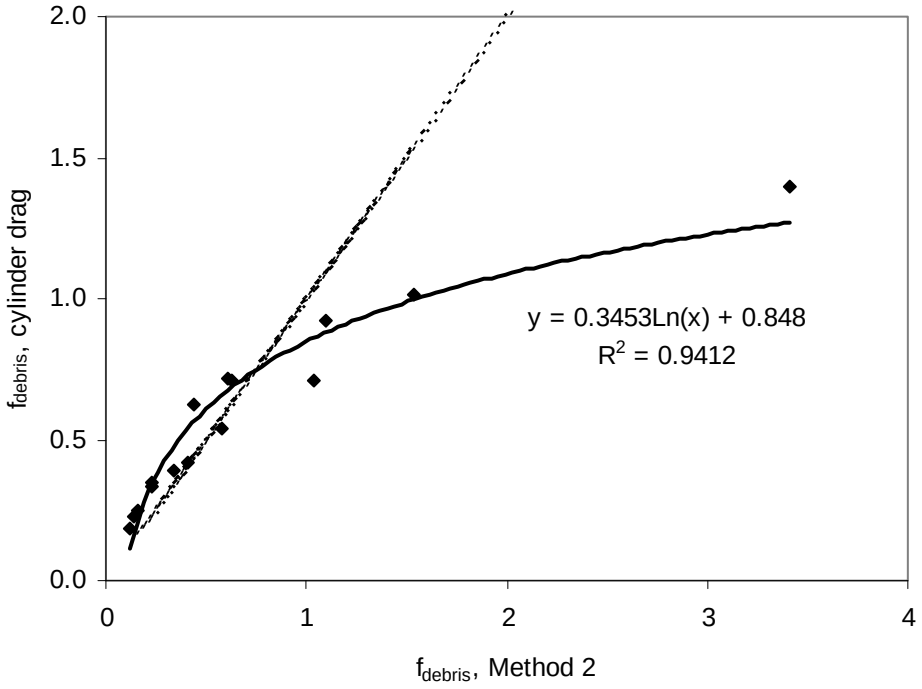

Figure 4.9. Comparison of f_{debris} for plane-bed runs using additive approach (Method 2), where $f_{debris} = f_{total} - f_{grain}$, and cylinder drag approach, based on cylinder drag coefficients, approach velocities, and LWD spacing. Dashed line illustrates 1:1 relationship.

that this method tends to inflate the values assigned to the "leftover" component. Partitioning estimates produced by the additive approach are therefore highly sensitive to the choice of "measurable" versus "unmeasurable" terms and to how each term is calculated. In this approach, leftover or unmeasurable values become catch-all terms whose values may incorporate resistance from sources that are not included in the original delineation of resistance components, and they are sensitive to any errors in calculation of "measurable" terms.

Leftover terms also incorporate interaction effects between resistance components, whereby the presence or addition of one type of roughness (e.g., LWD) can substantially affect the momentum extraction by other types of roughness (e.g., steps).

For example, partitioning estimates based on Method 4 illustrate how interaction effects may skew results based on additive approaches. For flume runs with smooth steps (no grains) and LWD, certain debris pieces were not fully submerged at low flows, limiting calculated f_{debris} contributions. Addition of grains to step treads created sufficient additional roughness to increase flow depths enough to fully submerge debris, increasing the drag created by debris pieces. This increased debris resistance contribution is included in the f_{grain} term, however, because Method 4 assigns leftover values to f_{grain}. The inflated values of leftover terms illustrate the importance of interaction effects between resistance components. Such interactions have implications not only for partitioning of flow resistance but also for understanding flow resistance dynamics in general. My companion study quantifies these interactions using factorial analyses of variance that illustrate highly significant two-way interactions between steps and debris, grains and steps, and grains and debris in affecting total flow resistance, and concludes that such interactions are an important factor driving flow resistance dynamics in step-pool channels (Chapter 3). Interaction effects between roughness components are therefore likely a central source of error in additive approaches to resistance partitioning that attempt to quantify unmeasurable resistance components by subtraction, resulting in the inflation of leftover values.

In the context of step-pool channels, the delineation of flow resistance into grain, spill, and debris components provides a useful conceptual framework for considering resistance partitioning, but my analysis illustrates the extent to which these components are not independent, as the additive approach assumes, and their synergistic effects in creating flow resistance. Delineations between resistance components in step-pool

channels are less clear-cut than in low-gradient channels. The concept of resistance partitioning originally was applied to sand-bedded channels, where a sharper distinction can be drawn between grain and form roughness, with individual sand grains on the bed responsible for grain roughness and grains organized into ripples, dunes, or other bedforms creating form roughness. In step-pool channels, grains contribute to skin friction resistance, form resistance, and spill resistance, and LWD also contributes to multiple types of flow resistance.

Despite the complications in delineating resistance components in step-pool channels and the errors introduced by the additive approach to partitioning, this flume study does allow a number of conclusions to be drawn about resistance partitioning in step-pool channels. My results show that LWD is an important source of flow resistance in step-pool channels where it is present. This is because LWD creates both form resistance as a result of drag created by LWD pieces and increases the spill resistance effect of steps compared to steps without LWD. Although my flume study delineated f_{debris} as a separate component from f_{spill}, the results suggest that woody debris can in fact be a substantial contributor to f_{spill}. This is because LWD pieces positioned near the lip of steps contribute to the structure of steps, increasing their effective height. LWD can therefore substantially increase the energy dissipation in step-pool channels and reduce the shear stress available for erosion of the bed and banks and sediment transport. LWD removal from mountain streams and reduced recruitment as a result of forestry practices may have therefore altered flow resistance dynamics in these channels, by reducing debris resistance and increasing the shear stress available for erosion and sediment transport, potentially altering sediment transport dynamics and aquatic habitat suitability.

The importance of debris resistance has previously been documented in lower-gradient channels (Shields and Gippel, 1995; Manga and Kirchner, 2000), as reviewed by Gippel (1995).

My results also indicated that although spill resistance from steps was a large component of total resistance, the spill resistance effect was much greater when LWD was present than for steps lacking LWD. Although my results suggested that calculated values of spill and debris resistance are sensitive to the partitioning methods employed, the general conclusion that form resistance, incorporating both LWD and spill, is dominant in step-pool channels was universal to all the methods tested here.

Further, grain roughness produced by bed sediments on step treads was a small component of total resistance when steps and/or debris were present. This result partly reflects the treatment of grain roughness as representative only of grains on step treads and the oversimplifications of grain size heterogeneity employed in the flume model. In natural step-pool channels, form and spill resistance from large, step-forming particles are undoubtedly significant, but the general conclusion that grain resistance on step treads is only a small contributor to overall resistance was well supported by flume runs. This result agrees with the field results of Curran and Wohl (2003) and MacFarlane and Wohl (2003).

Partitioning between grains, steps, and LWD was also found to be strongly mediated by discharge. For example, as discharge increases, steps are drowned out and spill resistance declines. The reduction in spill resistance with discharge can be conceptualized in terms of the transition from nappe flow to skimming flow (Chanson, 1994). At lower flows, steps produce nappe flow, where flow bounces over each step as

a succession of overfalls, resulting in a high f_{spill} contribution. At higher flows, the water surface profile flattens and a transition to skimming flow occurs, reducing the f_{spill} contribution. A procedure developed for calculating the discharge at which the onset of skimming flow occurs in stepped spillways (Boes and Hager, 2003) suggests that in my flume and with the step geometry employed here, this transition occurs at approximately 50 L/s, which is intermediate between the two highest discharges I modeled (32 L/s and 64 L/s). Although the Boes and Hager (2003) method was developed for steeper slopes than those used in my flume, this calculation provides further conceptual support for the explanation for reduced f_{spill} contributions at high discharges.

The increases in the relative contributions of f_{debris} and f_{grain} with discharge indicated by the additive approach (Method 1) likely reflect the effect of additional turbulence generation at high discharges when combinations of roughness sources are present. Turbulence effects associated with interactions between roughness features were not directly measurable in this study, but such effects likely contributed to the inflation of resistance estimates assigned to leftover or unmeasurable values (for Method 1, f_{debris}). Grain resistance is largely a function of relative submergence (d/D_x, where d is flow depth and D_x is a characteristic grain-size scale) and its effect is therefore diminished with increasing depth or discharge (Knighton, 1998; Wohl, 2000a), although the proportion of total resistance attributable to grain resistance may increase with increasing stage as other resistance components are drowned out (Parker and Peterson, 1980).

These results suggest a distinctive pattern of resistance partitioning in step-pool channels compared to lower-gradient channels. Spill resistance is substantial in step-pool channels, in contrast to low-gradient systems, and therefore must be accounted for in

estimates of flow resistance. Grain resistance, which some authors have suggested can be the dominant source of resistance in gravel- and cobble-bed channels (Bray, 1982; Knighton, 1998), was found to be relatively unimportant here, although this result reflects my treatment of grain resistance as consisting only of roughness from grains on step treads. The grain resistance contribution of large clasts to form resistance in step-pool channels, which was not modeled here, may be substantial, highlighting the difficulties of assigning roughness features to distinct categories for partitioning purposes in these channels. Further, the sensitivity of how resistance is partitioned to discharge variations may be much greater here than in lower-gradient channels.

My results also indicate that methods developed to calculate flow resistance components in lower-gradient rivers perform poorly in step-pool channels. Cylinder-drag approaches are likely to underestimate the hydraulic effect of woody debris in step-pool channels, in contrast to successful applications of this approach in lower-gradient rivers (Shields and Gippel, 1995; Manga and Kirchner, 2000). Cylinder-drag-based approaches underestimate debris resistance because they do not account for the synergistic interaction effects of woody debris and steps, including the increased spill and ponding effects of step-forming debris. In addition, my results suggest that equations for calculating f_{grain} are sensitive to the choice of characteristic grain size and/or roughness height and can introduce error into additive approaches to resistance partitioning.

4.5 Conclusions

This study has illustrated patterns of flow resistance partitioning between LWD, spill over steps, and grains in step-pool channels. The combined effect of LWD and spill

over steps dominates flow resistance in these channels, and grain resistance along step treads is only a small component of total resistance. Resistance from spill and LWD therefore substantially reduce the shear stress applied to the bed and available for sediment transport in step-pool channels, which is likely important for maintaining channel stability in these high-energy systems. The relative contributions of different sources of resistance are mediated by discharge, because steps and associated spill resistance are drowned out at high flows, and, to a lesser extent, by LWD density, because adding LWD increases the proportion of total resistance created by LWD.

Flow resistance partitioning in step-pool channels is complicated by the substantial interaction effects that occur between roughness variables. Momentum extraction associated with LWD, steps, and grains varies depending on the presence of other roughness variables, and the flow resistance created by these features cannot always be delineated into a clear category such as spill resistance. Interaction effects between roughness components therefore can create error in additive approaches to resistance partitioning that attempt to quantify unmeasurable resistance components by subtraction from measured components. Such approaches, which are commonly used in partitioning analyses, assign interaction effects to unmeasurable components, thereby inflating these leftover values. Furthermore, methods developed for lower-gradient channels, including cylinder-drag-based approaches to calculating debris resistance, are unreliable in step-pool channels because they do not capture interaction effects.

CHAPTER 5. THREE-DIMENSIONAL HYDRAULICS IN A STEP-POOL CHANNEL

Abstract

The effects of morphologic position and discharge on flow structure in a steep (0.10 m/m) mountain channel were investigated by collecting three-dimensional measurements of time-averaged and turbulent velocity components with a SonTek FlowTracker Handheld ADV (acoustic Doppler velocimeter) on a 30-m reach of a step-pool channel in the Colorado Rockies. Velocity profiles were measured at positions associated with various bed morphologies (upstream from steps, step lips, pools below steps, cascades, runs), and at five different discharges. A marked three-dimensionality of flow structure was documented in East St. Louis Creek. Velocities in the streamwise component were the largest contributors to overall velocity vector magnitudes, but cross-stream and vertical components were also substantial. Turbulence intensities were especially multi-dimensional, however, with large contributions to turbulent kinetic energy from the vertical component of velocity. Analysis of variance indicated that discharge and morphologic position significantly affected mean streamwise velocities, with substantially higher velocities upstream from steps than in pools. Discharge and morphology effects on cross-stream and vertical velocity components were not significant, however. Discharge and morphologic position also significantly affected turbulence intensities for all flow components, with the greatest turbulence intensities occurring in pools and at high discharges. These results illustrate both the strong discharge-dependence of hydraulics in step-pool channels, where relative submergence of bedforms changes rapidly with discharge, and the substantial spatial variation in

hydraulics created by step-pool sequences. The FlowTracker ADV employed here often produced questionable data in near-boundary and highly aerated environments, necessitating extensive data filtering and complicating interpretation of velocity and turbulence characteristics in these locations.

5.1 Introduction

Step-pool channels are an important class of mountain channels that are characterized by steep gradients (0.02–0.20 m/m) and repeating sequences of boulder, log, or bedrock steps and intervening pools. Hydraulics and morphology in step-pool channels are tightly coupled, with flow resistance resulting from the form drag of step-forming clasts and/or logs and from spill over steps into downstream pools (Curran and Wohl, 2003; MacFarlane and Wohl, 2003). Flow hydraulics in step-pool channels have been described in terms of a "tumbling" flow regime in which critical or supercritical flow over step crests plunges into downstream pools, where velocity abruptly decreases and hydraulic jumps and roller eddies generate substantial turbulence (Peterson and Mohanty, 1960; Wohl and Thompson, 2000).

Despite the apparently multi-dimensional character of flow structure created by step-pool sequences, hydraulics in step-pool channels have not been previously investigated in a three-dimensional framework, which is emblematic of a general lag in research on hydraulics in steep stream channels behind related work on lower-gradient channels. Recent work has nevertheless substantially advanced knowledge of physical processes in steep channels, including investigations of flow resistance dynamics and partitioning (Lee and Ferguson, 2002; Yager et al., 2002; Curran and Wohl, 2003;

MacFarlane and Wohl, 2003); formative processes of step-pool sequences (Whittaker and Jaeggi, 1982; Abrahams et al., 1995); controls on step spacing and geometry (Grant et al., 1990; Wohl and Grodek, 1994; Chin, 1999a; Chartrand and Whiting, 2000; Zimmermann and Church, 2001; Curran and Wilcock, 2005); mathematical treatment of flow structure (Furbish, 1993; Furbish, 1998); pool scour and jet characteristics (Comiti, 2003); hydraulic jumps (Valle and Pasternack, in press); and the morphologic effects of woody debris (Jackson and Sturm, 2002; Faustini and Jones, 2003). Building on these studies with further work exploring the interactions between hydraulics and bedforms is critical to developing insight into sediment transport and formative processes in step-pool channels.

One field study of hydraulics in step-pool channels (Wohl and Thompson, 2000) described velocity fluctuations in a step-pool channel using measurements with a one-dimensional electromagnetic current meter at various discharges and positions with respect to bedform type. Velocity profiles suggested that sites in pools immediately downstream from bed steps are dominated by wake turbulence from mid-profile shear layers associated with roller eddies, whereas sites upstream from steps, at steps, and in runs are dominated by bed-generated turbulence (Wohl and Thompson, 2000). Wohl and Thompson (2000) suggest that higher energy dissipation results from the wake-generated turbulence and form drag of step-pool reaches compared to the bed-generated turbulence found in more uniform-gradient reaches such as runs. Wohl and Thompson also found that as discharge increases, the magnitude of velocity fluctuations increases, with the largest increases recorded downstream from steps.

In lower-gradient river systems, several workers have completed field studies of flow structure and turbulence characteristics in a multi-dimensional framework. These studies have investigated a range of processes in sand- and gravel-bed rivers, including for example the role of vortex shedding around roughness elements and development of separation zones as a mechanism of momentum exchange (Robert et al., 1992; Robert, 1993; Buffin-Belanger and Roy, 1998); reach-scale variability in velocity and turbulence (Lamarre and Roy, 2005; Legleiter et al., in review); the size, scale, and dynamics of macro-turbulent flow structures (Roy et al., 2004); the effect of roughness transitions on turbulence intensities (Robert et al., 1996); the role of burst events in sand suspension (Lapointe, 1992); and analysis of three-dimensional velocities and/or turbulence at confluences (Sukhodolov and Rhoads, 2001) and associated with woody debris (Daniels and Rhoads, 2003).

This work has been facilitated by technological advances in instrumentation, including the development of current meters capable of field measurements of velocity and turbulence in a two- or three-dimensional framework (Lane et al., 1998; Walker and Roy, 2005). Application of acoustic Doppler methods for measuring three-dimensional velocity fields, including acoustic Doppler velocimeters (ADVs) (Lane et al., 1998) and acoustic Doppler current profilers (ADCPs) (Kostaschuk et al., 2005), has become increasingly well established in low- and moderate-gradient river systems (see for example the list of ADV studies in Buffin-Belanger and Roy, 2005, Table 1). Analogous data collection has not been previously performed in high-gradient stream channels, however, reflecting the challenges presented by complex topography and hydraulics in these systems. Flow that can be locally highly aerated and turbulent, coarse and

heterogeneous bed substrates, and remote settings create unique challenges for any method of velocity measurement in steep stream channels.

This study seeks to develop new insights into the hydraulics of step-pool channels using detailed three-dimensional measurements of velocity structure and turbulence characteristics in a small step-pool channel in the Colorado Rockies. I investigate how three-dimensional velocity structure and turbulence features vary with discharge, are controlled by step-pool bed morphology, and differ from lower-gradient systems. This research builds on the work of Wohl and Thompson (2000) by using three-dimensional measurement methods in the same step-pool channel they examined. This work is based on application of a recently developed three-dimensional current meter, the SonTek FlowTracker Handheld ADV, and is the first study that has employed the FlowTracker ADV or any other acoustic Doppler method to characterize hydraulics in a high-gradient stream channel (although see Legleiter et al. (in review) for a FlowTracker application in a pool-riffle channel). An evaluation of this instrument's usefulness for studies of velocity and turbulence in steep channels is therefore also included in this paper.

5.2 Methods

5.2.1 Field area

Data collection was completed on a 30-m step-pool reach of East St. Louis Creek, which is located in the Colorado Rockies approximately 80 km west of Denver, CO, in the Fraser Experimental Forest (Figure 5.1). Discharges have been recorded since 1943 at a gauging station maintained by the U.S. Forest Service that is located approximately 300 m downstream from the study reach. Discharge data show that East St. Louis Creek has a

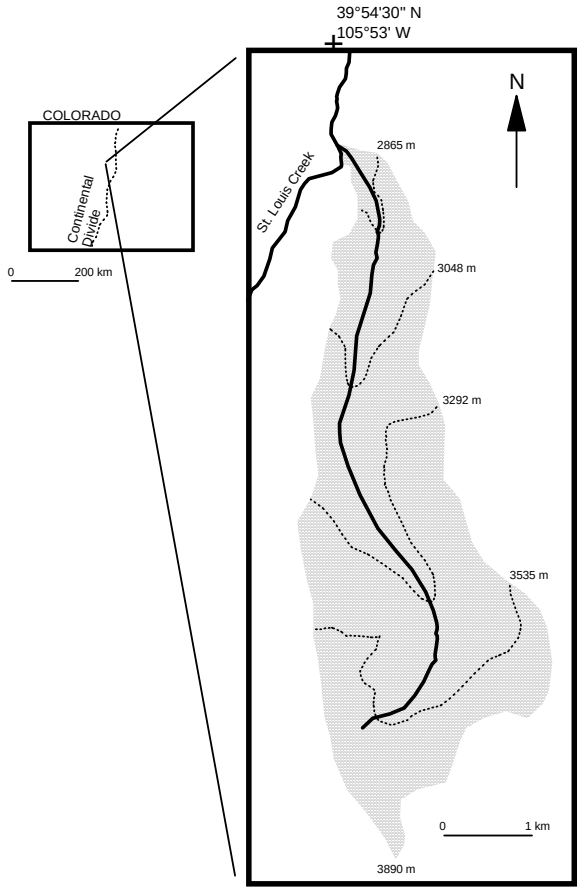

Figure 5.1. East St. Louis Creek location map. Study reach is located at approximately 2930 m elevation.

snowmelt-driven hydrologic regime, with average peak discharges occurring in mid-June and 80% of total flows occurring between April and October. East St. Louis Creek is characterized by low sediment supply, cold temperate climate (mean annual precipitation of 740 mm) (Alexander et al., 1985), and relatively abundant woody debris compared to many streams in the Colorado Rockies. Woody debris dynamics may have been altered by limited timber harvest in the vicinity of the study reach in the early 20th century, although the upstream drainage area has been largely undisturbed by anthropogenic land

uses. The study reach encompasses four distinct step-pool sequences, including both log steps and boulder steps (Figures 5.2, 5.3). Additional characteristics of the study reach are shown in Table 5.1.

Table 5.1. Summary of East St. Louis Creek study reach characteristics

Gradient	0.10 m/m
Average bankfull width	4.2 m
Drainage area	8 km^2
Average elevation	2930 m
Grain size (Reach composite)	D_{50}=78 mm D_{84}=260 mm
Average step height (H)	0.5 m
Average step length (L)	4.3 m

5.2.2 Field measurements

Repeat measurements of three-dimensional velocity profiles were performed across a range of discharges at various positions representative of bedform types found in steep channels. These positions are: (1) upstream from step (0.5 m upstream from step lip), (2) step lip, (3) base of step (at the base of the step riser, where flow from the step lands; generally 0.5–1 m downstream from the step lip), (4) pool (further downstream in pools below steps; generally 0.5 m downstream from base of step positions), (5) cascade (areas of the study reach with tumbling flow but lacking pools), and (6) run (lower-gradient portions of the study reach). Nineteen cross sections were established in positions representative of each of these morphologies (Table 5.2, Figure 5.2).

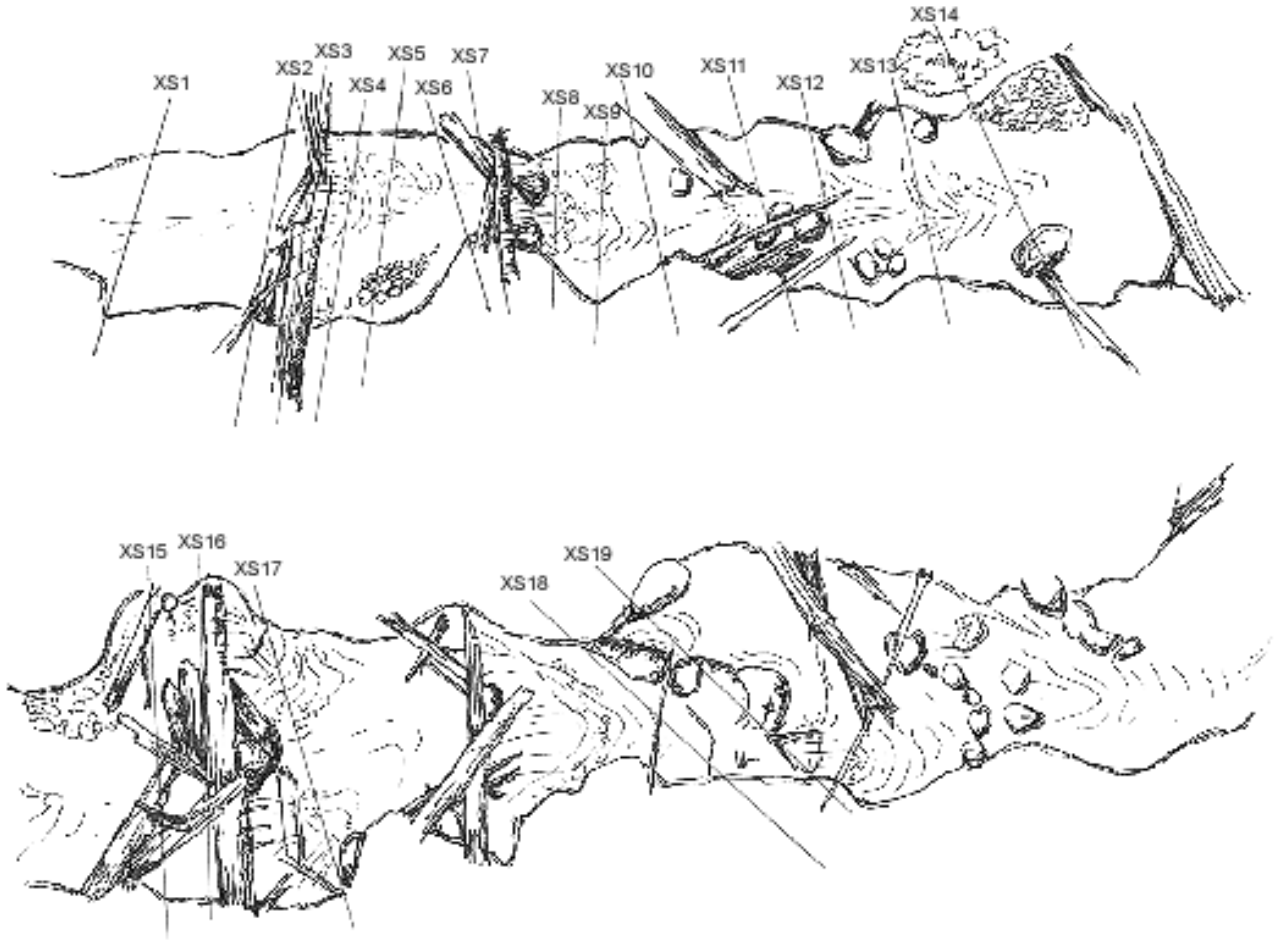

Figure 5.2. Sketch of study reach showing step-pool sequences and cross sections along which velocity was measured; flow is from left to right, and right side of upper sketch approximately connects with left side of bottom sketch. Channel length depicted here is 30 m; average channel width is approximately 4 m (sketch by Julie Kray).

5.3a **5.3b** **5.3c**

Figure 5.3. Photographs of East St. Louis Creek study reach: downstream portion of study reach at low discharge (a) and upstream portion of study reach at high (b) and low (c) discharges.

Table 5.2. Positions surveyed to characterize effects of morphology on hydraulics, and cross sections associated with each morphologic position

Morphologic position	Cross section
Upstream from step	2,6,15,18
Step lip	3,7,16
Base of step	4,8,17,19
Pool	5,9,14
Cascade	10–13
Run	1

Velocity measurements were repeated at each position during five different discharge periods (Table 5.3). The study period (2001–2003) coincided with a multi-year drought, skewing the range of sampled discharges downward. Discharges during each measurement period were determined using hourly flow data from the USFS gage located downstream from the study reach and were compared to the mean annual flow of 0.76 m^3/s from 1943 to 2003. Measurements during snowmelt periods, especially in June 2001, were subject to diurnal and inter-daily discharge fluctuations (Table 5.3).

Table 5.3. East St. Louis Creek discharge during field data collection periods, based on data from U.S. Forest Service gaging station.

Measurement period	Discharge range (m^3/s)	Average percent of mean annual flow	Date
High	0.58-0.64	80	June 2003
Moderately high	0.29-0.41	45	June 2001
Moderate	0.12-0.15	17	July 2001
Low	0.075-0.08	10	June 2002
Very low	0.054-0.058	7	August-September 2001

During all five measurement periods, thalweg velocity profiles were collected along monumented cross-sections. Additional non-thalweg profiles were also measured at 0.5-m intervals along each cross section during three of the measurement periods

(moderately high, moderate, and very low). The data presented here are derived from thalweg-only measurements; non-thalweg data will be treated in a future analysis to provide insights into lateral variations in hydraulics along cross-sections in step-pool channels. Measurement positions were relocated during each data-collection period based on distances from rebar benchmarks placed on one bank of each cross section. During the moderately high-flow data collection period, measurements were taken at z/h = 0.2, 0.6, and 0.8, where z is position in the water column and h is local flow depth (modified from USGS, 1977; Byrd et al., 2000). During all other field efforts, vertical velocity profiles consisting of 4–8 data points were measured at intervals of 0.1h–0.2h. Although concentrating measurements in the near-bed region would have facilitated analysis of Reynolds stresses, instrument limitations precluded this approach, as discussed further below. Time series of either 180 seconds (moderately high- and moderate-flow data collection periods) or 90 seconds (all other periods) were measured at each position. Buffin-Belanger and Roy (2005) found that 60–90 second time series are typically sufficient in length to capture turbulence characteristics for high-frequency (20–25 Hz) instruments. Their suggested duration comprises a much larger number of time steps than I measured, however, because of the lower frequency (1 Hz) of the FlowTracker ADV. My record lengths were selected in part as a compromise between record length and number of sampling points.

Cross-section and longitudinal-profile (water surface and thalweg) surveys were completed using a total station in order to characterize channel geometry and local- and reach-average gradients. Pebble counts were completed during the low-flow field work period using a transect method to characterize grain sizes (Table 5.1).

5.2.3 Instrumentation

Velocity was measured using a SonTek FlowTracker Handheld ADV (acoustic Doppler velocimeter) (Version 2.0), which records streamwise, cross-stream, and vertical velocity components at a frequency of 1 Hz (SonTek, 2001). The FlowTracker ADV has a sideways-facing probe that measures a 0.25 cm^3 sampling volume located 10 cm away to the side of the instrument. The FlowTracker reports velocities in *x*-*y*-*z* coordinates relative to the probe orientation (V_x, V_y, V_z), where, with the probe oriented with the *x*-axis downstream, *x* is the streamwise direction (positive downstream), *y* is the cross-stream direction (positive towards the left bank), and *z* is vertical (positive upward). In this analysis, the streamwise (*x*), cross-stream (*y*), and vertical (*z*) velocities are denoted as *u*, *v*, and *w*, respectively. This notation is consistent with usage in many previous studies, although it is worth noting that some studies employ a different coordinate system, where *v* is the vertical component and *w* is the cross-stream component.

Acoustic Doppler velocimeters measure flow velocity by transmitting an acoustic pulse that bounces off suspended sediment, air bubbles or other scattering particles in the flow and back to the instrument; velocity is recorded based on the resulting frequency shift in the transmitted signal. Signal-to-noise ratio (SNR), which is reported by the FlowTracker for each one-second velocity reading, measures the strength of the reflected acoustic signal compared to instrument noise and is largely a function of whether sufficient particulate matter is present in the water (SonTek, 2001). The principles of operation for ADVs have been described elsewhere (Lane et al., 1998; Nikora and Goring, 1998; McLelland and Nicholas, 2000), although the FlowTracker differs in important respects from ADVs used in previous turbulence studies. Those ADVs record

velocities at higher frequencies than the FlowTracker (up to 100 Hz), increasing their suitability for detailed turbulence analysis, report correlation (COR), a data-quality metric typically recorded by other types of ADVs that facilitates post-processing data filtering (Wahl, 2000), allow programming of velocity ranges, and have smaller sampling volumes. The FlowTracker was selected for this study because of its field-deployment advantages compared to other ADVs. The FlowTracker can be mounted on a standard top-setting rod, is suitable for operation in shallow flows because of its sideways-facing probe, does not require an external power source or data-logger, and is smaller and lighter than other ADVs.

5.2.4 Data analysis

Mean velocities in the streamwise (U), cross-stream (V), and vertical (W) directions were calculated for each time series. These orthogonal velocity components were used to calculate the magnitude of the three-dimensional velocity vector (M_{uvw}):

$$M_{uvw} = \sqrt{U^2 + V^2 + W^2}\,. \qquad \text{(Eq. 5.1)}$$

The relative influence of each orthogonal component on the velocity field was calculated by dividing U^2, V^2, and W^2, respectively, by M_{uvw}^2.

Each one-second velocity measurement was separated into mean and fluctuating components by Reynolds decomposition; for example: $u=U+u'$, where u is the instantaneous (one-second) streamwise velocity measurement, U is the mean streamwise velocity for a time series, and u' is the fluctuating component of the instantaneous velocity measurement. Cross-stream and vertical velocities were similarly decomposed ($v=V+v'$; $w=W+w'$). Turbulence intensities, which reflect the magnitude of the

fluctuating velocity components around the mean, were calculated as the root mean squares of velocity in each orthogonal direction (RMS_u, RMS_v, RMS_w) for each time series (Clifford and French, 1993; Middleton and Wilcock, 1994). To facilitate comparisons of turbulence intensities between measurement locations and periods, dimensionless RMS values, denoted RMS_u', RMS_v', and RMS_w', were calculated by dividing each orthogonal RMS component by M_{uvw}. In addition, to represent overall, three-dimensional turbulence intensity, average turbulent kinetic energy density (*TKE*) was calculated for each time series (Clifford and French, 1993):

$$TKE = \frac{1}{2}\rho\left(RMS_u^{\,2} + RMS_v^{\,2} + RMS_w^{\,2}\right), \qquad \text{(Eq. 5.2)}$$

where ρ is the fluid-mixture density (assumed to equal 1000 kg/m^3) and TKE has units of N/m^2. Similar to the manner in which the relative influence of each orthogonal component on the velocity field was calculated, the contributions of turbulence intensity in the streamwise, cross-stream, and vertical components to TKE were calculated by dividing each squared RMS component (multiplied by 0.5*ρ) by TKE.

Because of limitations associated with the FlowTracker ADV, including its sampling frequency (1 Hz) and its poor performance in near-bed environments, as discussed in Section 4, turbulence analysis is confined here to RMS and TKE. More detailed turbulence analysis may include calculation of Reynolds shear stresses, characteristic length scales of turbulence features, spectral properties, and quadrant analysis of deviatoric velocity terms to characterize turbulence event structure (Clifford and French, 1993; Nezu and Nakagawa, 1993).

For comparisons between discharge periods and morphologic positions, vertical averages of velocity and turbulence intensity data were calculated for each profile using

Riemann averaging. Froude numbers were calculated for each velocity profile based on vertically averaged downstream velocities (U) and flow depth. To characterize flow resistance in the study reach, Darcy Weisbach friction factor (f) was calculated for each cross-section:

$$f = \frac{8gRS_f}{V^2} \qquad \text{(Eq. 5.3)}$$

where g is gravitational acceleration (m/s^2), R=hydraulic radius (m), S_f=friction slope, and V=flow velocity (m/s). Using cross-section and longitudinal profile survey data, R and local water surface slope (which was substituted for S_f) were calculated for each cross section. Cross-section averages of flow velocity were calculated from FlowTracker data.

Analyses of variance (ANOVA) were completed to assess the influence of morphologic position and discharge on three-dimensional mean velocity, RMS, RMS', and TKE. Log transformations were applied to RMS and TKE values to stabilize variances. For the analysis of variance, the data collection was treated as a repeated measures design where cross-section position was treated as a random effect nested within morphology, morphology was treated as a blocking effect, and discharge period represented the repeated measure effect. A Satterthwaite approximation was applied in the mixed effects model for computing the denominator degrees of freedom (SAS, 2004). Discharge was treated as fixed during each field measurement period, and the average discharge during each period was used in statistical models. Discharge variations that occurred during these field sessions (Table 5.3) introduced variability that was not explicitly accounted for in the statistical models employed here, thereby reducing significance levels. All analyses of variance were completed using thalweg-only data.

5.2.5 Data filtering

Because the FlowTracker produces erroneous data in certain measurement environments, data filtering was an important initial component of data analysis. Filtering was necessary in order to eliminate data that may have been compromised as a result of factors such as obstructions within or near the sampling volume (particularly with respect to near-bed measurements), excessive aeration of flows, proximity to the surface, and/or difficult measurement positions; these topics are discussed further in Section 4.

A conservative, multi-step approach to data filtering was adopted. First, individual one-second velocity measurements with mean SNR values <10 dB and >35 dB were excluded from further analysis. These SNR criteria were based on the manufacturer's recommendation for optimal operating conditions (SonTek, 2001) and on initial data analysis, which indicated that data points with SNRs outside of this range often appeared erroneous. Next, "spikes" were removed, where spikes are defined as individual measurement points more than 3 standard deviations away from the SNR-filtered mean. This step is also performed by SonTek's summary-file software, although my method differed in that I removed spikes after the initial SNR-based filtering. If velocity readings for either the *u* or *v* components were filtered by the above methods, the remaining orthogonal velocity components were also excluded. In cases where only the *w* data were removed, however, *u* and *v* data were retained. The processing algorithm employed by the FlowTracker allows it to record valid *u* and *v* data even when *w* data are corrupted, but not vice versa (Huhta, 2003). Time series in which more than half of the

individual data points were removed by SNR- and spike-filtering were automatically excluded from further analysis. To avoid artificially reducing RMS values, time-series means or other data were not substituted for filtered points.

All time series in which any of the orthogonal dimensionless RMS values were greater than five were also removed from further analysis. Time series exceeding this threshold typically consisted of near-zero mean velocities with very large fluctuations, suggesting that constituent data were likely erroneous.

Because erroneous data could result from factors that are not measured by SNR and could produce standard deviations large enough to limit the effectiveness of spike filtering, I also manually filtered individual data points and/or time series that appeared erroneous following visual inspection. Manual filtering was performed after review of numerous time series suggested certain characteristic patterns of erroneous data produced by the FlowTracker ADV, as discussed further in section 5.4.2. Finally, time series in which the standard deviation of recorded SNRs was zero were removed because of the likelihood that such time series were corrupted (Huhta, 2003). Filtering resulted in the removal of a considerable amount of the data that were originally collected, although because of the large volume of data collected here, sufficient data remained to address the study objectives.

During field measurements, the FlowTracker was aligned to the extent possible so that its frame of reference was parallel to flow streamlines, which was equivalent in most but not all cases to a perpendicular alignment with respect to cross sections. Based on the complexity of the flow field in the study reach and the likelihood that deviations of mean vertical velocity from zero result primarily from velocity vector orientation rather than

sensor misalignment, no rotation was applied to instantaneous velocity measurements (Roy et al., 1996). Further, because the FlowTracker reports velocities in *x*-*y*-*z* coordinates relative to the probe orientation, no rotation of velocity data is required if the probe is oriented with the *x*-axis pointed downstream (Huhta, 2003).

In addition to the data filtering procedure described here, the quality of FlowTracker velocity data were assessed using other methods of determining both local and reach-averaged velocity. Vertical velocity profile measurements performed with the FlowTracker were repeated at 12 thalweg locations using a one-dimensional March-McBirney Flo-Mate 2000 electromagnetic current meter (ECM) during one of the field sessions. Reach-average velocities were also back-calculated for the June 2001 measurement period using the continuity equation for discharge ($Q=vA$). Measured discharges (Q) were determined at the downstream gaging station, and surveyed channel dimensions were used for cross-section area (A).

5.3 Results

5.3.1 Overview

Analysis of the relative influence of each orthogonal velocity component on M_{uvw} indicated that streamwise velocities (U) were the largest-magnitude components of the velocity field, contributing slightly less than two-thirds of the overall velocity vector magnitude. Mean cross-stream (V) and vertical velocities (W) contributed an average of 20% and 15% of the overall vector magnitude, respectively, averaging across discharges and morphologic positions (Figure 5.4). Linear regressions of mean U, V, and W values showed poor correlation ($r^2<0.10$) between these orthogonal components. In contrast,

RMS_u, RMS_v, and RMS_w values were all well correlated with each other, particularly RMS_u and RMS_w (r^2=0.72) and RMS_u and RMS_v (r^2=0.76) (Figure 5.5).

Mean values of dimensionless RMS_u, RMS_v, and RMS_w for thalweg velocity profiles were 0.7, 0.4, and 0.9, respectively (medians=0.5, 0.3, 0.6, respectively). This indicates that RMS values of the same order of magnitude as the overall velocity vector magnitude were typical, and that turbulence intensities that were larger than mean velocities were not uncommon (Figure 5.6). Turbulence intensities in the vertical component (RMS_w), including unstandardized and dimensionless values, were higher than in the streamwise and cross-stream components for nearly all measurement positions

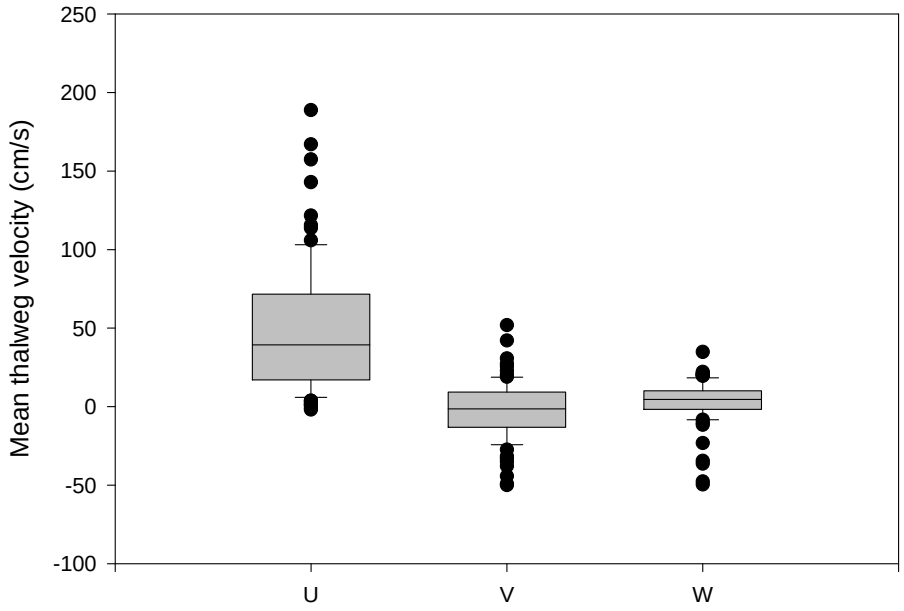

Figure 5.4. Distribution of vertically averaged mean streamwise (*U*), cross-stream (*V*) and vertical (*W*) velocities for thalweg positions at multiple morphologic positions and discharges in East St. Louis Creek study reach. Here and in Figures 5.6, 5.7, and 5.13, boxes represent 25th–75th percentiles, error bars above and below boxes show 10th and 90th percentiles.

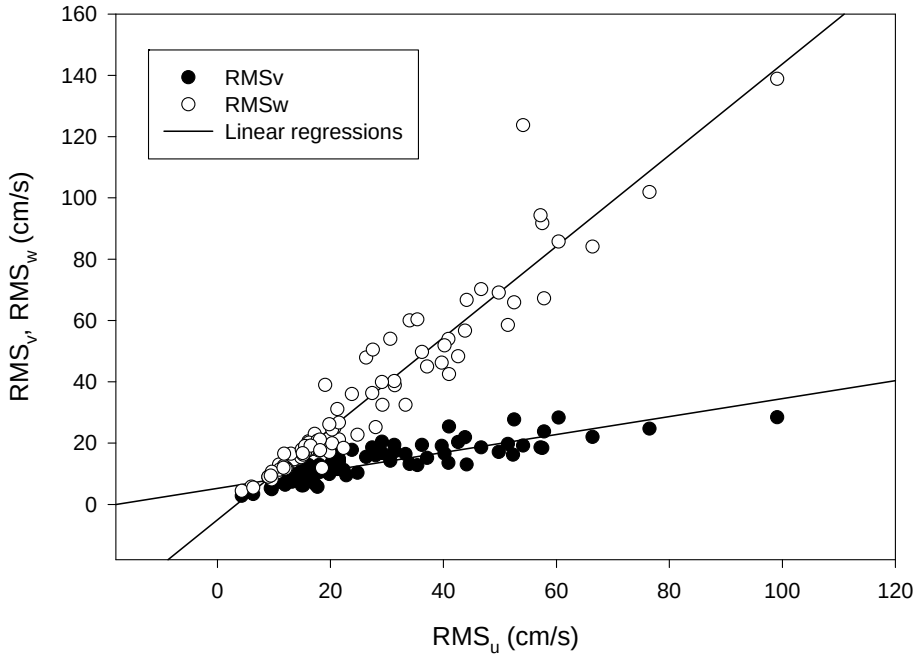

Figure 5.5. Linear regression of unstandardized turbulence intensities: RMS_u versus RMS_v and RMS_w

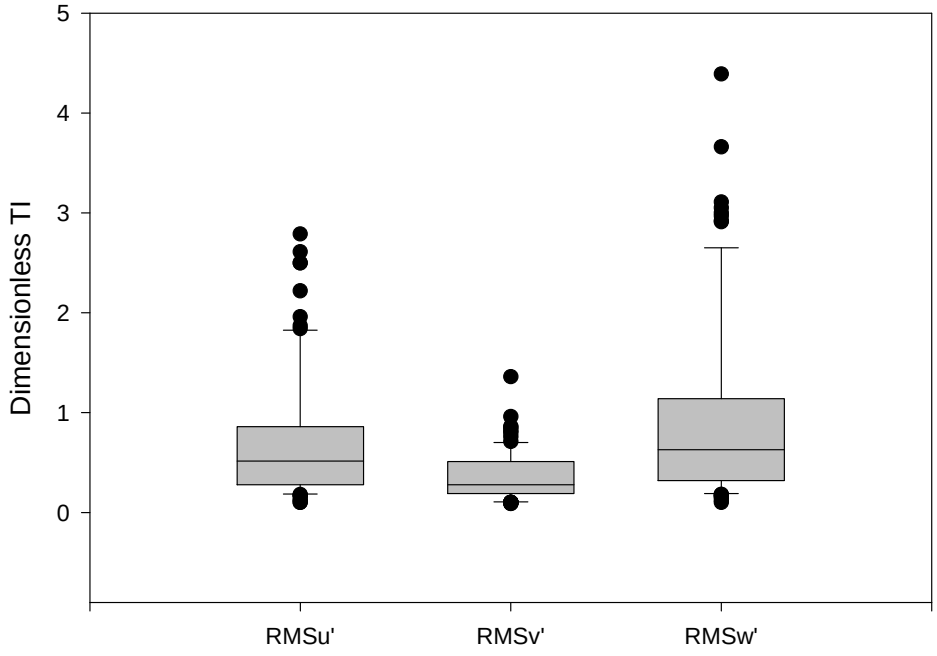

Figure 5.6. Distributions of measured dimensionless turbulence intensity (TI) (*RMS'*) values in the *u*, *v*, and *w* components, where *RMS'* consists of *RMS* divided by overall velocity vector magnitude.

(Figures 5.5, 5.6). This result may partly reflect the tendency of the FlowTracker to produce greater instrument noise in the vertical component than in the downstream component, as discussed in section 5.4.2. Turbulence intensities in the cross-stream velocity component were small compared to those in the streamwise and vertical components (Figures 5.5, 5.6).

5.3.2 Effects of morphologic position

Analyses of variance indicated that the effect of morphologic position was significant in the streamwise velocity component (*U*), but not in the cross-stream (*V*) and vertical (*W*) components (Table 5.4). In particular, significant differences in *U* were found between positions upstream from steps (above steps, step lips) versus downstream from steps (base of steps, pools). *U* measured in runs was significantly different than that in positions downstream from steps but not other positions. The pattern of mean velocity variation with morphologic position, which is evident both in the overall velocity vector magnitude (Figure 5.7) and in *U* (Figure 5.8), reflects the acceleration and deceleration caused by step-pool structures, whereby flow gains velocity along step treads until it reaches a maximum at the step lip, after which it plunges into downstream pool positions and decelerates sharply, before again repeating the sequence; intermediate velocities occur in runs and cascades.

Table 5.4. Summary of analyses of variance testing effects of morphology, discharge, and two-way morphology*discharge interactions on hydraulic parameters. Values shown are *p*-values produced by analyses of variance using mixed random effects models.

Effect	U	V	W	RMS_u	RMS_v	RMS_w	RMS_u'	RMS_v'	RMS_w'	TKE
Morphology	0.003	0.33	0.30	0.08	0.04	0.22	0.004	0.007	0.02	0.16
Q	<0.001	0.10	0.21	<0.001	<0.001	<0.001	0.88	0.86	0.98	<0.001
*Morphology*Q*	0.83	0.09	0.31	0.70	0.65	0.88	0.95	0.67	0.95	0.86

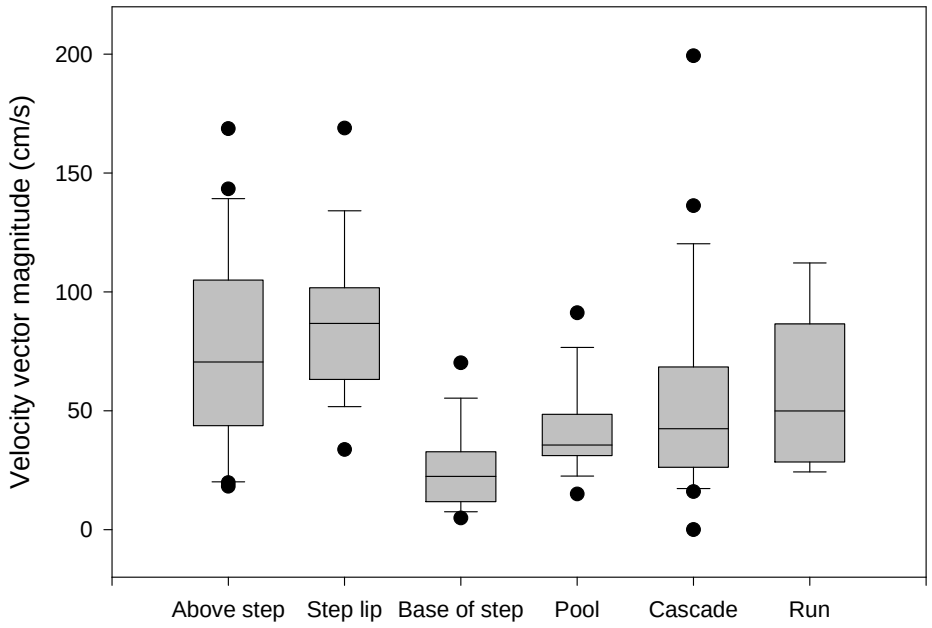

Figure 5.7. Distribution of velocity vector magnitudes at different morphologic positions, combining cross-section positions and measurement periods.

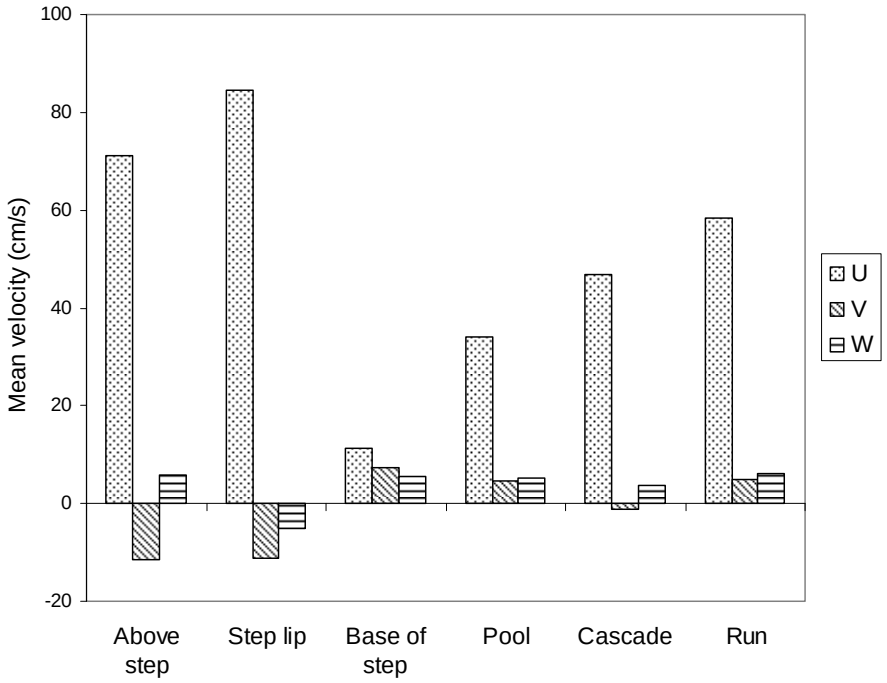

Figure 5.8. Variation in mean velocities (*U, V, W*) with morphologic position, averaged over all discharges.

Spatial variations in the relative influence of *U* and *W* components on the flow field were also evident between morphologic positions as a result of the limited variation between velocities in the vertical component between positions compared to streamwise velocities. For example, at the base of steps and in pools, the average of *W* values was 50% and 15%, respectively, as large as average *U*.

Although vertical velocities were not significantly different between morphologic positions, qualitative differences were evident (Figure 5.8). At most positions, vertically averaged *W* values were small but positive, averaging 2–6 cm/s and indicating weak flow away from the bed. At positions near step lips, in contrast, vertical velocities were typically negative, indicating flow towards the bed and/or downwards towards the overfall of plunging flow over the step lip. Absolute values of cross-stream velocities were similar between positions. The sign of cross-stream velocities (positive representing flow towards the left bank) varies between morphologic positions (Figure 5.8), reflecting the local effects of secondary circulation.

Morphologic position also significantly affected all dimensionless RMS components in the analyses of variance, although morphology effects on unstandardized RMS values were not significant (Table 5.4), reflecting the large variation in RMS values within each morphologic position. RMS values show the opposite spatial pattern of mean streamwise velocities, with high RMS values occurring at positions where velocities are low (at the base of steps and in pools) and low RMS values coinciding with high velocity positions (upstream from steps, step lips, runs) (Figure 5.9).

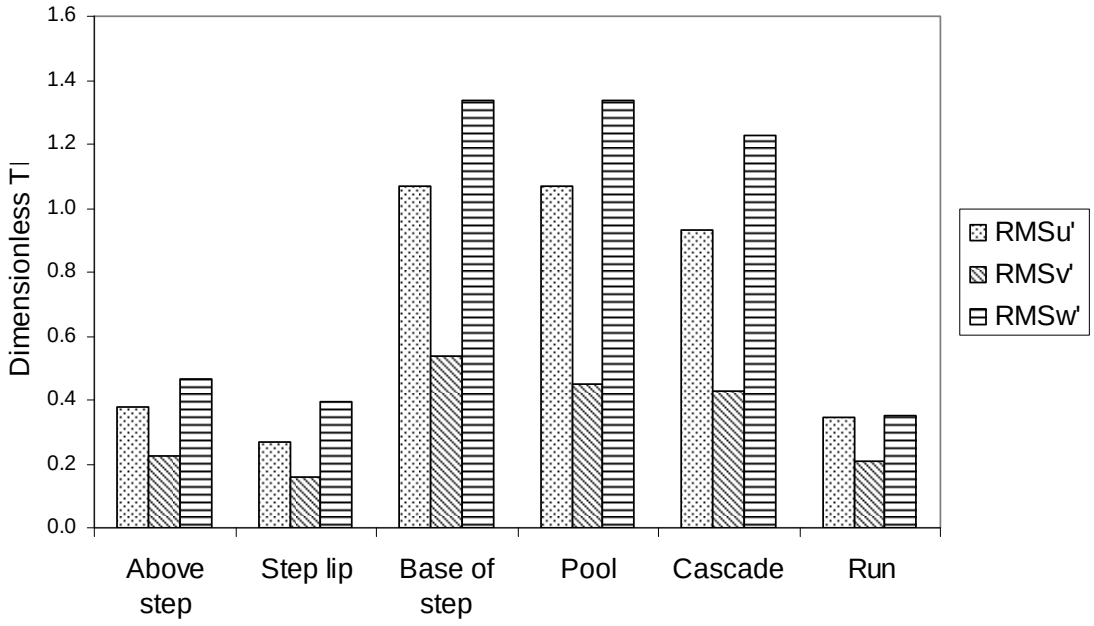

Figure 5.9. Dimensionless turbulence intensity (*RMS'*) values for each of three velocity components versus morphologic position.

5.3.3 Temporal variations

A highly significant discharge effect on *U* was observed in the analysis of variance (Table 5.4), with *U* consistently increasing with discharge (Figure 5.10). Discharge did not significantly affect *V* or *W*, and no consistent pattern of temporal variation was observed in *V* and *W* (Figure 5.10). The increase of *U* with *Q* was expected because of the collinearity between *U* and *Q* in a velocity field where the overall velocity vector magnitude is controlled by the streamwise component. The response of *V* and *W* to changes in *Q* was less predictable, however because of the potential influence of changes in relative submergence with changing *Q* on local patterns in these velocity components.

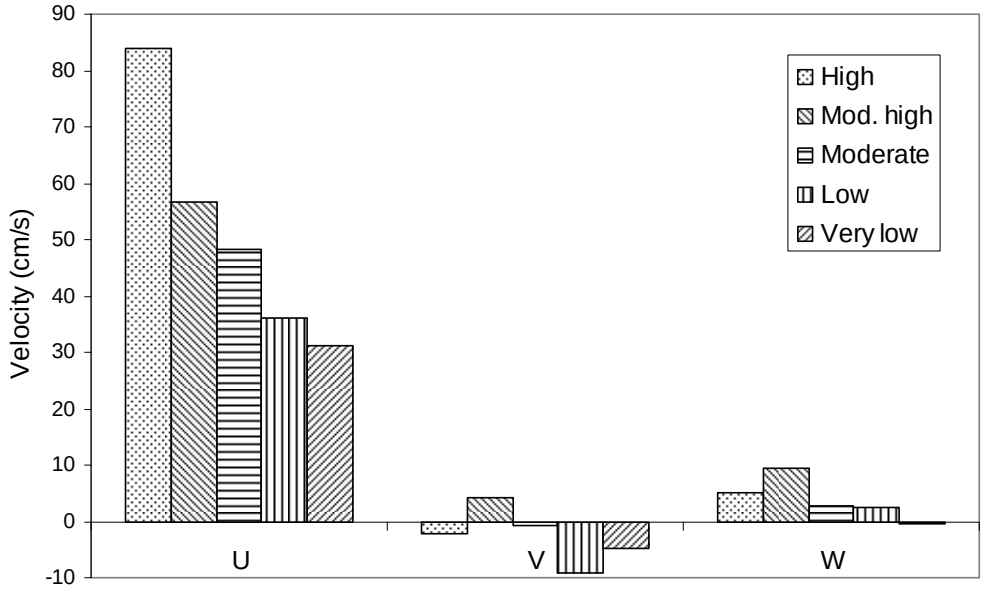

Figure 5.10. Mean velocities versus discharge, averaged over morphologic position.

The effect of discharge on unstandardized turbulence intensities (RMS) was highly significant (Table 5.4) for all flow components, with RMS values in all velocity components decreasing consistently with *Q*. Discharge did not significantly affect any of the dimensionless RMS components, however (Figure 5.11). Dimensionless RMS values tended to be highest during the lowest-discharge measurement period, but no consistent pattern of variation in dimensionless RMS with *Q* was evident (Figure 5.11). This suggests that the increase in turbulence with discharge is largely driven by velocity increases, but that the size of fluctuating components compared to mean velocity components does not change significantly with discharge. Interaction effects between discharge and morphologic position were not significant at α=0.10 for any components of velocity or RMS.

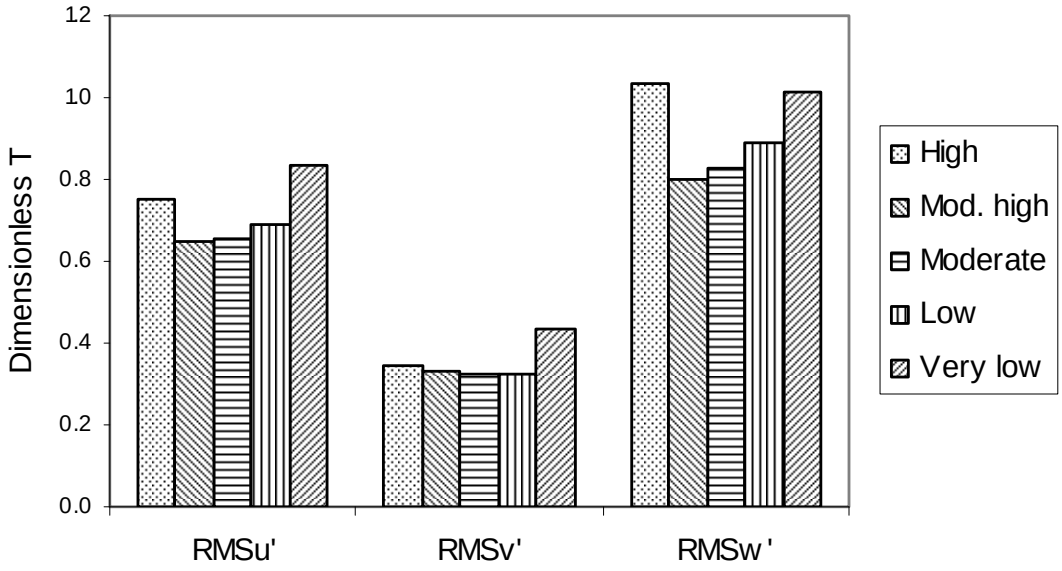

Figure 5.11. Dimensionless turbulence intensity TI (*RMS*') versus discharge.

Turbulent kinetic energy displayed similar patterns to those shown by the individual (unstandardized) RMS components (Table 5.4), as would be expected because TKE is calculated using the three orthogonal RMS components (Equation 5.2). At most morphologic positions, TKE decreased consistently with Q, although consistent patterns in TKE were not observed for step-lip and base-of-step positions. Very large TKE values were measured in pools, downstream from steps, and cascades (Figure 5.12).

Calculation of the relative contributions of the three orthogonal RMS components to TKE indicated that turbulence in the streamwise, cross-stream, and vertical velocity components contributed an average of 36%, 13%, and 51% of TKE, respectively, averaging over measurement positions. The greater noise produced by the FlowTracker ADV in the vertical component compared to other components (section 5.4.2) suggests

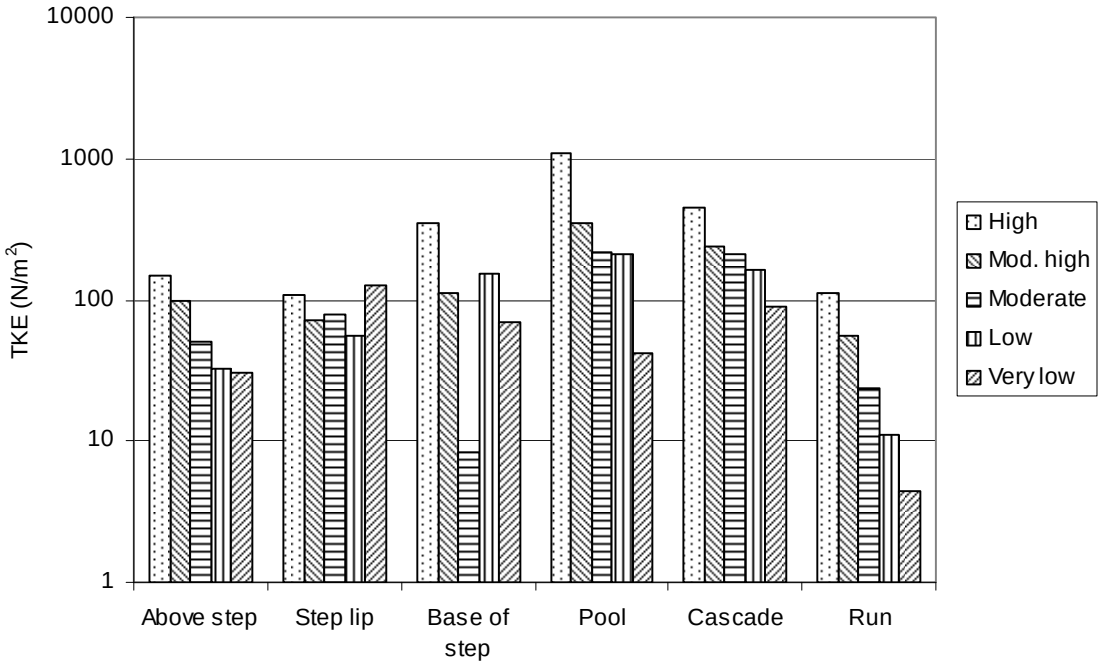

Figure 5.12. Average turbulent kinetic energy density (*TKE*) versus discharge, by morphologic position. Note log scale on y-axis.

that contributions of RMS_u and RMS_w to TKE are likely similar. Minimal variation in the relative TKE contributions was observed between discharge periods.

5.3.4 Other hydraulic parameters

Froude numbers were less than one at all measurement locations except one (a cascade bedform at "high" flow) (Figure 5.13), including at high flows and in measurement positions with high velocities (above steps and at step lips). These data suggest that subcritical flow is spatially predominant in this step-pool channel, despite the local occurrence of hydraulic jumps and supercritical flow (Figure 5.3). Locations of apparent supercritical flow were observed visually but were not measurable with the FlowTracker ADV because of shallow flow depths.

Darcy-Weisbach friction factors were calculated for each cross-section at one discharge (moderately high; June 2001) and ranged from 0.6 to 42. The highest *f* values were recorded downstream from steps; mean *f* values for base of step and pool positions

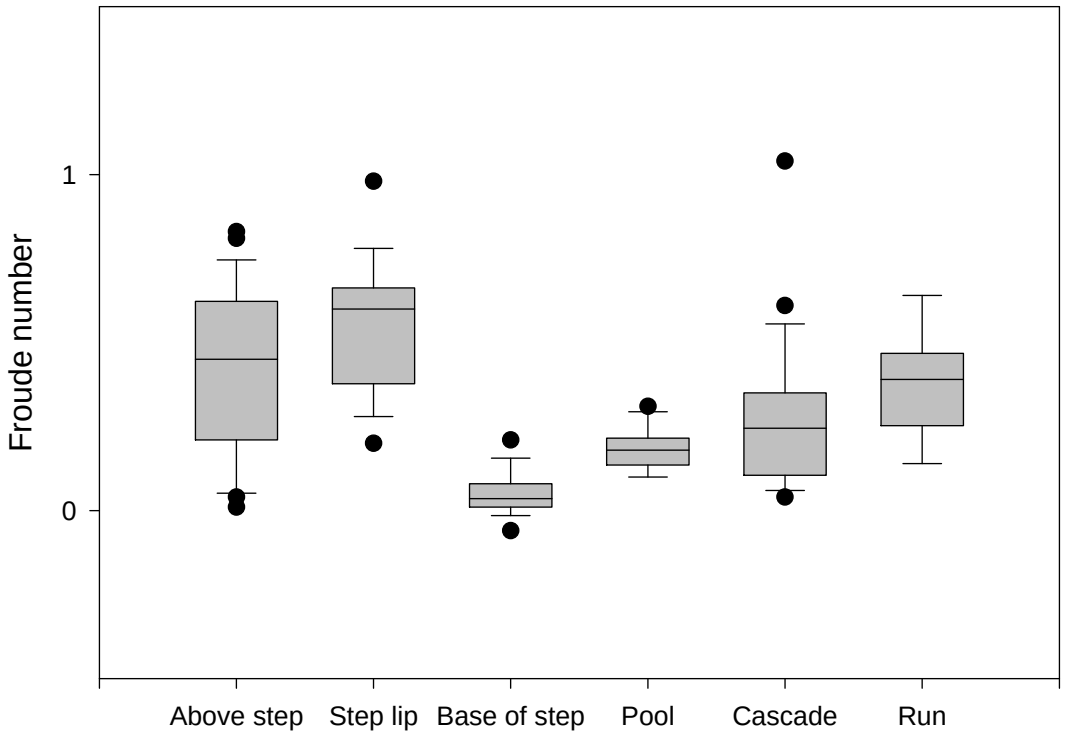

Figure 5.13. Variation in Froude number with morphologic position, averaged over discharge. These data suggest that flows are subcritical in nearly all measured positions in East St. Louis Creek, even in high-velocity locations.

were 29 and 9, respectively. Friction factors at positions upstream from steps and in cascades averaged approximately six, whereas *f* for the run position was approximately one. The ratio of step height to step length to slope (*H*/*L*/*S*), a parameter describing step geometry that has been linked with maximization of flow resistance (Abrahams et al., 1995), was 1.2 in the study reach (Table 5.1).

5.3.5 Comparisons with other velocity data

Comparison of time-average velocities measured with the FlowTracker ADV and a 1-D ECM indicated that, in locations with highly aerated flow (e.g., at the base of steps), ADV-measured values for downstream velocity were substantially lower than those recorded by the ECM at the same positions, although in other locations similar values were obtained. The overall average of FlowTracker measurements of U was approximately 60% as large as ECM measurements at the same positions.

Comparisons of reach-average FlowTracker velocities with reach-average velocities back-calculated from measured discharge and cross-section area data in June 2001 show good agreement (0.55 m/s versus 0.51 m/s). The cross-section averaged velocities used to calculate these reach averages showed greater deviations between FlowTracker and back-calculated velocities, however. Back-calculated velocities ranged from approximately 100% lower to 60% greater than FlowTracker velocities for individual cross sections.

5.4 Discussion

5.4.1 Three-dimensional hydraulics

These results illustrate the substantial spatial variability in hydraulics in this channel, where bed morphologies upstream from steps, which are associated with high velocities and low turbulence intensities, alternate with areas downstream from steps that are spatially proximal but hydraulically extremely different, having much lower velocities and much higher turbulence intensities. The grouping of RMS values between areas with high turbulence intensities (base of steps, pools, cascades) and areas with

relatively low turbulence intensities (runs, above steps, near step lips) (Figure 5.9) illustrate where energy dissipation is concentrated in this channel.

Temporal variability in the study reach was introduced not only by discharge variations, but also by morphologic changes. East St. Louis Creek is generally a stable channel, partly as a result of its low sediment supply and snowmelt-driven hydrologic regime that typically lacks flashy high-flow events. The study design employed here therefore assumed that morphologic changes would be minimal between study periods, allowing repeat measurements in the same positions that would represent only the effects of changing discharges. During the first two years of this study (2001–2002), which corresponded to a drought period in the study area, no morphologic changes were visibly evident in the study reach. The final data collection period, corresponding to the highest flow measured (Table 5.2), followed an above-bankfull event that caused the partial breaching of one of the log steps in the study reach (as is visible in the upstream-most step in Figures 5.3b and 5.3c) and shifting of a step-forming log in a second step. At the breached step (cross section 3), evidence of the effect of the reduction in drag at this step is provided by a doubling of the velocity vector magnitude, from 0.85 m/s to 1.7 m/s, between the moderately high and high discharge periods, a substantially greater rate of increase than was observed at other positions between these periods.

It was expected that increasing discharge would reduce the effect of bed morphology on average velocities and turbulence intensities, even in the absence of the type of flow-induced morphologic changes observed at cross section 3. At higher discharges in step-pool channels, steps and other roughness features are drowned out and the water surface profiles becomes more smooth, with the height of overfalls over steps

decreasing (Chin, 2003). Flume studies examining flow resistance dynamics in step-pool channels have quantified the effect of increasing discharges on bed roughness in terms of strong two-way interactions between Q and bed roughness features, including model LWD and steps (Chapter 3). This effect was tested in the study reach as well using two-way ANOVAs to examine the morphology*Q interaction effect on mean velocity components and turbulence intensities. Such an interaction effect could be viewed as analogous to the velocity convergence effect that has been observed in pool-riffle channels, where velocity differences between pools and riffles decrease as flow increases (Keller and Melhorn, 1978). No statistically significant interaction effects on any of the hydraulic parameters measured here were observed between morphologic position and Q, however (Table 5.4). This may be because a sufficiently large range of discharges was not measured, although it is more likely that the considerable variability in FlowTracker ADV data between measurement positions and periods reduced the significance of any interaction effect.

Qualitative assessment of the East St. Louis Creek study reach suggests that the effect of bed morphology on hydraulics did change with discharge, despite the lack of statistical significance for this effect. For example, Figures 5.3b and 5.3c illustrate how step-pool sequences become submerged as stage increases. At low flows, these features generate substantial localized turbulence as flow plunges over steps and decelerates in downstream pools, whereas at higher flows velocities and turbulence intensities are consistently higher throughout the channel, with less variation caused by underlying bed morphology. Further, several small step-pool features in the study reach that are evident at low discharges are completely drowned out at higher flows, assuming a more cascade-

like morphology. This includes several of the measurement locations that were classified as cascades (cross sections 12 and 13).

The presence of non-negligible vertical and cross-stream velocities illustrates the contributions of roller eddies, lateral eddies, and other non-streamwise flow to flow structure. Because of the effect of plunging flow over steps and upwelling in pools, it was expected that vertical velocity components would constitute an important part of the flow field. This was indeed the case, as mean velocities in the vertical contributed an average of 15% to overall velocity vector magnitudes. Vertical velocities had an even greater influence locally, indicating flow movement towards or away from the bed in areas of plunging and upwelling flow. The relatively large average contribution of cross-steam velocity components (20%) to M_{uvw} was unexpected, however, given the relatively straight nature of the study reach. As discussed in Section 5.2.5, a rotation was not applied to velocity data, and the possibility that V and W components were inflated as a result of sensor misalignment cannot be discounted. Furthermore, the common application of a rotation to three-dimensional velocity data in lower-gradient systems limits the availability of comparable data regarding the relative contributions of velocities in the cross-stream and vertical components to flow structure. The quantification of the contributions of V and W to vector magnitudes reported here does, however, suggest a potential source of error in one-dimensional methods of computational modeling in step-pool channels.

Turbulence intensities in the vertical component of velocity were an important component of turbulence in the study reach. Studies in lower-gradient systems, as reviewed by Sukhodolov et al. (1998), often have assumed that the contribution of

streamwise velocity to TKE amounts to 60–80%. Sukhodolov et al. (1998) found that the streamwise component is responsible for 45–55% of TKE, irrespective of flow depth. The remaining contributions from the cross-stream and vertical components varied with depth; with the vertical component lowest near the bed and the surface, and mid-profile contributions to TKE averaging approximately 20% and 30% in the vertical and cross-stream components, respectively. In my study, vertical variation within the water column in the relative contributions of each orthogonal component to TKE was not observed. Furthermore, TKE contributions from streamwise velocities were smaller in my study (an average of 36% in the study reach, averaging over measurement positions), whereas turbulence in the vertical velocity component contributed approximately half of TKE. Although RMS values in the vertical velocity component may be inflated by instrument noise, as discussed below, such that contributions to TKE from RMS_u and RMS_w are likely similar, the general conclusion regarding the multi-dimensional contributions to turbulence in this channel is likely valid.

The turbulence intensities measured in East St. Louis Creek, as represented by dimensionless RMS values, were very large compared to low-gradient channels. Whereas RMS values recorded here were between 50 and 100% of overall velocity vector magnitudes, on average, limited data from lower-gradient rivers suggest that turbulence intensities are typically on the order of 5 to 20% of mean velocity values (Middleton and Southard, 1984; Sukhodolov et al., 1998).

The results presented here characterizing Froude numbers add to the body of data on the prevalence of supercritical (Fr>1) flows in step-pool channels. Peterson and Mohanty's (1960) description of tumbling flow regimes suggests that supercritical flows

are typical upstream from steps, and descriptions of step-pool channels often refer to the presence of supercritical flows. Grant (1997) reviews data on Froude numbers and hypothesizes that interactions between hydraulics and bedforms maintain competent flows to $Fr \leq 1$ in step-pool and other channels. In East St. Louis Creek, hydraulic jumps were evident in the study reach and supercritical flow was likely present in positions that were not measured (e.g., in plunging flow jets and in shallow near-lip flows); the FlowTracker ADV was not capable of measuring velocity in these positions because of inadequate flow depths. Measured Froude number values were in the subcritical range ($Fr < 1$) at all positions except one (within a cascade bedform), even in positions upstream from steps with high (>1 m/s) flow velocities. These data suggest that, despite locally high flow velocities, the drag created by coarse substrates, step-pool structure, and woody debris increases flow depth sufficiently to maintain flow in the subcritical range across a large majority of the area of East St. Louis Creek.

Step-pool roughness features also create high flow resistance values compared to lower-gradient channels, as illustrated by the Darcy-Weisbach friction factors measured here. The spatial variation in friction factors in the study reach, with the lowest values in runs and the highest along step-pool sequences, supports Wohl and Thompson's (2000) model of energy dissipation in step-pool channels. Wohl and Thompson (2000) suggest that the wake-generated turbulence and form drag of step-pool reaches leads to higher energy dissipation relative to more uniform-gradient reaches such as runs that are dominated by bed-generated turbulence and skin friction.

5.4.2 Evaluation of FlowTracker ADV

In the East St. Louis study reach, the FlowTracker ADV operated most effectively in flows with depths greater than 10 cm, low to moderate aeration, and in mid-profile regions. In terms of the morphologic positions sampled here, data quality were most consistent in runs and positions upstream from steps. The FlowTracker ADV performed poorly in certain environments, however, and produced several characteristic data problems, necessitating the intensive and time-consuming filtering procedure described above and resulting in the elimination of a considerable amount of the data collected in the field. Here I discuss some of the problems that encountered with the use of a FlowTracker ADV in a steep, rough channel.

Questionable data were characterized by large RMS values, even after SNR-and spike-filtering. Several types of measurement environments often produced questionable data: highly aerated flows, near-boundary (bed or water surface) positions, and shallow high velocity flows. Noise can be produced by acoustic Doppler methods as a result of factors including sampling errors resulting from difficulties in resolving the phase shift of return acoustic pulses to the instrument, errors caused by random scatter motions within the sampling volume (i.e., Doppler noise), velocity gradients within the sampling volume, and boundary interference (Lane et al., 1998; Voulgaris and Trowbridge, 1998). The signal correlation reported by high-frequency ADVs can represent these types of problems (Lane et al., 1998; Wahl, 2000), thus facilitating data filtering, but as noted above, the FlowTracker does not report correlation.

In highly aerated positions, low (near-zero) mean velocities with large fluctuations in instantaneous velocity measurements around the mean were often recorded (Figure 5.14). Such problems were most common in pools below steps and/or near the surface. Because high turbulence intensities would be expected in these positions, it was sometimes difficult to determine whether high RMS values represented

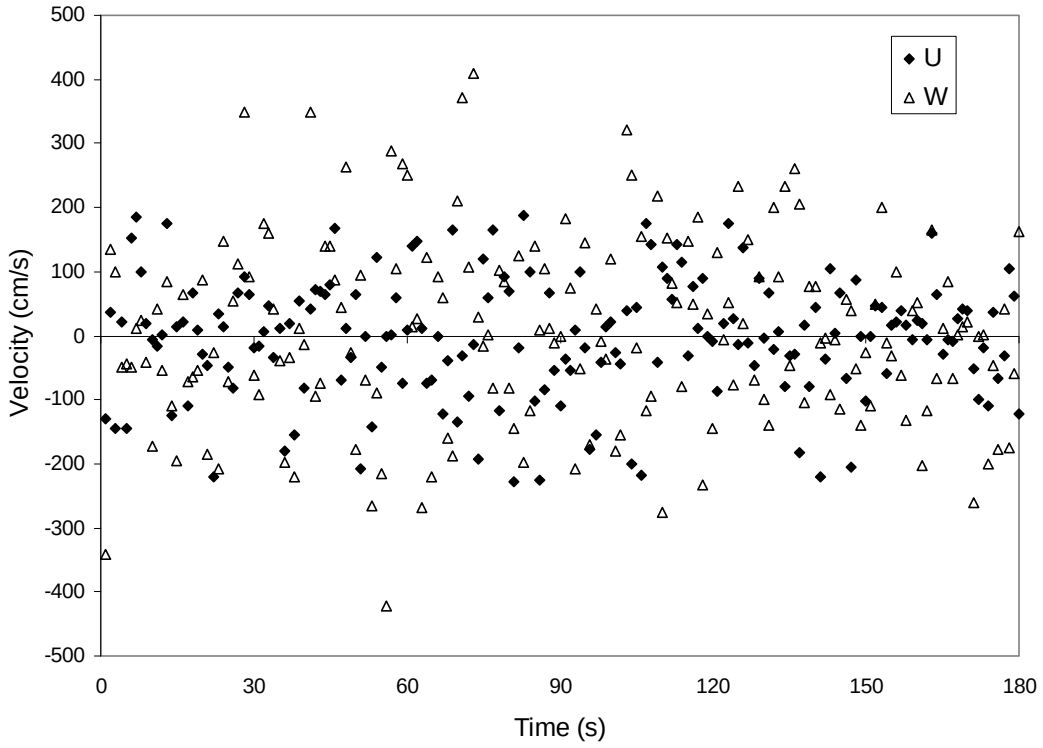

Figure 5.14. Time series characterized by low mean velocities and very large RMS values (only *u* and *w* components are shown to facilitate interpretation).

real turbulence or instrument noise resulting from ADV difficulties in aerated flows. These difficulties arise because of the sources of noise cited above and because the method employed by ADVs for measuring velocity relies on the assumption that any scattering particles in the flow are traveling at the same velocity as the overall flow. Although air bubbles can serve as accurate scattering particles, at high air concentrations

acoustic Doppler methods are compromised. A field method for measuring the aeration of hydraulic jumps using Time Domain Reflectometry (TDR) (Valle and Pasternack, 2002) could potentially be useful, in conjunction with ADV measurements in aerated flows, to help define the aeration limits under which ADVs are able to collect valid data.

Near-boundary measurements also frequently produced questionable data. Near the water surface, increased aeration and/or rapidly varying flow that intermittently exposed one or more of the instrument's probes reduced data quality. Because the beam that records vertical velocities is oriented upward on the FlowTracker, problems with near-surface measurements especially affected w and RMS_w data. In some cases where measurement of vertical velocity components was not possible because of protrusion of the top-most probe above the water surface, valid u and v data could still be collected.

In addition, data collection near the bed was often compromised by the presence of boulders, logs, or other submerged obstacles either within or close to the sampling volume. These obstacles were typically not visible from the surface and their presence was inferred from poor-quality data that were often characterized by low (<10) SNR values and near-zero velocities. In cases where the sampling volume includes the boundary, data are compromised because the ADV measures the Doppler shift of boundary reflection, rather than reflection from particles in water. Because boundary objects are stationary, resulting velocities are biased toward zero (SonTek/YSI, 2001). Furthermore, high noise is produced in such situations because objects in the sampling volume compromise the validity of pulse-lag measurements, which are used to process signals into velocity by the ADV (SonTek/YSI, 2001).

The FlowTracker also sometimes recorded erroneous data in areas where a strong positive downstream velocity was evident in the field, particularly in shallow flows. For example, highly negative downstream velocity components (on the order of -1 m/s) were sometimes recorded throughout the velocity profile near step lips despite the apparent physical implausibility of such flows. These types of errors occur as a result of velocity ambiguities or aliasing, where the FlowTracker incorrectly interprets positive velocities as negative values and readings fluctuate between large positive and large negative values (Figure 5.15) (Wahl, 2000; Huhta, 2003). Aliasing problems in very high velocity locations may have been caused where flows exceeded the maximum velocity that could be measured by one of the FlowTracker's beams. Algorithms are available to correct for ambiguity jumps (Huhta, 2003), although data affected by this problem were omitted here.

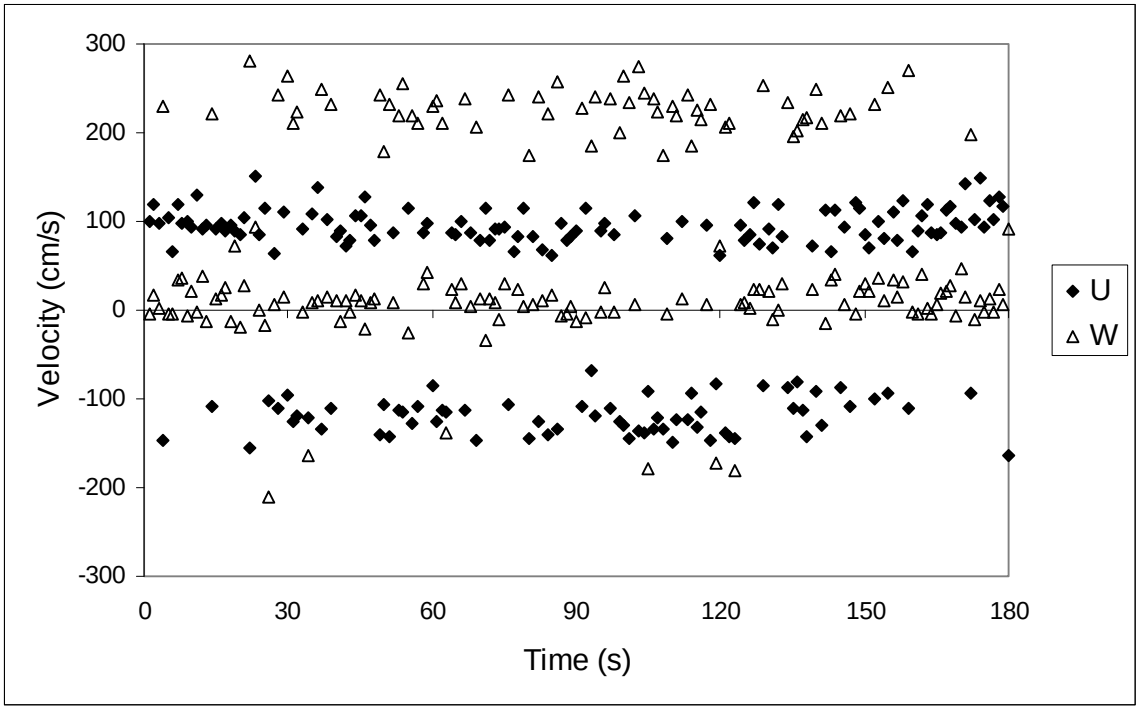

Figure 5.15. Time series affected by aliasing, where positive velocities are interpreted as negative values.

In addition, low SNR's or suspiciously high RMS values were most often associated with the *w* component, particularly in shallow flows. This results partly from the asymmetry of the FlowTracker's probe configuration, which increases instrument noise in the vertical component such that noise in the vertical should be approximately 50% higher than in the downstream component, inflating RMS_w values. Some of the results presented above with respect to the importance of turbulence intensities in the vertical direction are therefore likely affected to some extent by noise. FlowTracker noise in the downstream component is typically approximately four times greater than in the cross-stream component (Huhta, 2003).

Approximately 30% of the data that were originally collected were filtered and not used. This substantially exceeds the amount of data filtering reported in previous studies, which has ranged from 8–20% of data collected using a FlowTracker in a riffle (Legleiter et al., in review); 8% of values collected using a high-frequency ADV with an upward-facing probe in a marine surf zone (Elgar et al., 2001); and an average of 4.6% of data points per time series using ADVs in gravel-bed rivers Because I attempted to use conservative methods of filtering, valid data may have been removed in some cases, although it is also likely that some noise-dominated time series were not filtered. The amount of data filtering required (i.e., the quality of data produced by the FlowTracker) varied substantially between morphologic positions. Whereas the majority of data in positions upstream from steps and in runs were retained, much of the data collected at the base of steps, where aeration was greatest, were eliminated. Measurement of velocity in highly aerated flows in field settings is challenging, regardless of instrumentation, and three-dimensional measurements may be impossible using available technology in some

of the environments I attempted to quantify, such as the base of steps. Methods for measuring aeration of water flows in closed conduits (Naghash, 1994) and for measuring velocities in highly aerated flows in flume settings, such as employing Pitot tubes coupled with air concentration probes (Frizell et al., 1994), have been developed, but application of these methods to field settings such as East St. Louis Creek appears impractical.

Overall, except for in positions at the base of steps, the FlowTracker ADV usually produced valid mean velocity data, particularly on a vertically averaged basis and following data filtering. Turbulence intensity data produced by the FlowTracker appear to be more sensitive to instrument errors, however, particularly in the vertical component. I therefore conclude that the FlowTracker is appropriate for illustrating spatial and temporal variations in three-dimensional mean velocities, even in a challenging field setting such as this one, but that spatial and temporal variations in turbulence intensities documented by the FlowTracker should perhaps be viewed as more qualitative in nature.

Data on spatial and temporal patterns of Reynolds shear stresses, turbulence event structure, and length scales of turbulence features would provide additional insights into shear generation, sediment-transport mechanics, and morphology in steep mountain channels. Collection of such data would require instrumentation capable of measuring at high frequencies in near-boundary and potentially aerated positions, which is not currently available. The three-dimensional velocity and turbulence intensity data reported here represent an advance over existing characterizations of flow in steep channels. Although the FlowTracker data are not adequate for the type of detailed turbulence analysis listed above, they do provide insights into spatial and temporal

patterns of hydraulics and into the multi-dimensional nature of hydraulics in step-pool channels.

5.5 Conclusions

This study has characterized velocity and turbulence characteristics in a three-dimensional framework in East St. Louis Creek, the first such data set that I know of for a step-pool channel or for any other type of high-gradient (S>0.05 m/m) channel. The data presented here suggest that flow structure in step-pool channels is more three-dimensional than in lower-gradient systems, where streamwise velocities dominate overall velocity vector magnitude and turbulence intensities (i.e., flow is more one-dimensional). In particular, the contributions of mean velocities and especially turbulence intensities in the vertical component to overall flow structure were found to be substantial. Whereas the non-streamwise components of velocity and turbulence intensity were found to be broadly important to flow structure, cross-stream and vertical components exhibited less variation than streamwise components with either morphology (i.e., spatially) or discharge (i.e., temporally). Largely as a result of variations in the streamwise component, the results presented here illustrate the large spatial variations in hydraulics created by step-pool bedforms and the sensitivity of hydraulics in these channels to discharge variations, reflecting the rapid changes in relative submergence in these channels with respect to discharge. Future research, which will likely require improved instrumentation, is needed to gain further insight into step-pool hydraulics comparable to results for lower-gradient systems. For example, interactions between large-scale turbulence structures, vortex shedding, and bedforms, which have been

extensively examined in lower-gradient systems (e.g., Nelson et al., 1995; Roy et al., 2004), may be important in explaining sediment-transport processes and bedform development in step-pool channels and merit further study.

CHAPTER 6. CONCLUSIONS

The substantial influences of large woody debris on hydraulics, sediment transport and storage, channel morphology, and habitat and substrate diversity have been well documented across a range of channel types, but especially in gravel-bed pool-riffle channels (Bilby and Likens, 1980; Lisle, 1986; Robison and Beschta, 1990; Shields and Smith, 1992; Nakamura and Swanson, 1993; Smith et al., 1993; Gippel, 1995; Richmond and Fausch, 1995; Abbe and Montgomery, 1996; Buffington and Montgomery, 1999; Manga and Kirchner, 2000; Gurnell et al., 2002; Faustini and Jones, 2003). The research presented here provides new insights into the effects of LWD on hydraulics in steep channels, building on a relatively small body of previous work (Keller and Swanson, 1979; Heede, 1985; Curran and Wohl, 2003) compared to LWD studies in lower-gradient systems.

This research shows that LWD is an important source of flow resistance in step-pool channels where it is present, because LWD both creates form resistance as a result of drag created by LWD pieces and increases the spill resistance effect of steps compared to steps without LWD. Because woody debris can be a substantial contributor to spill resistance, delineating between debris resistance and spill resistance is problematic in field settings where step-forming debris is present. The delineation adopted in the flume study here is useful, however, for illustrating that step-pool sequences containing LWD, sometimes referred to as forced step-pool systems (Montgomery and Buffington, 1997), create substantially greater flow resistance than those lacking LWD, as discussed further below. LWD position appears to have a particularly important effect on flow resistance

and, in some cases, mediates LWD density effects, where additional pieces located along step treads rather than near step lips have only small incremental effects on flow resistance. LWD pieces positioned near the lip of steps contribute to the structure of steps, increasing their effective height. LWD can therefore substantially increase drag in step-pool channels and reduce the shear stress available for erosion of the bed and banks and sediment transport.

Where LWD abundance has been reduced in mountain channels as a result of removal or reduced recruitment, these reductions have likely substantially decreased overall flow resistance in step-pool channels. Reductions in the drag created by LWD would be expected to greatly increase the shear stress applied to the bed and available for sediment transport, potentially altering sediment-transport dynamics and aquatic habitat suitability and/or causing transitions from a forced step-pool morphology to a step-pool, cascade, or bedrock morphology (Montgomery and Buffington, 1997). Furthermore, reductions in LWD availability would be expected to decrease the spill resistance created by steps, because of the synergistic effect of LWD in increasing step height and creating upstream ponding. Reductions in the height of steps where step-forming LWD is absent may also, by limiting the overfall energy over steps, reduce downstream pool scour and potentially cause shifts from step-pool morphology to step-riffle or cascade morphology, where pools are largely absent and reach-scale hydraulic diversity is reduced. Management or restoration approaches in headwater stream channels that seek to maximize flow resistance through LWD placement or retention may achieve benefits in terms of sediment storage and aquatic habitat diversity.

In addition to documenting the hydraulic effect of LWD in step-pool channels, this research has provided insights into how hydraulics in steep channels differ from lower-gradient rivers. Whereas in lower-gradient channels, flow resistance is dominated by grain resistance and form resistance from features that depend on channel type such as bars, dunes, or channel sinuosity (e.g., Leopold et al., 1960; Parker and Peterson, 1980; Bray, 1982; Hey, 1988), in step-pool channels the combined effect of LWD and spill over steps dominates flow resistance, and grain resistance is only a small component of total resistance. Resistance from spill and LWD therefore substantially reduce the shear stress applied to the bed and available for sediment transport in step-pool channels, which is likely important for maintaining channel stability in these high-energy systems.

Interactions between roughness variables, including between steps, grains, and LWD, strongly influence flow resistance dynamics in step-pool channels. Momentum extraction associated with LWD, steps, and grains varies strongly depending on a range of factors including discharge, slope, the presence or absence of other roughness variables, and the density, orientation, length and arrangement of LWD pieces. Interactions among steps, grains, and LWD produce synergistic effects on flow resistance whereby the hydraulic effect of these roughness features is substantially greater in combination with each other than individually. This result suggests that there may be substantial differences in overall flow resistance and associated channel characteristics such as habitat complexity and sediment storage between step-pool systems in which LWD is present and contributes to step formation versus those lacking LWD as a result of either natural or anthropogenic influences.

Although interaction effects have not been documented in a similar manner for lower-gradient systems, the unique nature of step-pool bedforms and of how LWD functions in the context of such features suggest that interactions between roughness variables are likely more important in step-pool channels than in lower-gradient systems. The importance of interactions between roughness variables highlights the difficulties of flow resistance prediction in step-pool channels. Interaction effects between roughness components also can create error in partitioning methods that assume that resistance contributions from features such as grains or LWD are isolated and additive. Such approaches, which are commonly used in partitioning analyses, inflate the values of unmeasurable resistance components by implicitly assigning interaction effects to these components.

A discharge-dependence of roughness conditions occurs in many channel types, but the effect appears to be especially strong in step-pool channels as a result of the rapid variation in relative submergence of roughness objects with stage in step-pool channels. Because channel geometry in step-pool channels is often characterized by low width-to-depth ratios, discharge increases below the bankfull level are accommodated largely by velocity and depth increases. Further, because velocity increases more rapidly than depth as discharge increases, as observed here and by Lee and Ferguson (2002), significant decreases in flow resistance occur with increasing discharge. The effect of discharge on flow resistance was documented here in terms of strong direct discharge effects on total flow resistance, highly significant interactions between discharge and bed roughness variables, including steps, LWD, and grains, and variations in the partitioning of flow resistance between these roughness sources with changing discharge. The effect of these

variables on flow resistance was minimized at high discharges, when steps and other bed roughness features are drowned out and a transition to skimming flow (Chanson, 1994) occurs.

Strong discharge effects on hydraulics are also illustrated by the field research presented here. Discharge-driven velocity increases occur primarily as a result of changes in the streamwise velocity component; cross-stream and vertical velocity components do not appear to significantly change with discharge. Discharge increases produce substantial increases in turbulence intensity and turbulent kinetic energy, although analysis of dimensionless turbulence intensities, normalized by velocity vector magnitudes, suggests that such increases are driven by velocity increases. Little is known about the sensitivity of turbulence intensity to discharge increases in low-gradient channels.

Field studies provided evidence of a substantial "three-dimensionality" of flow structure, reflecting the complex topography and resulting hydraulics in step-pool channels. Turbulence intensities in the vertical component of velocity were an important component of turbulence in East St. Louis Creek, contributing a similar amount to turbulent kinetic energy as turbulence in the streamwise component. In contrast, turbulence intensities in the streamwise direction dominate turbulent kinetic energy in lower-gradient systems (Sukhodolov et al., 1998). In general, the turbulence intensities measured in East St. Louis Creek were very large compared to low-gradient channels, illustrating the importance of turbulence as a mechanism of energy dissipation in step-pool channels.

Although lower-gradient systems show spatial variability in velocity and turbulence characteristics as a result of features such as bars, pools, riffles, and bank irregularities, these spatial variations likely do not equal those observed in step-pool channels. As illustrated in East St. Louis Creek, sharp variations in velocity and turbulence occur over relatively small areas as a result of flow that accelerates towards and over step lips and decelerates sharply below steps.

Several directions for future study can be suggested that would build on the research presented here. The stream classification framework of Montgomery and Buffington (1997) suggests several categories of mountain stream channels, including step-pool, cascade, plane-bed, and pool-riffle. Many channels fall neatly into one of these categories on a reach-scale, and the Montgomery-Buffington delineations have, to some extent, guided studies of mountain rivers into these categories. Little is known, however, about channels that are transitional between the Montgomery-Buffington classifications and that are also recognized by those authors. For example, many steep channels have steps but lack well defined pools ("riffle-step") or have small pools but no distinct steps ("cascade-pool") (Montgomery and Buffington, 1997). Jackson and Sturm (2002) observed riffle-step channels within second-growth forests where small woody debris was available but large wood was not. Although they developed an alternative explanation for the lack of pools in their study reaches, the possibility that a lack of large wood limits pool formation in such channels merits exploration. In general, the factors determining whether steps and/or pools form in steep channels are poorly understood, including why a channel of a given gradient (e.g., 0.10 m/m) may have step-pool, cascade, or some intermediate morphology.

Investigation of factors (including LWD availability) driving transitional channel types and transitions between channel types is merited. For example, have reductions in the abundance of LWD in mountain stream channels caused shifts from forced step-pool to riffle-step, cascade, or plane-bed configurations, analogous to the transformation of alluvial to bedrock reaches proposed by Montgomery et al. (1996) as a result of LWD reductions? Such transitions may have important implications for aquatic habitat in steep channels, where steps generate substantial flow resistance and pools likely represent important velocity refugia for aquatic organisms in otherwise high-energy environments.

A related research question that demands further study pertains to the susceptibility of steep channels to changes in the supply of water, sediment and LWD as a result of either anthropogenic or natural factors, including timber harvest, water diversion, and climate change. Step-pool channels are often considered transport reaches (Montgomery and Buffington, 1997) that are resilient to anthropogenic effects because of their resistant boundaries and high sediment transport capacity (Gordon, 1995; Ryan, 1997). The research presented here, however, highlights the potential changes in flow resistance dynamics in step-pool channels as a result of factors such as altered flow and LWD regimes. Other work has also suggested a range of related morphologic changes that could result from channel disturbances, including altered step-pool geometry (i.e., step height and spacing between steps), grain size, and pool depths (Montgomery and Buffington, 1997). The sensitivity of step-pool channels to factors such as changes in LWD availability merit further study, however.

Although a broad flow resistance equation that captures the complexities of flow resistance dynamics described by this research has not been developed here, several

guidelines for flow resistance estimation are suggested by this work. Flow resistance prediction based on Keulegan-type relations, cylinder-drag calculations, or other methods developed for low-gradient channels have substantial error when applied to step-pool systems because such methods do not account for interaction effects between roughness features, various types of LWD configurations and step geometries, and the marked effects of changing discharge on relative submergence of roughness features and associated flow resistance. Because resistance from spill over steps and LWD substantially reduces the shear stress applied to the bed and available for sediment transport in step-pool channels, analyses of incipient motion of bed material and sediment transport rates that do not account for such resistance are likely to overestimate transport rates and the particle sizes that are mobile under certain flow conditions, as explored further by other studies (Zimmermann and Church, 2001; Yager et al., 2002).

Further study of the effect of step architecture on flow resistance and step-pool stability would provide insights into step mobility and formative processes in step-pool channels. My research has explored these factors to a limited extent, illustrating for example in a flume setting how forced steps incorporating LWD function differently than steps lacking LWD. Field investigations of the effect of imbrication and porosity of step-forming clasts and/or debris, the effect of woody debris presence/absence and configuration, and other elements of step architecture would complement the flume studies presented here. Field studies examining the relationship between local flow hydraulics, bed morphology, and aquatic biota would further enrich understanding of step-pool systems.

REFERENCES

Abbe, T.B. and Montgomery, D.R., 1996. Large woody debris jams, channel hydraulics and habitat formation in large rivers. Regulated Rivers-Research & Management, 12(2-3): 201-221.

Abrahams, A.D., Li, G. and Atkinson, J.F., 1995. Step-pool streams - adjustment to maximum flow resistance. Water Resources Research, 31(10): 2593-2602.

Alexander, R.R., Troendle, C.A., Kaufmann, M.R., Sheppard, W.D., Crouch, G.L. and Watkins, R.K., 1985. The Fraser Experimental Forest, Colorado: Research program and published research 1937-1985. USDA Forest Service General Technical Report RM-118, Fort Collins, CO.

ASCE, 1963. Progress report of the Task Force on Friction Factor in Open Channels of the Committee of Hydromechanics, Hydraulics Division. Journal of Hydraulics Division-Asce, 89(HY2): 97-143.

Ashida, K., Egashira, S. and Nishino, T., 1986. Structure and friction law of flow over a step-pool bedform. Disaster Prevention Research Annuals, 29(B-2): 391-403 (Japanese, English abstract).

Bathurst, J.C., 1978. Flow resistance of large-scale roughness. Journal of the Hydraulics Division, 104(12): 1587-1603.

Bathurst, J.C., 1985. Flow resistance estimation in mountain rivers. Journal of Hydraulic Engineering, 111(4): 625-643.

Bathurst, J.C., 1993. Flow resistance through the channel network. In: K. Beven and M.J. Kirkby (Editors), Channel Network Hydrology. Wiley, Chichester, pp. 69-98.

Bathurst, J.C., 2002. At-a-site variation and minimum flow resistance for mountain rivers. Journal of Hydrology, 269(1-2): 11-26.

Beebe, J.T., 2000. Flume studies of the effect of perpendicular log obstructions on flow patterns and bed topography. The Great Lakes Geographer, 7: 9-25.

Beschta, R.L., 1983. The effects of large organic debris upon channel morphology: a flume study. In: R.M. Li and P.F. Lagasse (Editors), Proceedings of the D.B. Simons Symposium on Erosion and Sedimentation. Simons, Li & Associates, Fort Collins, CO, pp. 8.63-8.78.

Beven, K., Gilman, K. and Newson, M., 1979. Flow and flow routing in upland channel networks. Hydrological Sciences Bulletin, 24: 303-325.

Bilby, R.E. and Likens, G.E., 1980. Importance of organic debris dams in the structure and function of stream ecosystems. Ecology, 61(5): 1107-1113.

Bilby, R.E. and Ward, J.W., 1989. Changes in characteristics and function of woody debris with increasing size of streams in western Washington. Transactions of the American Fisheries Society, 118(4): 368-378.

Bisson, P.A., Bilby, R.E., Bryant, M.D., Dolloff, C.A., Grette, G.B., House, R.A., Murphy, M.L., Koski, K.V. and Sedell, J.R., 1987. Large woody debris in forested streams in the Pacific Northwest: past, present, and future. In: E.O. Salo and T.W. Cundy (Editors), Streamside Management: Forestry and Fishery Interactions. University of Washington Institute of Forest Resources, Seattle, pp. 143-190.

Boes, R.M. and Hager, W.H., 2003. Hydraulic design of stepped spillways. Journal of Hydraulic Engineering, 129(9): 671-679.

Braudrick, C.A. and Grant, G.E., 2000. When do logs move in rivers? Water Resources Research, 36(2): 571-583.

Braudrick, C.A., Grant, G.E., Ishikawa, Y. and Ikeda, H., 1997. Dynamics of wood transport in streams: A flume experiment. Earth Surface Processes and Landforms, 22(7): 669-683.

Bray, D.I., 1982. Flow resistance in gravel-bed rivers. In: R.D. Hey, J.C. Bathurst and C.R. Thorne (Editors), Gravel-Bed Rivers: Fluvial Processes, Engineering and Management. Wiley, New York, pp. 109-137.

Brayshaw, A.C., 1985. Bed microtopography and entrainment thresholds in gravel-bed rivers. Geological Society of America Bulletin, 96(2): 218-223.

Brookes, A. and Shields, F.D. (Editors), 1996. River Channel Restoration : Guiding Principles for Sustainable Projects. John Wiley, Chichester.

Brownlie, W.R., 1982. Prediction of flow depth and sediment discharge in open channels. Ph.D. Thesis, California Institute of Technology, Pasadena, CA, 425 pp.

Buffin-Belanger, T. and Roy, A.G., 1998. Effects of a pebble cluster on the turbulent structure of a depth-limited flow in a gravel-bed river. Geomorphology, 25(3-4): 249-267.

Buffington, J.M. and Montgomery, D.R., 1999. Effects of hydraulic roughness on surface textures of gravel-bed rivers. Water Resources Research, 35(11): 3507-3521.

Byrd, T.C., Furbish, D.J. and Warburton, J., 2000. Estimating depth-averaged velocities in rough channels. Earth Surface Processes and Landforms, 25(2): 167-173.

Carbonneau, P.E. and Bergeron, N.E., 2000. The effect of bedload transport on mean and turbulent flow properties. Geomorphology, 35(3-4): 267-278.

Chanson, H., 1994. Hydraulic Design of Stepped Cascades, Channels, Weirs and Spillways. Pergamon, Oxford, 261 pp.

Chartrand, S.M. and Whiting, P.J., 2000. Alluvial architecture in headwater streams with special emphasis on step-pool topography. Earth Surface Processes and Landforms, 25(6): 583-600.

Cherry, J. and Beschta, R.L., 1989. Coarse woody debris and channel morphology - a flume study. Water Resources Bulletin, 25(5): 1031-1036.

Chin, A., 1989. Step pools in stream channels. Progress in Physical Geography, 13(3): 390-407.

Chin, A., 1999a. The morphologic structure of step-pools in mountain streams. Geomorphology, 27(3-4): 191-204.

Chin, A., 1999b. On the origin of step-pool sequences in mountain streams. Geophysical Research Letters, 26(2): 231-234.

Chin, A., 2003. The geomorphic significance of step-pools in mountain streams. Geomorphology, 55(1-4): 125-137.

Chow, V.T., 1959. Open-Channel Hydraulics. McGraw Hill, New York, 680 pp.

Clifford, N.J. and French, J.R., 1993. Monitoring and modelling turbulent flow: historical and contemporary perspectives. In: N.J. Clifford, J.R. French and J. Hardisty (Editors), Turbulence: Perspectives on Flow and Sediment Transport. Wiley, Chichester, pp. 1-34.

Comiti, F., 2003. Local scouring in natural and artificial step pool systems. Ph.D. Thesis, University of Padua, Padua, 209 pp.

Curran, J.C. and Wilcock, P.R., 2005. Characteristic dimensions of the step-pool bed configuration: An experimental study. Water Resources Research, 41(2): W02030, doi:10.1029/2004WR003568.

Curran, J.H., 1999. Hydraulics of large woody debris in step-pool channels. M.S. Thesis, Colorado State University, Fort Collins, CO, 197 pp.

Curran, J.H. and Wohl, E.E., 2003. Large woody debris and flow resistance in step-pool channels, Cascade Range, Washington. Geomorphology, 51(1-3): 141-157.

Daniels, M.D. and Rhoads, B.L., 2003. Influence of a large woody debris obstruction on three-dimensional flow structure in a meander bend. Geomorphology, 51(1-3): 159-173.

Einstein, H.A. and Barbarossa, N.L., 1952. River channel roughness. ASCE Transactions, 117: 1121-1146.

Elgar, S., Raubenheimer, B. and Guza, R.T., 2001. Current meter performance in the surf zone. Journal of Atmospheric and Oceanic Technology, 18(10): 1735-1746.

Engelund, F., 1966. Hydraulic resistance of alluvial streams. Journal of the Hydraulics Division ASCE, 92: 315-326.

Faustini, J.M. and Jones, J.A., 2003. Influence of large woody debris on channel morphology and dynamics in steep, boulder-rich mountain streams, western Cascades, Oregon. Geomorphology, 51(1-3): 187-205.

Ferguson, R.I., 1986. Hydraulics and hydraulic geometry. Progress in Physical Geography, 10(1): 1-31.

Frizell, K.H., Ehler, D.G. and Mefford, B.W., 1994. Developing air concentration and velocity probes for measuring highly aerated, high-velocity flow. In: C.A. Pugh (Editor), Fundamentals and Advancements in Hydraulic Measurements and Experimentation. ASCE, Buffalo, NY, pp. 268-277.

Furbish, D.J., 1993. Flow structure in a bouldery mountain stream with complex bed topography. Water Resources Research, 29(7): 2249-2263.

Furbish, D.J., 1998. Irregular bed forms in steep, rough channels - 1. Stability analysis. Water Resources Research, 34(12): 3635-3648.

Gao, P. and Abrahams, A.D., 2004. Bedload transport resistance in rough open-channel flows. Earth Surface Processes and Landforms, 29(4): 423-435.

Gippel, C.J., 1995. Environmental hydraulics of large woody debris in streams and rivers. Journal of Environmental Engineering-Asce, 121(5): 388-395.

Gippel, C.J., O'Neill, I.C. and Finlayson, B.L., 1992. The hydraulic basis of snag management, Center for Environmental Hydrology, University of Melbourne, Victoria, Australia.

Gippel, C.J., O'Neill, I.C., Finlayson, B.L. and Schnatz, I., 1996. Hydraulic guidelines for the re-introduction and management of large woody debris in lowland rivers. Regulated Rivers-Research & Management, 12(2-3): 223-236.

Gomez, B., 1993. Roughness of stable, armored gravel beds. Water Resources Research, 29(11): 3631-3642.

Gordon, N., 1995. Summary of technical testimony in the Colorado Water Division 1 trial. RM-270.

Grant, G.E., 1997. Critical flow constrains flow hydraulics in mobile-bed streams: A new hypothesis. Water Resources Research, 33(2): 349-358.

Grant, G.E. and Mizuyama, T., 1992. Origin of step-pool sequences in high-gradient streams: a flume experiment. In: M. Tominaga (Editor), Japan-U.S. Workshop on Snow Avalanche, Landslide, and Debris Flow Prediction and Control, Tsukuba, Japan, pp. 523-532.

Grant, G.E., Swanson, F.J. and Wolman, M.G., 1990. Pattern and origin of stepped-bed morphology in high-gradient streams, western Cascades, Oregon. Geological Society of America Bulletin, 102(3): 340-352.

Griffiths, G.A., 1989. Form resistance in gravel channels with mobile beds. Journal of Hydraulic Engineering, 115(3): 340-355.

Gurnell, A.M., Piegay, H., Swanson, F.J. and Gregory, S.V., 2002. Large wood and fluvial processes. Freshwater Biology, 47(4): 601-619.

Hayward, J.A., 1980. Hydrology & stream sediment from Torlesse stream catchment. Special Publication No. 17, Lincoln College.

Heede, B.H., 1981. Dynamics of selected mountain streams in the western United States of America. Zeitschrift fur Geomorphologie N.F., 25: 17-32.

Heede, B.H., 1985. Channel adjustments to the removal of log steps - an experiment in a mountain stream. Environmental Management, 9(5): 427-432.

Heritage, G.L., Moon, B.P., Broadhurst, L.J. and James, C.S., 2004. The frictional resistance characteristics of a bedrock-influenced river channel. Earth Surface Processes and Landforms, 29(5): 611-627.

Hey, R.D., 1979. Flow resistance in gravel-bed rivers. Journal of the Hydraulics Division-Asce, 105(4): 365-379.

Hey, R.D., 1988. Bar form resistance in gravel-bed rivers. Journal of Hydraulic Engineering, 114(12): 1498-1508.

Hilderbrand, R.H., Lemly, A.D., Dolloff, C.A. and Harpster, K.L., 1997. Effects of large woody debris placement on stream channels and benthic macroinvertebrates. Canadian Journal of Fisheries and Aquatic Sciences, 54(4): 931-939.

Hilderbrand, R.H., Lemly, A.D., Dolloff, C.A. and Harpster, K.L., 1998. Design considerations for large woody debris placement in stream enhancement projects. North American Journal of Fisheries Management, 18: 161-167.

Hu, S.X. and Abrahams, A.D., 2004. Resistance to overland flow due to bed-load transport on plane mobile beds. Earth Surface Processes and Landforms, 29(13): 1691-1701.

Huhta, C., 2003. Personal communication. SonTek, Fort Collins, CO.

Hygelund, B. and Manga, M., 2003. Field measurements of drag coefficients for model large woody debris. Geomorphology, 51(1-3): 175-185.

Jackson, C.R. and Sturm, C.A., 2002. Woody debris and channel morphology in first- and second-order forested channels in Washington's coast ranges. Water Resources Research, 38(9): 1177 doi:10.1029/2001WR001138.

Jarrett, R.D., 1984. Hydraulics of high-gradient streams. Journal of Hydraulic Engineering, 110(11): 1519-1539.

Jarrett, R.D., 1992. Hydraulics of mountain rivers. In: B.C. Yen (Editor), Channel Flow Resistance: Centennial of Manning's Formula. Water Resources Publications, Littleton, CO, pp. 287-298.

Julien, P.Y., 1998. Erosion and Sedimentation. Cambridge University Press, Cambridge, 280 pp.

Kamphuis, J.W., 1974. Determination of sand roughness for fixed beds. Journal of Hydraulic Research, 12(2): 193-203.

Keller, E.A. and Melhorn, W.N., 1978. Rhythmic spacing and origin of pools and riffles. Geological Society of America Bulletin, 89(5): 723-730.

Keller, E.A. and Swanson, F.J., 1979. Effects of large organic material on channel form and fluvial processes. Earth Surface Processes and Landforms, 4(4): 361-380.

Kennedy, J.F., 1963. The mechanics of dunes and antidunes in erodible-bed channels. Journal of Fluid Mechanics, 16: 521-544.

Kennedy, J.F., 1975. Hydraulic relations for alluvial streams. In: V.A. Vanoni (Editor), Sedimentation Engineering, Manual 54. ASCE, pp. 114-154.

Keulegan, G.H., 1938. Laws of turbulent flow in open channels. Journal National Bureau of Standards, 21(Research Paper 1151): 707-741.

Knighton, D., 1998. Fluvial Forms and Processes. Arnold, London, 383 pp.

Kostaschuk, R., Best, J., Villard, P., Peakall, J. and Franklin, M., 2005. Measuring flow velocity and sediment transport with an acoustic Doppler current profiler. Geomorphology, 68(1-2): 25-37.

Lamarre, H. and Roy, A.G., 2005. Reach scale variability of turbulent flow characteristics in a gravel-bed river. Geomorphology, 68(1-2): 95-113.

Lane, S.N., Biron, P.M., Bradbrook, K.F., Butler, J.B., Chandler, J.H., Crowell, M.D., McLelland, S.J., Richards, K.S. and Roy, A.G., 1998. Three-dimensional measurement of river channel flow processes using acoustic Doppler velocimetry. Earth Surface Processes and Landforms, 23(13): 1247-1267.

Lapointe, M., 1992. Burst-like sediment suspension events in a sand bed river. Earth Surface Processes and Landforms, 17(3): 253-270.

Larson, M.G., Booth, D.B. and Morley, S.A., 2001. Effectiveness of large woody debris in stream rehabilitation projects in urban basins. Ecological Engineering, 18(2): 211-226.

Lee, A.J., 1998. The hydraulics of steep streams. Ph.D. Thesis, University of Sheffield.

Lee, A.J. and Ferguson, R.I., 2002. Velocity and flow resistance in step-pool streams. Geomorphology, 46(1-2): 59-71.

Legleiter, C.J., Phelps, T.L. and Wohl, E.E., in review. Geostatistical analysis of the effects of stage and roughness on reach-scale spatial patterns of velocity and turbulence intensity. Geomorphology.

Lenzi, M.A., 2001. Step-pool evolution in the Rio Cordon, northeastern Italy. Earth Surface Processes and Landforms, 26(9): 991-1008.

Leopold, L.B., Bagnold, R.A., Wolman, M.G. and Brush, L.M.J., 1960. Flow resistance in sinuous or irregular channels. United States Geological Survey Professional Paper 282-D, Washington DC.

Leopold, L.B. and Maddock, T., 1953. The hydraulic geometry of streams and some physiographic implications. United States Geological Survey Professional Paper 252, Washington DC.

Leopold, L.B., Wolman, M.G. and Miller, J.P., 1964. Fluvial Processes in Geomorphology. Dover, New York, 522 pp.

Lienkaemper, G.W. and Swanson, F.J., 1987. Dynamics of large woody debris in streams in old-growth Douglas-fir forests. Canadian Journal of Forest Research-Revue Canadienne De Recherche Forestiere, 17(2): 150-156.

Lisle, T.E., 1986. Effects of woody debris on anadromous salmonid habitat, Prince of Wales Island, southeast Alaska. North American Journal of Fisheries Management, 6: 538-550.

Lisle, T.E., 1995. Effects of coarse woody debris and its removal on a channel affected by the 1980 eruption of Mount-St-Helens, Washington. Water Resources Research, 31(7): 1797-1808.

MacFarlane, W.A., 2001. Flow resistance in step-pool streams of the Washington Cascades. M.S. Thesis, Colorado State University, Fort Collins, CO, 158 pp.

MacFarlane, W.A. and Wohl, E., 2003. Influence of step composition on step geometry and flow resistance in step-pool streams of the Washington Cascades. Water Resources Research, 39(2): 1037, doi:10.1029/2001WR001238.

Manga, M. and Kirchner, J.W., 2000. Stress partitioning in streams by large woody debris. Water Resources Research, 36(8): 2373-2379.

Marcus, W.A., Roberts, K., Harvey, L. and Tackman, G., 1992. An evaluation of methods for estimating Mannings-n in small mountain streams. Mountain Research and Development, 12(3): 227-239.

Marston, R.A., 1982. The geomorphic significance of log steps in forest streams. Annals of the Association of American Geographers, 72: 99-108.

Maxwell, A.R. and Papanicolaou, A.N., 2001. Step-pool morphology in high-gradient streams. International Journal of Sediment Research, 16: 380-390.

McLelland, S.J. and Nicholas, A.P., 2000. A new method for evaluating errors in high-frequency ADV measurements. Hydrological Processes, 14(2): 351-366.

Middleton, G.V. and Southard, J.B., 1984. Mechanics of Sediment Movement. Lecture notes for S.E.P.M Short Course No. 3, 2nd ed., Providence, RI.

Middleton, G.V. and Wilcock, P.R., 1994. Mechanics in the Earth and Environmental Sciences. Cambridge University Press, Cambridge.

Millar, R.G. and Quick, M.C., 1994. Flow resistance of high-gradient gravel channels. In: G.V. Cotroneo and R.R. Rumer (Editors), Hydraulic Engineering '94. ASCE, Buffalo, NY, pp. 717-721.

Montgomery, D.R., Abbe, T.B., Buffington, J.M., Peterson, N.P., Schmidt, K.M. and Stock, J.D., 1996. Distribution of bedrock and alluvial channels in forested mountain drainage basins. Nature, 381(6583): 587-589.

Montgomery, D.R. and Buffington, J.M., 1997. Channel-reach morphology in mountain drainage basins. Geological Society of America Bulletin, 109(5): 596-611.

Montgomery, D.R., Collins, B.D., Buffington, J.M. and Abbe, T.B., 2003. Geomorphic effects of wood in rivers. In: S.V. Gregory, K.L. Boyer and A.M. Gurnell (Editors), The Ecology and Management of Wood in World Rivers. American Fisheries Society, Bethesda, MD, pp. 21-47.

Mussetter, R.A., 1989. Dynamics of mountain streams. Ph.D. Thesis, Colorado State University, Fort Collins.

Naghash, M., 1994. Void fraction measurement techniques for gas-liquid bubbly flow in closed conduits; a literature review. In: C.A. Pugh (Editor), Fundamentals and Advancements in Hydraulic Measurements and Experimentation. American Society of Civil Engineers, Buffalo, NY, pp. 278-288.

Nakamura, F. and Swanson, F.J., 1993. Effects of coarse woody debris on morphology and sediment storage of a mountain stream system in western Oregon. Earth Surface Processes and Landforms, 18(1): 43-61.

Nelson, J.M., McLean, S.R. and Wolfe, S.R., 1993. Mean flow and turbulence fields over two-dimensional bed forms. Water Resources Research, 29(12): 3935-3953.

Nelson, J.M., Shreve, R.L., McLean, S.R. and Drake, T.G., 1995. Role of near-bed turbulence structure in bed-load transport and bed form mechanics. Water Resources Research, 31(8): 2071-2086.

Nepf, H.M., 1999. Drag, turbulence, and diffusion in flow through emergent vegetation. Water Resources Research, 35(2): 479-489.

Nezu, I. and Nakagawa, H., 1993. Turbulence in Open-Channel Flows. IAHR Monograph Series. A.A. Balkema, Rotterdam, 281 pp.

Nikora, V.I. and Goring, D.G., 1998. ADV measurements of turbulence: Can we improve their interpretation? Journal of Hydraulic Engineering, 124(6): 630-634.

O'Connor, M.D. and Ziemer, R.R., 1989. Coarse woody debris ecology in a second-growth *Sequoia sempervirens* forest stream. General Technical Report PSW-110, USDA Forest Service, Pacific Southwest Forest and Range Experiment Station, Arcata, CA.

Ott, R.L. and Longnecker, M., 2001. An Introduction to Statistical Methods and Data Analysis. Duxbury, Pacific Grove, CA, 1152 pp.

Parker, G., 2004. 1D Sediment Transport Morphodynamics with Applications to Rivers and Turbidity Currents. In: S.A.F. Laboratory (Editor). University of Minnesota, pp. e-book.

Parker, G. and Peterson, A.W., 1980. Bar resistance of gravel-bed streams. Journal of the Hydraulics Division-Asce, 106(10): 1559-1573.

Peakall, J., Ashworth, P. and Best, J.L., 1996. Physical modelling in fluvial geomorphology: Principles, applications and unresolved issues. In: B.L. Rhoads and C.R. Thorne (Editors), The Scientific Nature of Geomorphology. Wiley, pp. 221-253.

Peterson, D.F. and Mohanty, P.K., 1960. Flume studies of flow in steep, rough channels. Journal of the Hydraulics Division-Asce, 86(HY9): 55-76.

Petryk, S. and Bosmajian, G.I., 1975. Analysis of flow through vegetation. Journal of the Hydraulics Division-Asce, 101(HY7): 871-884.

Prestegaard, K.L., 1983a. Variables influencing water-surface slopes in gravel-bed streams at bankfull stage. Geological Society of America Bulletin, 94: 673-678.

Prestegaard, K.L., 1983b. Bar resistance in gravel bed streams at bankfull stage. Water Resources Research, 19(2): 472-476.

Ranga Raju, K.G., Rana, O.P.S., Asawa, G.L. and Pillai, A.S.N., 1983. Rational assessment of blockage effect in channel flow past smooth circular cylinders. Journal of Hydraulic Research, 21(4): 289-302.

Richmond, A.D. and Fausch, K.D., 1995. Characteristics and function of large woody debris in sub-alpine Rocky-Mountain streams in northern Colorado. Canadian Journal of Fisheries and Aquatic Sciences, 52(8): 1789-1802.

Roberson, J.A. and Crowe, C.T., 1993. Engineering Fluid Mechanics. Wiley, New York, 823 pp.

Robert, A., 1993. Bed configuration and microscale processes in alluvial channels. Progress in Physical Geography, 17(2): 123-136.

Robert, A., Roy, A.G. and Deserres, B., 1992. Changes in velocity profiles at roughness transitions in coarse-grained channels. Sedimentology, 39(5): 725-735.

Robert, A., Roy, A.G. and DeSerres, B., 1996. Turbulence at a roughness transition in a depth limited flow over a gravel bed. Geomorphology, 16(2): 175-187.

Robison, E.G. and Beschta, R.L., 1990. Coarse woody debris and channel morphology interactions for undisturbed streams in southeast Alaska, USA. Earth Surface Processes and Landforms, 15(2): 149-156.

Roni, P. and Quinn, T.P., 2001. Density and size of juvenile salmonids in response to placement of large woody debris in western Oregon and Washington streams. Canadian Journal of Fisheries and Aquatic Sciences, 58(2): 282-292.

Roy, A.G., Biron, P. and DeSerres, B., 1996. On the necessity of applying a rotation to instantaneous velocity measurements in river flows. Earth Surface Processes and Landforms, 21(9): 817-827.

Roy, A.G., Buffin-Belanger, T., Lamarre, H. and Kirkbride, A.D., 2004. Size, shape and dynamics of large-scale turbulent flow structures in a gravel-bed river. Journal of Fluid Mechanics, 500: 1-27.

Ryan, S., 1997. Morphologic response of subalpine streams to transbasin flow diversion. Journal of the American Water Resources Association, 33(4): 839-854.

SAS, 2004. Statistical Analysis Software, Cary, NC.

Shields, F.D. and Gippel, C.J., 1995. Prediction of effects of woody debris removal on flow resistance. Journal of Hydraulic Engineering, 121(4): 341-354.

Shields, F.D. and Smith, R.H., 1992. Effects of large woody debris removal on physical characteristics of a sand-bed river. Aquatic Conservation-Marine and Freshwater Ecosystems, 2(2): 145-163.

Simons, D.B. and Richardson, E.V., 1966. Resistance to flow in alluvial channels. United States Geological Survey Professional Paper 422J.

Smith, R.D., Sidle, R.C. and Porter, P.E., 1993. Effects on bedload transport of experimental removal of woody debris from a forest gravel-bed stream. Earth Surface Processes and Landforms, 18(5): 455-468.

SonTek, 2001. FlowTracker Handheld ADV Technical Documentation, San Diego, CA.

SonTek/YSI, 2001. Acoustic Doppler Velocimeter Principles of Operation, San Diego, CA.

Sukhodolov, A., Thiele, M. and Bungartz, H., 1998. Turbulence structure in a river reach with sand bed. Water Resources Research, 34(5): 1317-1334.

Sukhodolov, A.N. and Rhoads, B.L., 2001. Field investigation of three-dimensional flow structure at stream confluences 2. Turbulence. Water Resources Research, 37(9): 2411-2424.

Tritton, D.J., 1988. Physical Fluid Dynamics. Clarendon Press, Oxford.

USGS, 1977. National handbook of recommended methods for water-data acquisition, USGS, Reston, VA.

Valle, B.L. and Pasternack, G.B., 2002. TDR measurements of hydraulic jump aeration in the South Fork of the American River, California. Geomorphology, 42(1-2): 153-165.

Valle, B.L. and Pasternack, G.B., in press. Submerged and unsubmerged natural hydraulic jumps in a bedrock step-pool mountain channel. Geomorphology.

van Rijn, L.C., 1984. Sediment transport, part III: Bedforms and alluvial roughness. Journal of the Hydraulics Division ASCE, 110: 1733-1754.

Vanoni, V.A. and Nomicos, G.N., 1960. Resistance properties of sediment-laden streams. ASCE Transactions, 125: 1140-1167.

Voulgaris, G. and Trowbridge, J.H., 1998. Evaluation of the acoustic Doppler velocimeter (ADV) for turbulence measurements. Journal of Atmospheric and Oceanic Technology, 15(1): 272-289.

Wahl, T.L., 2000. Analyzing ADV data using WinADV, Joint Conference on Water Resources Engineering and Water Resources Planning & Management, Minneapolis, MN.

Walker, I.J. and Roy, A.G., 2005. Fluid flow and sediment transport processes in geomorphology: innovations, insights, and advances in measurement. Geomorphology, 68(1-2): 1-2.

Wallerstein, N.P., Alonso, C.V., Bennett, S.J. and Thorne, C.R., 2001. Distorted Froude-scaled flume analysis of large woody debris. Earth Surface Processes and Landforms, 26(12): 1265-1283.

Wallerstein, N.P., Alonso, C.V., Bennett, S.J. and Thorne, C.R., 2002. Surface wave forces acting on submerged logs. Journal of Hydraulic Engineering, 128(3): 349-353.

Whiting, P.J. and Dietrich, W.E., 1990. Boundary shear-stress and roughness over mobile alluvial beds. Journal of Hydraulic Engineering, 116(12): 1495-1511.

Whittaker, J.G. and Jaeggi, M.N.R., 1982. Origin of step-pool systems in mountain streams. Journal of the Hydraulics Division, 108(6): 758-773.

Wiberg, P.L. and Rubin, D.M., 1989. Bed roughness produced by saltating sediment. Journal of Geophysical Research-Oceans, 94(C4): 5011-5016.

Wiberg, P.L. and Smith, J.D., 1991. Velocity distribution and bed roughness in high-gradient streams. Water Resources Research, 27(5): 825-838.

Williams, G., 1970. Flume width and water depth effects in sediment- transport experiments. United States Geological Survey Professional Paper 562-H.

Wohl, E., 2000a. Mountain Rivers. Water Resources Monograph, 14. American Geophysical Union, Washington DC, 320 pp.

Wohl, E.E., 2000b. Substrate influences on step-pool sequences in the Christopher Creek drainage, Arizona. Journal of Geology, 108(1): 121-129.

Wohl, E.E. and Grodek, T., 1994. Channel bed-steps along Nahal-Yael, Negev Desert, Israel. Geomorphology, 9(2): 117-126.

Wohl, E.E. and Thompson, D.M., 2000. Velocity characteristics along a small step-pool channel. Earth Surface Processes and Landforms, 25(4): 353-367.

Wooldridge, C.L. and Hickin, E.J., 2002. Step-pool and cascade morphology, Mosquito Creek, British Columbia: a test of four analytical techniques. Canadian Journal of Earth Sciences, 39(4): 493-503.

Wright, S. and Parker, G., 2004. Flow resistance and suspended load in sand-bed rivers: Simplified stratification model. Journal of Hydraulic Engineering, 130(8): 796-805.

Yager, E., Kirchner, J.W., Dietrich, W.E. and Furbish, D.J., 2002. Prediction of sediment transport in steep boulder-bed channels. EOS Trans. AGU Fall Meet. Suppl., 83(47): Abstract H21G-03.

Young, W.J., 1991. Flume study of the hydraulic effects of large woody debris in lowland rivers. Regulated Rivers: Research and Management, 6: 203-211.

Zimmermann, A. and Church, M., 2001. Channel morphology, gradient profiles and bed stresses during flood in a step-pool channel. Geomorphology, 40(3-4): 311-327.

APPENDIX A: HYDRAULICS DATA AND ROUGHNESS CONFIGURATIONS FOR FLUME RUNS

Hydraulics data and roughness configurations for flume runs. Abbreviations are as follows: *Q*=discharge, *V*=reach-average velocity, *d*=flow depth, *f*=Darcy-Weisbach friction factor, *Fr*=Froude number, perp=perpendicular, comb=combination (of perpendicular and ramped pieces). Missing data (denoted ".") represent runs that were eliminated because of flow calibration problems.

Run	*Q* (L/s)	Bed slope (m/m)	LWD density	LWD orient.	LWD length	LWD arrange-ment	Steps?	Grains?	*V* (m/s)	*d* (m)	*f*	*Fr*
1	4	0.14	none	n/a	n/a	n/a	N	N	1.08	0.01	0.06	4.5
2	8	0.14	none	n/a	n/a	n/a	N	N	1.37	0.01	0.06	4.4
3	16	0.14	none	n/a	n/a	n/a	N	N	1.59	0.02	0.07	3.9
4	32	0.14	none	n/a	n/a	n/a	N	N	1.80	0.03	0.10	3.3
5	64	0.14	none	n/a	n/a	n/a	N	N	2.19	0.05	0.11	3.2
6	4	0.14	none	n/a	n/a	n/a	N	Y	0.39	0.02	1.17	1.0
7	8	0.14	none	n/a	n/a	n/a	N	Y	0.56	0.02	0.82	1.2
8	16	0.14	none	n/a	n/a	n/a	N	Y	0.78	0.03	0.60	1.4
9	32	0.14	none	n/a	n/a	n/a	N	Y	1.26	0.04	0.29	2.0
10	64	0.14	none	n/a	n/a	n/a	N	Y	1.50	0.07	0.34	1.8
11	4	0.14	none	n/a	n/a	n/a	Y	Y	0.18	0.04	12.69	0.3
12	8	0.14	none	n/a	n/a	n/a	Y	Y	0.28	0.05	6.42	0.4
13	16	0.14	none	n/a	n/a	n/a	Y	Y	0.54	0.05	1.80	0.8
14	32	0.14	none	n/a	n/a	n/a	Y	Y	1.05	0.05	0.51	1.5
15	64	0.14	none	n/a	n/a	n/a	Y	Y	1.37	0.08	0.44	1.6
16	4	0.14	low	perp	long	single	N	Y	0.39	0.02	1.22	1.0
17	8	0.14	low	perp	long	single	N	Y	0.52	0.03	1.00	1.1
18	16	0.14	low	perp	long	single	N	Y	0.73	0.04	0.73	1.2
19	32	0.14	low	perp	long	single	N	Y	.	.	.	.
20	64	0.14	low	perp	long	single	N	Y	1.37	0.08	0.44	1.6
21	4	0.14	medium	perp	long	single	N	Y	0.37	0.02	1.43	0.9
22	8	0.14	medium	perp	long	single	N	Y	0.47	0.03	1.41	0.9
23	16	0.14	medium	perp	long	single	N	Y	0.68	0.04	0.91	1.1
24	32	0.14	medium	perp	long	single	N	Y	.	.	.	.
25	64	0.14	medium	perp	long	single	N	Y	1.23	0.09	0.61	1.3
26	4	0.14	high	perp	long	single	N	Y	0.35	0.02	1.67	0.8
27	8	0.14	high	perp	long	single	N	Y	0.39	0.03	2.48	0.7

Run	*Q* (L/s)	Bed slope (m/m)	LWD density	LWD orient.	LWD length	LWD arrange-ment	Steps?	Grains?	*V* (m/s)	*d* (m)	*f*	*Fr*
28	16	0.14	high	perp	long	single	N	Y	0.58	0.05	1.52	0.9
29	32	0.14	high	perp	long	single	N	Y	.	.	.	.
30	64	0.14	high	perp	long	single	N	Y	1.09	0.10	0.88	1.1
31	4	0.14	low	perp	long	single	Y	N	0.26	0.03	4.10	0.5
32	8	0.14	low	perp	long	single	Y	N	0.30	0.04	5.14	0.5
33	16	0.14	low	perp	long	single	Y	N	0.55	0.05	1.70	0.8
34	32	0.14	low	perp	long	single	Y	N	0.83	0.07	1.07	1.0
35	64	0.14	low	perp	long	single	Y	N	1.27	0.08	0.56	1.4
36	4	0.14	medium	perp	long	single	Y	N	0.19	0.03	10.04	0.3
37	8	0.14	medium	perp	long	single	Y	N	0.21	0.06	16.11	0.3
38	16	0.14	medium	perp	long	single	Y	N	0.35	0.08	6.95	0.4
39	32	0.14	medium	perp	long	single	Y	N	0.57	0.10	3.23	0.6
40	64	0.14	medium	perp	long	single	Y	N	1.12	0.09	0.81	1.2
41	4	0.14	high	perp	long	single	Y	N	0.18	0.04	13.23	0.3
42	8	0.14	high	perp	long	single	Y	N	0.21	0.06	15.60	0.3
43	16	0.14	high	perp	long	single	Y	N	0.34	0.08	7.28	0.4
44	32	0.14	high	perp	long	single	Y	N	0.53	0.10	4.14	0.5
45	64	0.14	high	perp	long	single	Y	N	1.06	0.10	0.94	1.1
46	4	0.14	none	none	none	none	Y	N	0.35	0.02	1.71	0.8
47	8	0.14	none	none	none	none	Y	N	0.65	0.02	0.53	1.4
48	16	0.14	none	none	none	none	Y	N	1.01	0.03	0.28	2.0
49	32	0.14	none	none	none	none	Y	N	1.16	0.05	0.37	1.7
50	64	0.14	none	none	none	none	Y	N	1.54	0.07	0.31	1.9
51	4	0.14	low	perp	long	single	Y	Y	0.16	0.04	16.72	0.3
52	8	0.14	low	perp	long	single	Y	Y	0.23	0.06	12.06	0.3
53	16	0.14	low	perp	long	single	Y	Y	0.39	0.07	4.77	0.5
54	32	0.14	low	perp	long	single	Y	Y	0.91	0.06	0.76	1.2
55	64	0.14	low	perp	long	single	Y	Y	1.16	0.09	0.73	1.2
56	4	0.14	medium	perp	long	single	Y	Y	0.16	0.04	19.38	0.2
57	8	0.14	medium	perp	long	single	Y	Y	0.20	0.07	18.29	0.2
58	16	0.14	medium	perp	long	single	Y	Y	0.33	0.08	8.32	0.4
59	32	0.14	medium	perp	long	single	Y	Y	0.57	0.09	2.93	0.6

Run	*Q* (L/s)	Bed slope (m/m)	LWD density	LWD orient.	LWD length	LWD arrange-ment	Steps?	Grains?	*V* (m/s)	*d* (m)	*f*	*Fr*
60	64	0.14	medium	perp	long	single	Y	Y	1.01	0.10	1.13	1.0
61	4	0.14	high	perp	long	single	Y	Y	0.14	0.05	24.98	0.2
62	8	0.14	high	perp	long	single	Y	Y	0.20	0.07	17.76	0.3
63	16	0.14	high	perp	long	single	Y	Y	0.33	0.08	7.95	0.4
64	32	0.14	high	perp	long	single	Y	Y	0.59	0.09	2.86	0.6
65	64	0.14	high	perp	long	single	Y	Y	1.02	0.10	1.08	1.0
66	8	0.14	high	ramp	long	single	Y	Y	0.26	0.05	8.27	0.4
67	32	0.14	high	ramp	long	single	Y	Y	0.54	0.10	3.66	0.6
68	8	0.14	medium	ramp	long	single	Y	Y	0.27	0.05	7.34	0.4
69	32	0.14	medium	ramp	long	single	Y	Y	0.75	0.07	1.36	0.9
70	8	0.14	low	ramp	long	single	Y	Y	0.27	0.05	7.18	0.4
71	32	0.14	low	ramp	long	single	Y	Y	0.80	0.07	1.14	1.0
72	8	0.14	high	comb	long	single	Y	Y	0.20	0.07	18.85	0.2
73	32	0.14	high	comb	long	single	Y	Y	0.48	0.11	5.14	0.5
74	8	0.14	medium	comb	long	single	Y	Y	0.24	0.05	10.51	0.3
75	32	0.14	medium	comb	long	single	Y	Y	0.57	0.09	2.98	0.6
76	8	0.14	low	comb	long	single	Y	Y	0.26	0.05	8.15	0.4
77	32	0.14	low	comb	long	single	Y	Y	0.78	0.07	1.23	1.0
78	8	0.14	high	perp	short	single	Y	Y	0.19	0.07	19.96	0.2
79	32	0.14	high	perp	short	single	Y	Y	0.51	0.10	4.12	0.5
80	8	0.14	medium	perp	short	single	Y	Y	0.27	0.05	7.48	0.4
81	32	0.14	medium	perp	short	single	Y	Y	0.60	0.09	2.75	0.6
82	8	0.14	low	perp	short	single	Y	Y	0.22	0.06	13.94	0.3
83	32	0.14	low	perp	short	single	Y	Y	0.69	0.07	1.73	0.8
84	8	0.14	high	ramp	short	single	Y	Y	0.27	0.05	7.66	0.4
85	32	0.14	high	ramp	short	single	Y	Y	0.63	0.08	2.29	0.7
86	8	0.14	medium	ramp	short	single	Y	Y	0.31	0.04	4.97	0.5
87	32	0.14	medium	ramp	short	single	Y	Y	0.61	0.08	2.49	0.7
88	8	0.14	low	ramp	short	single	Y	Y	0.33	0.04	4.12	0.5
89	32	0.14	low	ramp	short	single	Y	Y	0.81	0.06	1.08	1.0
90	8	0.14	high	comb	short	single	Y	Y	0.23	0.06	11.79	0.3
91	32	0.14	high	comb	short	single	Y	Y	0.48	0.11	5.17	0.5

Run	*Q* (L/s)	Bed slope (m/m)	LWD density	LWD orient.	LWD length	LWD arrange-ment	Steps?	Grains?	*V* (m/s)	*d* (m)	*f*	*Fr*
92	8	0.14	medium	comb	short	single	Y	Y	0.26	0.05	8.57	0.4
93	32	0.14	medium	comb	short	single	Y	Y	0.59	0.08	2.57	0.7
94	8	0.14	low	comb	short	single	Y	Y	0.26	0.05	8.34	0.4
95	32	0.14	low	comb	short	single	Y	Y	0.77	0.07	1.34	0.9
96	8	0.14	high	perp	long	stacked	Y	Y	0.17	0.08	30.46	0.2
97	32	0.14	high	perp	long	stacked	Y	Y	0.40	0.13	9.25	0.3
98	8	0.14	medium	perp	long	stacked	Y	Y	0.25	0.05	8.98	0.4
99	32	0.14	medium	perp	long	stacked	Y	Y	0.64	0.08	2.19	0.7
100	8	0.14	low	perp	long	stacked	Y	Y	0.29	0.05	5.99	0.4
101	32	0.14	low	perp	long	stacked	Y	Y	0.80	0.07	1.15	1.0
102	8	0.14	high	ramp	long	stacked	Y	Y	0.27	0.05	7.49	0.4
103	32	0.14	high	ramp	long	stacked	Y	Y	0.55	0.09	3.39	0.6
104	8	0.14	medium	ramp	long	stacked	Y	Y	0.30	0.04	5.30	0.5
105	32	0.14	medium	ramp	long	stacked	Y	Y	0.71	0.07	1.57	0.8
106	8	0.14	low	ramp	long	stacked	Y	Y	0.28	0.05	6.20	0.4
107	32	0.14	low	ramp	long	stacked	Y	Y	0.80	0.07	1.13	1.0
108	8	0.14	high	comb	long	stacked	Y	Y	0.24	0.05	10.45	0.3
109	32	0.14	high	comb	long	stacked	Y	Y	0.50	0.10	4.49	0.5
110	8	0.14	medium	comb	long	stacked	Y	Y	0.26	0.05	8.28	0.4
111	32	0.14	medium	comb	long	stacked	Y	Y	0.66	0.08	1.98	0.8
112	8	0.14	low	comb	long	stacked	Y	Y	0.28	0.05	6.38	0.4
113	32	0.14	low	comb	long	stacked	Y	Y	0.78	0.07	1.20	1.0
114	8	0.14	high	comb	n/a	jam	Y	Y	0.23	0.06	11.95	0.3
115	32	0.14	high	comb	n/a	jam	Y	Y	0.62	0.09	2.47	0.7
116	8	0.14	medium	comb	n/a	jam	Y	Y	0.25	0.05	9.15	0.3
117	32	0.14	medium	comb	n/a	jam	Y	Y	0.75	0.07	1.35	0.9
118	8	0.14	low	comb	n/a	jam	Y	Y	0.27	0.05	7.41	0.4
119	32	0.14	low	comb	n/a	jam	Y	Y	0.82	0.06	1.06	1.0
120	8	0.14	high	perp	rootwad	single	Y	Y	0.23	0.06	11.36	0.3
121	32	0.14	high	perp	rootwad	single	Y	Y	0.52	0.10	4.00	0.5
122	8	0.14	medium	perp	rootwad	single	Y	Y	0.27	0.05	7.46	0.4
123	32	0.14	medium	perp	rootwad	single	Y	Y	0.63	0.08	2.29	0.7

Run	*Q* (L/s)	Bed slope (m/m)	LWD density	LWD orient.	LWD length	LWD arrange-ment	Steps?	Grains?	*V* (m/s)	*d* (m)	*f*	*Fr*
124	8	0.14	low	perp	rootwad	single	Y	Y	0.25	0.05	9.13	0.3
125	32	0.14	low	perp	rootwad	single	Y	Y	0.67	0.08	1.86	0.8
126	8	0.14	high	ramp	rootwad	single	Y	Y	0.26	0.05	7.81	0.4
127	32	0.14	high	ramp	rootwad	single	Y	Y	0.62	0.08	2.41	0.7
128	8	0.14	medium	ramp	rootwad	single	Y	Y	0.29	0.05	5.92	0.4
129	32	0.14	medium	ramp	rootwad	single	Y	Y	0.77	0.07	1.26	0.9
130	8	0.14	low	ramp	rootwad	single	Y	Y	0.31	0.04	4.83	0.5
131	32	0.14	low	ramp	rootwad	single	Y	Y	0.83	0.06	0.98	1.1
132	4	0.10	none	n/a	n/a	n/a	N	N	1.03	0.01	0.05	4.1
133	8	0.10	none	n/a	n/a	n/a	N	N	1.32	0.01	0.05	4.2
134	16	0.10	none	n/a	n/a	n/a	N	N	1.46	0.02	0.07	3.5
135	32	0.10	none	n/a	n/a	n/a	N	N	1.81	0.03	0.07	3.4
136	64	0.10	none	n/a	n/a	n/a	N	N	1.98	0.05	0.11	2.7
137	4	0.10	none	n/a	n/a	n/a	N	Y	0.35	0.02	1.28	0.8
138	8	0.10	none	n/a	n/a	n/a	N	Y	0.55	0.02	0.66	1.1
139	16	0.10	none	n/a	n/a	n/a	N	Y	0.77	0.03	0.48	1.3
140	32	0.10	none	n/a	n/a	n/a	N	Y	1.19	0.04	0.25	1.8
141	64	0.10	none	n/a	n/a	n/a	N	Y	1.53	0.07	0.24	1.9
142	4	0.10	none	n/a	n/a	n/a	Y	N	0.24	0.03	3.98	0.5
143	8	0.10	none	n/a	n/a	n/a	Y	N	0.68	0.02	0.34	1.6
144	16	0.10	none	n/a	n/a	n/a	Y	N	1.07	0.02	0.17	2.2
145	32	0.10	none	n/a	n/a	n/a	Y	N	1.25	0.04	0.22	1.9
146	64	0.10	none	n/a	n/a	n/a	Y	N	1.54	0.07	0.23	1.9
147	4	0.10	low	perp	long	single	Y	N	0.24	0.03	3.95	0.5
148	8	0.10	low	perp	long	single	Y	N	0.37	0.04	2.17	0.6
149	16	0.10	low	perp	long	single	Y	N	0.41	0.06	3.04	0.5
150	32	0.10	low	perp	long	single	Y	N	1.16	0.05	0.28	1.7
151	64	0.10	low	perp	long	single	Y	N	1.36	0.08	0.33	1.6
152	4	0.10	medium	perp	long	single	Y	N	0.14	0.05	19.65	0.2
153	8	0.10	medium	perp	long	single	Y	N	0.21	0.06	10.75	0.3
154	16	0.10	medium	perp	long	single	Y	N	0.35	0.08	5.02	0.4
155	32	0.10	medium	perp	long	single	Y	N	0.70	0.08	1.29	0.8

Run	*Q* (L/s)	Bed slope (m/m)	LWD density	LWD orient.	LWD length	LWD arrange-ment	Steps?	Grains?	*V* (m/s)	*d* (m)	*f*	*Fr*
156	64	0.10	medium	perp	long	single	Y	N	1.20	0.09	0.49	1.3
157	4	0.10	high	perp	long	single	Y	N	0.11	0.06	44.60	0.1
158	8	0.10	high	perp	long	single	Y	N	0.19	0.07	16.76	0.2
159	16	0.10	high	perp	long	single	Y	N	0.33	0.08	6.01	0.4
160	32	0.10	high	perp	long	single	Y	N	0.52	0.10	3.12	0.5
161	64	0.10	high	perp	long	single	Y	N	0.99	0.10	0.87	1.0
162	4	0.10	none	none	none	none	Y	Y	0.18	0.04	9.71	0.3
163	8	0.10	none	none	none	none	Y	Y	0.28	0.05	4.66	0.4
164	16	0.10	none	none	none	none	Y	Y	0.46	0.06	2.21	0.6
165	32	0.10	none	none	none	none	Y	Y	0.88	0.06	0.63	1.1
166	64	0.10	none	none	none	none	Y	Y	1.37	0.08	0.33	1.6
167	4	0.10	low	perp	long	single	Y	Y	0.16	0.04	12.02	0.3
168	8	0.10	low	perp	long	single	Y	Y	0.22	0.06	9.80	0.3
169	16	0.10	low	perp	long	single	Y	Y	0.35	0.07	5.00	0.4
170	32	0.10	low	perp	long	single	Y	Y	0.66	0.08	1.48	0.7
171	64	0.10	low	perp	long	single	Y	Y	1.14	0.09	0.59	1.2
172	4	0.10	medium	perp	long	single	Y	Y	0.14	0.05	18.79	0.2
173	8	0.10	medium	perp	long	single	Y	Y	0.20	0.07	13.72	0.2
174	16	0.10	medium	perp	long	single	Y	Y	0.31	0.08	7.27	0.3
175	32	0.10	medium	perp	long	single	Y	Y	0.58	0.09	2.16	0.6
176	64	0.10	medium	perp	long	single	Y	Y	1.10	0.09	0.64	1.1
177	4	0.10	high	perp	long	single	Y	Y	0.14	0.05	20.99	0.2
178	8	0.10	high	perp	long	single	Y	Y	0.19	0.07	16.76	0.2
179	16	0.10	high	perp	long	single	Y	Y	0.31	0.09	7.47	0.3
180	32	0.10	high	perp	long	single	Y	Y	0.58	0.09	2.17	0.6
181	64	0.10	high	perp	long	single	Y	Y	1.03	0.10	0.76	1.0
182	8	0.10	high	perp	long	stacked	Y	Y	0.17	0.08	20.33	0.2
183	32	0.10	high	perp	long	stacked	Y	Y	0.43	0.12	5.59	0.4
184	8	0.10	medium	perp	long	stacked	Y	Y	0.20	0.07	14.30	0.2
185	32	0.10	medium	perp	long	stacked	Y	Y	0.48	0.11	3.74	0.5
186	8	0.10	low	perp	long	stacked	Y	Y	0.25	0.05	7.21	0.3
187	32	0.10	low	perp	long	stacked	Y	Y	0.68	0.08	1.32	0.8

Run	*Q* (L/s)	Bed slope (m/m)	LWD density	LWD orient.	LWD length	LWD arrange-ment	Steps?	Grains?	*V* (m/s)	*d* (m)	*f*	*Fr*
188	8	0.10	low	comb	long	stacked	Y	Y	0.24	0.05	7.82	0.3
189	32	0.10	low	comb	long	stacked	Y	Y	0.66	0.08	1.50	0.7
190	8	0.10	medium	comb	long	stacked	Y	Y	0.23	0.06	8.51	0.3
191	32	0.10	medium	comb	long	stacked	Y	Y	0.55	0.10	2.57	0.6
192	8	0.10	high	comb	long	stacked	Y	Y	0.18	0.07	18.12	0.2
193	32	0.10	high	comb	long	stacked	Y	Y	0.45	0.11	4.54	0.4
194	8	0.10	high	ramp	long	stacked	Y	Y	0.24	0.06	8.12	0.3
195	32	0.10	high	ramp	long	stacked	Y	Y	0.60	0.09	1.98	0.6
196	8	0.10	medium	ramp	long	stacked	Y	Y	0.25	0.05	6.64	0.4
197	32	0.10	medium	ramp	long	stacked	Y	Y	0.65	0.08	1.55	0.7
198	8	0.10	low	ramp	long	stacked	Y	Y	0.25	0.05	6.45	0.4
199	32	0.10	low	ramp	long	stacked	Y	Y	0.78	0.07	0.91	1.0
200	8	0.10	high	comb	long	single	Y	Y	0.19	0.07	16.05	0.2
201	32	0.10	high	comb	long	single	Y	Y	0.53	0.10	2.81	0.5
202	8	0.10	medium	comb	long	single	Y	Y	0.21	0.06	11.50	0.3
203	32	0.10	medium	comb	long	single	Y	Y	0.61	0.09	1.91	0.7
204	8	0.10	low	comb	long	single	Y	Y	0.24	0.06	8.06	0.3
205	32	0.10	low	comb	long	single	Y	Y	0.73	0.07	1.11	0.9
206	8	0.10	high	ramp	long	single	Y	Y	0.24	0.05	7.65	0.3
207	32	0.10	high	ramp	long	single	Y	Y	0.62	0.08	1.77	0.7
208	8	0.10	medium	ramp	long	single	Y	Y	0.25	0.05	7.31	0.3
209	32	0.10	medium	ramp	long	single	Y	Y	0.73	0.07	1.06	0.9
210	8	0.10	low	ramp	long	single	Y	Y	0.26	0.05	6.34	0.4
211	32	0.10	low	ramp	long	single	Y	Y	0.84	0.06	0.71	1.1
212	8	0.10	high	ramp	rootwad	single	Y	Y	0.25	0.05	6.77	0.4
213	32	0.10	high	ramp	rootwad	single	Y	Y	0.65	0.08	1.50	0.7
214	8	0.10	medium	ramp	rootwad	single	Y	Y	0.26	0.05	6.24	0.4
215	32	0.10	medium	ramp	rootwad	single	Y	Y	0.69	0.07	1.22	0.8
216	8	0.10	low	ramp	rootwad	single	Y	Y	0.26	0.05	5.95	0.4
217	32	0.10	low	ramp	rootwad	single	Y	Y	0.90	0.06	0.61	1.2
218	8	0.10	high	comb	rootwad	single	Y	Y	0.21	0.06	11.50	0.3
219	32	0.10	high	comb	rootwad	single	Y	Y	0.53	0.10	2.80	0.5

Run	*Q* (L/s)	Bed slope (m/m)	LWD density	LWD orient.	LWD length	LWD arrange-ment	Steps?	Grains?	*V* (m/s)	*d* (m)	*f*	*Fr*
220	8	0.10	medium	comb	rootwad	single	Y	Y	0.24	0.05	7.76	0.3
221	32	0.10	medium	comb	rootwad	single	Y	Y	0.71	0.07	1.22	0.8
222	8	0.10	low	comb	rootwad	single	Y	Y	0.26	0.05	6.10	0.4
223	32	0.10	low	comb	rootwad	single	Y	Y	0.88	0.06	0.64	1.1
224	8	0.10	high	perp	rootwad	single	Y	Y	0.19	0.07	14.73	0.2
225	32	0.10	high	perp	rootwad	single	Y	Y	0.53	0.10	2.81	0.5
226	8	0.10	medium	perp	rootwad	single	Y	Y	0.20	0.06	12.43	0.3
227	32	0.10	medium	perp	rootwad	single	Y	Y	0.54	0.10	2.66	0.6
228	8	0.10	low	perp	rootwad	single	Y	Y	0.23	0.06	8.37	0.3
229	32	0.10	low	perp	rootwad	single	Y	Y	0.68	0.08	1.35	0.8
230	8	0.10	high	perp	short	single	Y	Y	0.20	0.06	13.05	0.3
231	32	0.10	high	perp	short	single	Y	Y	0.62	0.09	1.83	0.7
232	8	0.10	medium	perp	short	single	Y	Y	0.20	0.07	13.68	0.2
233	32	0.10	medium	perp	short	single	Y	Y	0.62	0.08	1.82	0.7
234	8	0.10	low	perp	short	single	Y	Y	0.21	0.06	10.81	0.3
235	32	0.10	low	perp	short	single	Y	Y	0.69	0.08	1.32	0.8
236	8	0.10	high	comb	short	single	Y	Y	0.21	0.06	10.84	0.3
237	32	0.10	high	comb	short	single	Y	Y	0.63	0.08	1.73	0.7
238	8	0.10	medium	comb	short	single	Y	Y	0.24	0.05	7.77	0.3
239	32	0.10	medium	comb	short	single	Y	Y	0.75	0.07	1.04	0.9
240	8	0.10	low	comb	short	single	Y	Y	0.25	0.05	7.07	0.3
241	32	0.10	low	comb	short	single	Y	Y	0.69	0.08	1.29	0.8
242	8	0.10	high	ramp	short	single	Y	Y	0.22	0.06	9.96	0.3
243	32	0.10	high	ramp	short	single	Y	Y	0.56	0.09	2.39	0.6
244	8	0.10	medium	ramp	short	single	Y	Y	0.25	0.05	7.07	0.3
245	32	0.10	medium	ramp	short	single	Y	Y	0.75	0.07	1.04	0.9
246	8	0.10	low	ramp	short	single	Y	Y	0.25	0.05	7.04	0.3
247	32	0.10	low	ramp	short	single	Y	Y	0.72	0.07	1.17	0.8
248	8	0.10	high	comb	n/a	jam	Y	Y	0.20	0.07	13.65	0.2
249	32	0.10	high	comb	n/a	jam	Y	Y	0.61	0.09	1.92	0.7
250	8	0.10	medium	comb	n/a	jam	Y	Y	0.23	0.06	8.78	0.3
251	32	0.10	medium	comb	n/a	jam	Y	Y	0.77	0.07	0.96	0.9

Run	*Q* (L/s)	Bed slope (m/m)	LWD density	LWD orient.	LWD length	LWD arrange-ment	Steps?	Grains?	*V* (m/s)	*d* (m)	*f*	*Fr*
252	8	0.10	low	comb	n/a	jam	Y	Y	0.25	0.05	6.84	0.3
253	32	0.10	low	comb	n/a	jam	Y	Y	0.91	0.06	0.57	1.2
254	4	0.10	none	n/a	n/a	n/a	Y; H/L=0.2	Y	0.17	0.04	10.52	0.3
255	8	0.10	none	n/a	n/a	n/a	Y; H/L=0.2	Y	0.26	0.05	5.81	0.4
256	16	0.10	none	n/a	n/a	n/a	Y; H/L=0.2	Y	0.43	0.06	2.67	0.6
257	32	0.10	none	n/a	n/a	n/a	Y; H/L=0.2	Y	0.82	0.06	0.78	1.0
258	4	0.10	none	n/a	n/a	n/a	Y; H/L=0.07	Y	0.27	0.02	2.59	0.6
259	8	0.10	none	n/a	n/a	n/a	Y; H/L=0.07	Y	0.38	0.03	1.93	0.7
260	16	0.10	none	n/a	n/a	n/a	Y; H/L=0.07	Y	0.66	0.04	0.73	1.1
261	32	0.10	none	n/a	n/a	n/a	Y; H/L=0.07	Y	1.14	0.05	0.30	1.7
262	4	0.05	none	n/a	n/a	n/a	N	N	0.88	0.01	0.04	3.2
263	8	0.05	none	n/a	n/a	n/a	N	N	1.04	0.01	0.05	2.9
264	16	0.05	none	n/a	n/a	n/a	N	N	1.20	0.02	0.07	2.6
265	32	0.05	none	n/a	n/a	n/a	N	N	.	.	.	.
266	64	0.05	none	n/a	n/a	n/a	N	N	1.68	0.06	0.09	2.1
267	4	0.05	none	n/a	n/a	n/a	N	Y	0.32	0.02	0.89	0.7
268	8	0.05	none	n/a	n/a	n/a	N	Y	0.45	0.03	0.62	0.8
269	16	0.05	none	n/a	n/a	n/a	N	Y	0.65	0.04	0.40	1.0
270	32	0.05	none	n/a	n/a	n/a	N	Y	.	.	.	.
271	64	0.05	none	n/a	n/a	n/a	N	Y	1.20	0.09	0.26	1.3
272	4	0.05	low	perp	long	single	N	Y	0.29	0.02	1.19	0.6
273	8	0.05	low	perp	long	single	N	Y	0.40	0.03	0.90	0.7
274	16	0.05	low	perp	long	single	N	Y	0.58	0.05	0.59	0.9
275	32	0.05	low	perp	long	single	N	Y	.	.	.	.
276	64	0.05	low	perp	long	single	N	Y	1.07	0.10	0.36	1.1
277	4	0.05	medium	perp	long	single	N	Y	0.26	0.03	1.64	0.5
278	8	0.05	medium	perp	long	single	N	Y	0.32	0.04	1.71	0.5
279	16	0.05	medium	perp	long	single	N	Y	0.50	0.05	0.91	0.7
280	32	0.05	medium	perp	long	single	N	Y	.	.	.	.
281	64	0.05	medium	perp	long	single	N	Y	0.99	0.10	0.45	1.0

Run	*Q* (L/s)	Bed slope (m/m)	LWD density	LWD orient.	LWD length	LWD arrange-ment	Steps?	Grains?	*V* (m/s)	*d* (m)	*f*	*Fr*
282	4	0.05	high	perp	long	single	N	Y	0.19	0.04	4.27	0.3
283	8	0.05	high	perp	long	single	N	Y	0.25	0.05	3.72	0.3
284	16	0.05	high	perp	long	single	N	Y	0.40	0.07	1.78	0.5
285	32	0.05	high	perp	long	single	N	Y	.	.	.	.
286	64	0.05	high	perp	long	single	N	Y	0.89	0.12	0.64	0.8
287	4	0.05	none	n/a	n/a	n/a	Y	N	0.29	0.02	1.21	0.6
288	8	0.05	none	n/a	n/a	n/a	Y	N	0.58	0.02	0.28	1.2
289	16	0.05	none	n/a	n/a	n/a	Y	N	0.86	0.03	0.18	1.6
290	32	0.05	none	n/a	n/a	n/a	Y	N	1.17	0.05	0.14	1.7
291	64	0.05	none	n/a	n/a	n/a	Y	N	1.56	0.07	0.12	1.9
292	4	0.05	low	perp	long	single	Y	N	0.22	0.03	2.54	0.4
293	8	0.05	low	perp	long	single	Y	N	0.20	0.06	6.63	0.3
294	16	0.05	low	perp	long	single	Y	N	0.32	0.08	3.45	0.4
295	32	0.05	low	perp	long	single	Y	N	.	.	.	.
296	64	0.05	low	perp	long	single	Y	N	0.98	0.11	0.49	0.9
297	4	0.05	medium	perp	long	single	Y	N	0.18	0.04	5.09	0.3
298	8	0.05	medium	perp	long	single	Y	N	0.19	0.07	7.57	0.2
299	16	0.05	medium	perp	long	single	Y	N	0.31	0.08	3.63	0.3
300	32	0.05	medium	perp	long	single	Y	N	.	.	.	.
301	64	0.05	medium	perp	long	single	Y	N	0.79	0.13	0.91	0.7
302	4	0.05	high	perp	long	single	Y	N	0.16	0.04	6.80	0.3
303	8	0.05	high	perp	long	single	Y	N	0.19	0.07	8.09	0.2
304	16	0.05	high	perp	long	single	Y	N	0.31	0.09	3.86	0.3
305	32	0.05	high	perp	long	single	Y	N	.	.	.	.
306	64	0.05	high	perp	long	single	Y	N	0.71	0.15	1.25	0.6
307	4	0.05	none	n/a	n/a	n/a	Y	Y	0.18	0.04	4.51	0.3
308	8	0.05	none	n/a	n/a	n/a	Y	Y	0.29	0.05	2.41	0.4
309	16	0.05	none	n/a	n/a	n/a	Y	Y	0.48	0.05	1.03	0.7
310	32	0.05	none	n/a	n/a	n/a	Y	Y	0.85	0.06	0.36	0.0
311	64	0.05	none	n/a	n/a	n/a	Y	Y	1.26	0.08	0.22	0.0
312	4	0.05	low	perp	long	single	Y	Y	0.15	0.04	8.85	0.2
313	8	0.05	low	perp	long	single	Y	Y	0.18	0.07	9.27	0.2

Run	*Q* (L/s)	Bed slope (m/m)	LWD density	LWD orient.	LWD length	LWD arrange-ment	Steps?	Grains?	*V* (m/s)	*d* (m)	*f*	*Fr*
314	16	0.05	low	perp	long	single	Y	Y	0.30	0.09	3.97	0.3
315	32	0.05	low	perp	long	single	Y	Y	0.58	0.09	1.11	0.6
316	64	0.05	low	perp	long	single	Y	Y	0.95	0.11	0.52	0.9
317	4	0.05	medium	perp	long	single	Y	Y	0.13	0.05	12.77	0.2
318	8	0.05	medium	perp	long	single	Y	Y	0.18	0.07	9.26	0.2
319	16	0.05	medium	perp	long	single	Y	Y	0.31	0.08	3.82	0.3
320	32	0.05	medium	perp	long	single	Y	Y	0.56	0.10	1.34	0.6
321	64	0.05	medium	perp	long	single	Y	Y	0.93	0.11	0.55	0.9
322	4	0.05	high	perp	long	single	Y	Y	0.12	0.05	16.34	0.2
323	8	0.05	high	perp	long	single	Y	Y	0.19	0.07	8.75	0.2
324	16	0.05	high	perp	long	single	Y	Y	0.30	0.09	4.30	0.3
325	32	0.05	high	perp	long	single	Y	Y	0.66	0.08	0.76	0.4
326	64	0.05	high	perp	long	single	Y	Y	0.89	0.12	0.65	0.7
327	8	0.05	low	perp	short	single	Y	Y	0.20	0.06	6.73	0.3
328	32	0.05	low	perp	short	single	Y	Y	0.65	0.08	0.80	0.7
329	8	0.05	medium	perp	short	single	Y	Y	0.20	0.07	6.98	0.2
330	32	0.05	medium	perp	short	single	Y	Y	0.56	0.09	1.26	0.6
331	8	0.05	high	perp	short	single	Y	Y	0.20	0.07	6.95	0.3
332	32	0.05	high	perp	short	single	Y	Y	0.62	0.08	0.94	0.7
333	8	0.05	low	comb	short	single	Y	Y	0.21	0.06	5.90	0.3
334	32	0.05	low	comb	short	single	Y	Y	0.65	0.08	0.81	0.7
335	8	0.05	medium	comb	short	single	Y	Y	0.20	0.07	7.06	0.2
336	32	0.05	medium	comb	short	single	Y	Y	0.58	0.09	1.13	0.6
337	8	0.05	high	comb	short	single	Y	Y	0.19	0.07	8.23	0.2
338	32	0.05	high	comb	short	single	Y	Y	0.61	0.09	1.03	0.7
339	8	0.05	low	ramp	short	single	Y	Y	0.24	0.05	4.17	0.3
340	32	0.05	low	ramp	short	single	Y	Y	0.68	0.08	0.71	0.8
341	8	0.05	medium	ramp	short	single	Y	Y	0.23	0.06	4.76	0.3
342	32	0.05	medium	ramp	short	single	Y	Y	0.62	0.08	0.92	0.7
343	8	0.05	high	ramp	short	single	Y	Y	0.21	0.06	6.28	0.3
344	32	0.05	high	ramp	short	single	Y	Y	0.58	0.09	1.18	0.6
345	8	0.05	low	comb	long	single	Y	Y	0.21	0.06	5.87	0.3

Run	*Q* (L/s)	Bed slope (m/m)	LWD density	LWD orient.	LWD length	LWD arrange-ment	Steps?	Grains?	*V* (m/s)	*d* (m)	*f*	*Fr*
346	32	0.05	low	comb	long	single	Y	Y	0.65	0.08	0.83	0.7
347	8	0.05	medium	comb	long	single	Y	Y	0.19	0.07	8.69	0.2
348	32	0.05	medium	comb	long	single	Y	Y	0.58	0.09	1.14	0.6
349	8	0.05	high	comb	long	single	Y	Y	0.18	0.07	9.29	0.2
350	32	0.05	high	comb	long	single	Y	Y	0.54	0.10	1.39	0.6
351	8	0.05	low	ramp	long	single	Y	Y	0.26	0.05	3.16	0.4
352	32	0.05	low	ramp	long	single	Y	Y	0.71	0.08	0.64	0.8
353	8	0.05	medium	ramp	long	single	Y	Y	0.23	0.06	4.94	0.3
354	32	0.05	medium	ramp	long	single	Y	Y	0.63	0.08	0.90	0.7
355	8	0.05	high	ramp	long	single	Y	Y	0.22	0.06	5.48	0.3
356	32	0.05	high	ramp	long	single	Y	Y	0.58	0.09	1.17	0.6
357	8	0.05	low	ramp	long	stacked	Y	Y	0.25	0.05	3.73	0.3
358	32	0.05	low	ramp	long	stacked	Y	Y	0.62	0.08	0.92	0.7
359	8	0.05	medium	ramp	long	stacked	Y	Y	0.24	0.06	4.05	0.3
360	32	0.05	medium	ramp	long	stacked	Y	Y	0.54	0.09	1.38	0.6
361	8	0.05	high	ramp	long	stacked	Y	Y	0.20	0.07	7.42	0.2
362	32	0.05	high	ramp	long	stacked	Y	Y	0.49	0.11	1.93	0.5
363	8	0.05	low	comb	long	stacked	Y	Y	0.22	0.06	5.62	0.3
364	32	0.05	low	comb	long	stacked	Y	Y	0.54	0.10	1.41	0.6
365	8	0.05	medium	comb	long	stacked	Y	Y	0.20	0.07	7.23	0.2
366	32	0.05	medium	comb	long	stacked	Y	Y	0.45	0.12	2.41	0.4
367	8	0.05	high	comb	long	stacked	Y	Y	0.18	0.07	9.50	0.2
368	32	0.05	high	comb	long	stacked	Y	Y	0.40	0.13	3.34	0.4
369	8	0.05	low	perp	long	stacked	Y	Y	0.19	0.07	8.70	0.2
370	32	0.05	low	perp	long	stacked	Y	Y	0.43	0.12	2.73	0.4
371	8	0.05	medium	perp	long	stacked	Y	Y	0.17	0.08	10.95	0.2
372	32	0.05	medium	perp	long	stacked	Y	Y	0.37	0.14	4.55	0.3
373	8	0.05	high	perp	long	stacked	Y	Y	0.15	0.08	15.11	0.2
374	32	0.05	high	perp	long	stacked	Y	Y	0.37	0.14	4.26	0.3
375	8	0.05	low	ramp	rootwad	single	Y	Y	0.26	0.05	3.03	0.4
376	32	0.05	low	ramp	rootwad	single	Y	Y	0.75	0.07	0.55	0.9
377	8	0.05	medium	ramp	rootwad	single	Y	Y	0.24	0.05	4.01	0.3

Run	*Q* (L/s)	Bed slope (m/m)	LWD density	LWD orient.	LWD length	LWD arrange-ment	Steps?	Grains?	*V* (m/s)	*d* (m)	*f*	*Fr*
378	32	0.05	medium	ramp	rootwad	single	Y	Y	0.59	0.09	1.09	0.6
379	8	0.05	high	ramp	rootwad	single	Y	Y	0.24	0.05	3.86	0.3
380	32	0.05	high	ramp	rootwad	single	Y	Y	0.63	0.09	0.96	0.7
381	8	0.05	low	comb	rootwad	single	Y	Y	0.23	0.06	4.49	0.3
382	32	0.05	low	comb	rootwad	single	Y	Y	0.60	0.09	1.03	0.6
383	8	0.05	medium	comb	rootwad	single	Y	Y	0.20	0.06	6.60	0.3
384	32	0.05	medium	comb	rootwad	single	Y	Y	0.58	0.09	1.19	0.6
385	8	0.05	high	comb	rootwad	single	Y	Y	0.19	0.07	7.77	0.2
386	32	0.05	high	comb	rootwad	single	Y	Y	0.55	0.10	1.36	0.6
387	8	0.05	low	perp	rootwad	single	Y	Y	0.22	0.06	5.46	0.3
388	32	0.05	low	perp	rootwad	single	Y	Y	0.59	0.09	1.10	0.6
389	8	0.05	medium	perp	rootwad	single	Y	Y	0.20	0.06	6.65	0.3
390	32	0.05	medium	perp	rootwad	single	Y	Y	0.54	0.10	1.38	0.6
391	8	0.05	high	perp	rootwad	single	Y	Y	0.18	0.07	9.38	0.2
392	32	0.05	high	perp	rootwad	single	Y	Y	0.51	0.10	1.63	0.5
393	8	0.05	low	comb	n/a	jam	Y	Y	0.23	0.06	4.66	0.3
394	32	0.05	low	comb	n/a	jam	Y	Y	0.57	0.10	1.27	0.6
395	8	0.05	medium	comb	n/a	jam	Y	Y	0.18	0.07	9.10	0.2
396	32	0.05	medium	comb	n/a	jam	Y	Y	0.45	0.12	2.51	0.4
397	8	0.05	high	comb	n/a	jam	Y	Y	0.17	0.08	11.13	0.2
398	32	0.05	high	comb	n/a	jam	Y	Y	0.42	0.13	3.13	0.4
399[a]	8	0.05	low	perp	long	single	Y	Y	0.25	0.05	3.58	0.3
400[a]	32	0.05	low	perp	long	single	Y	Y	0.65	0.08	0.84	0.7
401[a]	8	0.05	medium	perp	long	single	Y	Y	0.23	0.06	4.42	0.3
402[a]	32	0.05	medium	perp	long	single	Y	Y	0.58	0.09	1.12	0.6
403[a]	8	0.05	low	perp	long	single	Y	Y	0.24	0.05	3.87	0.3
404[a]	32	0.05	low	perp	long	single	Y	Y	0.60	0.09	1.06	0.6

a. Runs 399–404 tested the effects of LWD position and entailed preferential placement of model LWD in positions away from the step lip. Arrangement of model LWD pieces on the step tread differed slightly between Runs 399–400 and 403–404.

APPENDIX B: GRAIN SIZE DISTRIBUTION OF SEDIMENTS USED IN FLUME

Grain size distribution of sediments used in flume

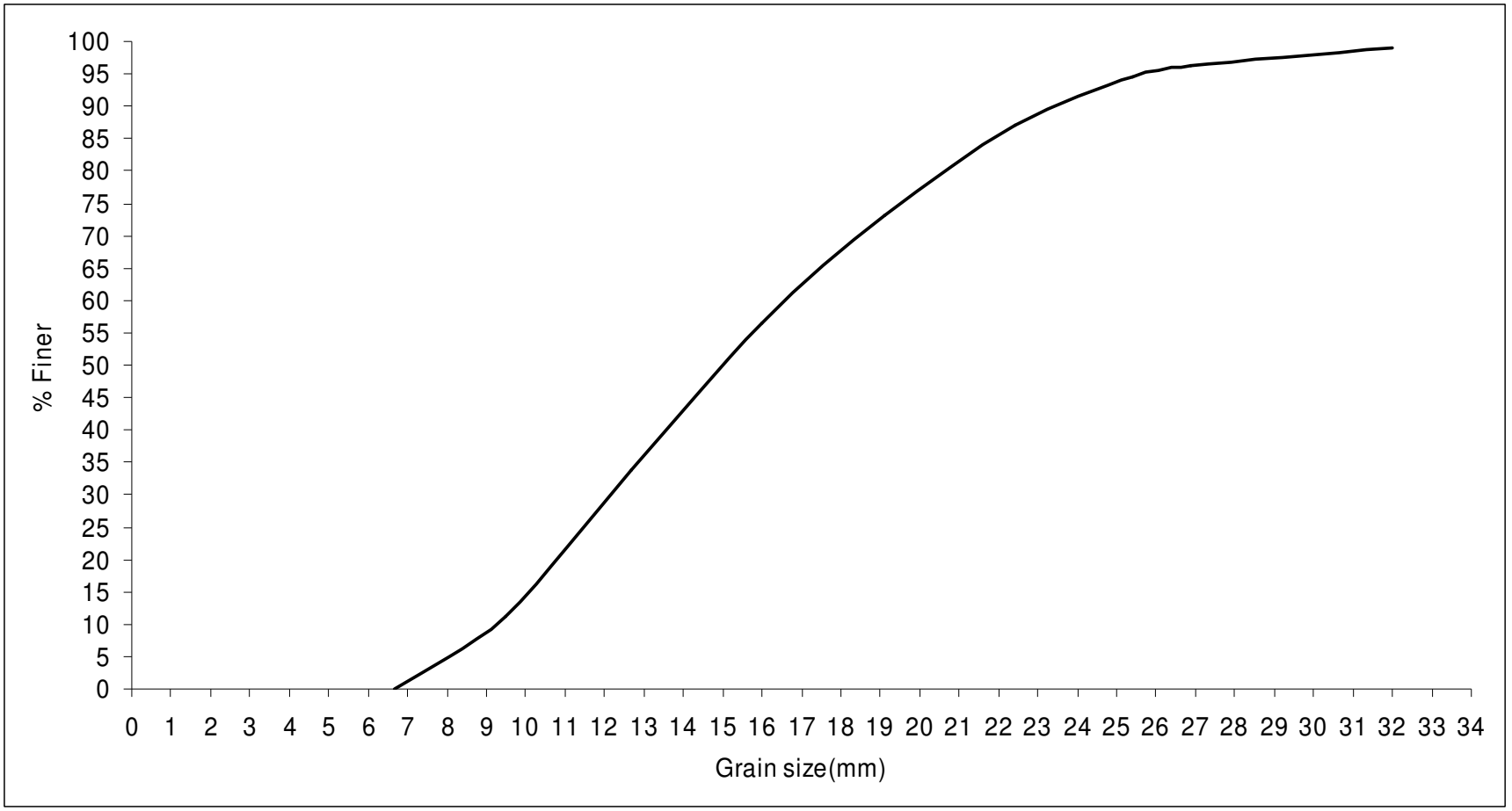

APPENDIX C: STATISTICAL OUTPUT FOR FACTORIAL ANALYSES OF VARIANCE PERFORMED TO TEST CONTROLS ON TOTAL FLOW RESISTANCE

1. **ALL 388 FLUME RUNS**
2. **LWD CONFIGURATION**
3. **LWD POSITION**
4. **STEP-GRAIN-LWD**
5. **STEP GEOMETRY**

Note: Dependent variable in all runs is log-transformed Darcy-Weisbach friction factor, abbreviated in statistical output as lff

1. Statistical output for ANOVA on all 388 flume runs, using SAS Proc GLM

Class Level Information

Class	Levels	Values
S	3	0.055 0.104 0.139
Q	5	4 8 16 32 64
LWD	2	n y
step	2	n y
grain	2	n y

Number of Observations Read 388
Number of Observations Used 388

Dependent Variable: lff

Source	DF	Sum of Squares	Mean Square	F Value	Pr > F
Model	38	615.8202721	16.2057966	69.03	<.0001
Error	349	81.9282441	0.2347514		
Corrected Total	387	697.7485162			

R-Square	Coeff Var	Root MSE	lff Mean
0.882582	55.57370	0.484512	0.871836

Source	DF	Type III SS	Mean Square	F Value	Pr > F
S	2	1.96458594	0.98229297	4.18	0.0160
Q	4	45.44770297	11.36192574	48.40	<.0001
S*Q	8	1.66767910	0.20845989	0.89	0.5266
LWD	1	31.33127805	31.33127805	133.47	<.0001
S*LWD	2	0.55636541	0.27818271	1.19	0.3070
Q*LWD	4	3.49634071	0.87408518	3.72	0.0055
step	1	30.43416470	30.43416470	129.64	<.0001
S*step	2	1.39494368	0.69747184	2.97	0.0525
Q*step	4	16.86353553	4.21588388	17.96	<.0001
LWD*step	1	0.17527943	0.17527943	0.75	0.3881
grain	1	24.56828973	24.56828973	104.66	<.0001
S*grain	2	0.11310606	0.05655303	0.24	0.7860
Q*grain	4	3.91987210	0.97996802	4.17	0.0026
LWD*grain	1	8.27963068	8.27963068	35.27	<.0001
step*grain	1	1.40420372	1.40420372	5.98	0.0149

Least Squares Means

Q	lff LSMEAN	LSMEAN Number
4	0.51548113	1
8	0.15322358	2
16	-0.25234619	3
32	-0.78607684	4
64	-1.09954560	5

Least Squares Means for effect Q
Pr > |t| for H0: LSMean(i)=LSMean(j)

i/j	1	2	3	4	5
1		0.0040	<.0001	<.0001	<.0001
2	0.0040		0.0013	<.0001	<.0001
3	<.0001	0.0013		0.0022	<.0001
4	<.0001	<.0001	0.0022		0.0713
5	<.0001	<.0001	<.0001	0.0713	

Least Squares Means

S	lff LSMEAN	LSMEAN Number
0.055	-0.45464505	1
0.104	-0.27549841	2
0.139	-0.15141489	3

Least Squares Means for effect S
Pr > |t| for H0: LSMean(i)=LSMean(j)

i/j	1	2	3
1		0.1418	0.0041
2	0.1418		0.2822
3	0.0041	0.2822	

LWD	lff LSMEAN	H0:LSMean1=LSMean2 Pr > |t|
n	-1.02561015	<.0001
y	0.43790459	

step	lff LSMEAN	H0:LSMean1=LSMean2 Pr > |t|
n	-1.02195596	<.0001
y	0.43425039	

grain	lff LSMEAN	H0:LSMean1=LSMean2 Pr > |t|
n	-0.83871295	<.0001
y	0.25100738	

2. Results of LWD configuration factorial test

Class Level Information

Class	Levels	Values
Q	2	8 32
density	3	hig low medium
orientation	3	comb perp ramp
length	4	loVS lsin root ssin
slope	3	0.055 0.104 0.139

Number of Observations Read 216
Number of Observations Used 210

Dependent Variable: lff

Source	DF	Sum of Squares	Mean Square	F Value	Pr > F
Model	122	186.1002316	1.5254117	47.13	<.0001
Error	87	2.8161045	0.0323690		
Corrected Total	209	188.9163361			

R-Square	Coeff Var	Root MSE	lff Mean
0.985093	13.94770	0.179914	1.289918

Source	DF	Type III SS	Mean Square	F Value	Pr > F
Q	1	128.0500469	128.0500469	3955.94	<.0001
density	2	12.9954697	6.4977348	200.74	<.0001
Q*density	2	1.0596714	0.5298357	16.37	<.0001
orientation	2	10.5880513	5.2940256	163.55	<.0001
Q*orientation	2	0.2700286	0.1350143	4.17	0.0186
density*orientation	4	0.1482658	0.0370665	1.15	0.3408
Q*density*orientatio	4	0.1847590	0.0461897	1.43	0.2318
length	3	2.6683825	0.8894608	27.48	<.0001
Q*length	3	1.8007108	0.6002369	18.54	<.0001
density*length	6	1.1869940	0.1978323	6.11	<.0001
Q*density*length	6	0.0685758	0.0114293	0.35	0.9063
orientation*length	6	0.8032989	0.1338831	4.14	0.0011
Q*orientation*length	6	0.4732157	0.0788693	2.44	0.0317
densit*orient*length	12	0.9301517	0.0775126	2.39	0.0100
slope	2	7.2487874	3.6243937	111.97	<.0001
Q*slope	2	0.9110268	0.4555134	14.07	<.0001
density*slope	4	1.6584785	0.4146196	12.81	<.0001
Q*density*slope	4	0.8307701	0.2076925	6.42	0.0001
orientation*slope	4	0.0599331	0.0149833	0.46	0.7628
Q*orientation*slope	4	0.1733383	0.0433346	1.34	0.2620
densit*orienta*slope	8	0.6823380	0.0852923	2.63	0.0124
length*slope	6	1.7928759	0.2988126	9.23	<.0001
Q*length*slope	6	0.6585838	0.1097640	3.39	0.0047
density*length*slope	12	0.4307107	0.0358926	1.11	0.3635
orienta*length*slope	11	1.0430024	0.0948184	2.93	0.0025

Least Squares Means

length	lff LSMEAN	LSMEAN Number
loVS	1.47357861	1
lsin	1.30078398	2
root	1.16138077	3
ssin	1.23581826	4

Least Squares Means for effect length
Pr > |t| for H0: LSMean(i)=LSMean(j)

Dependent Variable: lff

i/j	1	2	3	4
1		<.0001	<.0001	<.0001
2	<.0001		0.0010	0.0921
3	<.0001	0.0010		0.0742
4	<.0001	0.0921	0.0742	

Least Squares Means for effect Q*length

Q	length	lff LSMEAN	LSMEAN Number
8	loVS	2.13934891	1
8	lsin	2.21721878	2
8	root	1.94484045	3
8	ssin	2.07571444	4
32	loVS	0.80780830	5
32	lsin	0.38434918	6
32	root	0.37792110	7
32	ssin	0.39592209	8

Pr > |t| for H0: LSMean(i)=LSMean(j)

Dependent Variable: lff

i/j	1	2	3	4
1		0.1525	0.0012	0.2416
2	0.1525		<.0001	0.0102
3	0.0012	<.0001		0.0271
4	0.2416	0.0102	0.0271	
5	<.0001	<.0001	<.0001	<.0001
6	<.0001	<.0001	<.0001	<.0001
7	<.0001	<.0001	<.0001	<.0001
8	<.0001	<.0001	<.0001	<.0001

i/j	5	6	7	8
1	<.0001	<.0001	<.0001	<.0001
2	<.0001	<.0001	<.0001	<.0001
3	<.0001	<.0001	<.0001	<.0001
4	<.0001	<.0001	<.0001	<.0001
5		<.0001	<.0001	<.0001
6	<.0001		0.9125	0.8308
7	<.0001	0.9125		0.7583
8	<.0001	0.8308	0.7583	

Least Squares Means

density	slope	lff LSMEAN	LSMEAN Number
hig	0.055	1.18060904	1
hig	0.104	1.69650376	2
hig	0.139	1.94065228	3
low	0.055	0.81561952	4
low	0.104	1.03784081	5
low	0.139	1.08824698	6
medium	0.055	1.10289040	7
medium	0.104	1.37488466	8
medium	0.139	1.39876621	9

Least Squares Means for effect density*slope
Pr > |t| for HO: LSMean(i)=LSMean(j)
Dependent Variable: lff

i/j	1	2	3	4	5
1		<.0001	<.0001	<.0001	0.0144
2	<.0001		0.0001	<.0001	<.0001
3	<.0001	0.0001		<.0001	<.0001
4	<.0001	<.0001	<.0001		0.0002
5	0.0144	<.0001	<.0001	0.0002	
6	0.1317	<.0001	<.0001	<.0001	0.4088
7	0.1780	<.0001	<.0001	<.0001	0.2589
8	0.0010	<.0001	<.0001	<.0001	<.0001
9	0.0005	<.0001	<.0001	<.0001	<.0001

i/j	6	7	8	9
1	0.1317	0.1780	0.0010	0.0005
2	<.0001	<.0001	<.0001	<.0001
3	<.0001	<.0001	<.0001	<.0001
4	<.0001	<.0001	<.0001	<.0001
5	0.4088	0.2589	<.0001	<.0001
6		0.8101	<.0001	<.0001
7	0.8101		<.0001	<.0001
8	<.0001	<.0001		0.6951
9	<.0001	<.0001	0.6951	

Least Squares Means

Q	density	lff LSMEAN	LSMEAN Number
8	hig	2.35015518	1
8	low	1.88245068	2
8	medium	2.05023608	3
32	hig	0.86168821	4
32	low	0.07868753	5
32	medium	0.53412477	6

Least Squares Means for effect Q*density
Pr > |t| for HO: LSMean(i)=LSMean(j)

Dependent Variable: lff

i/j	1	2	3	4	5	6
1		<.0001	<.0001	<.0001	<.0001	<.0001
2	<.0001		0.0007	<.0001	<.0001	<.0001
3	<.0001	0.0007		<.0001	<.0001	<.0001
4	<.0001	<.0001	<.0001		<.0001	<.0001
5	<.0001	<.0001	<.0001	<.0001		<.0001
6	<.0001	<.0001	<.0001	<.0001	<.0001	

Least Squares Means

Q	orientation	lff LSMEAN	LSMEAN Number
8	comb	2.14141790	1
8	perp	2.38186460	2
8	ramp	1.75955945	3
32	comb	0.54618079	4
32	perp	0.68891675	5
32	ramp	0.23940296	6

Least Squares Means for effect Q*orientation
Pr > |t| for H0: LSMean(i)=LSMean(j)
Dependent Variable: lff

i/j	1	2	3	4	5	6
1		<.0001	<.0001	<.0001	<.0001	<.0001
2	<.0001		<.0001	<.0001	<.0001	<.0001
3	<.0001	<.0001		<.0001	<.0001	<.0001
4	<.0001	<.0001	<.0001		0.0049	<.0001
5	<.0001	<.0001	<.0001	0.0049		<.0001
6	<.0001	<.0001	<.0001	<.0001	<.0001	

Least Squares Means

Q	density	slope	lff LSMEAN	LSMEAN Number
8	hig	0.055	2.04944498	1
8	hig	0.104	2.49401635	2
8	hig	0.139	2.50700421	3
8	low	0.055	1.64754838	4
8	low	0.104	2.00972354	5
8	low	0.139	1.99008010	6
8	medium	0.055	1.86531309	7
8	medium	0.104	2.23059995	8
8	medium	0.139	2.05479521	9
32	hig	0.055	0.31177309	10
32	hig	0.104	0.89899117	11
32	hig	0.139	1.37430035	12
32	low	0.055	-0.01630934	13
32	low	0.104	0.06595807	14
32	low	0.139	0.18641386	15
32	medium	0.055	0.34046771	16
32	medium	0.104	0.51916938	17
32	medium	0.139	0.74273721	18

Least Squares Means for effect Q*density*slope
Pr > |t| for H0: LSMean(i)=LSMean(j)

i/j	1	2	3	4	5	6
1		<.0001	<.0001	<.0001	0.6250	0.4866
2	<.0001		0.8789	<.0001	<.0001	<.0001
3	<.0001	0.8789		<.0001	<.0001	<.0001
4	<.0001	<.0001	<.0001		<.0001	0.0001
5	0.6250	<.0001	<.0001	<.0001		0.8177
6	0.4866	<.0001	<.0001	0.0001	0.8177	
7	0.0252	<.0001	<.0001	0.0084	0.0778	0.1454
8	0.0276	0.0016	0.0016	<.0001	0.0076	0.0057
9	0.9499	<.0001	<.0001	<.0001	0.5972	0.4636
10	<.0001	<.0001	<.0001	<.0001	<.0001	<.0001
11	<.0001	<.0001	<.0001	<.0001	<.0001	<.0001
12	<.0001	<.0001	<.0001	0.0018	<.0001	<.0001
13	<.0001	<.0001	<.0001	<.0001	<.0001	<.0001
14	<.0001	<.0001	<.0001	<.0001	<.0001	<.0001
15	<.0001	<.0001	<.0001	<.0001	<.0001	<.0001
16	<.0001	<.0001	<.0001	<.0001	<.0001	<.0001
17	<.0001	<.0001	<.0001	<.0001	<.0001	<.0001
18	<.0001	<.0001	<.0001	<.0001	<.0001	<.0001

i/j	7	8	9	10	11	12
1	0.0252	0.0276	0.9499	<.0001	<.0001	<.0001
2	<.0001	0.0016	<.0001	<.0001	<.0001	<.0001
3	<.0001	0.0016	<.0001	<.0001	<.0001	<.0001
4	0.0084	<.0001	<.0001	<.0001	<.0001	0.0018
5	0.0778	0.0076	0.5972	<.0001	<.0001	<.0001
6	0.1454	0.0057	0.4636	<.0001	<.0001	<.0001
7		<.0001	0.0281	<.0001	<.0001	<.0001
8	<.0001		0.0413	<.0001	<.0001	<.0001
9	0.0281	0.0413		<.0001	<.0001	<.0001
10	<.0001	<.0001	<.0001		<.0001	<.0001
11	<.0001	<.0001	<.0001	<.0001		<.0001
12	<.0001	<.0001	<.0001	<.0001	<.0001	
13	<.0001	<.0001	<.0001	0.0001	<.0001	<.0001
14	<.0001	<.0001	<.0001	0.0031	<.0001	<.0001
15	<.0001	<.0001	<.0001	0.1435	<.0001	<.0001
16	<.0001	<.0001	<.0001	0.7240	<.0001	<.0001
17	<.0001	<.0001	<.0001	0.0120	<.0001	<.0001
18	<.0001	<.0001	<.0001	<.0001	0.0691	<.0001

i/j	13	14	15	16	17	18
1	<.0001	<.0001	<.0001	<.0001	<.0001	<.0001
2	<.0001	<.0001	<.0001	<.0001	<.0001	<.0001
3	<.0001	<.0001	<.0001	<.0001	<.0001	<.0001
4	<.0001	<.0001	<.0001	<.0001	<.0001	<.0001
5	<.0001	<.0001	<.0001	<.0001	<.0001	<.0001
6	<.0001	<.0001	<.0001	<.0001	<.0001	<.0001
7	<.0001	<.0001	<.0001	<.0001	<.0001	<.0001
8	<.0001	<.0001	<.0001	<.0001	<.0001	<.0001
9	<.0001	<.0001	<.0001	<.0001	<.0001	<.0001
10	0.0001	0.0031	0.1435	0.7240	0.0120	<.0001
11	<.0001	<.0001	<.0001	<.0001	<.0001	0.0691
12	<.0001	<.0001	<.0001	<.0001	<.0001	<.0001
13		0.3124	0.0190	<.0001	<.0001	<.0001
14	0.3124		0.1597	0.0010	<.0001	<.0001
15	0.0190	0.1597		0.0730	0.0002	<.0001
16	<.0001	0.0010	0.0730		0.0297	<.0001
17	<.0001	<.0001	0.0002	0.0297		0.0099
18	<.0001	<.0001	<.0001	<.0001	0.0099	

3. Results of LWD position factorial test

```
                    Class Level Information
                  Class         Levels    Values
                  Q                 2    8 32
                  dens              2    low medium
                  posit             3    a b c
               Number of Observations Read          10
               Number of Observations Used          10

Dependent Variable: lff
                                 Sum of
Source                    DF       Squares   Mean Square  F Value  Pr > F
Model                      6    6.45202279    1.07533713   143.86  0.0009
Error                      3    0.02242457    0.00747486
Corrected Total            9    6.47444736

           R-Square     Coeff Var      Root MSE      lff Mean
           0.996536      8.170340      0.086457      1.058184

Source                    DF   Type III SS   Mean Square  F Value  Pr > F
Q                          1    3.84908347    3.84908347   514.94  0.0002
dens                       1    0.05287830    0.05287830     7.07  0.0764
posit                      2    1.94807137    0.97403568   130.31  0.0012
Q*posit                    2    0.01891018    0.00945509     1.26  0.3996

                                      H0:LSMean1=
                                        LSMean2
                  Q       lff LSMEAN       Pr > |t|
                  8       1.68051669         0.0002
                  32      0.37257794

                                     H0:LSMean1=
                                       LSMean2
                dens      lff LSMEAN       Pr > |t|
                low       0.94524671         0.0764
                medium    1.10784792

                Least Squares Means for effect posit
                                        LSMEAN
                 posit      lff LSMEAN      Number
                 a          1.61746019           1
                 b          0.67511945           2
                 c          0.78706231           3

                Pr > |t| for H0: LSMean(i)=LSMean(j)
              i/j             1            2            3
                 1                     0.0006       0.0020
                 2        0.0006                    0.2603
                 3        0.0020       0.2603
```

4. Results of Step-grain-LWD factorial test

Class Level Information

Class	Levels	Values
Q	5	4 8 16 32 64
LWD	4	hig low medium none
S	3	0.05 0.1 0.14
step	2	n y
grain	2	n y

Number of Observations Read 180
Number of Observations Used 168

Dependent Variable: lff

Source	DF	Sum of Squares	Mean Square	F Value	Pr > F
Model	56	417.6707214	7.4584057	64.37	<.0001
Error	111	12.8622585	0.1158762		
Corrected Total	167	430.5329799			

R-Square	Coeff Var	Root MSE	lff Mean
0.970125	95.55918	0.340406	0.356225

Source	DF	Type III SS	Mean Square	F Value	Pr > F
Q	4	52.25061570	13.06265393	112.73	<.0001
LWD	3	42.67678342	14.22559447	122.77	<.0001
Q*LWD	12	4.99661090	0.41638424	3.59	0.0002
S	2	0.87994136	0.43997068	3.80	0.0254
Q*S	8	1.20953777	0.15119222	1.30	0.2485
LWD*S	6	1.67076998	0.27846166	2.40	0.0320
step	1	25.76307976	25.76307976	222.33	<.0001
Q*step	4	20.67874051	5.16968513	44.61	<.0001
LWD*step	3	1.94014927	0.64671642	5.58	0.0013
S*step	2	1.83415608	0.91707804	7.91	0.0006
grain	1	10.18529306	10.18529306	87.90	<.0001
Q*grain	4	5.26710572	1.31677643	11.36	<.0001
LWD*grain	3	8.98334367	2.99444789	25.84	<.0001
S*grain	2	0.14567364	0.07283682	0.63	0.5352
step*grain	1	0.92525489	0.92525489	7.98	0.0056

Least Squares Means

Q	lff LSMEAN	LSMEAN Number
4	0.81830145	1
8	0.64425275	2
16	0.17380381	3
32	-0.52590692	4
64	-0.88622519	5

Least Squares Means for effect Q
Pr > |t| for HO: LSMean(i)=LSMean(j)
Dependent Variable: lff

i/j	1	2	3	4	5
1		0.0644	<.0001	<.0001	<.0001
2	0.0644		<.0001	<.0001	<.0001
3	<.0001	<.0001		<.0001	<.0001
4	<.0001	<.0001	<.0001		0.0033
5	<.0001	<.0001	<.0001	0.0033	

Least Squares Means

LWD	lff LSMEAN	LSMEAN Number
hig	0.92050551	1
low	-0.20076008	2
medium	0.46192407	3
none	-1.00228878	4

Least Squares Means for effect LWD
Pr > |t| for H0: LSMean(i)=LSMean(j)
Dependent Variable: lff

i/j	1	2	3	4
1		<.0001	<.0001	<.0001
2	<.0001		<.0001	<.0001
3	<.0001	<.0001		<.0001
4	<.0001	<.0001	<.0001	

grain	lff LSMEAN	H0:LSMean1=LSMean2 Pr > |t|
n	-0.39301812	<.0001
y	0.48270848	

step	lff LSMEAN	H0:LSMean1=LSMean2 Pr > |t|
n	-0.77499175	<.0001
y	0.86468211	

Least Squares Means

step	grain	lff LSMEAN	LSMEAN Number
n	n	-1.34194788	1
n	y	-0.20803563	2
y	n	0.55591163	3
y	y	1.17345260	4

Least Squares Means for effect step*grain
Pr > |t| for H0: LSMean(i)=LSMean(j)

i/j	1	2	3	4
1		<.0001	<.0001	<.0001
2	<.0001		<.0001	<.0001
3	<.0001	<.0001		<.0001
4	<.0001	<.0001	<.0001	

Least Squares Means

LWD	step	lff LSMEAN	LSMEAN Number
hig	n	0.27140439	1
hig	y	1.56960663	2
low	n	-1.19773676	3
low	y	0.79621659	4
medium	n	-0.48250643	5
medium	y	1.40635458	6
none	n	-1.69112822	7
none	y	-0.31344934	8

Least Squares Means for effect LWD*step
Pr > |t| for HO: LSMean(i)=LSMean(j)
Dependent Variable: lff

i/j	1	2	3	4
1		<.0001	<.0001	0.0068
2	<.0001		<.0001	<.0001
3	<.0001	<.0001		<.0001
4	0.0068	<.0001	<.0001	
5	0.0002	<.0001	0.0004	<.0001
6	<.0001	0.0806	<.0001	<.0001
7	<.0001	<.0001	0.0104	<.0001
8	0.0029	<.0001	<.0001	<.0001

i/j	5	6	7	8
1	0.0002	<.0001	<.0001	0.0029
2	<.0001	0.0806	<.0001	<.0001
3	0.0004	<.0001	0.0104	<.0001
4	<.0001	<.0001	<.0001	<.0001
5		<.0001	<.0001	0.3800
6	<.0001		<.0001	<.0001
7	<.0001	<.0001		<.0001
8	0.3800	<.0001	<.0001	

Least Squares Means

LWD	grain	lff LSMEAN	LSMEAN Number
hig	n	0.80193462	1
hig	y	1.03907640	2
low	n	-0.71756302	3
low	y	0.31604285	4
medium	n	0.21557777	5
medium	y	0.70827038	6
none	n	-1.87202187	7
none	y	-0.13255569	8

Least Squares Means for effect LWD*grain
Pr > |t| for HO: LSMean(i)=LSMean(j)
Dependent Variable: lff

i/j	1	2	3	4
1		0.1428	<.0001	0.0055
2	0.1428		<.0001	<.0001
3	<.0001	<.0001		<.0001
4	0.0055	<.0001	<.0001	
5	0.0010	<.0001	<.0001	0.5590
6	0.5859	0.0024	<.0001	0.0004
7	<.0001	<.0001	<.0001	<.0001
8	<.0001	<.0001	0.0008	<.0001

i/j	5	6	7	8
1	0.0010	0.5859	<.0001	<.0001
2	<.0001	0.0024	<.0001	<.0001
3	<.0001	<.0001	<.0001	0.0008
4	0.5590	0.0004	<.0001	<.0001
5		0.0027	<.0001	0.0419
6	0.0027		<.0001	<.0001
7	<.0001	<.0001		<.0001
8	0.0419	<.0001	<.0001	

5. Results of Step geometry factorial test

```
                    Class Level Information
                Class         Levels    Values
                geom               3    0.05 0.1 0.14
                Q                  4    4 8 16 32
               Number of Observations Read          12
               Number of Observations Used          12

Dependent Variable: lff
                                 Sum of
Source                    DF       Squares   Mean Square  F Value  Pr > F
Model                      5   14.10673690    2.82134738   140.59  <.0001
Error                      6    0.12041136    0.02006856
Corrected Total           11   14.22714825

           R-Square     Coeff Var      Root MSE      lff Mean
           0.991537      18.86044      0.141664      0.751115

Source                    DF   Type III SS   Mean Square  F Value  Pr > F
geom                       2    3.37925464    1.68962732    84.19  <.0001
Q                          3   10.72748225    3.57582742   178.18  <.0001

                         Least Squares Means
                                                LSMEAN
                    geom      lff LSMEAN      Number
                    0.05      0.00917940           1
                    0.1       1.02433003           2
                    0.14      1.21983535           3

                  Least Squares Means for effect geom
                  Pr > |t| for H0: LSMean(i)=LSMean(j)

                         Dependent Variable: lff
              i/j              1             2             3
                 1                        <.0001        <.0001
                 2         <.0001                       0.0988
                 3         <.0001        0.0988

                         Least Squares Means
                                                LSMEAN
                     Q       lff LSMEAN      Number

                     4       1.85967086           1
                     8       1.31575810           2
                     16      0.47501140           3
                     32     -0.64598066           4

                   Least Squares Means for effect Q
                  Pr > |t| for H0: LSMean(i)=LSMean(j)

                         Dependent Variable: lff
        i/j              1             2             3             4
           1                       0.0033        <.0001        <.0001
           2         0.0033                      0.0003        <.0001
           3         <.0001        0.0003                      <.0001
           4         <.0001        <.0001        <.0001
```

APPENDIX D: SUMMARY DATA FOR FLUME PARTITIONING ANALYSIS: GRAIN, SPILL, AND DEBRIS RESISTANCE CALCULATED BY FOUR METHODS

Values for grain (f_{grain}), spill (f_{spill}), and debris (f_{debris}) resistance and of their respective percent contributions to total resistance, calculated by four methods of additive approach to resistance partitioning. For each of the runs below, data on roughness configuration and hydraulics, including velocity, depth, discharge, and Darcy-Weisbach friction factor values (f_{total}) are listed in Appendix A. Values for f_{grain} and $\%f_{grain}$ for Method 2 are the same as for Method 1, and values for f_{spill} and $\%f_{spill}$ are the same for Methods 3 and 4. Calculation methods are described in Chapter 4.

	Method 1						Method 3						Method 2				Method 4			
Run	f_{grain}	$\%f_{grain}$	f_{spill}	$\%f_{spill}$	f_{debris}	$\%f_{debris}$	f_{grain}	$\%f_{grain}$	f_{spill}	$\%f_{spill}$	f_{debris}	$\%f_{debris}$	f_{spill}	$\%f_{spill}$	f_{debris}	$\%f_{debris}$	f_{grain}	$\%f_{grain}$	f_{debris}	$\%f_{debris}$
51	0.3	2	12.3	74	4.1	24	11.0	66	1.7	10	4.0	24	16.3	97	0.1	1	12.6	75	2.4	14
52	0.3	2	6.1	50	5.7	47	5.9	49	0.5	4	5.6	47	11.5	95	0.3	2	6.9	57	4.6	38
53	0.3	6	1.4	30	3.1	65	1.5	32	0.3	6	3.0	62	4.3	90	0.2	4	3.1	64	1.4	30
54	0.2	29	0.3	36	0.3	35	0.2	32	0.3	35	0.2	33								
55	0.3	36	0.1	19	0.3	45	0.1	18	0.3	43	0.3	39	0.3	46	0.1	19	0.2	24	0.2	34
56	0.3	2	12.3	64	6.7	35	11.0	57	1.7	9	6.7	35	18.7	96	0.4	2	9.3	48	8.3	43
57	0.2	1	6.1	33	12.0	65	5.9	32	0.5	3	11.9	65	17.3	94	0.8	4	2.2	12	15.6	85
58	0.2	3	1.4	17	6.7	80	1.5	18	0.3	3	6.5	78	7.7	92	0.4	5	1.4	16	6.7	80
59	0.2	5	0.3	9	2.5	85	0.2	8	0.3	9	2.4	83								
60	0.2	20	0.1	12	0.8	67	0.1	12	0.3	28	0.7	61	0.6	49	0.3	30	0.3	28	0.5	44
61	0.3	1	12.3	49	12.4	50	11.0	44	1.7	7	12.3	49	24.0	96	0.7	3	11.8	47	11.5	46
62	0.2	1	6.1	34	11.4	64	5.9	33	0.5	3	11.3	64	15.5	87	2.0	11	2.2	12	15.1	85
63	0.2	3	1.4	18	6.3	79	1.5	19	0.3	4	6.1	77	6.6	83	1.1	14	0.7	8	7.0	88
64	0.2	5	0.3	10	2.4	85	0.2	9	0.3	9	2.3	82								
65	0.2	21	0.1	13	0.7	66	0.1	12	0.3	29	0.6	59	0.2	20	0.6	58	0.1	13	0.6	58
66	0.3	4	6.1	74	1.9	23	5.9	71	0.5	6	1.8	22								
67	0.1	4	0.3	7	3.2	88	0.2	7	0.3	7	3.1	86								
68	0.3	4	6.1	83	0.9	13	5.9	80	0.5	7	0.9	12								
69	0.2	14	0.3	20	0.9	66	0.2	18	0.3	20	0.9	62								
70	0.3	5	6.1	85	0.8	11	5.9	82	0.5	7	0.8	11								
71	0.2	17	0.3	24	0.7	59	0.2	21	0.3	24	0.6	55								
78	0.2	1	6.1	30	13.6	68	5.9	30	0.5	3	13.5	68								
79	0.1	4	0.3	7	3.7	90	0.2	6	0.3	6	3.6	88								
80	0.3	4	6.1	81	1.1	14	5.9	79	0.5	7	1.1	14								
81	0.2	6	0.3	10	2.3	84	0.2	9	0.3	10	2.2	81								
82	0.3	2	6.1	44	7.6	54	5.9	42	0.5	4	7.5	54								
83	0.2	10	0.3	16	1.3	74	0.2	14	0.3	16	1.2	70								

	Method 1						Method 3						Method 2				Method 4			
Run	f_{grain}	$\%f_{grain}$	f_{spill}	$\%f_{spill}$	f_{debris}	$\%f_{debris}$	f_{grain}	$\%f_{grain}$	f_{spill}	$\%f_{spill}$	f_{debris}	$\%f_{debris}$	f_{spill}	$\%f_{spill}$	f_{debris}	$\%f_{debris}$	f_{grain}	$\%f_{grain}$	f_{debris}	$\%f_{debris}$
84	0.3	4	6.1	79	1.3	16	5.9	77	0.5	7	1.2	16								
85	0.2	7	0.3	12	1.8	81	0.2	11	0.3	12	1.8	78								
87	0.2	7	0.3	11	2.1	82	0.2	10	0.3	11	2.0	79								
89	0.2	19	0.3	25	0.6	56	0.2	23	0.3	25	0.6	53								
96	0.2	1	6.1	20	24.2	79	5.9	19	0.5	2	24.0	79								
97	0.1	1	0.3	3	8.9	96	0.2	3	0.3	3	8.7	94								
98	0.3	3	6.1	68	2.6	29	5.9	66	0.5	6	2.6	29								
99	0.2	8	0.3	12	1.8	80	0.2	11	0.3	12	1.7	77								
101	0.2	17	0.3	24	0.7	59	0.2	21	0.3	23	0.6	55								
167	0.4	4	9.3	77	2.3	19	5.7	48	4.0	33	2.3	19					8.0	67	0.0	0
168	0.2	2	4.4	44	5.2	53	4.3	44	0.3	3	5.1	52					7.6	78	1.8	19
169	0.2	4	1.9	39	2.9	57	2.0	41	0.2	3	2.8	56					2.0	39	2.9	57
170	0.2	11	0.4	29	0.9	60	0.4	28	0.2	15	0.8	57								
171	0.2	32	0.1	19	0.3	49	0.1	17	0.2	40	0.3	43					0.3	43	0.1	17
172	0.4	2	9.3	49	9.2	49	5.7	31	4.0	21	9.1	48					0.0	0	14.8	79
173	0.2	2	4.4	32	9.1	67	4.3	32	0.3	2	9.1	66					3.0	22	10.4	76
174	0.2	3	1.9	27	5.1	71	2.0	28	0.2	2	5.1	70					2.2	31	4.8	67
175	0.1	7	0.4	20	1.6	73	0.4	19	0.2	10	1.5	71								
176	0.2	29	0.1	18	0.3	53	0.1	16	0.2	37	0.3	48					0.1	23	0.3	40
177	0.3	2	9.3	44	11.4	54	5.7	27	4.0	19	11.3	54					0.0	0	17.0	81
178	0.2	1	4.4	26	12.2	73	4.3	26	0.3	2	12.1	72					0.0	0	16.4	98
179	0.2	3	1.9	26	5.3	71	2.0	27	0.2	2	5.3	70					1.5	20	5.8	78
180	0.1	7	0.4	20	1.6	73	0.4	19	0.2	10	1.5	71								
181	0.2	23	0.1	15	0.5	62	0.1	13	0.2	31	0.4	56					0.0	0	0.5	69
182	0.2	1	4.4	21	15.8	78	4.3	21	0.3	2	15.7	77								
183	0.1	2	0.4	8	5.0	90	0.4	7	0.2	4	5.0	89								
184	0.2	2	4.4	30	9.7	68	4.3	30	0.3	2	9.6	67								
185	0.1	4	0.4	12	3.2	85	0.4	11	0.2	6	3.1	83								
186	0.3	4	4.4	60	2.6	36	4.3	60	0.3	5	2.5	35								
187	0.2	13	0.4	33	0.7	55	0.4	31	0.2	17	0.7	52								
206	0.3	3	4.4	57	3.0	40	4.3	57	0.3	4	3.0	39								
207	0.2	9	0.4	25	1.2	67	0.4	23	0.2	12	1.1	64								
208	0.3	4	4.4	60	2.7	37	4.3	59	0.3	5	2.6	36								
209	0.2	17	0.4	41	0.5	43	0.4	39	0.2	21	0.4	41								

	Method 1						Method 3						Method 2				Method 4			
Run	f_{grain}	$\%f_{grain}$	f_{spill}	$\%f_{spill}$	f_{debris}	$\%f_{debris}$	f_{grain}	$\%f_{grain}$	f_{spill}	$\%f_{spill}$	f_{debris}	$\%f_{debris}$	f_{spill}	$\%f_{spill}$	f_{debris}	$\%f_{debris}$	f_{grain}	$\%f_{grain}$	f_{debris}	$\%f_{debris}$
210	0.3	4	4.4	69	1.7	27	4.3	68	0.3	5	1.7	26								
211	0.2	27	0.4	61	0.1	12	0.4	58	0.2	31	0.1	11								
230	0.2	2	4.4	33	8.5	65	4.3	33	0.3	3	8.4	64								
231	0.2	8	0.4	24	1.2	68	0.4	22	0.2	12	1.2	66								
232	0.2	2	4.4	32	9.1	67	4.3	32	0.3	2	9.0	66								
233	0.2	8	0.4	24	1.2	68	0.4	23	0.2	12	1.2	65								
234	0.2	2	4.4	40	6.2	57	4.3	40	0.3	3	6.1	57								
235	0.2	12	0.4	33	0.7	55	0.4	31	0.2	17	0.7	52								
242	0.2	2	4.4	44	5.4	54	4.3	43	0.3	3	5.3	53								
243	0.1	6	0.4	18	1.8	76	0.4	17	0.2	9	1.8	74								
244	0.3	4	4.4	62	2.4	35	4.3	61	0.3	5	2.4	34								
245	0.2	17	0.4	42	0.4	41	0.4	40	0.2	21	0.4	39								
246	0.3	4	4.4	62	2.4	34	4.3	61	0.3	5	2.4	34								
247	0.2	14	0.4	37	0.6	49	0.4	35	0.2	19	0.5	46								
312	0.3	4	4.1	46	4.4	50	3.3	37	1.2	14	4.3	49	8.1	91	0.4	5	6.3	71	1.3	15
313	0.2	3	2.1	22	7.0	75	2.1	23	0.3	3	6.9	74	8.7	93	0.4	4	2.6	28	6.3	68
314	0.2	5	0.7	19	3.0	76	0.9	22	0.2	4	2.9	74	3.5	89	0.2	6	0.5	13	3.3	82
316	0.2	37	0.1	9	0.3	54	0.2	33	0.1	20	0.3	47	0.2	42	0.1	21	0.1	15	0.4	65
317	0.3	2	4.1	32	8.4	66	3.3	26	1.2	9	8.3	65	11.5	90	1.0	8	7.7	60	3.9	30
318	0.2	3	2.1	22	7.0	75	2.1	23	0.3	3	6.8	74	7.7	83	1.3	14	1.7	18	7.3	79
319	0.2	5	0.7	19	2.9	75	0.9	22	0.2	5	2.8	73	3.0	79	0.6	16	0.2	5	3.4	90
321	0.2	26	0.1	7	0.5	67	0.2	25	0.1	15	0.5	60	0.3	44	0.2	30	0.0	0	0.6	85
322	0.3	2	4.1	25	12.0	73	3.3	20	1.2	7	11.8	72	12.2	75	3.8	23	9.5	58	5.6	34
323	0.2	3	2.1	23	6.5	74	2.1	24	0.3	3	6.3	72	5.1	58	3.4	39	0.7	8	7.8	89
324	0.2	4	0.7	17	3.4	78	0.9	20	0.2	4	3.3	76	2.6	60	1.5	36	0.4	10	3.7	86
326	0.2	25	0.1	7	0.5	68	0.2	24	0.1	15	0.5	61	0.1	19	0.4	56	0.0	0	0.7	85
327	0.3	4	2.1	31	4.4	66	2.1	32	0.3	4	4.3	64								
329	0.3	4	2.1	29	4.7	67	2.1	30	0.3	4	4.6	66								
331	0.3	4	2.1	30	4.6	67	2.1	31	0.3	4	4.5	65								
339	0.3	7	2.1	49	1.8	44	2.1	51	0.3	7	1.8	42								
341	0.3	6	2.1	43	2.4	51	2.1	45	0.3	6	2.3	49								
343	0.3	4	2.1	33	4.0	63	2.1	34	0.3	4	3.9	62								
351	0.3	10	2.1	65	0.8	25	2.1	67	0.3	9	0.7	24								
353	0.3	6	2.1	42	2.6	53	2.1	43	0.3	6	2.5	51								

	Method 1						Method 3						Method 2				Method 4			
Run	f_{grain}	$\%f_{grain}$	f_{spill}	$\%f_{spill}$	f_{debris}	$\%f_{debris}$	f_{grain}	$\%f_{grain}$	f_{spill}	$\%f_{spill}$	f_{debris}	$\%f_{debris}$	f_{spill}	$\%f_{spill}$	f_{debris}	$\%f_{debris}$	f_{grain}	$\%f_{grain}$	f_{debris}	$\%f_{debris}$
355	0.3	5	2.1	37	3.2	58	2.1	39	0.3	5	3.1	56								
369	0.2	3	2.1	24	6.4	74	2.1	24	0.3	3	6.3	72								
371	0.2	2	2.1	19	8.7	79	2.1	19	0.3	3	8.5	78								
373	0.2	1	2.1	14	12.9	85	2.1	14	0.3	2	12.7	84								

APPENDIX E: SUMMARY OF EAST ST. LOUIS CREEK HYDRAULICS DATA: VELOCITY AND TURBULENCE CHARACTERISTICS

1. THALWEG DATA FOR EACH CROSS SECTION

2. MEANS BY DISCHARGE PERIOD

3. MEANS BY MORPHOLOGIC POSITION

1. Vertically averaged thalweg data for each cross section. Missing values were eliminated as a result of data filtering. Average Q indicates the average discharge during the field session in which each cross section was collected; Q indicates the hourly flow value that corresponds to the time in which each velocity profile was actually measured.

Cross Section	Morph. Position	U (cm/s)	V (cm/s)	W (cm/s)	Vector magnitude (cm/s)	RMS_u (cm/s)	RMS_v (cm/s)	RMS_w (cm/s)	TKE (N/m^2)	RMS_u'	RMS_v'	RMS_w'	Froude number	Average Q (m^3/s)	Q (m^3/s)	Date
1	Run	32	0.3	2.3	30	6	4	6	4	0.21	0.14	0.19	0.29	0.055	0.058	Aug-Sept 2001
1	Run	26	-1.89	1.43	24	9	5	9	11	0.46	0.25	0.42	0.14	0.077	0.08	June 2002
1	Run	50	-1.2	7.0	50	13	7	14	23	0.28	0.16	0.30	0.39	0.13	0.15	July 2001
1	Run	70	8.9	15.5	78	21	15	21	56	0.38	0.25	0.38	0.41	0.34	0.41	June 2001
1	Run	114	19.0	4.6	112	33	16	33	113	0.41	0.24	0.46	0.64	0.61	0.61	June 2003
2	Above	51	25.7	2.9	57	12	8	12	18	0.23	0.14	0.21	0.47	0.055	0.058	Aug-Sept 2001
2	Above	76	5.26	-0.86	79	18	11	21	44	0.22	0.13	0.27	0.42	0.077	0.08	June 2002
2	Above	75	13.2	6.1	71	16	10	18	34	0.24	0.14	0.25	0.60	0.13	0.15	July 2001
2	Above	143	4.5	14.6	143	18	11	12	22	0.09	0.08	0.08	0.81	0.34	0.41	June 2001
2	Above	157	18.8	7.0	169	28	18	50	211	0.17	0.11	0.30	0.83	0.61	0.61	June 2003
3	Step lip	43	6.7	-36.3	56	44	13	67	329	0.78	0.23	1.19	0.34	0.055	0.055	Aug-Sept 2001
3	Step lip	37	-8.83	-0.48	34	19	12	39	110	0.52	0.35	1.14	0.20	0.077	0.08	June 2002
3	Step lip	82	15.6	4.2	64	26	16	48	133	0.23	0.19	0.74	0.70	0.13	0.14	July 2001
3	Step lip	88	51.9	-6.1	85	24	18	36	102	0.24	0.21	0.42	0.60	0.34	0.31	June 2001
3	Step lip	167	-20.7	0.4	169	28	16	25	92	0.18	0.10	0.16	0.98	0.61	0.61	June 2003
4	Base	4	-6.1	7.4	12	16	8	20	37	1.56	0.76	1.82	0.03	0.055	0.055	Aug-Sept 2001
4	Base													0.077	0.08	June 2002
4	Base													0.13	0.14	July 2001
4	Base													0.34	0.41	June 2001
4	Base	52	10.9	12.4	54	41	25	43	204	0.86	0.58	0.93	0.21	0.61	0.61	June 2003
5	Pool	28	12.0	12.5	33	20	13	26	63	0.77	0.48	0.94	0.19	0.055	0.055	Aug-Sept 2001
5	Pool	52	3.29	21.22	57	41	14	54	322	0.71	0.24	0.94	0.29	0.077	0.08	June 2002
5	Pool	24	10.8	7.0	35	47	17	64	389	1.54	0.52	1.95	0.14	0.13	0.14	July 2001
5	Pool	21	16.2	4.8	36	66	22	84	631	2.47	0.73	3.02	0.10	0.34	0.29	June 2001
5	Pool	42	-7.1	-34.5	91	99	28	139	1743	1.37	0.37	1.99	0.23	0.61	0.61	June 2003
6	Above	45	-18.0			15	6						0.45	0.055	0.055	Aug-Sept 2001
6	Above	37	-17.96	6.51	49	16	8	19	38	0.33	0.19	0.38	0.21	0.077	0.08	June 2002
6	Above	84	-8.9	19.6	82	14	10	15	28	0.19	0.12	0.18	0.63	0.13	0.14	July 2001
6	Above	103	-33.2	15.3	110	16	13	21	43	0.15	0.12	0.19	0.59	0.34	0.31	June 2001
6	Above	115	-49.2	19.9	130	29	17	33	110	0.23	0.13	0.25	0.64	0.61	0.61	June 2003

Cross Section	Bedform type	U (cm/s)	V (cm/s)	W (cm/s)	Vector magnitude (cm/s)	RMS_u (cm/s)	RMS_v (cm/s)	RMS_w (cm/s)	TKE (N/m^2)	RMS_u'	RMS_v'	RMS_w'	Froude number	Average Q (m^3/s)	Q (m^3/s)	Date
7	Step lip	70	-44.3	-23.2	87	11	8	13	18	0.13	0.09	0.15	0.65	0.055	0.055	Aug-Sept 2001
7	Step lip	52	-50.05	-6.74	69	12	8	12	21	0.20	0.12	0.17	0.30	0.077	0.08	June 2002
7	Step lip	64	-27.4	-49.6	98	25	10	23	74	0.28	0.11	0.25	0.62	0.13	0.14	July 2001
7	Step lip													0.34	0.31	June 2001
7	Step lip													0.61	0.61	June 2003
8	Base	2	1.5	0.5	8	12	8	13	19	1.96	1.36	2.05	0.01	0.055	0.055	Aug-Sept 2001
8	Base													0.077	0.08	June 2002
8	Base													0.13	0.14	July 2001
8	Base													0.34	0.31	June 2001
8	Base													0.61	0.61	June 2003
9	Pool	22	0.6	8.9	24	20	12	20	46	0.83	0.54	0.91	0.10	0.055	0.055	Aug-Sept 2001
9	Pool	35	-0.53	8.77	40	40	17	52	266	1.84	0.65	2.54	0.21	0.077	0.08	June 2002
9	Pool	37	2.4	18.0	46	36	19	50	246	0.80	0.47	1.09	0.16	0.13	0.14	July 2001
9	Pool													0.34	0.31	June 2001
9	Pool													0.61	0.61	June 2003
10	Casc	6	-15.2	-11.6	21	13	10	16	32	0.67	0.49	0.76	0.04	0.055	0.055	Aug-Sept 2001
10	Casc	53	-11.71	-2.33	55	15	9	16	30	0.30	0.19	0.29	0.31	0.077	0.08	June 2002
10	Casc	9	-10.0	-1.7	16	11	8	10	15	0.74	0.60	0.73	0.06	0.13	0.14	July 2001
10	Casc	16	14.3	7.3	41	17	12	18	45	0.46	0.32	0.49	0.09	0.34	0.31	June 2001
10	Casc	12	6.3	-5.3	29	57	19	94	680	2.61	0.80	4.39	0.07	0.61	0.61	June 2003
11	Casc	46	18.2			23	10						0.42	0.055	0.055	Aug-Sept 2001
11	Casc	46	12.38	-1.95	49	22	11	18	32	0.55	0.27	0.26	0.28	0.077	0.08	June 2002
11	Casc	39	8.1	10.1	43	22	14	27	73	0.52	0.36	0.63	0.27	0.13	0.14	July 2001
11	Casc	66	42.1	8.6	86	43	20	48	348	0.54	0.25	0.60	0.35	0.34	0.31	June 2001
11	Casc	68	-1.8	19.9	77	44	22	57	284	0.73	0.40	0.84	0.35	0.61	0.61	June 2003
12	Casc	9	-10.5	10.1	19	40	19	46	199	2.50	0.96	2.92	0.06	0.055	0.055	Aug-Sept 2001
12	Casc													0.077	0.08	June 2002
12	Casc	24	-5.9	9.2	33	59	19	92	679	1.87	0.60	2.91	0.14	0.13	0.13	July 2001
12	Casc													0.34	0.33	June 2001
12	Casc	106	-0.4	-3.8	136	60	28	86	542	0.45	0.22	0.63	0.50	0.61	0.61	June 2003
13	Casc	17	-9.9	1.5	24	15	6	18	33	0.70	0.32	0.79	0.12	0.055	0.054	Aug-Sept 2001
13	Casc	41	-21.77	3.25	51	29	20	40	162	0.63	0.46	0.84	0.26	0.077	0.08	June 2002
13	Casc	32	-10.3	-3.4	37	21	9	25	68	1.22	0.44	1.55	0.18	0.13	0.13	July 2001
13	Casc	101	-20.7	8.2	104	51	20	58	325	0.49	0.19	0.56	0.61	0.34	0.33	June 2001
13	Casc	189	0.4	0.0	194	76	25	0		0.38	0.12		1.04	0.61	0.61	June 2003

Cross Section	Bedform type	U (cm/s)	V (cm/s)	W (cm/s)	Vector magnitude (cm/s)	RMS_u (cm/s)	RMS_v (cm/s)	RMS_w (cm/s)	TKE (N/m^2)	RMS_u'	RMS_v'	RMS_w'	Froude number	Average Q (m^3/s)	Q (m^3/s)	Date
14	Pool	13	-6.9	-1.3	15	11	7	11	16	0.76	0.50	0.78	0.12	0.055	0.054	Aug-Sept 2001
14	Pool	30	-4.65	8.59	32	16	9	19	37	0.51	0.29	0.59	0.20	0.077	0.08	June 2002
14	Pool	26	9.2	3.0	28	12	6	12	17	0.46	0.24	0.46	0.18	0.13	0.13	July 2001
14	Pool	29	22.8	10.6	38	21	16	25	66	0.54	0.42	0.66	0.14	0.34	0.29	June 2001
14	Pool	69	-2.6	12.8	73	58	24	67	410	0.78	0.33	0.88	0.31	0.61	0.61	June 2003
15	Above	93	-20.1	-2.9	90	12	7	16	29	1.30	0.51	1.85	0.65	0.055	0.054	Aug-Sept 2001
15	Above	10	-9.66	-8.49	20	15	7	17	29	0.81	0.37	0.91	0.07	0.077	0.08	June 2002
15	Above	97	-35.7	7.7	105	17	10	17	40	0.17	0.10	0.18	0.50	0.13	0.13	July 2001
15	Above	9	-7.0	6.5	18	20	14	24	57	1.09	0.75	1.27	0.04	0.34	0.29	June 2001
15	Above	80	-3.0	0.4	70	27	19	36	124	0.46	0.32	0.63	0.31	0.61	0.61	June 2003
16	Step lip	77	-18.4	0.4	91	15	9	17	31	0.17	0.10	0.19	0.62	0.055	0.054	Aug-Sept 2001
16	Step lip	54	-21.46	8.12	60	18	11	18	39	0.32	0.19	0.32	0.39	0.077	0.08	June 2002
16	Step lip	122	27.3	-8.3	125	15	11	15	30	0.12	0.09	0.12	0.73	0.13	0.13	July 2001
16	Step lip	94	-23.8	34.8	100	18	13	18	42	0.19	0.13	0.18	0.54	0.34	0.29	June 2001
16	Step lip	96	-37.9	-6.0	107	31	17	39	125	0.28	0.16	0.33	0.47	0.61	0.61	June 2003
17	Base	4	9.6	3.3	12	4	3	4	2	0.36	0.23	0.37	0.02	0.055	0.054	Aug-Sept 2001
17	Base	-1	1.32	1.69	21	35	13	60	303	1.78	0.64	3.11	-0.01	0.077	0.08	June 2002
17	Base	12	19.8	5.5	24	9	5	8	8	0.37	0.20	0.36	0.06	0.13	0.13	July 2001
17	Base	8	14.0	17.2	26	15	8	17	33	0.58	0.30	0.64	0.04	0.34	0.29	June 2001
17	Base	8	30.7	16.4	70	31	19	40	137	0.43	0.26	0.54	-0.06	0.61	0.61	June 2003
18	Above	19	-5.1	3.4	21	17	9	19	38	0.84	0.45	0.95	0.13	0.055	0.054	Aug-Sept 2001
18	Above	26	-15.56	-5.51	35	12	7	12	19	0.33	0.21	0.33	0.21	0.077	0.08	June 2002
18	Above	41	-24.2	13.0	57	21	11	31	103	0.41	0.22	0.53	0.21	0.13	0.13	July 2001
18	Above	25	-35.0	3.0	44	31	14	54	279	0.79	0.36	1.39	0.11	0.34	0.29	June 2001
18	Above													0.61	0.61	June 2003
19	Base	23	-8.8	-5.9	25	18	6	21	39	0.70	0.23	0.82	0.11	0.055	0.054	Aug-Sept 2001
19	Base	10	0.44	-1.72	10	6	3	5	4	0.64	0.37	0.51	0.08	0.077	0.08	June 2002
19	Base	0	4.8	-0.02	5	8	5	9	8	1.64	0.97	1.86	0.00	0.13	0.13	July 2001
19	Base	20	4.5	-10.3	33	37	15	45	187	1.07	0.50	1.34	0.08	0.34	0.29	June 2001
19	Base													0.61	0.61	June 2003

2. Thalweg hydraulics data averaged for each discharge period.

U (cm/s)	V (cm/s)	W (cm/s)	Vector magnitude (cm/s)	RMS_u (cm/s)	RMS_v (cm/s)	RMS_w (cm/s)	TKE (N/m^2)	RMS_u'	RMS_v'	RMS_w'	Froude number	Average Q (m^3/s)	Date
30	-4.5	-0.4	36	18	9	23	67	0.90	0.46	1.10	0.24	0.055	Aug-Sept 2001
36	-9.1	2.4	42	22	11	28	111	0.69	0.33	0.89	0.22	0.077	June 2002
48	-0.7	2.8	54	22	11	28	116	0.65	0.32	0.83	0.33	0.13	July 2001
57	4.2	9.3	67	29	15	34	160	0.65	0.33	0.80	0.32	0.34	June 2001
84	-2.3	5.0	99	47	21	58	387	0.75	0.34	1.03	0.43	0.61	June 2003

3. Thalweg hydraulics data averaged for each morphologic position.

Morphologic position	U (cm/s)	V (cm/s)	W (cm/s)	Vector magnitude (cm/s)	RMS_u (cm/s)	RMS_v (cm/s)	RMS_w (cm/s)	TKE (N/m^2)	RMS_u'	RMS_v'	RMS_w'	Froude number
Above step	70	-11.3	5.9	76	19	11	24	72	0.46	0.25	0.58	0.42
Step lip	85	-11.1	-5.2	92	22	13	28	88	0.27	0.16	0.39	0.56
Base of step	11	7.4	5.6	26	23	11	33	139	1.07	0.54	1.34	0.05
Pool	34	4.7	5.1	44	41	17	52	378	1.07	0.45	1.34	0.18
Cascade	47	-1.1	3.7	55	35	16	41	231	0.93	0.43	1.23	0.27
Run	58	5.0	6.2	59	17	10	17	42	0.35	0.21	0.35	0.38

APPENDIX F: EAST ST. LOUIS CREEK SURVEY DATA: LONGITUDINAL PROFILE, CROSS SECTIONS, PHOTOGRAPHS, GRAIN SIZE DISTRIBUTION

East St. Louis Creek
Longitudinal Profile
Surveyed June 16, 2003

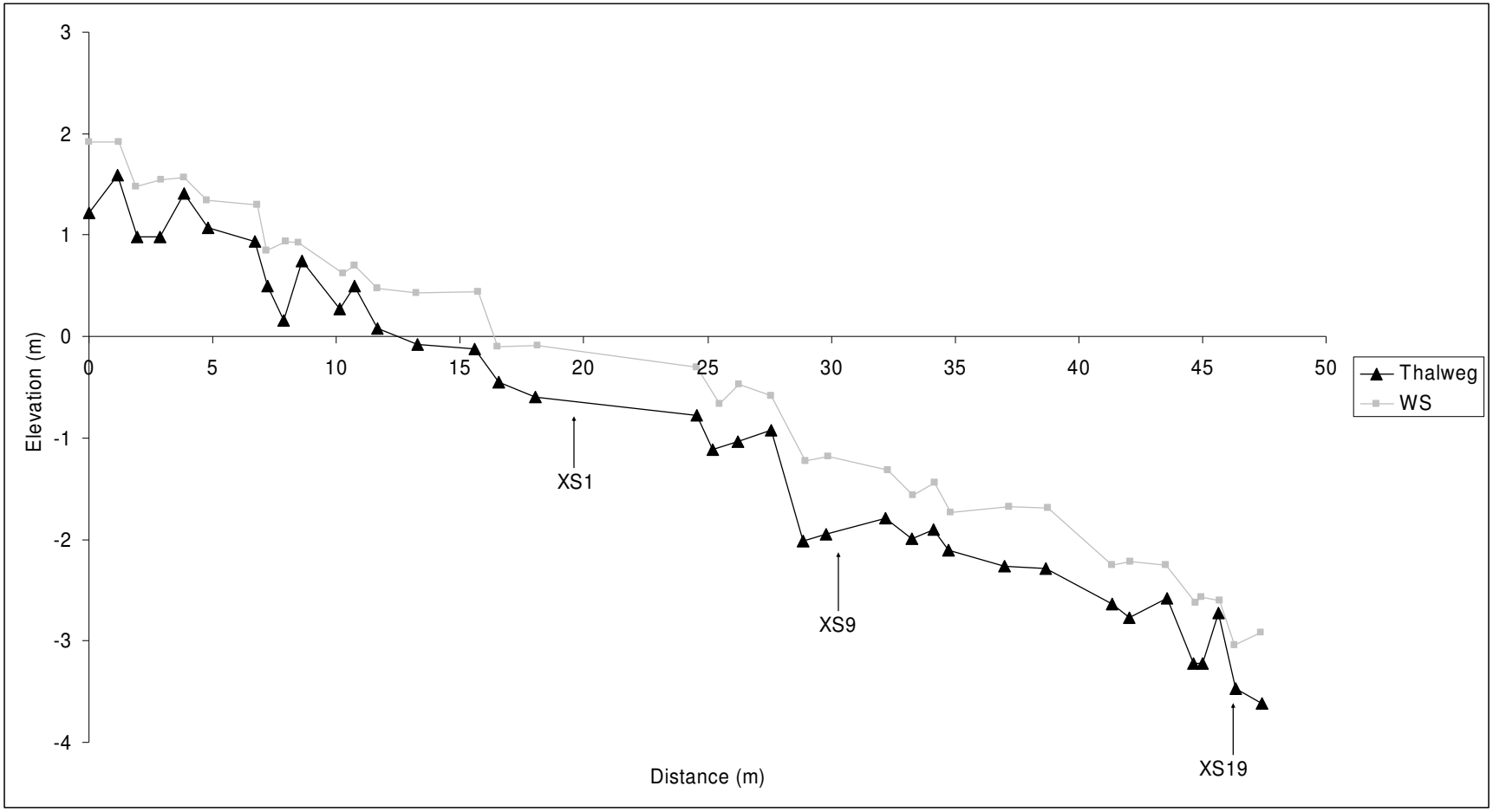

Cross Sections and Photos

Note: All elevations for cross sections based on arbitrary datum.

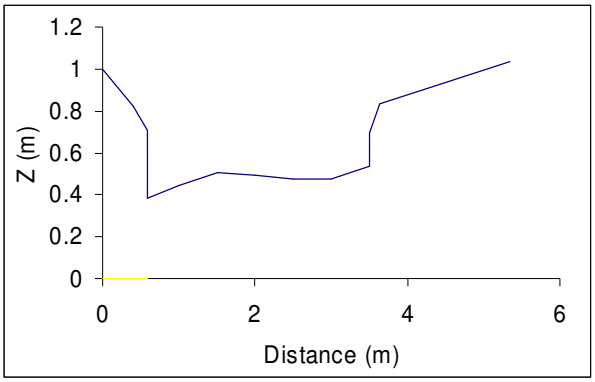

Cross Section 1. Surveyed June 12, 2001 (photo from left bank)

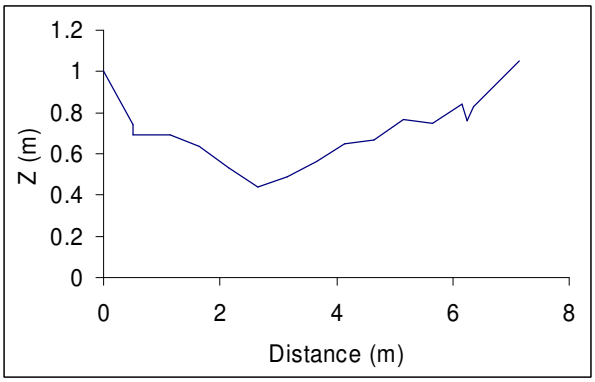

Cross Section 2. Surveyed June 12, 2001 (photo from right bank)

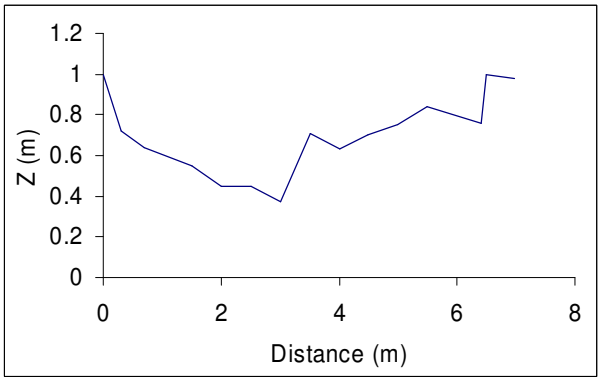

Cross Section 3. Surveyed June 15, 2001 (see photo below)

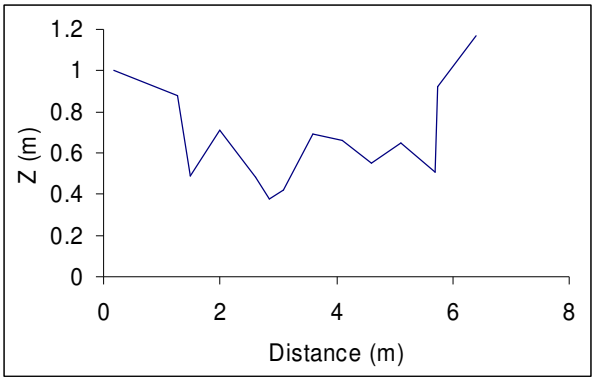

Cross Section 4. Surveyed June 12, 2001 (photo from right bank of cross sections 3 on left and 4 on right)

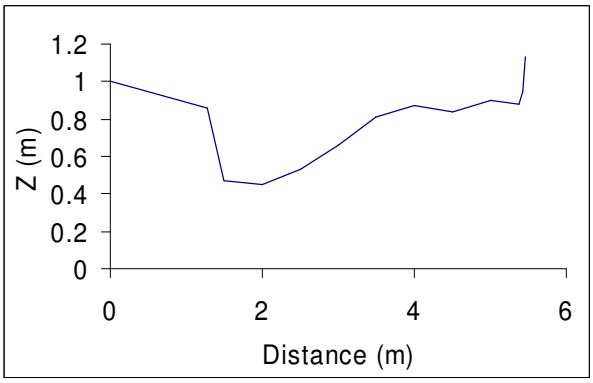

Cross Section 5. Surveyed June 16, 2001 (see photo below)

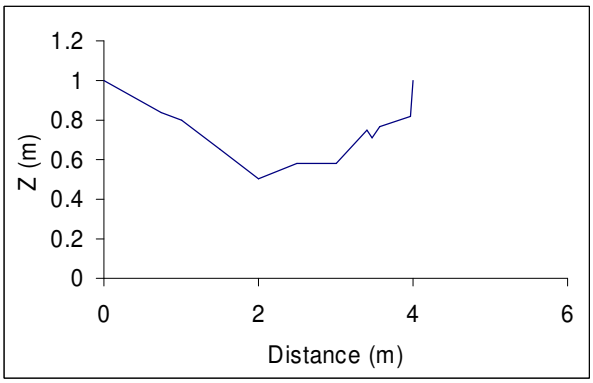

Cross Section 6. Surveyed June 15, 2001 (photo from left bank of cross sections 5 on right and 6 on left)

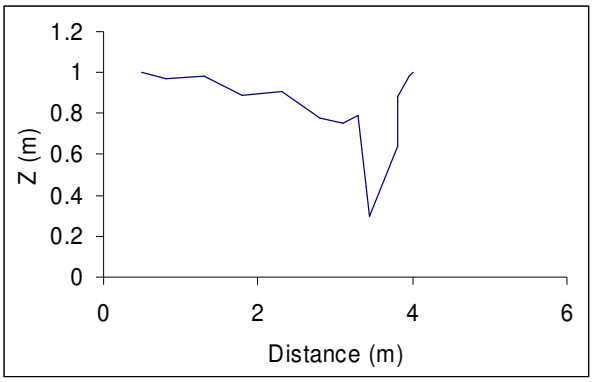

Cross Section 7. Surveyed June 15, 2001 (photo from left bank of cross sections 6 on right and 7 on left)

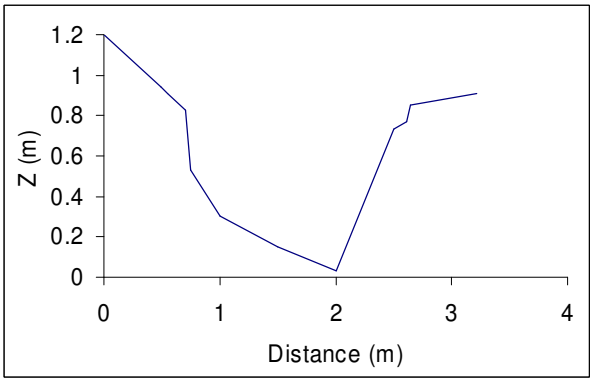

Cross Section 8. Surveyed June 15, 2001 (See photo above, cross section 8 located to left of tape at cross section 7 at base of step)

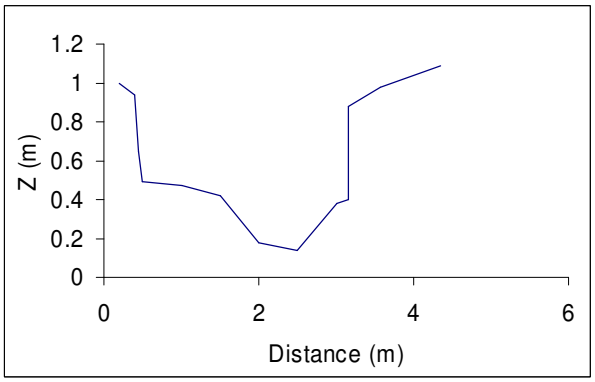

Cross Section 9. Surveyed June 15, 2001 (see photo below)

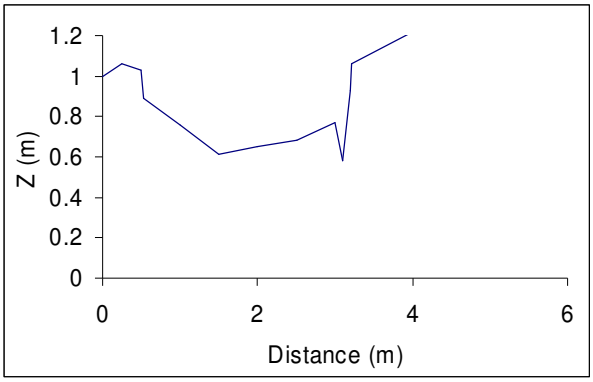

Cross Section 10. Surveyed June 15, 2001 (photo from right bank of cross sections 9 on left and 10 on right)

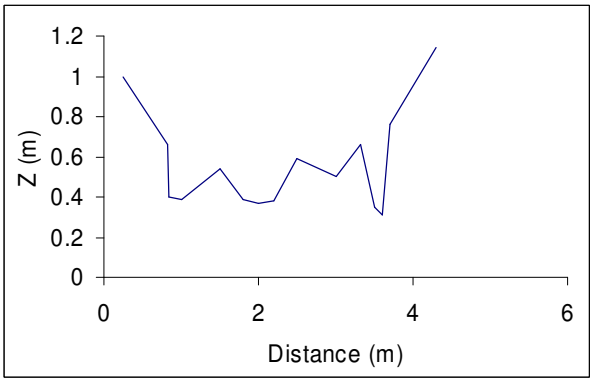

Cross Section 11. Surveyed June 15, 2001 (see photo below)

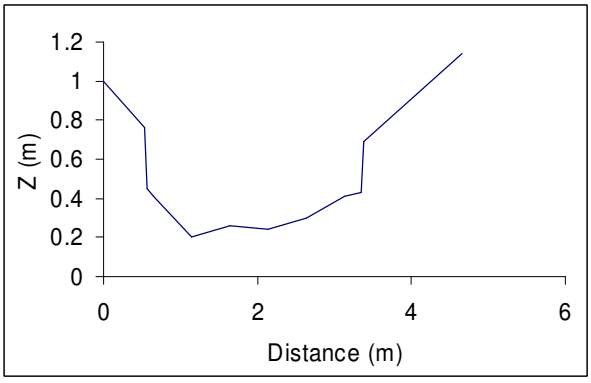

Cross Section 12. Surveyed June 15, 2001 (photo from right bank of cross sections 11 on left and 12 on right)

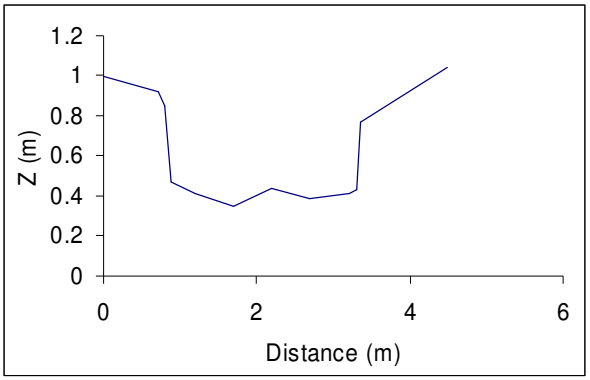

Cross Section 13. Surveyed June 15, 2001 (photo from left bank of cross sections 12 on right and 13 on left)

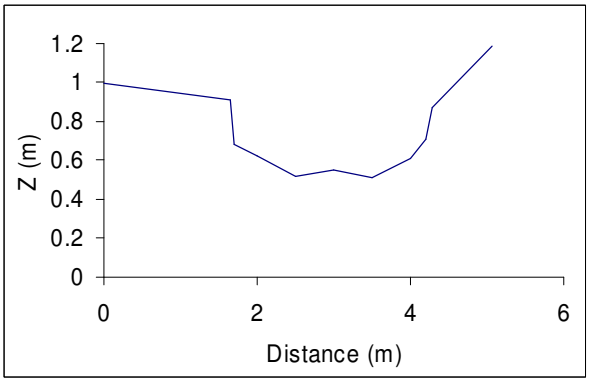

Cross Section 14. Surveyed June 16, 2001 (photo from right bank)

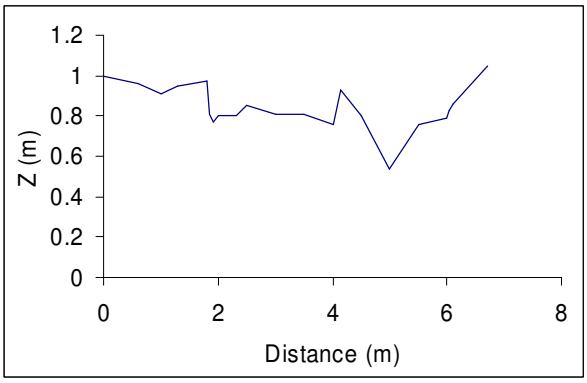

Cross Section 15. Surveyed June 16, 2001 (see photo below)

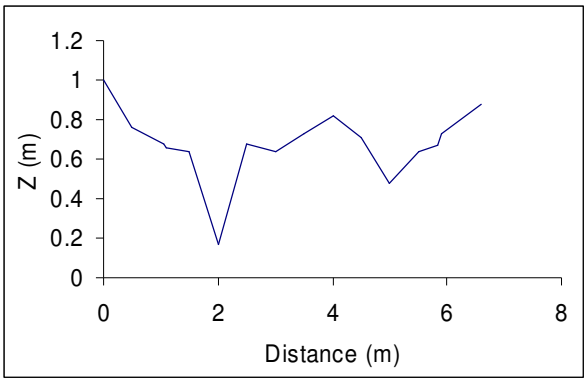

Cross Section 16. Surveyed June 16, 2001 (See photo below, cross section 16 is just upstream (right) of channel spanning log)

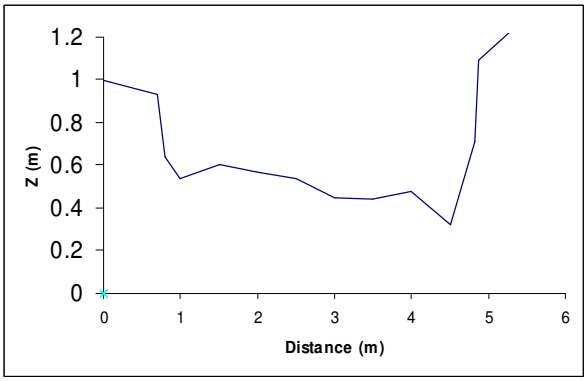

Cross Section 17. Surveyed June 16, 2001 (photo from left bank of cross sections 15 on right and 17 on left)

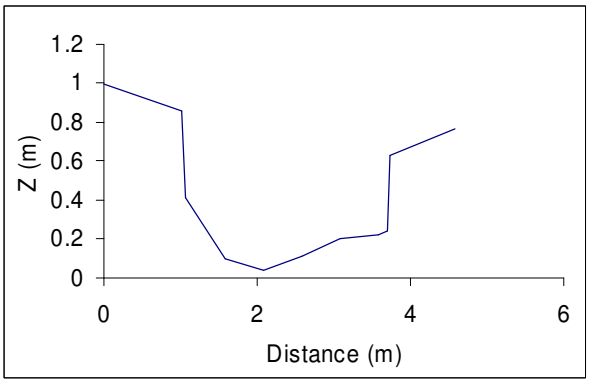

Cross Section 18. Surveyed June 16, 2001 (photo from right bank)

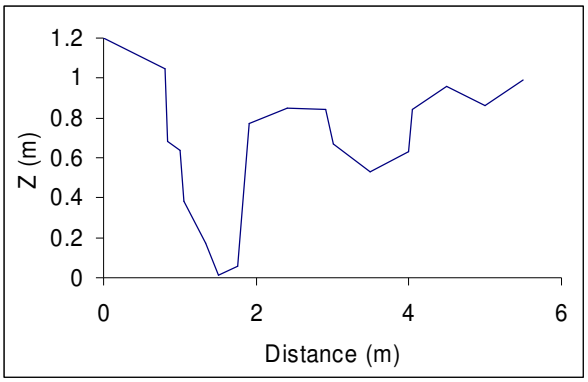

Cross Section 19. Surveyed June 16, 2001 (photo from left bank)

East St. Louis Creek
Grain size distribution